



University
of Glasgow

Smaranda, Dumitru Dan (2020) *Grand unified theories in extra dimensions*. PhD thesis.

<https://theses.gla.ac.uk/81357/>

Copyright and moral rights for this work are retained by the author

A copy can be downloaded for personal non-commercial research or study, without prior permission or charge

This work cannot be reproduced or quoted extensively from without first obtaining permission in writing from the author

The content must not be changed in any way or sold commercially in any format or medium without the formal permission of the author

When referring to this work, full bibliographic details including the author, title, awarding institution and date of the thesis must be given

Enlighten: Theses

<https://theses.gla.ac.uk/>
research-enlighten@glasgow.ac.uk

Grand Unified Theories in Extra Dimensions

Dumitru Dan Smaranda

Supervised by Dr. David J. Miller and Dr. Christoph Englert

*Submitted in fulfillment of the requirements for the degree of
Doctor of Philosophy*

April 2020



*University of Glasgow
College of Science and Engineering
School of Physics and Astronomy*

Abstract

Abstract: The Standard Model (SM) of Particle Physics is currently our best understanding of the laws of nature. At the same time it cannot account for a variety of phenomena, and has a series of shortcomings regarding its own structure.

Beyond the Standard Model physics aims to address these issues, where Grand Unified Theories (GUTs) provide a solution to some of questions regarding the structure, which in turn address some of the phenomenological problems present in the SM.

In the following thesis we explore the phenomenology of GUTs, along with their valid parameter spaces and experimental signatures. This is done within an extra dimensional scenario, where we look at 5D and 6D models, within flat and warped contexts. In this work we have ruled out a series of models and explored the use of unification metrics to guide model building via renormalisation group equation analysis within different regimes. To achieve this we have employed a variety of numerical and evolutionary algorithms.

Keywords: Grand Unified Theory, orbifold, $\mathcal{M}_4 \times S^1/\mathbb{Z}_2$, $\mathcal{M}_4 \times T^1/\mathbb{Z}_2$, extra dimensions, $SO(11)$, $SU(5)$, $SU(5) \times U(1)$, 4D, 5D, 6D, renormalisation group equations, unification, differential evolution, AdS_5 , Randal Sundrum.

Declaration of originality

This thesis is my own work, except where explicit attribution to others is made. Chapters 3, 7 are based on the following publications:

- Chapter 3:
“Scherk-Schwarz orbifolds at the LHC” [1], written in collaboration with Dr. David J. Miller.
- Chapter 7:
“Phenomenology of GUT-inspired gauge-Higgs unification” [2], written in collaboration with Dr. Christoph Englert and Dr. David J. Miller.

“The Weinberg Angle and 5D RGE effects in a SO(11) GUT theory” [3], written in collaboration with Dr. Christoph Englert and Dr. David J. Miller.

All results and figures presented in these chapters are my own, except for the calculation in Sec. 7.3.1 which was done by Dr. Christoph Englert.

'There is no answer.'

Acknowledgments

Firstly, I would like to thank David Miller for being an excellent supervisor throughout my PhD, giving me the freedom and support to explore all the interesting topics and problems that I found along the way. I would like to thank Christoph Englert for always pointing me in the right direction along with providing me with his insight, knowledge and help of which I would have been lost without. I would also like to thank Christine Davies for being an amazing group leader and for always providing support whenever it was needed.

I would like to thank all my friends and colleagues from the PPT group Dan Hatton, Stephen Brown, Euan Mclean, Donatas Zaripovas, John McDowall, and Karl Nordstrom, for being pillars that have supported me and endured my poor humour over the past couple of years, with a special mention to Andres Luna and Natalia Campos Rivera who made me feel at home. And to the new Ph.D. students, Will Parrott, Panayiotis Stylianou, and Esther Pertiñez Ruiz, good luck!

I would also like to thank the various PPE and nuclear PhD students, Dwayne Spiteri, Lauren Douglas, Abby Powell, Sarah Karodia, and Will Breaden Madden for being excellent to me and providing a long sheet of anecdotes that I will fondly remember. I would also like to thank the postdocs, Andrew Lyle, Sarah Boutle, Federica Fabbri, Giuseppe Callea, Ian Connelly, John Nugent, and Chris Pollard that have helped me form into a better physicist and a better person.

I would like to thank my good friends Brian and Elizabeth Alden, which have become my family from over the pond over the past couple of years. They have played an immense role in shaping me into who I am today.

Pe aceeași notă, aş dori să îi mulțumesc mamei mele Lăcrămioara și fratelui meu Cezar, pentru că au fost un sprijin toți anii aceștia, alături de prietenii mei Mara Solomon, Daniel Budeanu, Flavia Vereș, Maria Sârzea, Ana Iuteș, Ionuț Aruxandei, și Emilia Gherman. Într-un final, aş vrea să îi mulțumesc prietenei mele Cara, pentru dragostea și suportul ei, pentru ultimele luni, și pentru că a râs la glumele mele proaste.

Contents

1	The Standard Model	1
1.1	The Legacy of the Standard Model	1
1.2	Poincaré and Lorentz Algebras	2
1.2.1	Representations of $SL(2, \mathbb{C})$	3
1.3	The Standard Model - Introduction	5
1.4	The Standard Model - Gauge and Higgs Sector	6
1.5	The Standard Model - Lepton Sector	10
1.6	The Standard Model - Quark Sector	13
1.7	Shortcomings of the SM	17
1.8	Grand Unification, and Hierarchies	18
1.8.1	The Gildener Problem	18
1.8.2	A non Supersymmetric $SU(5)$ GUT	19
1.8.3	The Effective Action and Conformal Symmetry	24
1.8.4	Scalar QED and Radiatively Induced SSB	27
1.8.5	Conformal Symmetry doesn't work	29
1.8.6	Supersymmetric $SU(5)$	29
2	Supersymmetry and the MSSM	31
2.1	Graded Algebra	31
2.2	Representations of the Poincaré Group	33
2.3	Representations of the $\mathcal{N} = 1$ SUSY Algebra	34
2.3.1	Massless Supermultiplet	35
2.3.2	Massive Supermultiplet	36
2.4	Extended Supersymmetry	38
2.4.1	Massless Representations of $\mathcal{N} > 1$ SUSY	39
2.5	Superspace and Superfields	41
2.5.1	Groups and Cosets	42
2.5.2	Scalar Superfield	44
2.6	Vector Superfields	47
2.6.1	Abelian Superfield Field Strength	48
2.6.2	Non-abelian Superfield Field Strength	49
2.7	4D, $\mathcal{N} = 1$ SUSY	50

2.8	The Minimal Supersymmetric Model (MSSM)	54
2.8.1	Soft SUSY Breaking in the MSSM	58
2.8.2	Mass Spectrum of the MSSM - Higgs Sector	62
2.8.3	Mass Spectrum of the MSSM - Neutralinos & Charginos	65
2.8.4	Mass Spectrum of the MSSM - Squarks and sleptons	68
2.9	SUSY in GUTs	71
3	Orbifolds and Scherk-Schwarz breaking	73
3.1	Introduction	73
3.2	Extra Dimensions, Compactifications, and SS Twists	74
3.3	$5D \mathcal{N} = 1$ SUSY to $4D \mathcal{N} = 1$	81
3.3.1	Gauge Lagrangian	85
3.3.2	Matter Lagrangian	85
3.4	Breaking Symmetries	86
3.4.1	SUSY Breaking	86
3.4.2	Gauge Breaking	89
3.5	Fermionic Matter: Brane vs. Bulk	92
3.6	Models	94
3.6.1	Methodology	95
3.6.2	Barbieri, Hall and Nomura $SU(5)$: Brane and Bulk	98
3.6.3	$SU(5)$ with an additional scalar	101
3.6.4	$SU(5) \times U(1)$ via $SO(10)$ and E_6	107
3.6.5	An E_6 Model	110
3.7	Conclusions	111
3.7.1	Back to the Gildener Problem	112
4	The Hosotani Mechanism	113
4.1	Introduction	113
4.2	Orbifolds, Boundary Conditions & the Hosotani Mechanism	113
4.3	Residual Gauge Invariance of the Boundary Conditions	116
4.4	Wilson Line Phases	117
4.4.1	Geometry of Gauge Invariance	117
4.4.2	Wilson Line Phases on Multiply Connected Manifolds	121
4.4.3	Caveat	123
4.5	The Hosotani Mechanism	124
4.6	Orbifolds in $SU(5)$ Gauge Theory	126

4.7	Effective Potentials	127
4.8	Non-SUSY $SU(5)$ Theory	130
4.8.1	Equivalence Classes	133
4.9	Conclusions	136
5	Flat & Warped Extra Dimensions	137
5.1	Extra Dimensions: Equations of Motion	137
5.1.1	Fermions in a Flat Extra Dimension	137
5.1.2	Fermions in a Warped Extra Dimension	141
5.2	Stepping Stones	145
6	$SO(11)$ GHGUT - The Model	147
6.1	6D Orbifold Compactification	147
6.2	6D Spacetime and Gauge Symmetry	149
6.3	Matter Content	152
6.3.1	6D Fields	152
6.3.2	5D Fields	154
6.4	Parity Assignments	154
6.4.1	Gauge Fields	154
6.4.2	Spinor Fields	156
6.4.3	Vector Fields	158
6.5	Lagrangians	159
6.5.1	Bulk Lagrangian	159
6.5.2	Brane Lagrangians	161
6.6	Symmetry Breaking	163
6.6.1	Orbifold Breaking	164
6.6.2	Brane gauge breaking via $\langle \Phi_{\mathbf{32}} \rangle$	165
6.6.3	Hosotani EW Breaking	168
6.7	EOMs, $V_{\text{eff}}(\theta_H)$ & the Parameter Space	170
6.7.1	Boson Equations of Motion	170
6.7.2	Fermion Equations of Motion	173
6.7.3	The Effective Higgs Potential $V_{\text{eff}}(\theta_H)$	176
6.8	A Brief Pause	178
7	$SO(11)$ GHGUT - RGEs & spectra	179
7.1	Scanning Algorithm	179

7.2	Mass Spectra	185
7.3	Low Energy Phenomenology Implications	186
7.3.1	Di-Higgs Physics	186
7.3.2	Exotics	188
7.4	Gauge Coupling RGE Running in (4D & 5D) EFTs	191
7.4.1	Methodology	193
7.4.2	4D Approximation and RGEs	195
7.4.3	5D RGEs and Cut-offs	200
7.4.4	Weinberg Angle: $SU(5)$ Prediction vs. Running	207
7.5	Results	210
7.6	Conclusions	215
8	Summary & Conclusions	217
	Appendices	219
A	Bessel Equation	221
A.1	Bessel Equation & Bessel Functions	221
B	$SO(11)$ GHGUT	225
B.1	Threshold Corrections	225
B.2	Gauge Couplings	226
B.3	$N_{(\pm,\pm)}(\mu)$ Functions	227
B.4	Bessel Basis Functions	229
B.5	Bessel Tower Equations Solutions	230

The Standard Model

1.1 The Legacy of the Standard Model

The Standard Model (SM) of particle physics [4–6] has been for the past 50 years or so, the most accurate description of the fundamental laws of nature via its description of the strong and electroweak interactions, that has been validated by experiment over and over again. Furthermore, in July 2012 the ATLAS and CMS [7, 8] experiments at the LHC discovered the Higgs boson, and measured its mass $m_H = 125.10 \pm 0.14$ GeV [9], further confirming the validity of the SM.

Even though the SM has been enormously successful in explaining a lot of features of the universe, it still has a series of shortcomings and cannot accurately account for a variety of phenomena (see Ref. [10] for a detailed overview). These range from lacking an explanation as to why gravity is so much weaker than the other fundamental forces [11–14], to producing a realistic value for the cosmological constant [15]. Amongst the series of problems, the SM does not account for neutrino masses, cannot account for the strong CP problem [16], or describe the matter antimatter asymmetry in the universe [17], and struggles to provide a phenomenologically viable dark matter candidate or a source for dark energy. These shortcomings have in turn pointed towards the need of physics Beyond the Standard Model (BSM). Throughout this thesis we will be looking at how we formulate and scrutinise certain BSM theories.

In the following chapter we will review the structure of the SM and then come back to answer some of the shortcomings, within the context of Grand Unified Theories (GUTs).

The following section will summarise the matter constituents of the SM, its gauge groups, how the matter representations transform under the various Lie algebras, and how the Weyl basis relates to the Dirac basis post electroweak symmetry breaking. The review is based mostly on Chapters 87–89 from [18].

1.2 Poincaré and Lorentz Algebras

The Poincaré group consists of the symmetries of special relativity, i.e. translations a_μ and Lorentz transformations $\Lambda^\mu{}_\nu$. These, in turn act on space-time coordinates x^μ as

$$x^\mu \rightarrow x'^\mu = \Lambda^\mu{}_\nu x^\nu + a^\mu, \quad (1.1)$$

where the metric tensor ($\eta_{\mu\nu} = \text{diag}(+, -, -, -)$) is invariant under Lorentz transformation $\Lambda^T \eta \Lambda = \eta$. The Lorentz matrices can have a determinant of $\det \Lambda = \pm 1$, which separates them into two classes, the ones which are connected to the identity matrix ($\det \Lambda = +1$) and the ones which are not ($\det \Lambda = -1$). The ones that are not connected contain discrete actions (i.e. non-continuous discrete transformations such as parity, time reversal or charge conjugation P, T, C), whilst the connected ones form a continuous group named the *proper orthochronous group* $SO_+^\uparrow(3, 1)$. In this section we will be discussing the latter. To this extent, the generators of the Poincaré algebra consist of the Lorentz generators $M^{\mu\nu}$ and the translational generators P^σ that obey the commutation relations

$$\begin{aligned} [P^\mu, P^\nu] &= 0, \\ [M^{\mu\nu}, P^\sigma] &= i(P^\mu \eta^{\nu\sigma} - P^\nu \eta^{\mu\sigma}), \\ [M^{\mu\nu}, M^{\rho\sigma}] &= i(M^{\mu\sigma} \eta^{\nu\rho} + M^{\nu\rho} \eta^{\mu\sigma} - M^{\mu\rho} \eta^{\nu\sigma} - M^{\nu\sigma} \eta^{\mu\rho}). \end{aligned} \quad (1.2)$$

Locally the proper orthochronous group is isomorphic to

$$SO_+^\uparrow(3, 1) \simeq SU(2) \oplus SU(2), \quad (1.3)$$

which in turn allows us to write the Lorentz generators in terms of two $SU(2)$ commutative algebras with generators A_i, B_i , where

$$[A_i, A_j] = i\varepsilon_{ijk} A_k, \quad [B_i, B_j] = i\varepsilon_{ijk} B_k, \quad [A_i, B_j] = 0. \quad (1.4)$$

Simultaneously we can define the Lorentz rotation generators J_i , and the Lorentz boost generators K_i , with respect to $M^{\mu\nu}$

$$J_i = \frac{1}{2} \varepsilon_{ijk} M_j, \quad K_i = M_{0,i} \quad (1.5)$$

which in conjunction with the isomorphism relates the generator sets as linear combinations

$$A_i = \frac{1}{2} (J_i + iK_i), \quad B_i = \frac{1}{2} (J_i - iK_i), \quad (1.6)$$

where $\vec{J} = \vec{A} + \vec{B}$ can be interpreted as physical spin. We also note that one can find the homeomorphism

$$SO_+^\uparrow(3, 1) \simeq SL(2, \mathbb{C}) \quad (1.7)$$

by noting that we can construct a mapping between a 4-vector $\mathbf{X} = x_\mu e^\mu$ and a 2×2 matrix $\tilde{x} = x_\mu \sigma^\mu$ where x^μ are the Minkowski coordinates and e^μ are the basis vectors, and σ^μ are the the Pauli sigma matrices along with the identity matrix $\sigma^\mu = \{\mathbb{1}, \sigma^i\}$. Writing these out explicitly we have

$$\mathbf{X} = x_\mu e^\mu = (x_0, x_1, x_2, x_3), \quad \tilde{x} = x_\mu \sigma^\mu = \begin{pmatrix} x_0 + x_3 & x_1 - ix_2 \\ x_1 + ix_2 & x_0 - x_3 \end{pmatrix}. \quad (1.8)$$

The two constructs transform under $SO_+^\uparrow(3, 1)$ and $SL(2, \mathbb{C})$ as

$$\mathbf{X} \rightarrow \Lambda \mathbf{X}, \quad \tilde{x} \rightarrow N \tilde{x} N^\dagger, \quad (1.9)$$

where N is a general $SL(2, \mathbb{C})$ matrix parametrising the transformation.

The magnitude of the 4-vector $|\mathbf{X}|^2 = x_0^2 - x_1^2 - x_2^2 - x_3^2$ is invariant under $SO_+^\uparrow(3, 1)$ transformations. Similarly, the determinant $\det \tilde{x} = x_0^2 - x_1^2 - x_2^2 - x_3^2$ is also invariant under the $SL(2, \mathbb{C})$ mapping. Therefore we have induced a mapping between $SO_+^\uparrow(3, 1)$ and $SL(2, \mathbb{C})$, where the map is 2 to 1 since identical \pm choices in N result in the same correspondence to the specific Λ . In addition, since $SL(2, \mathbb{C})$ is simply connected, it acts as the universal covering group for $SO_+^\uparrow(3, 1)$.

1.2.1 Representations of $SL(2, \mathbb{C})$

We now list the relevant representations of $SL(2, \mathbb{C})$ to our discussion, and how they behave under a specific transformation N .

- The fundamental representation

$$\psi'_\alpha = N_\alpha{}^\beta \psi_\beta, \quad (1.10)$$

where $\alpha, \beta = 1, 2$. The fundamental ψ_α is referred to as a *left-handed (LH) Weyl spinor*.

- The conjugate representation

$$\bar{\chi}'_{\dot{\alpha}} = (N_{\dot{\alpha}}{}^{\dot{\beta}})^* \bar{\chi}_{\dot{\beta}}, \quad (1.11)$$

where $\dot{\alpha}, \dot{\beta} = 1, 2$. The conjugate $\bar{\chi}_{\dot{\beta}}$ is referred to as a *right-handed (RH) Weyl spinor*.

- The fundamental and the conjugate representations have respective contravariant representations

$$\psi'^{\alpha} = \psi^{\beta} (N^{-1})_{\beta}^{\alpha}, \quad \bar{\chi}'^{\dot{\alpha}} = \bar{\chi}^{\dot{\beta}} (N^{*-1})_{\dot{\beta}}^{\dot{\alpha}}. \quad (1.12)$$

The contravariant representation is related to the fundamental/conjugate via the $SL(2, \mathbb{C})$ invariant tensor

$$\varepsilon^{\alpha\beta} = \varepsilon^{\dot{\alpha}\dot{\beta}} = \begin{pmatrix} 0 & 1 \\ -1 & 0 \end{pmatrix} = -\varepsilon_{\alpha\beta} = -\varepsilon_{\dot{\alpha}\dot{\beta}}, \quad (1.13)$$

which acts to raise/lower representation indices

$$\psi^{\alpha} = \varepsilon^{\alpha\beta} \psi_{\beta}, \quad \bar{\chi}^{\dot{\alpha}} = \varepsilon^{\dot{\alpha}\dot{\beta}} \bar{\chi}_{\dot{\beta}}. \quad (1.14)$$

similar to the metric tensor $\eta_{\mu\nu}$ acting on 4-vector indices. Note that transformations that involve both $SO_+^{\uparrow}(3, 1)$ and $SL(2, \mathbb{C})$ indices will in general involve the construct

$$(\bar{\sigma}^{\mu})^{\dot{\alpha}\alpha} \equiv \varepsilon^{\alpha\beta} \varepsilon^{\dot{\alpha}\dot{\beta}} (\sigma^{\mu})_{\beta\dot{\beta}} = (\mathbb{1}_2, -\vec{\sigma}). \quad (1.15)$$

Along the same line of thought, one can find a representation for the Lorentz generators by defining the antisymmetric tensors

$$\begin{aligned} (\sigma^{\mu\nu})_{\alpha}^{\beta} &\equiv \frac{i}{4} (\sigma^{\mu} \bar{\sigma}^{\nu} - \sigma^{\nu} \bar{\sigma}^{\mu})_{\alpha}^{\beta}, \\ (\bar{\sigma}^{\mu\nu})_{\dot{\alpha}}^{\dot{\beta}} &\equiv \frac{i}{4} (\bar{\sigma}^{\mu} \sigma^{\nu} - \bar{\sigma}^{\nu} \sigma^{\mu})_{\dot{\alpha}}^{\dot{\beta}}, \end{aligned} \quad (1.16)$$

which can be shown that satisfy the Lorentz algebra

$$[\sigma^{\mu\nu}, \sigma^{\lambda\rho}] = i \left(\eta^{\mu\rho} \sigma^{\nu\lambda} + \eta^{\nu\lambda} \sigma^{\mu\rho} - \eta^{\mu\lambda} \sigma^{\nu\rho} - \eta^{\nu\rho} \sigma^{\mu\lambda} \right). \quad (1.17)$$

Furthermore the $\sigma^{\mu\nu}, \bar{\sigma}^{\mu\nu}$ tensors are self-dual and anti-self dual which in turn halves the components via the identities

$$\sigma^{\mu\nu} = \frac{1}{2i} \varepsilon^{\mu\nu\rho\sigma} \sigma_{\rho\sigma}, \quad \bar{\sigma}^{\mu\nu} = -\frac{1}{2i} \varepsilon^{\mu\nu\rho\sigma} \bar{\sigma}_{\rho\sigma}. \quad (1.18)$$

Therefore we can parametrise a Lorentz transformation as $\Lambda = \exp(-\frac{i}{2} \omega_{\mu\nu} \sigma^{\mu\nu})$, where $\omega_{\mu\nu}$ is the infinitesimal transformation parameter, under which the spinors transform as

$$\begin{aligned} \psi_{\alpha} &\rightarrow \exp\left(-\frac{i}{2} \omega_{\mu\nu} \sigma^{\mu\nu}\right)_{\alpha}^{\beta} \psi_{\beta}, \\ \bar{\chi}^{\dot{\alpha}} &\rightarrow \exp\left(-\frac{i}{2} \omega_{\mu\nu} \bar{\sigma}^{\mu\nu}\right)^{\dot{\alpha}}_{\dot{\beta}} \bar{\chi}^{\dot{\beta}}. \end{aligned} \quad (1.19)$$

1.3 The Standard Model - Introduction

The SM of elementary particle physics is our current best theory that describes the real world. It is formulated along the lines of invariant symmetries present in nature, and more specifically how conserved quantities can be modelled in a Lagrangian formalism via the use of continuous or discrete symmetries. The SM is constructed under the assumptions of Poincaré invariance, along with invariance under an internal gauge symmetry, the form of which is dictated by the Coleman-Mandula theorem [19]. By constructing a theory based on these principles, the SM can accommodate, and accurately describe our experimental observations of nature.

The SM marries together the Glashow-Weinberg-Salam electroweak model [5, 20, 21] with quantum chromodynamics (QCD). In its unbroken phase, it consists of the Poincaré invariant gauge theory with the internal gauge group

$$SU(3)_C \times SU(2)_L \times U(1)_Y \equiv G_{\text{SM}}. \quad (1.20)$$

$SU(3)_C$ is the QCD gauge group, where the C index stands for colour, $SU(2)_L$ is the weak gauge group, where L stands for left denoting weak isospin, and $U(1)_Y$ is the hypercharge group, where Y denotes the namesake's charge. The SM then undergoes electroweak (EW) symmetry breaking which causes the gauge group to break down to

$$SU(3)_C \times SU(2)_L \times U(1)_Y \rightarrow SU(3)_C \times U(1)_{\text{EM}}, \quad (1.21)$$

where $U(1)_{\text{EM}}$ is identified as the electromagnetic (EM) $U(1)$ gauge group. This in turn is referred to as the “broken phase” which we will discuss at length in the following section/s.

The matter content of the SM consists of 3 copies of LH Weyl fields, their RH counterparts obtained via Hermitian conjugation, a complex scalar field known as the Higgs boson, which is responsible for EW symmetry breaking, and the corresponding massless gauge bosons. The fields, number of copies, nomenclature and their representations under the SM gauge group G_{SM} are summarised in Tabs. 1.1, 1.2.

We will build up the SM over the next couple of sections, where we will gradually introduce the various elements, along with explaining electroweak symmetry breaking and how the weak gauge bosons acquire mass.

Field	Copies	Field Name	Spin 0	Spin $\frac{1}{2}$	G_{SM} rep.
q	3 (gens.)	LH quark doublet	-	(u_L, d_L)	$(\mathbf{3}, \mathbf{2}, +\frac{1}{6})$
\bar{u}	3 (gens.)	LH up-type anti-quark	-	\bar{u}_L	$(\bar{\mathbf{3}}, 1, -\frac{2}{3})$
\bar{d}	3 (gens.)	LH down-type anti-quark	-	\bar{d}_L	$(\bar{\mathbf{3}}, 1, +\frac{1}{3})$
ℓ	3 (gens.)	LH lepton doublet	-	(ν_{eL}, e_L)	$(1, \mathbf{2}, -\frac{1}{2})$
\bar{e}	3 (gens.)	LH anti-electron	-	\bar{e}_L	$(1, 1, +1)$
φ	1	complex Higgs doublet	(φ^\pm, φ^0)	-	$(1, \mathbf{2}, -\frac{1}{2})$

Table 1.1: Table summarising the matter fields in the SM, where the columns contain the name of the field, the nomenclature, the notation for the spin 1/2 components, and the charges under the SM gauge group $G_{\text{SM}} = SU(3)_C \times SU(2)_L \times U(1)_Y$. The RH version of the fields is obtained via Hermitian conjugation.

Field	Field Name	Spin 1	G_{SM} rep.
G^a	Gluons	G^a	$(\mathbf{8}, 1, 0)$
W^a	W bosons	W^\pm, W^0	$(1, \mathbf{3}, 0)$
B	B boson	B	$(1, 1, 0)$

Table 1.2: Table summarising the gauge fields in the SM, where the columns contain the name of the field, the nomenclature, the notation for the spin 1 components, and the charges under the SM gauge group $G_{\text{SM}} = SU(3)_C \times SU(2)_L \times U(1)_Y$.

1.4 The Standard Model - Gauge and Higgs Sector

In the following section we will review the electroweak component of the SM denoted by the gauge group product $SU(2)_L \times U(1)_Y$. This will be followed by explaining EW symmetry breaking via the introduction of a $(\mathbf{2}, +1) \sim SU(2)_L \times U(1)_Y$ complex scalar field. This is the aforementioned Higgs field, and it acquires a vacuum expectation value (VEV) that causes the spontaneous breaking $SU(2)_L \times U(1)_Y \rightarrow U(1)_{\text{EM}}$.

First off, we have the covariant derivative that acts on the i th component ($i = 1, 2$) of Higgs field $SU(2)_L$ doublet φ_i as

$$(D_\mu \varphi)_i = \partial_\mu \varphi_i - i [g_2 W_\mu^a T^a + g_1 B_\mu Y]_i^j \varphi_j, \quad (1.22)$$

where T^a are the $SU(2)_L$ generators, Y is the hypercharge generator, W_μ^a are the

$SU(2)_L$ gauge fields, B_μ is the hypercharge field, and g_2, g_1 are the $SU(2)_L, U(1)_Y$ gauge couplings. The i, j indices refer to the representation indices for the gauge group generators, where $T^a = \frac{1}{2}\sigma^a, Y = -\frac{1}{2}\mathbb{1}_2$. Therefore the explicit form of the gauge components is

$$g_2 W_\mu^a T^a + g_1 B_\mu Y = \frac{1}{2} \begin{pmatrix} g_2 W_\mu^3 - g_1 B_\mu & g_2(W_\mu^1 - iW_\mu^2) \\ g_2(W_\mu^1 + iW_\mu^2) & -g_2 W_\mu^3 - g_1 B_\mu \end{pmatrix}. \quad (1.23)$$

In the SM, the Higgs potential $V(\varphi)$ consists of a quadratic, and a quartic interaction which are chosen such that the Higgs field acquires a non-zero VEV. The form of the Higgs potential is

$$V(\varphi) = \frac{1}{4}\lambda \left(\varphi^\dagger \varphi - \frac{1}{2}\nu^2 \right)^2, \quad (1.24)$$

where λ is the quartic coupling, and ν is the Higgs field VEV. Note that the $\sim \lambda\nu^4$ term is a constant and doesn't affect the equations of motion. This form of the potential ensures a non-zero VEV, which in turn triggers EW symmetry breaking. According to the breaking chain $SU(2)_L \times U(1)_Y \rightarrow U(1)_{\text{EM}}$, only one of the gauge fields remains massless (corresponding to the unbroken $U(1)$ symmetry), whilst the others acquire a tree level mass dictated by the Higgs VEV.

Using the gauge freedom associated with $SU(2)_L$, we can perform a global gauge transformation to bring the VEV entirely into the 1st component. Similarly, using the $U(1)_Y$ invariance we can further make it purely real, such that

$$\langle 0 | \varphi(x) | 0 \rangle = \frac{1}{\sqrt{2}} \begin{pmatrix} \nu \\ 0 \end{pmatrix}. \quad (1.25)$$

Under this choice we can parametrise the Higgs field as

$$\varphi(x) = \begin{pmatrix} \nu + \varphi_1 \\ \varphi_2 \end{pmatrix} = \frac{1}{\sqrt{2}} \begin{pmatrix} ((\nu + H(x)) \exp(-i\chi_1(x)/\nu)) \\ \chi_2(x) \exp(-i\chi_3(x)/\nu) \end{pmatrix}, \quad (1.26)$$

where $\chi_i, i = 1, 2, 3$ are the real scalar components absorbed by the newly massive gauge bosons that provide their longitudinal modes, and $H(x)$ is the remaining real propagating scalar degree of freedom. Under the choice of the unitary gauge $\chi_i(x) = 0$, Eqn. (1.26) becomes

$$\varphi(x) = \begin{pmatrix} \nu + H(x) \\ 0 \end{pmatrix}. \quad (1.27)$$

To this extent, the kinetic term $-(D_\mu\varphi)^\dagger D_\mu\varphi$ makes the connection between the covariant derivative and the VEV, giving a mass basis for the gauge matrix in Eqn. (1.23), which is expressed as

$$-\frac{1}{8}\begin{pmatrix}\nu^2 & 0\end{pmatrix}\begin{pmatrix}g_2W_\mu^3 - g_1B_\mu & g_2(W_\mu^1 - iW_\mu^2) \\ g_2(W_\mu^1 + iW_\mu^2) & -g_2W_\mu^3 - g_1B_\mu\end{pmatrix}^2\begin{pmatrix}\nu^2 \\ 0\end{pmatrix}. \quad (1.28)$$

By diagonalising the above, we obtain the mass eigenstates for the fields. This can be done analytically by defining the weak mixing angle (also known as the Weinberg angle)

$$\theta_W \equiv \text{atan}\left(\frac{g_1}{g_2}\right), \quad (1.29)$$

and by defining the mass eigenstate fields

$$W^\pm \equiv \frac{1}{2}(W_\mu^1 \mp iW_\mu^2), \quad Z_\mu \equiv \cos\theta_W W_\mu^3 - \sin\theta_W B_\mu, \quad A_\mu \equiv \sin\theta_W W_\mu^3 + \cos\theta_W B_\mu. \quad (1.30)$$

Putting this all together gives us the mass eigenstate form of the gauge boson Lagrangian

$$\begin{aligned} \mathcal{L} &= -\frac{1}{8}g_2^2\nu^2\begin{pmatrix}1 & 0\end{pmatrix}\begin{pmatrix}\frac{1}{\cos\theta_W}Z_\mu & \sqrt{2}W_\mu^+ \\ \sqrt{2}W_\mu^+ & \dots\end{pmatrix}^2\begin{pmatrix}1 \\ 0\end{pmatrix} \\ &= -M_W^2 W^{+\mu}W_\mu^- - \frac{1}{2}M_Z^2 Z^\mu Z_\mu, \end{aligned} \quad (1.31)$$

where $M_W = g_2\nu/2$ and $M_Z = M_W/\cos\theta_W$ are the identified W^\pm boson and Z^0 boson masses. The observed masses of the W^\pm, Z^0 therefore set the electroweak breaking scale. The most recent experimental measurements of these are $M_{W^\pm} = 80.4$ GeV and $M_{Z^0} = 91.4$ GeV [22]. This in turn sets the Weinberg angle at the EW scale as $\sin^2\theta_W = 0.223$. Note that if we introduce a renormalisation scheme, e.g. $\overline{\text{MS}}$, the loop corrected gauge couplings become dependent on the renormalisation scale μ . In $\overline{\text{MS}}$, at $\mu = M_Z$, the Weinberg angle is $\sin^2\theta_W = 0.2312$ [22], and the VEV takes the value $\nu = 246$ GeV.

We note that the mass matrix does not involve any mass terms for the newly defined A_μ field, since it is the gauge field that transforms under the remaining unbroken $U(1)_{\text{EM}}$ symmetry, which is identified as the EM gauge group.

Coming back to the Higgs field post EW symmetry breaking, we can write out the potential in Eqn. (1.24) in terms of the remaining scalar degree of freedom $H(x)$, which gives us

$$V(\varphi) = \frac{1}{4}\lambda\nu^2 H^2 + \frac{1}{4}\lambda\nu H^3 + \frac{1}{16}\lambda H^4. \quad (1.32)$$

By reading off the H^2 term's coefficient we get the mass term for the Higgs field $m^2 = \frac{1}{2}\lambda\nu^2$. The most recent measured experimental value for the mass of the Higgs boson is $m_H = 125.9$ GeV [22]. The kinetic term for the Higgs field remains unchanged, with $\varphi \rightarrow H$, and its couplings to the W^\pm, Z^0 become

$$\mathcal{L} = -\frac{1}{2}\partial^\mu H \partial_\mu H - \left(M_W^2 W^{+\mu} W_\mu^- + \frac{1}{2} M_Z^2 Z^\mu Z_\mu \right) (1 + \nu^{-1} H)^2. \quad (1.33)$$

Before symmetry breaking, the gauge fields have their kinetic terms dictated by the usual field strength tensors for a non-abelian/abelian gauge field

$$\mathcal{L} = -\frac{1}{4} W^{a\mu\nu} W_{\mu\nu}^a - \frac{1}{4} B^{\mu\nu} B_{\mu\nu}, \quad (1.34)$$

where $B_{\mu\nu} = \partial_\mu B_\nu - \partial_\nu B_\mu$ and $W_{\mu\nu}^a = \partial_\mu W_\nu^a - \partial_\nu W_\mu^a + ig_2 f^{abc} W_\mu^b W_\nu^c$. Post EW-symmetry breaking, in our W^\pm, Z^0 basis, the gauge kinetic terms are now expressed as

$$\begin{aligned} \mathcal{L} = & -\frac{1}{4} F^{\mu\nu} F_{\mu\nu} - \frac{1}{4} Z^{\mu\nu} Z_{\mu\nu} - D^\dagger{}^\mu W^{-\nu} D_\mu W_\nu^+ + D^\dagger{}^\mu W^{-\nu} D_\nu W_\mu^+ \\ & + ie (F^{\mu\nu} + \cot \theta_W Z^{\mu\nu}) W_\mu^+ W_\nu^- \\ & - \frac{1}{2} \left(\frac{e^2}{\sin^2 \theta_W} \right) (W^{+\mu} W_\mu^- W^{+\nu} W_\nu^- - W^{+\mu} W_\mu^+ W^{-\nu} W_\nu^-). \end{aligned} \quad (1.35)$$

where we have defined the EM coupling constant

$$e = g_2 \sin \theta_W = \frac{g_1 g_2}{\sqrt{g_1^2 + g_2^2}}, \quad (1.36)$$

the field strength tensors $F^{\mu\nu} = \partial_\mu A_\nu - \partial_\nu A_\mu$, $Z^{\mu\nu} = \partial_\mu Z_\nu - \partial_\nu Z_\mu$, and $D_\mu = \partial_\mu - ie (A_\mu + \cot \theta_W Z_\mu)$.

Note that by assigning EM charge $Q = +1$ to the W_μ^+ field the post-symmetry breaking Lagrangians exhibit manifest EM invariance. Similarly we note that the choice of the unitary gauge for the Higgs field hides the underlying $SU(2)_L \times U(1)_Y$ gauge invariance.

Lastly, the QCD gauge sector consists of the traditional terms associated with a non-abelian gauge theory, where the gauge group is $SU(3)$. QCD remains unbroken post EW symmetry breaking. The Lagrangian for the gauge sector consists of the invariant construct formed by the gluon strength tensor $G_{\mu\nu}$,

$$\mathcal{L} = -\frac{1}{2} \text{Tr} (G_{\mu\nu} G^{\mu\nu}) = -\frac{1}{4} G_{\mu\nu}^a G^{a\mu\nu}, \quad (1.37)$$

where $G_{\mu\nu} = G_{\mu\nu}^a T^a$, and T^a are the generators of $SU(3)$. The gluon field strength tensor components are defined as

$$G_{\mu\nu}^a = \partial_\mu G_\nu^a - \partial_\nu G_\mu^a + g f^{bca} G_\mu^b G_\nu^c, \quad (1.38)$$

where G_μ^a are the gluon gauge fields that transform as the adjoint **8** representation under $SU(3)_C$, and f^{abc} are the totally antisymmetric $SU(3)$ structure constants defined by the generator commutation relationships

$$[T^a, T^b] = if^{abc}T^c. \quad (1.39)$$

Lastly we note that in order to have a consistent quantisation of non-abelian gauge theories, we require gauge fixing. This is done by introducing two complex Grassman-valued scalar fields c, \bar{c} which are referred to as ghosts and have the Lagrangian

$$\mathcal{L}_{\text{Ghost}} = \partial^\mu \bar{c}^a D_\mu^{ac} c^c = \partial^\mu \bar{c}^a \left(\delta^{ac} \partial_\mu + g f^{abc} A_\mu^b \right) c^c. \quad (1.40)$$

The ghost fields do not represent physical states, but rather act as a tool, removing unphysical degrees of freedom from virtual gauge bosons.

1.5 The Standard Model - Lepton Sector

Leptons are spin 1/2 particles that transform as singlets under the $SU(3)_C$ QCD gauge group. There are 6 types (flavours) of leptons, which are grouped into three families/generations. Namely these are the electron and the electron neutrino \bar{e}, ν_e , the muon and the muon neutrino $\bar{\mu}, \nu_\mu$ and the tau and tau neutrino $\bar{\tau}, \nu_\tau$. The SM treats them as 3 copies of the same G_{SM} representation.

A lepton family is described by the corresponding electron and neutrino. Referring back to Tab. 1.1, we now introduce two LH Weyl fields ℓ, \bar{e} in the representations $\ell \sim (\mathbf{2}, -\frac{1}{2})$ and $\bar{e} \sim (1, +1)$ of $SU(2)_L \times U(1)_Y$. Note that the bar is part of the nomenclature of the field, and does not denote any type of conjugation.

The covariant derivative acts on the fields as

$$(D_\mu \ell)_i = \partial_\mu \ell_i - ig_2 W_\mu^a (T^a)_i^j \ell_j - ig_1 \left(-\frac{1}{2} \right) B_\mu \ell_i, \quad (1.41)$$

$$D_\mu \bar{e} = \partial_\mu \bar{e} - ig_1 (+1) B_\mu \bar{e}, \quad (1.42)$$

where $i = 1, 2$ is a $SU(2)$ index. This in turn gives us the kinetic terms in the Lagrangian

$$\mathcal{L} = i \ell^\dagger \bar{\sigma}^\mu (D_\mu \ell)_i + i \bar{e}^\dagger \bar{\sigma}^\mu D_\mu \bar{e}. \quad (1.43)$$

We note that, with the available fields, we cannot write down any gauge-invariant mass terms for the doublet or singlet, since none of the product representation combinations

$$(\mathbf{2}, -\frac{1}{2}) \otimes (\mathbf{2}, -\frac{1}{2}), \quad (\mathbf{2}, -\frac{1}{2}) \otimes (1, +1), \quad (1, +1) \otimes (1, +1), \quad (1.44)$$

provide us with a gauge singlet in their deconstructed form whilst maintaining a chiral theory. Fortunately, we can couple the Higgs to the lepton fields, and more specifically use its VEV to impart masses by writing down a Yukawa coupling of the form

$$\mathcal{L} = -y\varepsilon^{ij}\varphi_i\ell_j\bar{e} + \text{h.c.} , \quad (1.45)$$

where y is the Yukawa coupling constant. We note that the above construction is gauge invariant since the product contains a singlet representation $(\mathbf{2}, -\frac{1}{2}) \otimes (\mathbf{2}, -\frac{1}{2}) \otimes (1, +1) = (1, 0) \oplus (\mathbf{3}, 0)$. We also note that this term is unique within the context of a gauge invariant renormalisable theory.

Going to the unitary gauge, in which $\varphi_1 \rightarrow (\nu + H)/\sqrt{2}$, $\varphi_2 \rightarrow 0$, and denoting the $SU(2)$ components of ℓ as $\ell = \begin{pmatrix} \nu_e \\ e \end{pmatrix}$, our Lagrangian now becomes

$$\begin{aligned} \mathcal{L} &= -\frac{1}{\sqrt{2}}y(\nu + H)(e\bar{e} + \bar{e}^\dagger e^\dagger). \\ &\equiv -\frac{1}{\sqrt{2}}y(\nu + H)\bar{\mathcal{E}}\mathcal{E}. \end{aligned} \quad (1.46)$$

Note that we rely on context to distinguish the field e from the EM coupling constant e . In the last line of the above, we have introduced a Dirac field definition for our electron, post symmetry breaking, namely

$$\mathcal{E} \equiv \begin{pmatrix} e \\ \bar{e}^\dagger \end{pmatrix}. \quad (1.47)$$

We also note that the electron acquires a mass dictated by the VEV and Yukawa coupling of $m_e = y\nu/\sqrt{2}$. Reading the mass terms in the Lagrangian, we can see that the neutrino has remained massless, which can now be described by a Majorana field

$$\mathcal{N} \equiv \begin{pmatrix} \nu_e \\ \nu_e^\dagger \end{pmatrix}. \quad (1.48)$$

The above is also used in conjuncture with the LH projection operator $P_L = \frac{1}{2}(1 - \gamma_5)$, which acting on \mathcal{N} gives $\mathcal{N}_L \equiv P_L\mathcal{N} = \begin{pmatrix} \nu_e \\ 0 \end{pmatrix}$ in the 4-component notation. With this in mind, we can now move on to the form of the covariant derivative and look at the EM generator and what charges the fields possess under the unbroken $U(1)_{\text{EM}}$. More specifically we look at the terms that are responsible

for the construction of A_μ , namely

$$\begin{aligned} g_2 W_\mu^3 T^3 + g_1 B_\mu Y &= \frac{e}{\sin \theta_W} (\sin \theta_W A_\mu + \cos \theta_W Z_\mu) T^3 \\ &\quad + \frac{e}{\cos \theta_W} (\cos \theta_W A_\mu - \sin \theta_W Z_\mu) Y \\ &= e(T^3 + Y)A_\mu + e(\cot \theta_W T^3 - \tan \theta_W Y)Z_\mu. \end{aligned} \quad (1.49)$$

Recalling that A_μ is identified as the field corresponding to the surviving $U(1)_{\text{EM}}$ symmetry, with $e > 0$ as the EM coupling constant, we identify the electric charge generator Q as

$$Q = T^3 + Y. \quad (1.50)$$

Working within the representations $T^3 = \frac{1}{2}\sigma^3$, $Y = -\frac{1}{2}\mathbb{1}_2$, the LH Weyl fields ν_e, e, \bar{e} have the corresponding charges

$$\begin{aligned} T^3 \nu_e &= +\frac{1}{2}\nu_e, & T^3 e &= -\frac{1}{2}e, & T^3 \bar{e} &= 0, \\ Y \nu_e &= -\frac{1}{2}\nu_e, & Y e &= -\frac{1}{2}e, & Y \bar{e} &= +\bar{e}. \end{aligned} \quad (1.51)$$

Post-symmetry breaking, the fields have their EM charges as multiples of e dictated by the action of the charge generator in Eqn. (1.50) as

$$Q \nu_e = 0, \quad Q e = -e, \quad Q \bar{e} = +\bar{e}. \quad (1.52)$$

Therefore we have recovered what we expected the charges to be for the neutrino and electron, i.e. a neutral particle and a charged particle with charge e . Moving on, in terms of the covariant derivative component action on the 4-component Dirac fields $\mathcal{E}, \mathcal{N}_L$, this can now be expressed as

$$(g_2 W_\mu^3 T^3 + g_1 B_\mu Y) \mathcal{E} = \left[-e A_\mu + \frac{e}{\sin \theta_W \cos \theta_W} \left(-\frac{1}{2} P_L + \sin^2 \theta_W \right) Z_\mu \right] \mathcal{E}, \quad (1.53)$$

$$(g_2 W_\mu^3 T^3 + g_1 B_\mu Y) \mathcal{N}_L = \frac{e}{\sin \theta_W \cos \theta_W} \left(+\frac{1}{2} \right) Z_\mu \mathcal{N}_L. \quad (1.54)$$

Furthermore, we can look at the conserved currents in the broken phase of the SM. Writing down the mass basis definition

$$g_2 W_\mu^1 T^1 + g_2 W_\mu^2 T^2 = \frac{g_2}{\sqrt{2}} \begin{pmatrix} 0 & W_\mu^+ \\ W_\mu^- & 0 \end{pmatrix}, \quad (1.55)$$

which taken along with the Dirac field definitions and the EM invariant, provides us with the gauge field couplings to the lepton currents

$$\mathcal{L} = \frac{1}{\sqrt{2}} g_2 W_\mu^+ J^{-\mu} + \frac{1}{\sqrt{2}} g_2 W_\mu^- J^{+\mu} + \frac{e}{\sin \theta_W \cos \theta_W} Z_\mu J_Z^\mu + e A_\mu J_{\text{EM}}^\mu. \quad (1.56)$$

In the above we have defined the leptonic currents as

$$\begin{aligned} J^{+\mu} &\equiv \bar{\mathcal{E}}_L \gamma^\mu \mathcal{N}_L, & J^{-\mu} &\equiv \bar{\mathcal{N}}_L \gamma^\mu \mathcal{E}_L, & J_Z^\mu &\equiv J_3^\mu - \sin^2 \theta_W J_{\text{EM}}^\mu, \\ J_3^\mu &\equiv \frac{1}{2} \bar{\mathcal{N}}_L \gamma^\mu \mathcal{N}_L - \frac{1}{2} \bar{\mathcal{E}}_L \gamma^\mu \mathcal{E}_L, & J_{\text{EM}}^\mu &\equiv -\bar{\mathcal{E}} \gamma^\mu \mathcal{E}. \end{aligned} \quad (1.57)$$

Similarly, we can extend our construct to include interactions of multiple generations by promoting the fields and the respective Yukawa terms with a generational index $I = 1, 2, 3$. The kinetic term for the fields now reads

$$\mathcal{L} = i \ell_I^\dagger \bar{\sigma}^{\mu\nu} (D_\nu)_i^j \ell_{jI} + i \bar{e}_I^\dagger \bar{\sigma}^{\mu\nu} (D_\nu)_i^j \bar{e}_{jI}. \quad (1.58)$$

Similarly, the Yukawa terms now become

$$\mathcal{L} = -\varepsilon^{ij} \varphi_i \ell_{jI} y^{IJ} \bar{e}_J + \text{h.c.} , \quad (1.59)$$

where y^{IJ} is a complex 3×3 matrix in flavour space, and we sum over the repeated flavour indices. Note that we can perform independent unitary transformations on ℓ, \bar{e} as $\ell_I \rightarrow L_{IJ} \ell_J$ and $\bar{e}_I \rightarrow \bar{E}_{IJ} \bar{e}_J$, which can be chosen such that we diagonalise the Yukawa matrix $L^T y \bar{E}$, along with making the components purely real. In turn this leaves us with the real diagonal form of the Yukawa y_I which gives the different masses for the 3 generations of leptons.

The most recent experimental masses for the leptons are $m_e = 0.51$ MeV, $m_\mu = 105.65$ MeV, $m_\tau = 1.77$ GeV [22]. We also note, experimentally neutrinos have small masses of the order $\mathcal{O}(\text{eV})$. The SM can be modified to accommodate small neutrino masses, by introducing a Majorana neutrino which provides the basis for the seesaw mechanism. This in turn introduces mixing between the neutrino families via the PMNS matrix [23, 24].

1.6 The Standard Model - Quark Sector

Lastly, we have the quarks, which are spin 1/2 particles that transform as triplets $\mathbf{3}, \bar{\mathbf{3}}$ under the $SU(3)_C$ QCD gauge group. There are 6 different types of quarks (flavours), which come as 3 copies of the same fields, grouped into 3 generations. These are the up and down quarks u, d , the charm and strange quarks c, s , and the top and bottom quarks t, b .

Similar to what we have done in the leptonic section, we will look at only one generation of quarks and then extend our discussion to encompass the entire flavour

sector. In line with Tab. 1.1, we introduce the LH spinor Weyl fields q, \bar{u}, \bar{d} which transform under the SM gauge group as

$$q \sim (\mathbf{3}, \mathbf{2}, +\frac{1}{6}), \quad \bar{u} \sim (\bar{\mathbf{3}}, 1, -\frac{2}{3}), \quad \bar{d} \sim (\bar{\mathbf{3}}, 1, +\frac{1}{3}). \quad (1.60)$$

Similar to the leptons, the \bar{u}, \bar{d} bars are part of the nomenclature of the field and do not denote any type of conjugation. The covariant derivatives acting on the fields are then expressed as

$$(D_\mu q)_{\alpha i} = \partial_\mu q_{\alpha i} - ig_3 G_\mu^a (T_{\mathbf{3}}^a)_\alpha{}^\beta q_{\beta i} - ig_2 W_\mu^a (T_{\mathbf{2}}^a)_i{}^j q_{\beta j} - ig_1 \left(+\frac{1}{6} \right) B_\mu q_{\alpha i}, \quad (1.61)$$

$$(D_\mu \bar{u})^\alpha = \partial_\mu \bar{u}^\alpha - ig_3 G_\mu^a (T_{\bar{\mathbf{3}}}^a)^\alpha{}_\beta \bar{u}^\beta - ig_1 \left(-\frac{2}{3} \right) B_\mu \bar{u}^\alpha, \quad (1.62)$$

$$(D_\mu \bar{d})^\alpha = \partial_\mu \bar{d}^\alpha - ig_3 G_\mu^a (T_{\bar{\mathbf{3}}}^a)^\alpha{}_\beta \bar{d}^\beta - ig_1 \left(+\frac{1}{3} \right) B_\mu \bar{d}^\alpha, \quad (1.63)$$

where $T_{\mathbf{3}}^a, T_{\bar{\mathbf{3}}}^a$ are the $SU(3)_C$ generators in the $\mathbf{3}, \bar{\mathbf{3}}$ representations, $T_{\mathbf{2}}^a$ are the $SU(2)$ generators in the doublet representation, i, j are $SU(2)$ indices, and α, β are $SU(3)$ indices. With this in mind, the kinetic terms for the q, \bar{u}, \bar{d} fields consist of

$$\mathcal{L} = iq^{\dagger \alpha i} \bar{\sigma}^\mu (D_\mu q)_{\alpha i} + i\bar{u}_\alpha^\dagger \bar{\sigma}^\mu (D_\mu \bar{u})^\alpha + i\bar{d}_\alpha^\dagger \bar{\sigma}^\mu (D_\mu \bar{d})^\alpha. \quad (1.64)$$

Again, we note, that we cannot write a gauge invariant mass term that involves the 3 quark fields since their various products do not contain any singlets. Fortunately, the Higgs field $\varphi \sim (1, \mathbf{2}, -\frac{1}{2})$ comes to the rescue, since it, and its complex conjugate $\varphi^\dagger \sim (1, \mathbf{2}, +\frac{1}{2})$, can be used to build Yukawa couplings which contain gauge singlets as part of their decomposition

$$(1, \mathbf{2}, -\frac{1}{2}) \otimes (\mathbf{3}, \mathbf{2}, +\frac{1}{6}) \otimes (\bar{\mathbf{3}}, 1, +\frac{1}{3}) = (1, 1, 0) \oplus \dots, \quad (1.65)$$

$$(1, \mathbf{2}, +\frac{1}{2}) \otimes (\mathbf{3}, \mathbf{2}, +\frac{1}{6}) \otimes (\bar{\mathbf{3}}, 1, -\frac{2}{3}) = (1, 1, 0) \oplus \dots \quad (1.66)$$

Therefore we introduce the following Yukawa mass terms

$$\mathcal{L} = -y' \varepsilon^{ij} \varphi_i q_{\alpha j} \bar{d}^\alpha - y'' \varphi^{\dagger i} q_{\alpha i} \bar{u}^\alpha + \text{h.c.}, \quad (1.67)$$

where y', y'' are the Yukawa coupling constants. We note that these are the only possible terms whilst keeping the Lagrangian renormalisable.

We now want to look at the broken phase of the SM. Therefore we switch to the unitary gauge, where the Higgs field transforms as $\varphi_1 \rightarrow \frac{1}{\sqrt{2}}(\nu + H)$, $\varphi_2 \rightarrow 0$ and the real scalar Higgs is denoted by H . Furthermore, by assigning notations to the

components of the $SU(2)$ quark doublet as $q = \begin{pmatrix} u \\ d \end{pmatrix}$, the Lagrangian in Eqn. (1.67) becomes

$$\begin{aligned}\mathcal{L} &= -\frac{1}{\sqrt{2}}y'(\nu + H) \left(d_\alpha \bar{d}^\alpha + \bar{d}_\alpha^\dagger d^{\dagger\alpha} \right) - \frac{1}{\sqrt{2}}y''(\nu + H) \left(u_\alpha \bar{u}^\alpha + \bar{u}_\alpha^\dagger u^{\dagger\alpha} \right) \\ &= -\frac{1}{\sqrt{2}}y'(\nu + H) \bar{\mathcal{D}}^\alpha \mathcal{D}_\alpha - \frac{1}{\sqrt{2}}y''(\nu + H) \bar{\mathcal{U}}^\alpha \mathcal{U}_\alpha.\end{aligned}\quad (1.68)$$

In the above we have introduced the Dirac fields for the up and down quark fields

$$\mathcal{D}_\alpha \equiv \begin{pmatrix} d_\alpha \\ \bar{d}_\alpha^\dagger \end{pmatrix}, \quad \mathcal{U}_\alpha \equiv \begin{pmatrix} u_\alpha \\ \bar{u}_\alpha^\dagger \end{pmatrix}, \quad (1.69)$$

which post EW symmetry breaking acquire masses dictated by the Higgs VEV and the Yukawa couplings

$$m_d = \frac{y'\nu}{\sqrt{2}}, \quad m_u = \frac{y''\nu}{\sqrt{2}}. \quad (1.70)$$

Looking now at the charge generator $Q = T_3 + Y$, one finds that the u, \bar{u}, d, \bar{d} fields have the EM charges

$$Qu = \left(+\frac{2}{3} \right) u, \quad Qd = \left(-\frac{1}{3} \right) d, \quad Q\bar{u} = \left(-\frac{2}{3} \right) \bar{u}, \quad Q\bar{d} = \left(+\frac{1}{3} \right) \bar{d}. \quad (1.71)$$

Similarly, we have recovered what we expected in terms of the quarks and their charges. Analogous to the lepton sector, we can express the covariant derivative action in terms of the 4-component fields as

$$(g_2 W_\mu^3 T^3 + g_1 B_\mu Y) \mathcal{U} = \left[+\frac{2}{3} e A_\mu + \frac{e}{\sin \theta_W \cos \theta_W} \left(\frac{1}{2} P_L - \frac{2}{3} \sin^2 \theta_W \right) Z_\mu \right] \mathcal{U}, \quad (1.72)$$

$$(g_2 W_\mu^3 T^3 + g_1 B_\mu Y) \mathcal{D} = \left[-\frac{1}{3} e A_\mu + \frac{e}{\sin \theta_W \cos \theta_W} \left(-\frac{1}{2} P_L + \frac{1}{3} \sin^2 \theta_W \right) Z_\mu \right] \mathcal{D}. \quad (1.73)$$

Using the above, along with the explicit form of the covariant derivative from Eqn. (1.55), the kinetic terms in Eqn. (1.64) are recast in terms of the SM quark currents as

$$\mathcal{L} = \frac{1}{\sqrt{2}} g_2 W_\mu^+ J^{-\mu} + \frac{1}{\sqrt{2}} g_2 W_\mu^- J^{+\mu} + \frac{e}{\sin \theta_W \cos \theta_W} Z_\mu J_Z^\mu + e A_\mu J_{\text{EM}}^\mu. \quad (1.74)$$

In the above we have defined the SM charged quark currents as

$$\begin{aligned}J^{+\mu} &\equiv \bar{\mathcal{D}}_L \gamma^\mu \mathcal{U}_L, & J^{-\mu} &\equiv \bar{\mathcal{U}}_L \gamma^\mu \mathcal{D}_L, & J_Z^\mu &\equiv J_3^\mu - \sin^2 \theta_W J_{\text{EM}}^\mu, \\ J_3^\mu &\equiv \frac{1}{2} \bar{\mathcal{U}}_L \gamma^\mu \mathcal{U}_L - \frac{1}{2} \bar{\mathcal{D}}_L \gamma^\mu \mathcal{D}_L, & J_{\text{EM}}^\mu &\equiv +\frac{2}{3} \bar{\mathcal{U}} \gamma^\mu \mathcal{U} - \frac{1}{3} \bar{\mathcal{D}} \gamma^\mu \mathcal{D}.\end{aligned}\quad (1.75)$$

where the L subscript indicates the inclusion of the LH projection operator P_L .

After having established the action for a single quark generation, we can now incorporate the full flavour structure of the theory by promoting the fields with a generational index $q_{\alpha i I}, \bar{u}_I^\alpha, \bar{d}_I^\alpha$ where $I = 1, 2, 3$. The kinetic term for the quark fields now reads

$$\mathcal{L} = iq^{\dagger\alpha i I} \bar{\sigma}^\mu (D_\mu)_{\alpha i}^{\beta j} q_{\beta j I} + i\bar{u}_{\alpha I}^\dagger \bar{\sigma}^\mu (D_\mu)_{\beta}^{\alpha} \bar{u}_I^\beta + i\bar{d}_{\alpha I}^\dagger \bar{\sigma}^\mu (D_\mu)_{\beta}^{\alpha} \bar{d}_I^\beta, \quad (1.76)$$

where the summation over the repeated generational index is implied. Similarly the Yukawa terms now become

$$\mathcal{L} = -y'_{IJ} \varepsilon^{ij} \varphi_i q_{\alpha j I} \bar{d}_J^\alpha - y''_{IJ} \varphi^\dagger_i q_{\alpha i I} \bar{u}_J^\alpha + \text{h.c.}, \quad (1.77)$$

where y'_{IJ}, y''_{IJ} are complex 3×3 matrices in flavour space. Analogous to the leptonic case, we can perform independent unitary transformations on the fields $d_I \rightarrow D_{IJ} d_J, \bar{d}_I \rightarrow \bar{D}_{IJ} \bar{d}_J, u_I \rightarrow U_{IJ} u_J, \bar{u}_I \rightarrow \bar{U}_{IJ} \bar{u}_J$, which can be chosen such that they diagonalise and rotate out the complex eigenvalue phases of the Yukawa matrices via the constructs $D^T y' \bar{D}, U^T y'' \bar{U}$.

Within this framework, the generations of quarks acquire masses dictated by the Higgs VEV and the real Yukawa eigenvalues $m_{d_I} = y'_I \nu \sqrt{2}, m_{u_I} = y''_I \nu \sqrt{2}$. In contrast to the leptonic case, we have an additional complication arising in the kinetic term, which picks up a unitary matrix V via the charged currents

$$J^{+\mu} = \bar{\mathcal{D}}_{LI} \left(V^\dagger \right)_{IJ} \gamma^\mu \bar{\mathcal{U}}_{LJ}, \quad J^{-\mu} = \bar{\mathcal{U}}_{LI} V_{IJ} \gamma^\mu \mathcal{D}_{LK}, \quad (1.78)$$

$V \equiv U^\dagger D$ is the Cabbibo-Kobayashi-Maskawa (CKM) matrix [25, 26] and it arises in the quark case, since now we are dealing with two Yukawa terms in the Lagrangian. By performing additional independent phase rotations, the CKM matrix can be brought into a form where the first row and column become real, eliminating 5 of the 9 complex parameters. The remaining 4 consist of $\theta_1, \theta_2, \theta_3, \delta$ where they appear in the CKM matrix as

$$V = \begin{pmatrix} c_1 & c_1 c_3 & c_1 c_3 \\ -c_1 c_2 & c_1 c_2 c_3 - c_2 c_3 e^{i\delta} & c_1 c_2 c_3 + c_2 c_3 e^{i\delta} \\ -c_1 c_2 & c_1 c_2 c_3 + c_2 c_3 e^{i\delta} & c_1 c_2 c_3 - c_2 c_3 e^{i\delta} \end{pmatrix}, \quad (1.79)$$

and we have defined the shorthand $\cos \theta_i = c_i$ and $\sin \theta_i = s_i$. The experimentally measured values of the angles are $\sin \theta_1 = 0.224, \sin \theta_2 = 0.041, \sin \theta_3 = 0.016$, $\delta = 40^\circ$ [22], where θ_1 is known as the Cabibbo angle and δ is often referred to as the CP violating phase.

1.7 Shortcomings of the SM

We now come back to the questions that we left open at the start of the chapter. In particular, we look at the Hierarchy problem and the related “naturalness” problem. The naturalness problem, can be stated as “why is there such a large mass gap between the Planck scale and the electroweak scale?”. This manifests itself explicitly in the SM via the radiative corrections received by the Higgs field, which in turn constitutes the source of the technical Hierarchy problem. More specifically, the dominant one loop corrections to the Higgs propagator come from top quarks t via the Feynman diagram in Eqn. (1.80).

$$\begin{array}{c}
 H \text{---} \times \text{---} H \\
 + \quad \text{---} H \text{---} \bigcirc \text{---} H \\
 \quad \quad \quad \begin{array}{c} \uparrow t \\ \downarrow \bar{t} \end{array}
 \end{array} \quad (1.80)$$

If we consider the cut-off scale $\Lambda_P \sim 10^{18}\text{GeV}$ at which the SM is no longer valid due to quantum gravitational effects coming into play, along with a momentum cutoff regularisation scheme, the one loop Feynman contribution in Eqn. (1.80), amounts to a radiatively corrected Higgs mass

$$m_{\text{Higgs}}^2 = \mu^2 - \frac{y_t}{8\pi^2} \Lambda_P^2. \quad (1.81)$$

This is the manifestation of the hierarchy problem. More specifically, why is there such a large discrepancy between the EW scale associated with the Higgs mass $m_{\text{Higgs}} \sim 10^2\text{GeV}$, and the Planck scale $\Lambda_P \sim 10^{18}\text{GeV}$. In particular, we now have to deal with a fine tuning problem as a direct consequence. In order to get the right Higgs mass of $m_{\text{Higgs}} \sim 125\text{GeV}$, we have to fine tune the mass parameter μ in Eqn. (1.81) to a precision of 36 digits. This fine tuning is in no way naturally compelling. This in turn hints at the idea that there is more physics beyond the SM.

Similarly there are questions regarding the structure of the SM itself, such as why did the universe choose the particular quark and lepton multiplet structure, why do quarks and leptons have their specific charges, and why are forces just partially unified? In addition one asks what is the origin of the 28 free parameters in the SM?

Some of these problems can be addressed within the context of Grand Unified Theories (GUTs). The main idea is that the SM gauge group is not the most

fundamental one, but is part of a larger gauge group which unifies all three forces. The following section will focus on explaining the hurdles related with implementing a grand unified theory, the need of an additional mechanism to overcome these hurdles and a brief mention on an attempt at incorporating conformal symmetry as said mechanism.

1.8 Grand Unification, and Hierarchies

1.8.1 The Gildener Problem

Grand Unified Theories are founded on the idea that the SM gauge group $G_{\text{SM}} = SU(3)_C \times SU(2)_L \times U(1)_Y$ is a subset of a larger gauge group G , where the SM representations arise from the breaking of more fundamental representations that transform under G . As a consequence of the gauge breaking $G \rightarrow G_{\text{SM}}$ we have the associated heavy bosons which mediate interactions between all the unified representations of the particles. Due to phenomenological considerations, such as the bosons inducing baryon number violating processes, it follows that they must have a large mass in comparison with the electroweak scale. Therefore we need to establish a mass hierarchy between the GUT scale, at which these heavy bosons become kinematically available, and the electroweak scale. Naively one thinks of being able to artificially adjust parameters in the Lagrangian to set these scales, but there are some associated issues.

The Gildener problem [13] states that one cannot establish an arbitrarily high mass hierarchy via the naive adjustment of the parameters of the bare Lagrangian in a non supersymmetric theory. It follows that within the context of naturalness, the hierarchy has an upper bound imposed by the radiative corrections. We will now present the original set-up in Ref. [13], and then move on to apply it to a realistic construct to see how it comes into effect.

Consider a theory based on $O(N)$ gauge group, that possesses two real scalar fields that transform as the fundamental representation, i.e. as \mathbf{n} dimensional vectors $\vec{\chi}, \vec{\eta}$, that cause two symmetry breaking stages $O(N) \rightarrow O(N-1) \rightarrow O(N-2)$. To this extent we write down the most general potential allowed by the symmetries,

$$\begin{aligned}
 V(\vec{\chi}, \vec{\eta}) = & -\frac{1}{2}m_1^2(\vec{\chi})^2 - \frac{1}{2}m_2^2(\vec{\eta})^2 + \frac{1}{4}f_1[(\vec{\chi})^2]^2 + \frac{1}{4}f_2[(\vec{\eta})^2]^2 \\
 & + \frac{1}{2}f_3(\vec{\chi})^2(\vec{\eta})^2 + \frac{1}{4}f_4(\vec{\chi} \cdot \vec{\eta})^2.
 \end{aligned} \tag{1.82}$$

This is accompanied by the fields couplings to the gauge fields via

$$\mathcal{L}_{\text{kin}} = (D_\mu \chi_i)(D^\mu \chi^i) + (D_\mu \eta_i)(D^\mu \eta^i), \quad (1.83)$$

where $D_\mu = \partial_\mu + igA_\mu^a T^a$ is the covariant derivative defined by the $O(N)$ gauge coupling g , the group generators T^a , and the gauge field A_μ^a which transforms as the adjoint representation. The $\vec{\chi}$ and $\vec{\eta}$ acquire VEVs and provide the vector bosons with a mass term, where the $n^2 - (n-1)^2$ “heavy” bosons M_H and the $(n-1)^2 - (n-2)^2$ “light” bosons M_L are associated with the $O(N) \rightarrow O(N-1)$, and $O(N-1) \rightarrow O(N-2)$ breakings. The masses are expressed as

$$M_H^2 = g^2(\vec{\chi}_m)^2, \quad M_L^2 = g^2(\vec{\eta}_m)^2, \quad (1.84)$$

where $\vec{\chi}_m, \vec{\eta}_m$ are the two vector’s VEVs. To this extent, we can define the aforementioned hierarchy as

$$\mathcal{H}^2 \equiv M_H^2/M_L^2. \quad (1.85)$$

By examining the dependence of the potential on the contact term f_3 , one finds that the hierarchy is bounded by the precision to which the coupling can be specified with respect to the gauge coupling, as

$$\mathcal{H} < \mathcal{O}(\alpha^{-1/2}), \quad (1.86)$$

where $\alpha^{-1} = 4\pi/g^2$. To see how this argument unfolds, we construct a $SU(5)$ GUT model and examine the contact terms in the potential to see how the bound comes into effect.

1.8.2 A non Supersymmetric $SU(5)$ GUT

In the following we follow Ref. [18] in building an $SU(5)$ GUT that incorporates the SM gauge group. Recalling from Tab. 1.1, under the SM gauge group $G_{\text{SM}} = SU(3)_C \times SU(2)_L \times U(1)_Y$ the LH matter SM fields transform as

$$\begin{aligned} \bar{u} &\sim (\bar{\mathbf{3}}, 1, -\frac{2}{3}), & \bar{d} &\sim (\bar{\mathbf{3}}, 1, +\frac{1}{3}), & \bar{e} &\sim (1, 1, +1), \\ q &= \begin{pmatrix} u \\ d \end{pmatrix} \sim (\mathbf{3}, \mathbf{2}, +\frac{1}{6}), & \ell &= \begin{pmatrix} \nu_e \\ e \end{pmatrix} \sim (1, \mathbf{2}, -\frac{1}{2}). \end{aligned} \quad (1.87)$$

The RH counterparts are obtained via Hermitian conjugation.

From a Lie algebra point of view, we require a group that has rank greater or equal to the SM gauge group (rank 4). To this extent, the minimal extension is the

$SU(5)$ group. Within this framework, we require $SU(5)$ representations that can host the SM matter fields. Following Georgi [27], under G_{SM} the $\bar{\mathbf{5}}$ representation of $SU(5)$ decomposes as

$$\bar{\mathbf{5}} \sim (\bar{\mathbf{3}}, 1, +\frac{1}{3}) \oplus (1, \mathbf{2}, -\frac{1}{2}) = \bar{d} \oplus \ell. \quad (1.88)$$

We still need a representation to host the rest of the matter fields. If we look at the next to minimal set of representations, we see that the antisymmetric $\mathbf{10}$ representation decomposes under the SM as

$$\mathbf{10} \sim (\bar{\mathbf{3}}, 1, -\frac{2}{3}) \oplus (\mathbf{3}, \mathbf{2}, \frac{1}{6}) \oplus (1, 1, 1) = \bar{u} \oplus q \oplus \bar{e}. \quad (1.89)$$

Therefore we can host all the LH SM fields in the $\bar{\mathbf{5}} \oplus \mathbf{10}$ representations of $SU(5)$. Equivalently, the Hermitian conjugate $\mathbf{5} \oplus \bar{\mathbf{10}}$ provides the embedding for the RH fields.

The $SU(5)$ gauge bosons transform under the adjoint representation $\mathbf{24}$, which decomposes under G_{SM} as

$$\mathbf{24} \sim (\mathbf{8}, 1, 0) \oplus (1, \mathbf{3}, 0) \oplus (1, 1, 0) \oplus (\mathbf{3}, \mathbf{2}, -\frac{5}{6}) \oplus (\bar{\mathbf{3}}, \mathbf{2}, \frac{5}{6}). \quad (1.90)$$

We identify $(\mathbf{8}, 1, 0)$ as the $SU(3)_C$ gluons G^a , $(1, \mathbf{3}, 0)$ are $SU(2)_L$ bosons W^a , $(1, 1, 0)$ as the hypercharge field B , and $(\mathbf{3}, \mathbf{2}, -\frac{5}{6}), (\bar{\mathbf{3}}, \mathbf{2}, \frac{5}{6})$ as the X_1, X_2 gauge bosons associated with the coset $SU(5)/G_{\text{SM}}$.

To better understand how the SM representations fit inside the $SU(5)$ ones we can look at the explicit matrix forms. We have the LH Weyl fermionic matter representations

$$\psi^i = \bar{\mathbf{5}} = \begin{pmatrix} \bar{d}^r & \bar{d}^b & \bar{d}^g & e & -\nu_e \end{pmatrix},$$

$$\chi^{ij} = -\chi^{ji} = \mathbf{10} = \begin{pmatrix} 0 & \bar{u}^g & -\bar{u}^b & u^r & d^r \\ -\bar{u}^g & 0 & \bar{u}^r & u^b & d^b \\ \bar{u}^b & -\bar{u}^r & 0 & u^g & d^g \\ -u^r & -u^b & -u^g & 0 & \bar{e} \\ -d^r & -d^b & -d^g & -\bar{e} & 0 \end{pmatrix}, \quad (1.91)$$

where the r, g, b indices refer to the QCD colour index. Similarly, looking at the gauge boson structure we have in a block diagram notation

$$A^a T^a = \left(\begin{array}{c|c} \mathbf{G} - \frac{1}{3} cB \mathbf{1}_3 & \mathbf{X} \\ \hline \mathbf{X}^\dagger & \mathbf{W} + \frac{1}{2} cB \mathbf{1}_2 \end{array} \right), \quad (1.92)$$

where c is a normalisation constant, and $\mathbf{G} \in \mathcal{M}_{3 \times 3}(\mathbb{C})$, $\mathbf{W} \in \mathcal{M}_{2 \times 2}(\mathbb{C})$ and $\mathbf{X} \in \mathcal{M}_{2 \times 3}(\mathbb{C})$ are the corresponding block matrices in the adjoint representation corresponding to the aforementioned fields transforming under the $SU(5)/G_{\text{SM}}$ coset.

Therefore we can build a $SU(5)$ invariant Lagrangian via the gauge covariant derivative $\mathcal{D}_\mu = \partial_\mu - ig_5 A_\mu^a T^a$, and the $SU(5)$ fields, that has the form

$$\mathcal{L} = i\psi_i^\dagger \bar{\sigma}^\mu (\mathcal{D}_\mu \psi)^i + \frac{1}{2} i(\chi^\dagger)^{ij} \bar{\sigma}^\mu (\mathcal{D}_\mu \chi)_{ij}, \quad (1.93)$$

where g_5 is the $SU(5)$ gauge coupling, and A_μ^a are the corresponding gauge fields the generators T^a .

We now want to break $SU(5) \rightarrow G_{\text{SM}}$, and subsequently, $G_{\text{SM}} \rightarrow SU(3)_C \times U(1)_{\text{EM}}$. The breaking of $SU(5)$ is implemented by coupling a $SU(5)$ scalar field $\Phi \sim \mathbf{24}$, to the gauge covariant derivative. Φ acquires a VEV V dictated by the structure

$$\langle \Phi \rangle = \text{diag} \left(-\frac{1}{3}, -\frac{1}{3}, -\frac{1}{3}, +\frac{1}{2}, +\frac{1}{2} \right) V. \quad (1.94)$$

This in turn breaks the $SU(5)$ gauge symmetry down to the SM gauge group, causing the X bosons to become massive, where they acquire a mass

$$M_X = \frac{5}{6\sqrt{2}} g_5 V \equiv C g_5 V, \quad (1.95)$$

where we have defined the constant C . Note that we still require a Higgs field H that transforms as $(1, \mathbf{2}, -\frac{1}{2}) \sim G_{\text{SM}}$ in order to achieve EW symmetry breaking. The smallest $SU(5)$ representation that can host it is the $\bar{\mathbf{5}}$, which has the explicit form

$$H^i = (\phi^r, \phi^b, \phi^g, \varphi^-, \varphi^0). \quad (1.96)$$

We identify the SM Higgs doublet components φ^-, φ^0 , and the introduced coloured Higgs states that can have potentially dangerous phenomenological consequences (see the following chapter). Coupling this field to the gauge fields and matter representations in order to impart the appropriate quark and lepton masses, we obtain the full $SU(5)$ GUT Lagrangian

$$\mathcal{L}_H = (\mathcal{D}_\mu H^i)^\dagger (\mathcal{D}^\mu H_i) - y H^i \psi^j \chi_{ij} - \frac{1}{8} y'' \varepsilon^{ijklm} H_i^\dagger \chi_{jk} \chi_{lm} + \text{h.c.}, \quad (1.97)$$

where ε^{ijklm} is the antisymmetric $SU(5)$ invariant tensor, and we have introduced the Yukawa couplings y, y'' . Note that the Yukawas are promoted to matrices in generation space when taking into account the two additional families.

We still require a scalar potential for Φ, H , such that the fields acquire the required VEVs and reproduce the SM Higgs sector. The most general renormalisable potential consistent with gauge invariance that can be written down has the form

$$\mathcal{V}(\Phi, H) = -\frac{1}{2}m_\Phi^2 \text{Tr } \Phi^2 + \frac{1}{4}\lambda_1 \text{Tr } \Phi^4 + \frac{1}{4}\lambda_2 (\text{Tr } \Phi^2)^2 \quad (1.98a)$$

$$+ m_H^2(H^\dagger H) + \frac{1}{4}\kappa_1(H^\dagger H)^2 - \frac{1}{2}\kappa_2(H^\dagger \Phi^2 H). \quad (1.98b)$$

The potential consists of the mass couplings m_Φ, m_H , quartic self interactions $\lambda_1, \lambda_2, \kappa_1$, and the contact coupling κ_2 .

With the model in place, we now turn to analysing it from the perspective of the Gildener problem. Since we are trying to establish an arbitrarily large mass hierarchy, we require a separation of the mass scales dictated by the VEVs of the two scalar fields $\langle H \rangle \ll \langle \phi \rangle$. Therefore we have a two stage gauge symmetry breaking, where the first consists of Φ acquiring a VEV V through the minimisation of the potential in Eqn. (1.98a), resulting in

$$V^2 = \frac{36}{7\lambda_1 + 30\lambda_2} m_\Phi^2 \equiv C_\lambda^{-1} m_\Phi^2. \quad (1.99)$$

Post symmetry breaking the contact term “drives down” the Higgs mass term in Eqn. (1.98b) causing it to become negative. Therefore the Higgs potential now develops a non trivial minimum away from 0 dictated by the corrected mass term

$$m_\varphi^2 = m_H^2 - \frac{1}{8}\kappa_2 V^2, \quad (1.100)$$

and the $SU(5)$ Higgs quartic self coupling κ_1 .

More specifically, after the H field induces EW symmetry breaking, the W^\pm, Z^0 bosons become massive. The mass of the W^\pm bosons is specified by $M_W^2 = g_5^2 \nu^2$, where $\nu^2 = m_\varphi^2 / \sqrt{\kappa_1}$. For a qualitative approximation, we identify g_5 evaluated at the EW scale as the EM coupling e . Similarly, we assume its RGE evolution from the GUT scale is negligible, with $g_5|_{\mu=M_{\text{GUT}}} \sim e$. The hierarchy \mathcal{H} defined in Eqn. (1.85) is determined by the W, X boson masses. In the current $SU(5)$ model this becomes

$$\mathcal{H}^2 = \frac{M_X^2}{M_W^2} = \frac{C^2 e^2 C_\lambda^{-1} m_\Phi^2}{e^2 \frac{m_\varphi^2}{\kappa_1}} \equiv \frac{C^2 \kappa_1}{C_\lambda \frac{m_H^2}{m_\Phi^2} - \frac{\kappa_2}{8}}. \quad (1.101)$$

Requiring a theory in which we maintain perturbative control of our couplings, and where the tree level terms are a good approximation of the potential dominating over the loop corrections, implies that the tree level approximation for the potential

\mathcal{V} is only valid for a range of coupling constants κ, λ within the $[\alpha^2, 1]$ interval. If $\kappa, \lambda < \alpha^2$ the loop gauge corrections become the dominant terms in the potential approximation, or if $\kappa, \lambda > 1$ we lose perturbative control of the theory. Here we have considered $\alpha \sim e^2$ as a qualitative approximation of $\alpha^{-1} = 4\pi/g^2$.

The hierarchy in Eqn. (1.101) can be arbitrarily extended depending on how closely we approach the limit $\kappa_2 \rightarrow 8C_\lambda m_H^2/m_\Phi^2$. To examine the behaviour of the dependency of \mathcal{H} as a function of κ_2 as it approaches the boundary parametrise κ_2 as

$$\kappa_2 = 8C_\lambda \frac{m_H^2}{m_\Phi^2} - \Delta\kappa_2. \quad (1.102)$$

In line with the precision to which we can specify couplings inside the potential \mathcal{V} up to which the tree level approximation still holds, the $\Delta\kappa_2$ term will in turn have an intrinsic effective lower bound $\Delta\kappa_2^{(e)}$ dictated by the gauge coupling corrections

$$\Delta\kappa_2 > \Delta\kappa_2^{(e)}. \quad (1.103)$$

To specify this term to a larger degree of accuracy, one needs to take into account loop corrections contributing to the $HH\Phi\Phi$ term, since the tree level becomes subdominant. Therefore requiring a larger hierarchy, has the consequence that the tree level diagram in Fig. 1.1a no longer serves as a good approximation to the potential, causing loop corrections, such as the one in Fig. 1.1b, to become the leading effect.

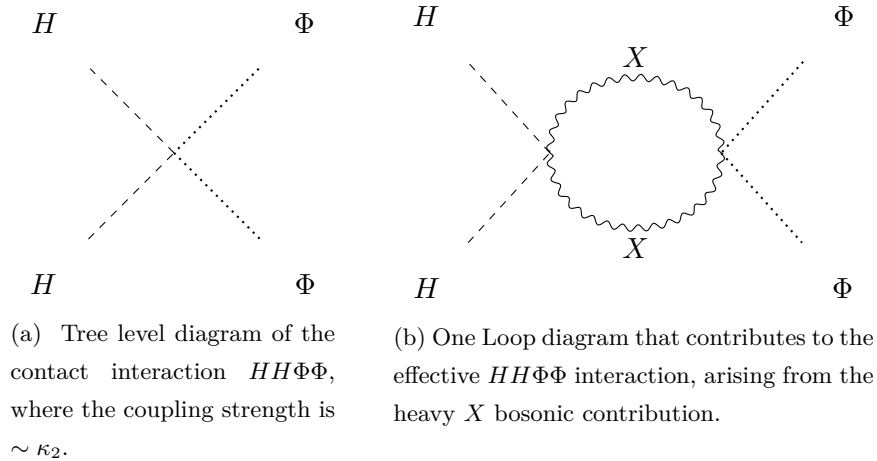


Figure 1.1: Diagrams contributing to the one loop effective $HH\Phi\Phi$ interaction.

Therefore, if we want to establish a mass hierarchy via this process, we have to go to the one loop approximation and repeat the entire process, only to run into the

same issue again via the two loop terms. The argument repeats itself ad infinitum. Going with the presumption that this degree of fine tuning is unnatural, we can only push the hierarchy up to the value allowed by the effective lower bound of the contact term, which depending on the various valid regions for $\kappa, \Delta\kappa \in [\alpha^2, 1]$ provides an upper bound

$$\mathcal{H}^2 = C^2 \frac{\kappa_1}{\Delta\kappa_2} < C^2 \frac{\kappa_1}{\Delta\kappa^{(e)}} < \mathcal{O}(\alpha^{-1}). \quad (1.104)$$

This is in essence the Gildener problem [13], one cannot establish a naturally occurring, arbitrarily large mass hierarchy in the context of gauge group symmetry breaking due to the loop corrections playing a role on how precise the contact terms can be specified before the relevant approximations break down.

While on the topic of hierarchies, even if one finds some sort of unknown mechanism to break the symmetry and establish the desired mass hierarchy, we are then left with an even more serious issue. The theory now suffers from, what is referred to as, the “real Hierarchy problem” [28]. This comprises of the fact that the Higgs now receives massive corrections from the heavy X bosons, which cannot be eliminated via renormalisation.

We will now look at radiative symmetry breaking as a potential solution to the Gildener problem, and examine why it is attractive but ultimately fails in solving it. We then turn our attention to how the Gildener problem can be resolved by postulating a supersymmetric GUT theory.

1.8.3 The Effective Action and Conformal Symmetry

We now follow Ref. [29] in constructing the effective action as a parallel to different quantities in thermodynamics. We note that in thermodynamics one defines the Gibbs free energy G of a system with a magnetisation M in an external magnetic field H as the Legendre transform of the Helmholtz free energy F defined via the partition function Z . More precisely

$$Z(H) = \exp(-\beta F(H)) \quad \Rightarrow \quad G = F + MH \quad \text{where } M \equiv \partial F / \partial H. \quad (1.105)$$

One can take into account the thermal fluctuations via the Gibbs free energy (for no external magnetic field, i.e. $H = 0$), and predict the favoured ground state of the system by finding the minimum free Gibbs potential (i.e. $\partial G / \partial M = 0$).

One can show (see Sec. 9.3 in Ref. [29]) that there exists a correspondence between the correlation functions of a statistical system and those of a related

quantum field, where the thermal fluctuations are replaced by quantum fluctuations. Due to this parallel, one can find the vacuum configuration in a quantum field theory (QFT) by examining the Gibbs free energy analogue. We start off with the partition function equivalent in a QFT, i.e. a generating functional of the form

$$Z(J) = \exp(-iE(J)) = \int \mathcal{D}\phi \exp \left\{ i \int d^4x (\mathcal{L} + J\phi) \right\}, \quad (1.106)$$

where $\int d^4x \mathcal{L}$ is the classical action for a scalar field ϕ , J is the classical current source term, $\mathcal{D}\phi$ is the path integral measure that denotes integration over all configurations of ϕ . We also define the classical field ϕ_{cl} analogous to the thermodynamic case as

$$\frac{\delta}{\delta J(x)} E(J) = -\langle \phi \rangle = -\phi_{\text{cl}}. \quad (1.107)$$

Therefore, we generate an effective action Γ_{eff} via the Legendre transform

$$\Gamma_{\text{eff}}(\phi) = -E(J) - \int d^4y J(y) \phi_{\text{cl}}(y). \quad (1.108)$$

For $J(x) = 0$ (i.e. no exterior source), we can find the preferred vacuum state (lowest energy state) of the field theory by minimising Γ_{eff} . Implicitly, since Γ_{eff} only depends on the classical field, minimising the effective action gives us the possible VEVs of ϕ .

Moreover, one can write the effective action as a derivative expansion as

$$\Gamma_{\text{eff}} = \int d^4x [-V_{\text{eff}}(\phi) + \frac{1}{2}(\partial_\mu \phi)^2 \mathcal{Z}(\phi)] + \dots \quad (1.109)$$

where we dropped the classic subscript for ϕ , and we have introduced the effective potential $V_{\text{eff}}(\phi)$ and $\mathcal{Z}(\phi)$ which are ordinary functions of ϕ (i.e. not functionals). Furthermore, since we are interested only in translationally invariant VEVs ($\phi \rightarrow \phi + \delta\phi$), the effective action becomes

$$\Gamma_{\text{eff}} = -(VT) \cdot V_{\text{eff}}. \quad (1.110)$$

VT is the 4 dimensional volume in the considered hyperspace. Therefore the minimisation of Γ_{eff} now reduces to finding the root of $\partial V_{\text{eff}}/\partial\phi = 0$. In other words, one can find the VEV of the theory by examining the effective potential.

Let us now compute the effective action. We start off by expanding $E(J)$ in Eqn. (1.106), around the classical field as $\phi(x) = \phi_{\text{cl}}(x) + \eta(x)$ for infinitesimal

variations in $\eta(x)$, which takes the form

$$\begin{aligned} \int d^4x (\mathcal{L} + J\phi) &= \int d^4x (\mathcal{L}|_{\phi=\phi_{\text{cl}}} + J\phi_{\text{cl}}) + \int d^4x \eta(x) \left(\frac{\delta \mathcal{L}}{\delta \phi} + J \right) \Big|_{\phi=\phi_{\text{cl}}} \\ &\quad + \frac{1}{2} \int d^4x d^4y \left(\eta(x) \frac{\delta^2 \mathcal{L}}{\delta \phi \delta \phi} \eta(y) \right) \Big|_{\phi=\phi_{\text{cl}}} + \dots, \end{aligned} \quad (1.111)$$

We note that the second term in the expansion is 0 due to the classical field equation arising from Eqn. (1.106), i.e.

$$\left. \frac{\delta \mathcal{L}}{\delta \phi} \right|_{\phi=\phi_{\text{cl}}} + J = 0. \quad (1.112)$$

Similarly, substituting the expansion for $E(J)$ from Eqn. (1.111) into Eqn. (1.108) we see that the effective action Γ_{eff} is a pure function of ϕ_{cl} where

$$\Gamma_{\text{eff}} = \left(\int d^4x \mathcal{L} + \frac{1}{2} \int d^4x d^4y \left(\eta(x) \frac{\delta^2 \mathcal{L}}{\delta \phi \delta \phi} \eta(y) \right) + \dots \right) \Big|_{\phi=\phi_{\text{cl}}}. \quad (1.113)$$

Examining the form of the expansion we can now understand how the higher order terms contribute to choosing the right vacuum state. Solving the second integral in the above via functional determinant methods, one finds it gives an explicit contribution of

$$\frac{i}{2} \log \det \left(-\frac{\delta^2 \mathcal{L}}{\delta \phi \delta \phi} \right). \quad (1.114)$$

Following Itzkinson and Zuber [30], if one expresses the above as a trace over the logarithm of the corresponding Green's functions $G_F(x, y)$ and second derivative of the potential $V''(\phi_{\text{cl}}(x))$ associated with the functional derivative of \mathcal{L} , we can then expand the logarithm and write the trace explicitly as

$$i \sum_{n=1}^{\infty} \frac{(-1)^n}{2n} \int d^4z_1 \dots d^4z_n [G_F(z_1 - z_2) V''(\phi(z_2))] \dots [G_F(z_n - z_1) V''(\phi(z_1))]. \quad (1.115)$$

To help us understand what this means, we substitute the results in a concrete potential. Consider a pure real scalar theory with a quartic interaction of the form $\lambda \phi^4$. Using Feynman diagrams to represent the terms in the above sum, we get the series of polygon graphs as shown in Fig. 1.2, where the dots at the vertex intersections correspond to the coupling strength associated with $V''(\phi)$.

Therefore the functional determinant is formed by the sum of all the 1 loop contributions with n propagators and n vertices. Similarly higher order terms in the effective action expansion will be comprised of 2 loop graphs and beyond. This

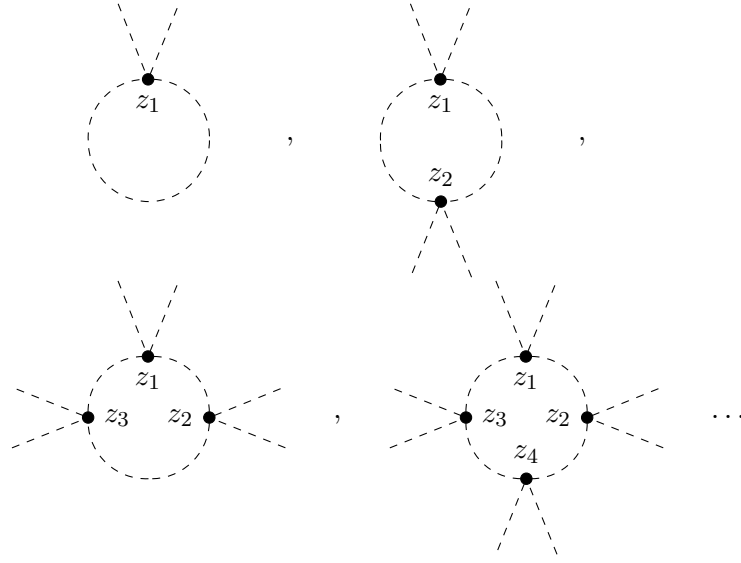


Figure 1.2: First order loop corrections in the ϕ^4 theory, where the diagrams correspond to the $n = 1, 2, 3, 4$ terms in the functional logarithm expansion in Eqn. (1.115).

is in a graphical sense, the statement that the effective action contains information about the quantum fluctuations of the system.

Furthermore, one can show that in the case of the ϕ^4 theory (see e.g. Ref. [31]), that this loop expansion is equivalent to a power series expansion of a dimensionless parameter a multiplying the Lagrangian \mathcal{L} that induces the transformation

$$\mathcal{L}(\phi, \partial_\mu \phi) \rightarrow \frac{1}{a} \mathcal{L}(\phi, \partial_\mu \phi). \quad (1.116)$$

This in turn can be made invariant by imposing that ϕ transforms under a conformal symmetry as $\phi \rightarrow a^{-1} \phi$. Looking back at our procedure, it was this implied invariance that allowed us to expand around the classical field and survey the VEVs of the theory.

1.8.4 Scalar QED and Radiatively Induced SSB

Let us now look at a particular ϕ^4 scalar QED theory considered by the authors in Ref. [31] and compute the effective potential. Consider the Lagrangian

$$\mathcal{L} = -\frac{1}{4} F_{\mu\nu} F^{\mu\nu} + (\mathcal{D}_\mu \phi)^\dagger (\mathcal{D}^\mu \phi) - \frac{\lambda}{4!} \phi^4, \quad (1.117)$$

consisting of a massless charged scalar field coupled to a gauge field A_μ via the covariant derivative $\mathcal{D}_\mu = \partial_\mu - ieA_\mu$. Choosing a regularisation scheme, in this

case dimensional regularisation, and working in the Landau gauge, one can find the effective one loop potential

$$V_{\text{eff}}(\phi) = \frac{\lambda}{4!} \phi^4 + \left(\frac{5\lambda^2}{1152\pi^2} + \frac{3e^4}{64\pi^2} \right) \phi^4 \left(\ln \frac{\phi^2}{M^2} - \frac{25}{6} \right), \quad (1.118)$$

where M is an arbitrary renormalisation scale. Diagrammatically this consists of incorporating the diagrammatic corrections $V^{(1)}(\lambda^2), V^{(1)}(e^4)$ to the tree level 4 point vertex $V^{(0)}(\lambda)$ as shown in Eqn. (1.119). For the purposes of our discussion and convenience, we choose M as the VEV of the scalar field $M = \langle \phi \rangle$.

(1.119)

If we consider the regime of $\lambda \sim e^4$ to produce a non-trivial VEV (i.e. where the 1 loop gauge coupling is of the same order of magnitude of the tree level quartic interaction), the λ^2 contribution becomes negligible, and the effective potential develops a minimum at $\langle \phi \rangle$ away from the origin. This new minimum in turn leads to a determination of λ in terms of e with $\lambda = \frac{33}{8\pi^2} e^4$. From the effective potential point of view we have traded a dimensionless parameter λ for a dimensional one $\langle \phi \rangle$. This is a direct consequence of eliminating the arbitrariness of the renormalisation scale via its association with the minimum; if kept arbitrary we would have a determination of the VEV in terms of M . Substituting everything back in, we have the full form of the effective potential

$$V_{\text{eff}} = \frac{3e^4}{64\pi^2} \phi^4 \left(\log \frac{\phi^2}{\langle \phi \rangle^2} - \frac{1}{2} \right). \quad (1.120)$$

Taking the second derivative one finds that after spontaneous symmetry breaking (SSB) ϕ has acquired a mass given by

$$m_\phi^2 = \left. \frac{\partial^2 V}{\partial \phi^2} \right|_{\phi=\langle \phi \rangle} = \frac{3e^4}{8\pi^2} \langle \phi \rangle^2. \quad (1.121)$$

Along with the scalar, the additional would-be Goldstone bosons associated with symmetry breaking are “swallowed” up by the gauge field to give a mass to the vector boson $m_V^2 = e^2 \langle \phi \rangle^2$. Therefore, the Coleman-Weinberg mechanism provides us with a symmetry breaking mechanism in a classically conformal invariant theory,

that provides a mass scale (which is typically small) determined by the coupling constants of the theory.

We note that we cannot incorporate this into the SM as a stand-alone mechanism. When Coleman and Weinberg applied it to the SM without the presence of heavy quarks or additional families in [31] (i.e. just with u, d, e^-), the authors got a prediction for the Higgs mass of the order of $\mathcal{O}(10 \text{ GeV})$. This gets a lot worse when adding in the heavy quarks, namely the top which drives the squared Higgs mass negative.

Note that the computation in Ref. [31] was done in the Landau gauge, which raises the question of gauge dependence. It follows that physically measurable quantities such as the existence of a non-trivial minimum, and its magnitude are gauge independent (see Refs. [32–34]).

1.8.5 Conformal Symmetry doesn't work

In lieu of evading the ever higher LHC bounds on supersymmetry, we initially tried to see if we could incorporate a different mechanism within a GUT that would circumvent or solve the Gildener problem. We looked at conformal symmetry breaking (see Secs. 1.8.3, 1.8.4) and how it can generate small effective scales. Unfortunately the Gildner problem cannot be solved via the introduction of conformal symmetry; because we are essentially breaking from an enlarged gauge group G to a subset \tilde{G} we do not have any residual or implicit symmetry to protect our parameters from the discussed issues (see Ref. [13]). Even more, this mechanism generates the real hierarchy problem, not having anything to protect it from the large mass contributions. We will in turn revisit the idea of effective potentials in a later Chapter, within the context of the Hosotani mechanism, which avoids the Gildener problem entirely by not possessing the traditional coupled VEV structure.

1.8.6 Supersymmetric $SU(5)$

We now look at a supersymmetric $SU(5)$ GUT model and examine how it gets around the Gildener issue. Supersymmetry is the only non-trivial extension of the space-time Poincare symmetry, via the introduction of a graded algebra. It follows that every field has a supersymmetric partner that has the same relevant coupling strengths to the other fields.

Therefore, if one tries to establish an arbitrarily high mass hierarchy, one runs into the same issue we had before, but with the addition that we now have a super-

partner fields associated with the loop diagrams. Considering the gauge corrections arising to the Feynman diagram in Fig. 1.1a, we now have two diagrams corresponding to the boson X and the superpartner \tilde{X} . The contributions from the two cancel out due to the negative sign associated with the fermionic superpartner

$$\begin{array}{c}
 \begin{array}{ccc}
 H & & \Phi \\
 \diagdown & & \diagup \\
 & \text{Loop } X & \\
 \diagup & & \diagdown \\
 H & & \Phi
 \end{array}
 +
 \begin{array}{ccc}
 H & & \Phi \\
 \diagdown & & \diagup \\
 & \text{Loop } \tilde{X} & \\
 \diagup & & \diagdown \\
 H & & \Phi
 \end{array}
 \simeq 0,
 \end{array}
 \quad (1.122)$$

therefore allowing us to establish the desired mass hierarchy. Since we have this cancellation present we can establish an arbitrarily large mass hierarchy since the tree level term remains a good approximation to the effective potential. By introducing the superpartner \tilde{X} , Eqn. (1.101) picks up a negative contribution to the denominator that sets it to ~ 0 allowing the hierarchy to be established reliably via the specificity of κ_1, κ_2 in the supersymmetric $SU(5)$ version.

Furthermore, SUSY also sorts out the “real Hierarchy problem” since the superpartner loop diagrams cancel the ones arising from the massive boson contributions.

Supersymmetry is therefore a recipe for a successful GUT that doesn’t suffer from the Gildener problem. The following chapters will be based around examining how one builds a SUSY theory, along with a class of supersymmetric models based on extra dimensional (5D, 6D) orbifold models [35–39]. These models are attractive for a few reasons: they provide SUSY breaking mass parameters via string theory arguments involved in the compactification, one can achieve suppression of proton decay processes via embedding the problematic matter representations into the bulks or UV branes, and possess the ability of hosting family symmetries that also arise from string theory like models. The idea behind this will be to establish an understanding on how the GUTs are built and broken on the orbifolds, and then examine their low energy predictions on the IR brane that can lead to a viable SM spectra. The next chapter will review SUSY and its relation with the SM.

Supersymmetry and the MSSM

The following chapter will examine the construction of supersymmetric theories via the introduction of graded algebras, and introduces a prescription on how to build representations and invariant constructs within the context of the various gradings. We then move on to introducing the Minimal Supersymmetric Model, and review how it reproduces the SM in the low energy limit, along with the phenomenology of the new fields. This chapter is mostly based on Refs. [40, 41].

2.1 Graded Algebra

The “no-go Coleman - Mandula theorem” [19] states that the most general symmetry allowed by the S-matrix in a quantum field theory, is Poincaré with an internal gauge symmetry that cannot mix different spins. Therefore if we want to enlarge the space-time algebra we require a generator Q that acts heuristically as

$$\begin{cases} Q |\text{boson}\rangle \sim |\text{fermion}\rangle, \\ Q |\text{fermion}\rangle \sim |\text{boson}\rangle. \end{cases} \quad (2.1)$$

This in turn can be accomplished by introducing a *graded algebra*. A graded algebra is a generalisation of a Lie algebra, where given the Lie algebra with generators O_a ($[O_a, O_b] = iC_{ab}^e O_e$), a graded algebra derived from it is defined by

$$O_a O_b - (-1)^{\eta_a \eta_b} O_b O_a = iC_{ab}^e O_e, \quad (2.2)$$

where C_{ab}^e are invariant tensors of the graded algebra, and η^a are the gradings where $\eta_a = 0$ if O_a is a “bosonic generator”, and $\eta_a = 1$ if O_a is a “fermionic generator”. A supersymmetric (SUSY) algebra, is a grading of the Poincaré algebra, where

- “Bosonic generators” are defined by the Poincaré translation and boost generators $P^\mu, M^{\mu\nu}$.
- “Fermionic generators” are defined by newly introduced *spinor generators*, $Q_\alpha^A, \bar{Q}_{\dot{\alpha}}^A$, where $A = 1, \dots, \mathcal{N}$ where \mathcal{N} is a constant that will determine the

nature of our supersymmetric theory, and $\alpha, \dot{\alpha}$ are spinorial indices associated with $SL(2, \mathbb{C})$. We refer to $\mathcal{N} > 1$ as extended SUSY algebras. We will see that these generators have the effect of changing a fermion into a boson and vice-versa.

In order to build a full SUSY theory we will need the full set of commutation relations between the bosonic and fermionic generators. Since we started with a Poincaré algebra we already have the ones involving $P^\mu, M^{\mu\nu}$, and still require

$$\left[Q_\alpha, M^{\mu\nu}\right], \quad \left[Q_\alpha, P^\mu\right], \quad \left\{Q_\alpha, Q_\beta\right\}, \quad \left\{Q_\alpha, \bar{Q}_{\dot{\beta}}\right\}, \quad \left[Q_\alpha, T_i\right], \quad (2.3)$$

where the last commutation relation encompasses the relation of the fermionic generators with the internal gauge symmetry generators T_i .

The first relation can be derived by looking at how Q_α transforms since it carries a spinorial index, and therefore transforms under $SL(2, \mathbb{C})$ which is determined by the group's generators $\sigma_{\mu\nu}$. Similarly, due to the homeomorphism to the proper orthochronous group, Q_α transforms under the Lorentz group. Together, in their infinitesimal limits these are

$$\begin{cases} Q_\alpha \rightarrow \left(1 - \frac{i}{2}\omega_{\mu\nu}\sigma^{\mu\nu}\right)_\alpha^\beta Q_\beta, \\ Q_\alpha \rightarrow \left(1 + \frac{i}{2}\omega_{\mu\nu}M^{\mu\nu}\right) Q_\alpha \left(1 - \frac{i}{2}\omega_{\rho\sigma}M^{\rho\sigma}\right). \end{cases} \quad (2.4)$$

Equating the transformations with one another results in the commutation relationship,

$$\left[Q_\alpha, M^{\mu\nu}\right] = (\sigma^{\mu\nu})_\alpha^\beta Q_\beta, \quad (2.5)$$

where similarly we can get the $\bar{Q}^{\dot{\alpha}}$ relationships by analysing its different transformations

$$\left[\bar{Q}^{\dot{\alpha}}, M^{\mu\nu}\right] = (\bar{\sigma}^{\mu\nu})^{\dot{\alpha}}_{\dot{\beta}} \bar{Q}^{\dot{\beta}}. \quad (2.6)$$

In order to derive $[Q_\alpha, P^\mu]$, we note that since we want to impose that the transformation has to be linear in Q , the only sensible way of writing a term that also incorporates the free indices α, μ is

$$\left[Q_\alpha, P^\mu\right] = c (\bar{\sigma}^\mu)^{\dot{\alpha}\alpha} Q_\alpha. \quad (2.7)$$

Equivalently, for the Hermitean conjugate, we have $\left[\bar{Q}^{\dot{\alpha}}, P^\mu\right] = c^* (\sigma^\mu)_{\alpha\dot{\alpha}} \bar{Q}^{\dot{\alpha}}$. The value of c is then set by looking at the Jacobi identity for P^μ, P^ν, Q_α which in turn

requires $|c|^2 = 0$, resulting in

$$\left[Q_\alpha, P^\mu\right] = \left[\bar{Q}^{\dot{\alpha}}, P^\mu\right] = 0. \quad (2.8)$$

Carrying out analogous arguments, one can show that the remaining anticommutation relations are

$$\left\{Q_\alpha, Q_\beta\right\} = 0, \quad \left\{Q_\alpha, \bar{Q}_{\dot{\beta}}\right\} = 0, \quad (2.9)$$

$$\left\{Q_\alpha, \bar{Q}_{\dot{\beta}}\right\} = 2(\sigma^\mu)_{\alpha\dot{\beta}} P_\mu. \quad (2.10)$$

Examining the last relation we notice that the combined action of $Q_\alpha \bar{Q}_{\dot{\beta}} \sim P_\mu$ has the effect of a translation,

$$Q_\alpha \bar{Q}_{\dot{\beta}} |B\rangle \rightarrow |B(x^\mu + c^\mu)\rangle, \quad (2.11)$$

where $|B\rangle$ denotes a bosonic state. Lastly $[Q_\alpha, T_i]$ vanishes due to the Coleman-Mandula theorem [19], with the exception of an $U(1)$ algebra automorphism, which is referred to as *R-symmetry* under which the fermionic generators transform as $Q_\alpha \rightarrow \exp(i\lambda)Q_\alpha$.

2.2 Representations of the Poincaré Group

We now want to examine the Casimirs of the graded algebra (to which we will refer to as the “super-algebra”), since they will label the irreducible representations of the theory, and denote the conserved quantities. We recall, that within the Poincaré algebra, the rotation group defined by generators J_i ($[J_i, J_j] = i\varepsilon_{ijk}J_k$) has the Casimir J^2 ,

$$J^2 = \sum_{i=1}^3 J_i^2. \quad (2.12)$$

We recall that it commutes with all J_i ’s, and labels irreducible representations by the $j(j+1)$ eigenvalues of J^2 along with the J_3 eigenvalue $j_3 = -j, \dots, j$ as $|j, j_3\rangle$. The rest of the Casimirs of the Poincaré algebra are defined by the translation vectors P^μ and the Pauli-Lyubanski pseudo-vector W^μ (that describes generalised spin $W_\mu = \frac{1}{2}\varepsilon_{\mu\nu\sigma\rho}P^\nu M^{\sigma\rho}$),

$$C_1 = P^\mu P_\mu, \quad C_2 = W^\mu W_\mu. \quad (2.13)$$

We now label Poincaré multiplets by the C_1, C_2 eigenvalues m^2, ω as $|m, \omega\rangle$, where m^2 is identified as the invariant mass. In addition the states carry the eigenvalue

of P^μ , p_μ as a label. Note that W_μ doesn't form a subalgebra, but provides a convenient way of expressing the C_2 Casimir.

Since massive particles have rotations as part of their little group, their 4-momentum can be written as $p^\mu = (m, 0, 0, 0)$ (in the centre of mass frame). This implies that W_μ takes the form $W_\mu = (0, -mJ_1, mJ_2, mJ_3)$. I.e. in terms of the Casimirs labelling the representations, we have $C_1 = m^2$, and $C_2 = -m^2 j(j+1)$. Therefore, *massive* particles are irreducible representation of the Poincaré group labeled by

$$|m, j; p^\mu, j_3\rangle. \quad (2.14)$$

Similarly, for massless particles, the 4-momentum has the general expression $p^\mu = (|\vec{p}|, \vec{p})$. This in turn implies that W_μ has eigenvalues of the form λp^μ , where $\lambda = \vec{j} \cdot \vec{p}/|\vec{p}|$ is identified as helicity. Therefore *massless* particles are irreducible representations of the Poincaré group labeled by

$$|p^\mu, \lambda\rangle. \quad (2.15)$$

In addition if we require the theory to be CPT invariant, it forces λ to be integer or half integer ($\lambda = 0, 1/2, 1, \dots$), where we perform the common identifications

$$\begin{aligned} \lambda = 0 &: \text{Scalars}, & \lambda = 1/2 &: \text{Fermions}, \\ \lambda = 1 &: \text{Bosons}, & \lambda = 3/2 &: \text{Gravitinos}, & \lambda = 2 &: \text{Gravitons}. \end{aligned} \quad (2.16)$$

2.3 Representations of the $\mathcal{N} = 1$ SUSY Algebra

We will now look at representations of the super-Poincaré algebra for the case of $\mathcal{N} = 1$. It can be shown that $C_1 = P^\mu P_\mu$ is still a good Casimir, but $C_2 = W^\mu W_\mu$ is not, since it does not commute with the spinorial generators $Q_\alpha, \bar{Q}_{\dot{\alpha}}$. To fix this we can define a new Casimir \tilde{C}_2 associated with *superspin*, which is constructed by “super” version of the Pauli-Lyubanski vector

$$B_\mu \equiv W_\mu - \frac{1}{4} \bar{Q}_{\dot{\alpha}} (\sigma_\mu)^{\dot{\alpha}\beta} Q_\beta. \quad (2.17)$$

B_μ is then used to form $C_{\mu\nu} \equiv B_\mu P_\nu - B_\nu P_\mu$ which is in turn used to define the new superspin quadratic Casimir

$$\tilde{C}_2 \equiv C_{\mu\nu} C^{\mu\nu}. \quad (2.18)$$

We are now equipped to label and deal with irreducible states of the super-Poincaré algebra, which we will refer to as supermultiplets. By construction the

supermultiplet will consist of bosons and fermions, where the $Q_\alpha, \bar{Q}_{\dot{\alpha}}$ generators will be responsible for switching between them, acting as raising/lowering operators. By examining how the fermion number operator $(-)^F$ (which as the name denotes acts on a state depending on its bosonic $(-)^F |B\rangle = |B\rangle$ and fermionic $(-)^F |F\rangle = -|F\rangle$ nature) acts on the components of a supermultiplet, one can show that the number of bosons n_B and the number of fermions n_F contained within the supermultiplet, are equal

$$n_B = n_F. \quad (2.19)$$

With this in mind we move on to looking at how we can form massless/massive supermultiplets.

2.3.1 Massless Supermultiplet

Analogous to the Poincaré case, a massless particle has a P_μ eigenvalue of $p_\mu = (E, 0, 0, E)$ (where we've chosen the simplifying case of a pure z direction component). Similarly to the Poincaré case, the supersymmetric version of the Casimir eigenvalues are $C_1 = \tilde{C}_2 = 0$. To get a better understanding of what a supermultiplet entails, we examine the $\{Q_\alpha, \bar{Q}_{\dot{\beta}}\}$ algebra (expressed in the chiral representation where $\sigma^\mu = (\sigma^0 = \mathbb{1}_2, \sigma^1, \sigma^2, \sigma^3)$) acting on a massless particle

$$\begin{aligned} \{Q_\alpha, \bar{Q}_{\dot{\beta}}\} |p^\mu, \lambda\rangle &= 2(\sigma^\mu)_{\alpha\dot{\beta}} P_\mu |p^\mu, \lambda\rangle = 2E(\sigma^0 + \sigma^3)_{\alpha\dot{\beta}} |p^\mu, \lambda\rangle \\ &= 4E \begin{pmatrix} 1 & 0 \\ 0 & 0 \end{pmatrix}_{\alpha\dot{\beta}} |p^\mu, \lambda\rangle, \end{aligned} \quad (2.20)$$

where $\alpha = 1, 2$, and $\dot{\beta} = \dot{1}, \dot{2}$. Therefore in this representation looking at the Q_2 component we have $\{Q_2, \bar{Q}_{\dot{2}}\} = 0$, or equivalently $\langle p^\mu, \lambda | \{Q_2, \bar{Q}_{\dot{2}}\} |p^\mu, \lambda\rangle = 0$. Therefore

$$\bar{Q}_{\dot{2}} |p^\mu, \lambda\rangle = Q_2 |p^\mu, \lambda\rangle = 0, \quad (\forall) \lambda. \quad (2.21)$$

Similarly, inspecting the $1, \dot{1}$ component $\{Q_1, \bar{Q}_{\dot{1}}\} = 4E$, which implies that there exists a unique state $|p^\mu, \Lambda\rangle$ such that $Q_1 |p^\mu, \Lambda\rangle = 0$. The latter, in conjunction with CPT implies that $\bar{Q}_{\dot{1}} |p^\mu, -\Lambda\rangle = 0$.

To see effect that $Q_\alpha, \bar{Q}^{\dot{\alpha}}$ have on helicity we look at the eigenvalue of $W_0(Q |p^\mu, \lambda\rangle)$, where the 0th component of W_μ is the only non-trivial one due to the p^μ eigenvalue. To this extent we have, the commutation relation

$$[W_\mu, \bar{Q}^{\dot{\alpha}}] = -\frac{1}{2} \varepsilon_{\mu\nu\rho\sigma} P^\nu (\bar{\sigma}^{\rho\sigma})^{\dot{\alpha}}_{\dot{\beta}} \bar{Q}^{\dot{\beta}}, \quad (2.22)$$

along with the eigenvalue relation $W_0 |p^\mu, \lambda\rangle = \lambda p_0 |p^\mu, \lambda\rangle$. Taking these together, we find in particular, the action of $\bar{Q}^{\dot{2}}$ on the helicity eigenvalue λ of a state

$$W_0 (\bar{Q}^{\dot{2}} |p^\mu, \lambda\rangle) = ([W_0, \bar{Q}^{\dot{2}}] + \bar{Q}^{\dot{2}} W_0) |p^\mu, \lambda\rangle = \left(\lambda - \frac{1}{2}\right) p_0 (\bar{Q}^{\dot{2}} |p^\mu, \lambda\rangle). \quad (2.23)$$

Therefore $\bar{Q}^{\dot{2}} \equiv -\bar{Q}_1$ has the effect of reducing the helicity of a state by $1/2$. The normalised state with a lowered helicity eigenvalue is then

$$\left| p^\mu, \lambda - \frac{1}{2} \right\rangle = \frac{1}{\sqrt{4E}} \bar{Q}_1 |p^\mu, \lambda\rangle. \quad (2.24)$$

Furthermore, one can show that $\bar{Q}_1 |p^\mu, \lambda - \frac{1}{2}\rangle = 0$. Since we have shown that the latter is unique, it implies that there are no other states in the supermultiplet. Therefore \bar{Q}_1 acts as the lowering $(-)$ operator. Similarly one can show that the Q_1 operator acts as the raising $(+)$ operator, where

$$|p^\mu, \lambda\rangle = \frac{1}{\sqrt{4E}} Q_1 \left| p^\mu, \lambda - \frac{1}{2} \right\rangle. \quad (2.25)$$

Analogously we have $Q_1 |p^\mu, \lambda\rangle = 0$, which in conjunction with the previous results show that a massless supermultiplet contains only two helicity states (in addition to their CPT conjugates). I.e. a “bosonic” state (corresponding to the λ helicity) and a “fermionic” state (corresponding to the $\lambda - \frac{1}{2}$ helicity)

$$|p^\mu, \pm\lambda\rangle, \quad \left| p^\mu, \pm \left(\lambda - \frac{1}{2} \right) \right\rangle. \quad (2.26)$$

This is what we identify within the classic supermultiplets present throughout the literature within the $\mathcal{N} = 1$ formulations, where we have listed the common representations in Tab. 2.1

2.3.2 Massive Supermultiplet

For the massive case, in the centre of mass frame we have the P^μ eigenvalue $p^\mu = (m, 0, 0, 0)$, which has the associated Casimirs

$$C_1 = P_\mu P^\mu, \quad \tilde{C}_2 = C_{\mu\nu} C^{\mu\nu} = 2m^4 Y^i Y_i. \quad (2.27)$$

Y^i denotes the *super-spin* vector, which obeys the Lie algebra $[Y_i, Y_j] = i\varepsilon_{ijk} Y_k$, and is defined by

$$Y_i = J_i - \frac{1}{4m^2} \bar{Q}_{\dot{\alpha}} (\bar{\sigma}_i)^{\dot{\alpha}\beta} Q_\beta = \frac{1}{m} B_i. \quad (2.28)$$

$\lambda = 0$	$\lambda = 1/2$
Squark \tilde{q}	Quark q
Slepton \tilde{l}	Lepton l
Higgs h	Higgsino \tilde{h}

$\lambda = 1/2$	$\lambda = 1$
Bino \tilde{B}	$U(1)_Y$ field B_μ
Winos \tilde{W}	W_μ^\pm weak bosons
Gluinos \tilde{G}	$SU(3)_C$ gluons G_μ

$\lambda = 3/2$	$\lambda = 2$
Gravitino ψ_μ	Graviton $\sigma_{\mu\nu}$

Table 2.1: Examples of common massless supermultiplets consisting of the two different helicity states along with their notation and name.

Analogous to J^2 , the squared superspin vector has eigenvalues $y(y+1)$ corresponding to $Y_i Y^i$. To this extent we label the massive supermultiplet representations as $|m, y\rangle$, along with the original p^μ and j_3 eigenvalues. Analogous to the massless case we now look at how the spinor generator algebra acts on a state $|m, y\rangle$

$$\left\{ Q_\alpha, \bar{Q}_{\dot{\beta}} \right\} |m, y\rangle = 2m (\sigma^0)_{\alpha\dot{\beta}} |m, y\rangle = 2m \begin{pmatrix} 1 & 0 \\ 0 & 1 \end{pmatrix}_{\alpha\dot{\beta}} |m, y\rangle. \quad (2.29)$$

Similar to what we did previously, we suppose that $|\Omega\rangle$ is the lowest state with Q_1, Q_2 annihilating it. Therefore if we look at the action of the superspin vector on $|\Omega\rangle$, we get

$$Y_i |\Omega\rangle = J_i |\Omega\rangle - \frac{1}{4m^2} \bar{Q}_{\dot{\alpha}} (\bar{\sigma}_i)^{\dot{\alpha}\beta} Q_\beta |\Omega\rangle = J_i |\Omega\rangle. \quad (2.30)$$

Therefore the lowest state for a given m and y is

$$|\Omega\rangle = |m, y = j; p^\mu, j^3\rangle. \quad (2.31)$$

Similar to what we did in the massless case, we can derive the rest of the states present in the SUSY multiplet via the action of $\bar{Q}^{\dot{1}}, \bar{Q}^{\dot{2}}$, by defining the normalised ladder operators

$$a_1^\dagger |j_3\rangle \equiv \frac{1}{\sqrt{2m}} \bar{Q}^{\dot{1}} |j_3\rangle = \left| j_3 - \frac{1}{2} \right\rangle, \quad a_2^\dagger |j_3\rangle \equiv \frac{1}{\sqrt{2m}} \bar{Q}^{\dot{2}} |j_3\rangle = \left| j_3 + \frac{1}{2} \right\rangle. \quad (2.32)$$

The relevant commutation relations are now

$$\begin{cases} [J^2, \overline{Q}^{\dot{\alpha}}] = \frac{3}{4} \overline{Q}^{\dot{\alpha}} - (\sigma^i)_{\dot{\beta}}^{\dot{\alpha}} \overline{Q}^{\dot{\beta}} J_i \\ [J_3, a_1^\dagger a_2^\dagger] = [J^2, a_1^\dagger a_2^\dagger] = 0 \end{cases} . \quad (2.33)$$

Depending on the y eigenvalue, we have two cases

- $y = 0$. For this case the supermultiplet consists of 3 states, where

$$\begin{aligned} |\Omega\rangle &= |m, j = 0; p^\mu, j_3 = 0\rangle, \\ a_{1,2}^\dagger |\Omega\rangle &= \left| m, j = \frac{1}{2}; p^\mu, j_3 = \pm \frac{1}{2} \right\rangle, \\ a_1^\dagger a_2^\dagger |\Omega\rangle &= |m, j = 0; p^\mu, j_3 = 0\rangle \equiv |\Omega'\rangle. \end{aligned} \quad (2.34)$$

Note that $|\Omega\rangle$ is annihilated by a_i , whereas $|\Omega'\rangle$ is annihilated by a_i^\dagger . Furthermore, since under a parity transformation we have the interchange $Q \leftrightarrow \overline{Q}$, this implies $|\Omega\rangle \leftrightarrow |\Omega'\rangle$. To this extent the linear combinations $|\pm\rangle = |\Omega\rangle \pm |\Omega'\rangle$ have a defined parity, where $|+\rangle$ is called a scalar and $|-\rangle$ a pseudoscalar.

- $y \neq 0$. In this case we have a number of $4y + 4$ states consisting of $2y + 2$ fermionic states with $j = y + \frac{1}{2}$, $2y$ fermionic states with $j = y - \frac{1}{2}$, and $4y + 2$ bosonic states with $j = y$

$$\begin{aligned} &2 \cdot |m, j = y; p^\mu, j_3\rangle, \\ &1 \cdot \left| m, j = y + \frac{1}{2}; p^\mu, j_3 \right\rangle, \\ &1 \cdot \left| m, j = y - \frac{1}{2}; p^\mu, j_3 \right\rangle, \end{aligned} \quad (2.35)$$

where $j_3 = -j, \dots, +j$, and the values for y, m are fixed.

2.4 Extended Supersymmetry

We will now briefly look at extended supersymmetric algebras, which will be referred back to in the next chapter where we will explore 5-dimensional $\mathcal{N} = 1$ models, which are equivalent to 4-dimensional $\mathcal{N} = 2$ models.

In Sec. 2.1 when we introduced the spinorial generators we saw that in its most general form the graded Poincaré algebra contains an additional label $A = 1, \dots, \mathcal{N}$ corresponding to the rank of \mathcal{N} . Generalising from the $\mathcal{N} = 1$ case we get the new

anticommutation relations for the extended SUSY spinor generators

$$\begin{aligned} \{Q_\alpha^A, \bar{Q}_{\dot{\beta}B}\} &= 2(\sigma^\mu)_{\alpha\dot{\beta}} P_\mu \delta_B^A, \\ \{Q_\alpha^A, Q_\beta^B\} &= \varepsilon_{\alpha\beta} Z^{AB}, \quad \{\bar{Q}_{\dot{\alpha}}^A, \bar{Q}_{\dot{\beta}}^B\} = \varepsilon_{\dot{\alpha}\dot{\beta}} (Z^\dagger)^{AB}, \end{aligned} \quad (2.36)$$

where $\varepsilon^{\alpha\beta} = \varepsilon^{\dot{\alpha}\dot{\beta}} = \begin{pmatrix} 0 & 1 \\ -1 & 0 \end{pmatrix}$, and $Z^{AB} = -Z^{BA}$ are the *antisymmetric central charges* that commute with all the generators of the graded algebra

$$[Z^{AB}, P^\mu] = [Z^{AB}, M^{\mu\nu}] = [Z^{AB}, Q_\alpha^A] = [Z^{AB}, Z^{CD}] = [Z^{AB}, T_a] = 0. \quad (2.37)$$

Analogous to the $\mathcal{N} = 1$ case we want to see if we have the same algebra automorphism caused by the spinorial generators with respect to the internal symmetry generators. Suppose we have a theory that possesses an internal symmetry group G with a Lie algebra $[T_a, T_b] = if_{abc}T_c$. We then define the R-symmetry, H as a subgroup of G , $H \subset G$, which is determined by the generators of the internal symmetry group that don't commute with the spinorial generators. To this extent H is defined by the non-trivial elements of the algebra automorphism

$$[Q_\alpha^A, T_a] = (S_\alpha)_B^A Q_\alpha^B, \quad (2.38)$$

where $(S_\alpha)_B^A$ is a structure constant determined by the central charges Z^{AB} . If the eigenvalues of Z^{AB} are all 0 then the R-symmetry $H = U(N)$, otherwise $H \subset U(N)$, where we've denoted $N \equiv \mathcal{N}$.

2.4.1 Massless Representations of $\mathcal{N} > 1$ SUSY

Finding a representation for the massless $\mathcal{N} > 1$ super-Poincaré algebra is now completely analogous to what we did in the $\mathcal{N} = 1$ case, with an additional complexity introduced by the central charges. Starting off with the $p^\mu = (E, 0, 0, E)$ eigenvalue for a massless particle, we now look at the effect of $\{Q_\alpha^A, \bar{Q}_{\dot{\beta}B}\}$ acting on an arbitrary state

$$\{Q_\alpha^A, \bar{Q}_{\dot{\beta}B}\} |p^\mu, \lambda\rangle = 4E \begin{pmatrix} 1 & 0 \\ 0 & 0 \end{pmatrix}_{\alpha\dot{\beta}} \delta_B^A |p^\mu, \lambda\rangle. \quad (2.39)$$

Therefore the Q_1^A, Q_2^A operators act as annihilation operators with $Q_2^A |p^\mu, \lambda\rangle = Q_1^A |p^\mu, \lambda\rangle = 0$. Furthermore we can derive the values of the antisymmetric central

State	Helicity	Number of States
$ \Omega\rangle$	λ_0	$\binom{\mathcal{N}}{1}$
$(a^A)^\dagger \Omega\rangle$	$\lambda_0 + \frac{1}{2}$	$\binom{\mathcal{N}}{2}$
$(a^B)^\dagger (a^A)^\dagger \Omega\rangle$	$\lambda_0 + 1$	$\binom{\mathcal{N}}{3}$
\vdots	\vdots	\vdots
$(a^\mathcal{N})^\dagger (a^{\mathcal{N}-1})^\dagger \dots (a^1)^\dagger \Omega\rangle$	$\lambda_0 + \frac{\mathcal{N}}{2}$	$\binom{\mathcal{N}}{\mathcal{N}}$

Table 2.2: The available states in a supermultiplet where the left column denotes how the state is obtained via applying successive raising operators, the middle column denotes the helicity of the obtained states, and the right column contains the number of states of equivalent helicity.

charges Z_{AB} by looking at the action of $\{Q_1^A, Q_2^B\}$, i.e.

$$\begin{aligned}
\{Q_1^A, Q_2^B\} |p^\mu, \lambda\rangle &= \varepsilon_{12} Z^{AB} |p^\mu, \lambda\rangle, \\
&= Q_1^A Q_2^B |p^\mu, \lambda\rangle + Q_2^B Q_1^A |p^\mu, \lambda\rangle = 0.
\end{aligned} \tag{2.40}$$

Since $\varepsilon_{12} \neq 0$, it follows that $Z^{AB} = 0, (\forall) A, B$. Therefore the R symmetry of the theory is $U(N)$.

Analogously to the $\mathcal{N} = 1$ case we now define a number of \mathcal{N} creation and annihilation operators $\{a^A\}$

$$(a^A)^\dagger \equiv \frac{Q_1^A}{2\sqrt{E}}, \quad a^A \equiv \frac{\bar{Q}_1^A}{2\sqrt{E}}, \tag{2.41}$$

which obey the algebra $\{a^A, a_B^\dagger\} = \delta_B^A$. Similar to how we have constructed our representations so far, we postulate the existence of the lowest state $|\Omega\rangle$, which in turns allows us to construct our algebra representation by applying the corresponding $(a^A)^\dagger$ operators to produce the states in Tab. 2.2.

Therefore the total number of states within the supermultiplet is given by $\sum_{k=1}^{\mathcal{N}} \binom{\mathcal{N}}{k} = 2^\mathcal{N}$.

With a bit of foresight we now look at the $\mathcal{N} = 2$ massless representations (which will show up later on when projecting from $5D, \mathcal{N} = 1$ down to $4D$).

A $\mathcal{N} = 2$ vector multiplet is defined by $\lambda_0 = 0$, and contains the helicity states

$$\left(\begin{array}{ccc} & \lambda = 0 & \\ \swarrow a_1^\dagger & & \searrow a_2^\dagger \\ \lambda = \frac{1}{2} & & \lambda = \frac{1}{2} \\ \searrow a_2^\dagger & & \swarrow a_1^\dagger \\ & \lambda = 1 & \end{array} \right), \quad (2.42)$$

where we have denoted the raising operators a_1^\dagger, a_2^\dagger used to obtain the states. The $\mathcal{N} = 2$ vector supermultiplet can be decomposed in terms of $\mathcal{N} = 1$ multiplets, namely a $\mathcal{N} = 1$ vector supermultiplet consisting of the $(\lambda = 1/2, \lambda = 1)$ states, where the $\lambda = 1/2$ is the one obtained via a_2^\dagger , and another chiral super multiplet consisting of the remaining states $(\lambda = 0, \lambda = 1/2)$.

Similarly, a $\mathcal{N} = 2$ hypermultiplet is defined by $\lambda_0 = -\frac{1}{2}$, and contains the helicity states

$$\left(\begin{array}{ccc} & \lambda = -\frac{1}{2} & \\ \swarrow a_1^\dagger & & \searrow a_2^\dagger \\ \lambda = 0 & & \lambda = 0 \\ \searrow a_2^\dagger & & \swarrow a_1^\dagger \\ & \lambda = \frac{1}{2} & \end{array} \right). \quad (2.43)$$

Similarly this decomposes under the $\mathcal{N} = 1$ sub-algebra into a chiral supermultiplet consisting of the $(\lambda = 0, \lambda = 1/2)$ states, where the $\lambda = 1/2$ is obtained via a_2^\dagger , and a anti-chiral supermultiplet consisting of the remaining states $(\lambda = 0, \lambda = -1/2)$

2.5 Superspace and Superfields

So far we have derived representations of the super-Poincaré group, where we saw how multiple particle states fit inside a supermultiplet. With this, we now want to derive a field theory that describes their interaction via a dimensionless action. To this extent we require objects $\Phi(X)$ which:

- are functions of the superspace coordinate X corresponding to the super-Poincaré group.
- transform under the super-Poincaré group.

2.5.1 Groups and Cosets

To derive the form of the super-space we look at how one derives Minkowski space from group theory arguments, such that we can then apply it to the super-Poincaré group.

Starting off, every continuous group G defines a manifold \mathcal{M}_G via its set of parameters $\{\alpha_a\}$. I.e. there exists a mapping $\Lambda : G \rightarrow \mathcal{M}_G$ between a group element $g = \exp(i\alpha_a T^a)$ and the set of parameters $\{\alpha_a\}$ such that

$$g = \exp(i\alpha_a T^a) \xrightarrow{\Lambda} \{\alpha_a\}, \quad (2.44)$$

where T_a are the group generators. From this mapping we see that $\text{rank } G = \dim \mathcal{M}_G$.

To get a better intuition on how we build up the Minkowski manifold, we now look at a series of examples involving continuous groups and cosets:

- $G = U(1)$: has elements defined by $g = \exp(i\alpha \mathbb{1}_1)$, where the parameter $\alpha \in [0, 2\pi]$. Therefore the corresponding manifold $\mathcal{M}_{U(1)}$ is defined by $\{\alpha\}$ and has the topology of a circle (or equivalently a 1-sphere)

$$\mathcal{M}_{U(1)} = S^1. \quad (2.45)$$

- $G = SU(2)$: has 3 generators corresponding to the Pauli Matrices $\{\sigma^a\}$, $a = 1, 2, 3$, and has a group element representation of the form $g = \begin{pmatrix} \alpha & \beta \\ -\beta^* & \alpha^* \end{pmatrix}$, where $\alpha, \beta \in \mathbb{C}$ and $|\alpha|^2 + |\beta|^2 = 1$. By writing the two complex parameters in terms of their real and imaginary parts, $\alpha = x_1 + ix_2, \beta = x_3 + ix_4$, where $x_i \in \mathbb{R}, i = 1, 2, 3, 4$, the determinant constraint becomes $\sum_{i=1}^4 x_i^2 = 1$. Therefore the corresponding manifold has the topology of a 3-sphere

$$\mathcal{M}_{SU(2)} = S^3. \quad (2.46)$$

Moving on, for coset groups of the form G/H , where H is a subgroup of G , $g \in G$ and $h \in H$, we identify the group element g with that of the coset $g \cdot h$ as

$$g \sim g \cdot h \quad (\forall) h \in H. \quad (2.47)$$

Similarly looking at a couple of examples

- $G = U_1(1) \times U_2(1)$; $H = U_1(1)$: we have the group elements $g = \exp(i(\alpha_1 Q_1 + \alpha_2 Q_2))$, and similarly $h = \exp(i\beta Q_1)$. Performing the identification for the coset $(U_1(1) \times U_2(1))/U_2(1)$

$$g \cdot h = \exp(i((\alpha_1 + \beta)Q_1 + \alpha_2 Q_2)) \sim \exp(i(\alpha_1 Q_1 + \alpha_2 Q_2)) = g, \quad (\forall)\beta. \quad (2.48)$$

Therefore α_2 is the only parameter containing any effective information. The identification has an element of the form $\exp(i\alpha_2 Q_2)$, which implies $G/H = U_2(1)$. Therefore the coset has a corresponding manifold with topology of a 1-sphere

$$\mathcal{M}_{(U_1(1) \times U_2(1))/U_2(1)} = S^1. \quad (2.49)$$

- $G = SU(2)$; $H = U(1)$: we first identify the isomorphisms $G/H = SU(2)/U(1) \simeq SU(2)/SO(2)$. Therefore we have the group elements $g = \begin{pmatrix} \alpha & \beta \\ -\beta^* & \alpha^* \end{pmatrix}$ and $h = \begin{pmatrix} \exp(i\gamma) & 0 \\ 0 & \exp(-i\gamma) \end{pmatrix}$, where $\gamma \in [0, 2\pi]$. Performing the identification $g \sim g \cdot h$ restricts us to those values of for which $\alpha \in \mathbb{R}$. Imposing the determinant constraint we get $(\text{Re}\{\beta\})^2 + (\text{Im}\{\beta\})^2 + \alpha = 1$. Therefore the coset manifold has the topology of a 2-sphere

$$\mathcal{M}_{SU(2)/U(1)} = S^2. \quad (2.50)$$

Minkowski space is the corresponding manifold of the translational group $\mathcal{R}^{1,3}$ which can be thought of as resulting from the coset of the Poincaré group and the Lorentz group, $(\mathcal{R}^{1,3} \rtimes \text{SL}(2, \mathbb{C}))/\text{SL}(2, \mathbb{C})$, where \rtimes stands for the semi-direct group product. In terms of the group parameters we have $\{\omega^{\mu\nu}, a^\mu\} / \{\omega^{\mu\nu}\} = \{a^\mu\}$.

Analogously to the Minkowski case, the $\mathcal{N} = 1$ superspace is defined as the coset

$$\text{super-Poincaré} / \text{Lorentz} = \{\omega^{\mu\nu}, a^\mu, \theta^\alpha, \bar{\theta}_{\dot{\alpha}}\} / \{\omega^{\mu\nu}\} \sim \{a^\mu, \theta^\alpha, \bar{\theta}_{\dot{\alpha}}\}. \quad (2.51)$$

A general group element of the super-Poincaré algebra is expressed as

$$g = \exp\left(i\left(\omega^{\mu\nu} M_{\mu\nu} + a^\mu P_\mu + \theta^\alpha Q_\alpha + \bar{\theta}_{\dot{\alpha}} \bar{Q}^{\dot{\alpha}}\right)\right), \quad (2.52)$$

where $\theta^\alpha, \bar{\theta}_{\dot{\alpha}}$ are Grassmann variables, that have the effect of reducing the *anticommutation* relation $\{Q_\alpha, \bar{Q}_{\dot{\beta}}\} = 2(\sigma^\mu)_{\alpha\dot{\beta}} P_\mu$ to a *commutation* relation

$$[\theta^\alpha Q_\alpha, \bar{\theta}^{\dot{\beta}} \bar{Q}_{\dot{\beta}}] = 2\theta^\alpha (\sigma^\mu)_{\alpha\dot{\beta}} \bar{\theta}^{\dot{\beta}} P_\mu. \quad (2.53)$$

2.5.2 Scalar Superfield

We will now look at the simplest case of a scalar superfield. In the case of a Poincaré scalar field, φ is a function of spacetime coordinates x^μ , transforms under the Poincaré group, and in particular under translations P^μ . More specifically, we can treat φ as an operator, which transforms under the P^μ by an amount a^μ as

$$\varphi \rightarrow \exp(-ia_\mu P^\mu) \varphi \exp(ia_\mu P^\mu). \quad (2.54)$$

We can also approach this from another point of view, namely treating $\varphi(x^\mu)$ as a Hilbert vector in a function space \mathcal{F} , which evolves under translations as

$$\varphi(x^\mu) \rightarrow \exp(-ia_\mu \mathcal{P}^\mu) \varphi(x^\mu) \equiv \varphi(x^\mu - a^\mu), \quad (2.55)$$

where \mathcal{P}^μ is some representation of P^μ acting on \mathcal{F} . Therefore $\mathcal{P}^\mu = -i\partial_\mu$.

Performing an expansion in a^μ and comparing the two transformations up to $\mathcal{O}(a^\mu)$ we can determine the variation in the scalar field $\delta\varphi$ under a small change in a^μ

$$i[\varphi, a_\mu P^\mu] = -ia^\mu \mathcal{P}_\mu = -a\partial_\mu \varphi = \delta\varphi. \quad (2.56)$$

Analogously, we can apply the same argument for the superfield case. A general scalar superfield S has to transform under the super-Poincaré algebra, and must be a function of super-space coordinates $S(x^\mu, \theta_\alpha, \bar{\theta}_{\dot{\alpha}})$. Similarly we treat S as an operator transforming under the super-Poincaré algebra. More specifically, the superfield transforms under the spinorial generators $Q_\alpha, \bar{Q}_{\dot{\alpha}}$ by infinitesimal amounts $\delta x^\mu, \delta\theta_\alpha = \epsilon_\alpha, \delta\bar{\theta}_{\dot{\alpha}} = \bar{\epsilon}_{\dot{\alpha}}$, as

$$S \rightarrow \exp(-i(\epsilon Q + \bar{\epsilon} \bar{Q})) S \exp(i(\epsilon Q + \bar{\epsilon} \bar{Q})). \quad (2.57)$$

Analogously $S(x^\mu, \theta_\alpha, \bar{\theta}_{\dot{\alpha}})$ is a operator acting on Hilbert space, which transforms as,

$$\begin{aligned} S(x^\mu, \theta_\alpha, \bar{\theta}_{\dot{\alpha}}) &\rightarrow \exp(-i(\epsilon \mathcal{Q} + \bar{\epsilon} \bar{\mathcal{Q}})) S(x^\mu, \theta_\alpha, \bar{\theta}_{\dot{\alpha}}), \\ &= S(x^\mu + \delta x^\mu, \theta_\alpha + \epsilon_\alpha, \bar{\theta}_{\dot{\alpha}} + \bar{\epsilon}_{\dot{\alpha}}), \end{aligned} \quad (2.58)$$

where $\mathcal{Q}, \bar{\mathcal{Q}}$ are representations of the spinorial generators. Since the spinorial generators have the additional effect of a translation, one can show that the variational amount δx^μ induced by $\mathcal{Q}, \bar{\mathcal{Q}}$ is determined by,

$$\delta x^\mu = -ic(\epsilon \sigma^\mu \bar{\theta}) + ic^*(\theta \sigma^\mu \bar{\epsilon}), \quad (2.59)$$

where c is a constant set by $[Q, \bar{Q}]$.

Putting all of this together, the representations for $P^\mu, Q_\alpha, \bar{Q}_{\dot{\alpha}}$ have the explicit form

$$Q_\alpha = -i \frac{\partial}{\partial \theta^\alpha} - c (\sigma^\mu)_{\alpha\dot{\beta}} \bar{\theta}^{\dot{\beta}} \frac{\partial}{\partial x^\mu}, \quad (2.60)$$

$$\bar{Q}_{\dot{\alpha}} = +i \frac{\partial}{\partial \bar{\theta}^{\dot{\alpha}}} + c^* \theta^\beta (\sigma^\mu)_{\beta\dot{\alpha}} \frac{\partial}{\partial x^\mu}, \quad (2.61)$$

$$\mathcal{P}_\mu = -i \partial_\mu. \quad (2.62)$$

Therefore if we compare the two transformation laws, the variation of the superfield induced by the infinitesimal variation corresponding to $P^\mu, Q_\alpha, \bar{Q}_{\dot{\alpha}}$, is determined by

$$i [S, \epsilon Q + \bar{\epsilon} \bar{Q}] = i (\epsilon Q + \bar{\epsilon} \bar{Q}) S = \delta S. \quad (2.63)$$

With this information we can look at how supermultiplets fit within the superfield formulation. For a general superfield $S(x^\mu, \theta_\alpha, \bar{\theta}_{\dot{\alpha}})$, we can perform a Taylor expansion in $\theta_\alpha, \bar{\theta}_{\dot{\alpha}}$

$$\begin{aligned} S(x^\mu, \theta_\alpha, \bar{\theta}_{\dot{\alpha}}) = & \varphi(x^\mu) + \theta\psi(x^\mu) + \bar{\theta}\bar{\chi}(x^\mu) + \theta\theta M(x^\mu) + (\theta\sigma^\mu\bar{\theta}) V_\mu(x^\mu) \\ & + (\theta\theta) \bar{\theta}\bar{\lambda}(x^\mu) + (\bar{\theta}\bar{\theta}) \theta\rho(x^\mu) + (\theta\theta) (\bar{\theta}\bar{\theta}) D(x^\mu), \end{aligned} \quad (2.64)$$

where the $\mathcal{O}(\theta^3)$ terms vanish since $\{\theta_\alpha, \theta_\beta\} = 0$ for $\alpha = \beta$. Under a supersymmetric transformation the various components of S transform as dictated by Eqn. (2.63), e.g. $\delta\varphi = \epsilon\psi + \bar{\epsilon}\bar{\chi}$.

We note that the number of bosons and fermions in a superfield are equal (identified by the powers of θ and $\bar{\theta}$), but are too many to be identified as the supermultiplets. This is due to the fact that in general the superfield is a reducible supersymmetric representation. The supermultiplets are obtained by imposing restrictions on generic superfields S , which in turn define the types of superfields:

- **Chiral superfield** Φ , defined by $\bar{\mathcal{D}}_{\dot{\alpha}}\Phi = 0$.
- **Anti-Chiral superfield** $\bar{\Phi}$, defined by $\mathcal{D}_\alpha\bar{\Phi} = 0$.
- **Vector superfield** V defined by $V^\dagger = V$.
- **Linear superfield** L defined by $\mathcal{D}_\alpha\mathcal{D}^\alpha L = 0$ and $L = L^\dagger$.

All the above are determined via the covariant derivatives $\mathcal{D}_\alpha, \bar{\mathcal{D}}_{\dot{\alpha}}$ which are defined as

$$\mathcal{D}_\alpha \equiv \partial_\alpha + i (\sigma^\mu)_{\alpha\dot{\beta}} \bar{\theta}^{\dot{\beta}} \partial_\mu, \quad (2.65)$$

$$\bar{\mathcal{D}}_{\dot{\alpha}} \equiv -\bar{\partial}_{\dot{\alpha}} - i \theta^\beta (\sigma^\mu)_{\beta\dot{\alpha}} \partial_\mu. \quad (2.66)$$

The forms of the constraints are related to constructing SUSY invariants and preserving their structure. E.g. the $\bar{\mathcal{D}}_{\dot{\alpha}}\Phi = 0$ condition, is equivalent to the statement that if we parallel transport Φ via the covariant derivative across superspace, this leaves Φ unchanged. We can find the components of the superfields by looking at these conditions and how they compare with the superfield variations. For convenience we define

$$y^\mu \equiv x^\mu + i(\theta\sigma^\mu\bar{\theta}). \quad (2.67)$$

Looking at the chiral superfield, if $\Phi = \Phi(y, \theta, \bar{\theta})$, then the $\bar{\mathcal{D}}_{\dot{\alpha}}\Phi = 0$ condition reduces to

$$\bar{\mathcal{D}}_{\dot{\alpha}}\Phi = -\bar{\partial}_{\dot{\alpha}}\Phi - \frac{\partial\Phi}{\partial y^\mu} \frac{\partial y^\mu}{\partial \bar{\theta}^{\dot{\alpha}}} - i\theta^\beta (\sigma^\mu)_{\beta\dot{\alpha}} \partial_\mu \Phi \quad (2.68)$$

$$= -\bar{\partial}_{\dot{\alpha}}\Phi = 0, \quad (2.69)$$

which a posteriori justifies our definition of y^μ . Therefore Φ has no dependence on the $\bar{\theta}$ Grassman variable, and only depends on y^μ, θ . Using the explicit form arising from the Taylor expansion one finds the components of the chiral superfield

$$\Phi(y^\mu, \theta^\alpha) = \varphi(y^\mu) + \sqrt{2}\theta\psi(y^\mu) + \theta\theta F(y^\mu), \quad (2.70)$$

where φ represents a scalar field, ψ a fermionic field and F is an auxiliary field, the purpose of which will be explained later on. Note that we have the same number of bosons and fermions in the superfield, with $n_B = 4$ (represented by the complex ϕ , and F), and $n_F = 4$ (represented by the complex ψ_α). E.g. when we introduce the Higgs fields, and matter supermultiplets in the minimal supersymmetric model (MSSM), the φ represents the scalar degrees of freedom, i.e. the squarks, sleptons, and the Higgs bosons, and ψ_α represent the fermion partners, i.e. the quarks, leptons and Higgsinos.

Recasting Φ in terms of x^μ , we have

$$\begin{aligned} \Phi(x^\mu, \theta^\alpha, \bar{\theta}^{\dot{\alpha}}) &= \varphi(x) + \sqrt{2}\theta\psi(y^\mu) + \theta\theta F(y^\mu) + i\theta\sigma^\mu\bar{\theta}\partial_\mu\varphi(x) \\ &\quad - \frac{i}{\sqrt{2}}(\theta\theta)\partial_\mu\psi(x)\sigma^\mu\bar{\theta} - \frac{1}{4}(\theta\theta)(\bar{\theta}\bar{\theta})\partial_\mu\partial^\mu\varphi(x). \end{aligned} \quad (2.71)$$

Under a supersymmetric transformation $\delta\Phi$, the components' variations are expressed as

$$\begin{aligned} \delta\varphi &= \sqrt{2}\epsilon\psi, & \delta\psi &= i\sqrt{2}\sigma^\mu\bar{\epsilon}\partial_\mu\varphi + \sqrt{2}\epsilon F, \\ \delta F &= i\sqrt{2}\bar{\epsilon}\bar{\sigma}^\mu\partial_\mu\psi. \end{aligned} \quad (2.72)$$

Note that δF is a total derivative term, which implies that the F term is invariant under a supersymmetry transformation, which will allow us to build an invariant object $\mathcal{L}(\Phi)$.

Regarding chiral superfields one can show a couple of useful things. The product of chiral superfields is a chiral superfield, and in general any holomorphic function $f(\Phi)$ (does not depend on conjugate terms of the form Φ^*) of a chiral superfield is also chiral. If Φ is chiral, then $\Phi^\dagger = \bar{\Phi}$ is antichiral. $\Phi^\dagger\Phi$ and $\Phi^\dagger + \Phi$ are real superfields but are neither chiral nor anti-chiral.

2.6 Vector Superfields

A vector superfield is defined by the hermiticity constraint $V(x^\mu, \theta, \bar{\theta}) = V^\dagger(x^\mu, \theta, \bar{\theta})$, and takes the general form

$$\begin{aligned} V(x, \theta, \bar{\theta}) = & C(x) + i\theta\chi(x) - i\bar{\theta}\bar{\chi}(x) + \frac{i}{2}\theta\theta(M(x) + iN(x)) - \frac{i}{2}\bar{\theta}\bar{\theta}(M(x) - iN(x)) \\ & + \theta\sigma^\mu\bar{\theta}V_\mu(x) + i\theta\theta\bar{\theta}\left(-i\bar{\lambda}(x) + \frac{i}{2}\bar{\sigma}^\mu\partial_\mu\chi(x)\right) - i\bar{\theta}\bar{\theta}\theta\left(i\bar{\lambda}(x) - \frac{i}{2}\sigma^\mu\partial_\mu\chi(x)\right) \\ & + \frac{1}{2}(\theta\theta)(\bar{\theta}\bar{\theta})\left(D - \frac{1}{2}\partial_\mu\partial^\mu C\right). \end{aligned} \quad (2.73)$$

Again we have the same number of bosonic and fermionic components with $n_B = 8$ (represented by C, M, N, D, V_μ) and $n_F = 8$ (represented by χ_α, ψ_α).

As a caveat we note that we can form a vector superfield from a chiral superfield Λ via the construct $i(\Lambda - \Lambda^\dagger)$. The constructed vector superfield then has its components determined by the Λ 's which have the explicit form

$$\begin{aligned} C = i(\varphi - \varphi^\dagger), \quad \chi(x) = \sqrt{2}\psi, \quad \frac{1}{2}(M + iN) = F, \\ V_\mu = -\partial_\mu(\varphi + \varphi^\dagger), \quad \lambda = D = 0. \end{aligned} \quad (2.74)$$

Using the vector construct, we can now define the generalised gauge transformation

$$V \rightarrow V - \frac{i}{2}(\Lambda - \Lambda^\dagger). \quad (2.75)$$

The reason behind this becomes clear when we recall that a vector field transforms under an abelian gauge transformation as $V_\mu \rightarrow V_\mu + \partial_\mu$, and examine the vector component of our generalised gauge transform

$$V_\mu \rightarrow V_\mu + \partial_\mu(\text{Re}(\varphi)) \equiv V_\mu - \frac{1}{2}\partial_\mu(\varphi + \varphi^\dagger). \quad (2.76)$$

We can gauge away certain components of V via the “gauge choice” associated with the parametric freedom of φ, ψ, F . One such gauge is the *Wess Zumino* (WZ) gauge, which aims to set $C = \chi = M = N = 0$. A vector superfield in the WZ gauge has the form

$$V_{\text{WZ}}(x, \theta, \bar{\theta}) = (\theta\sigma^\mu\bar{\theta})V_\mu(x) + (\theta\theta)(\bar{\theta}\bar{\lambda}(x)) + (\bar{\theta}\bar{\theta})(\theta\lambda(x)) + \frac{1}{2}(\theta\theta)(\bar{\theta}\bar{\theta})D(x). \quad (2.77)$$

Similarly, when we build the MSSM we will identify the V_μ as the SM gauge bosons $\gamma, W^\pm, Z^0, G_\mu$ and the $\lambda, \bar{\lambda}$ as the corresponding gauginos.

With these tools we are almost ready to build a supersymmetric theory that will in some limit resemble the structure of the SM, but we still require gauge invariant constructs and field strength tensors.

2.6.1 Abelian Superfield Field Strength

Given a non-supersymmetric theory, let us consider the case of a complex scalar field φ coupled to a abelian $U(1)$ gauge field V_μ via the covariant derivative contained in the Lagrangian

$$\mathcal{L}_{\varphi V_\mu} = (D_\mu\varphi)^\dagger(D^\mu\varphi). \quad (2.78)$$

The covariant derivative is defined as $D_\mu = \partial_\mu - iqV_\mu$, where q is the scalar field’s charge under the $U(1)$ gauge symmetry. Under a local gauge transformation $\alpha(x)$ the fields transform as

$$\varphi(x) \rightarrow \exp(iq\alpha(x))\varphi(x), \quad (2.79)$$

$$V_\mu(x) \rightarrow V_\mu + \partial_\mu\alpha(x). \quad (2.80)$$

Associated with V_μ we have the field strength tensor which is defined as

$$F_{\mu\nu} = \partial_\mu V_\nu - \partial_\nu V_\mu. \quad (2.81)$$

We now want to construct a supersymmetric analogue using our previously defined superfields. We saw earlier that we can induce a gauge transformation for a vector superfield V via the chiral superfield Λ construct $V \rightarrow V - \frac{i}{2}(\Lambda - \Lambda^\dagger)$. Analogous to the non-SUSY case, under our imposed generalised gauge transform, we can impose that Φ transforms as $\Phi \rightarrow \exp(iq\Lambda)\Phi$, which in turn results in the gauge invariant

$$\Phi^\dagger \exp(2qV)\Phi. \quad (2.82)$$

Similarly the supersymmetric field strength analogue is defined as

$$W_\alpha \equiv -\frac{1}{4}(\overline{\mathcal{D}}\mathcal{D})\mathcal{D}_\alpha V, \quad (2.83)$$

which, in addition to being invariant under the generalised SUSY gauge transformations, is chiral. In the Wess-Zumino gauge the components of W_α are expressed in terms of the $y^\mu = x^\mu + i\theta\sigma^\mu\bar{\theta}$ super-coordinate as

$$W_\alpha(y, \theta) = \lambda_\alpha(y) + \theta_\alpha D(y) + (\sigma^{\mu\nu}\theta)_\alpha F_{\mu\nu} - i(\theta\theta)(\sigma^\mu)_{\alpha\dot{\beta}}\partial_\mu\bar{\lambda}^{\dot{\beta}}(y). \quad (2.84)$$

2.6.2 Non-abelian Superfield Field Strength

We now want to generalise the above to the non-abelian case. Instead of the $U(1)$ symmetry, we now have a non-abelian gauge group defined by a Lie algebra spanned by hermitian generators T^a

$$[T^a, T^b] = if^{abc}T_c. \quad (2.85)$$

In the non-abelian case the gauge fields have an additional set of degrees of freedom, which have an index associated with the generators of the Lie algebra

$$\Lambda = \Lambda_a T^a, \quad V = V_a T^a. \quad (2.86)$$

Analogous to what we did in the abelian case, we want to keep the construct analogous to $\Phi^\dagger \exp(2qV)\Phi$ invariant under the super-gauge transformation $\Phi \rightarrow \exp(iq\Lambda)\Phi$. Due to the non-commutative nature of Λ, V , the generalised gauge transformation induces a non-linear transformation law $V \rightarrow V'$ defined by the gauge invariant

$$\begin{aligned} \exp(2qV') &= \exp(iq\Lambda^\dagger) \exp(2qV) \exp(-iq\Lambda) \\ &= \exp\left(iq\Lambda^\dagger + 2qV + \frac{1}{2}[iq\Lambda^\dagger, 2qV] + \dots\right) \exp(-iq\Lambda) \\ &= \exp\left(2qV + iq(\Lambda^\dagger - \Lambda) + \frac{1}{2}[iq\Lambda^\dagger, 2qV] - \frac{1}{2}[iq\Lambda^\dagger, 2qV] + \dots\right) \\ &= \exp\left(2qV - iq(\Lambda - \Lambda^\dagger) - iq^2[V, \Lambda + \Lambda^\dagger] + \dots\right) \end{aligned} \quad (2.87)$$

where we've used the Baker-Campbell-Hausdorff expansion for matrix exponentials [42]. Therefore the induced gauge transformation has the form

$$V \rightarrow V - \frac{i}{2}(\Lambda - \Lambda^\dagger) - \frac{iq}{2}[V, \Lambda + \Lambda^\dagger] + \dots \quad (2.88)$$

Similarly, the field strength is determined by the analogous invariance arguments. In the non-SUSY theory the field strength transformed as the adjoint $F_{\mu\nu} \rightarrow U F_{\mu\nu} U^{-1}$. The explicit supersymmetric form is then

$$W_\alpha \equiv -\frac{1}{8q}(\overline{D}\overline{D})(\exp(-2qV)\mathcal{D}_\alpha \exp(2qV)). \quad (2.89)$$

Analogous to the abelian case, in the Wess-Zumino gauge, the supersymmetric field strength can be expressed in terms of the super-coordinate y^μ as

$$W_\alpha^a(y, \theta) = \lambda_\alpha^a(y) + \theta_\alpha D^a(y) + (\sigma^{\mu\nu}\theta)_\alpha F_{\mu\nu}^a(y) - i(\theta\theta)(\sigma^\mu)_{\alpha\dot{\beta}} D_\mu \bar{\lambda}^{a\dot{\beta}}(y), \quad (2.90)$$

where $F_{\mu\nu}^a$, and $D_\mu \bar{\lambda}^a$ are the classic field strength, and gauge covariant derivative. These are identical to the non-SUSY case and are defined as $F_{\mu\nu}^a \equiv \partial_\mu V_\nu^a - \partial_\nu V_\mu^a + qf_{bc}^a V_\mu^b V_\nu^c$, and $D_\mu \bar{\lambda}^a = \partial_\mu \bar{\lambda}^a + qV_\mu^b \bar{\lambda}^c f_{bc}^a$ respectively.

2.7 4D, $\mathcal{N} = 1$ SUSY

We now have all the tools in place to be able to write a supersymmetric theory in 4 dimensions, which will resemble the SM. Using our $\mathcal{N} = 1$ SUSY representations we now need to build Lagrangians that are invariant under the SUSY transformation, i.e. the Lagrangian \mathcal{L} will have to be an object that under a supersymmetric transformation has a variation $\delta\mathcal{L}$ that is a total derivative.

The simplest construction comes from using chiral superfields. To be able to find objects formed by superfields that transform as total derivatives we note that a general scalar superfield S as shown in Eqn. (2.64) contains the “D-term” $\sim (\theta\theta)(\bar{\theta}\bar{\theta})D(x^\mu)$. The $D(x^\mu)$ field transforms under the supersymmetric transformation in Eqn. (2.63) as

$$\delta D = \frac{i}{2}\partial_\mu (\epsilon\sigma^\mu \bar{\lambda} - \rho\sigma^\mu \bar{\epsilon}), \quad (2.91)$$

where $\epsilon, \bar{\epsilon}$ are the SUSY transformation parameters, and $\rho, \bar{\lambda}$ are the fields contained in S corresponding to the $\sim (\bar{\theta}\bar{\theta})\theta, \sim (\theta\theta)\bar{\theta}$ terms.

Secondly we recall from Eqn. (2.72) that a chiral superfield Φ contains the “F-term” $\sim (\theta\theta)F(x)$, which also transforms as a total derivative

$$\delta F = i\sqrt{2}\bar{\epsilon}\sigma^\mu \partial_\mu \psi. \quad (2.92)$$

We can now use chiral superfields as the building blocks of our Lagrangian. Recalling that any holomorphic function of chiral superfields results in a chiral superfield,

and that a real function of a chiral superfield results in a general scalar superfield, the most general Lagrangian that we can form using a chiral superfield Φ consists of

$$\mathcal{L} = K(\Phi, \Phi^\dagger) \Big|_D + \left(W(\Phi) \Big|_F + \text{h.c.} \right). \quad (2.93)$$

The $\Big|_D$ and $\Big|_F$ evaluation refer to keeping only the D-terms and F-terms of the corresponding constructs. The real function K (known as the Kähler potential), is a function of Φ, Φ^\dagger , and W (known as the superpotential) is a holomorphic function of Φ .

We now have an object that satisfies our SUSY transformation requirement. Our proto-Lagrangian now needs further refinement such that it will be renormalisable and possess mass dimension 4. To this extent the mass dimension of the superfield is the same as its scalar component $[\Phi] = [\varphi]$, which can be seen from the Taylor expansion in θ . In the usual fashion the scalar and fermionic components have mass dimensions

$$[\varphi] = 1, \quad [\psi] = \frac{3}{2}. \quad (2.94)$$

For the Taylor expansion $\Phi \sim \varphi + \sqrt{2}\theta\psi + \theta\theta F$ to be consistent with the scalar and fermion's mass dimensions, it follows that $[\theta] = -\frac{1}{2}$, and $[F] = 2$. Therefore looking at the D ($\sim \theta^4$) and F ($\sim \theta^2$) terms of K, W , the renormalisability and mass dimension constraints require

$$[K] \leq 2, \quad [W] \leq 3. \quad (2.95)$$

Putting all of this together results in the most general expression for the Kähler potential and superpotential that can be built with only chiral superfields. This Lagrangian is known as the Wess-Zumino model [43]

$$\mathcal{L} = \Phi^\dagger \Phi \Big|_D + \left(\left(\alpha + \lambda\Phi + \frac{m}{2}\Phi^2 + \frac{g}{3}\Phi^3 \right) \Big|_F + \text{h.c.} \right), \quad (2.96)$$

where α, λ, m, g are coupling constants with appropriate mass dimensions. In terms of the bosonic and fermionic components, the breakdown of the Wess-Zumino model consists of

$$\begin{aligned} \mathcal{L} = & (\partial^\mu \varphi^* \partial_\mu \varphi - i\bar{\psi} \bar{\sigma}^\mu \partial_\mu \psi + F^* F) \\ & + \left(\left(\frac{\partial W}{\partial \varphi} F + \text{h.c.} \right) - \frac{1}{2} \left(\frac{\partial^2 W}{\partial \varphi^2} \psi \psi + \text{h.c.} \right) \right), \end{aligned} \quad (2.97)$$

where the first line corresponds to the D-term of $\Phi^\dagger \Phi$, and the 2nd line to the F-Term of the super-potential which is obtained via a Taylor expansion around

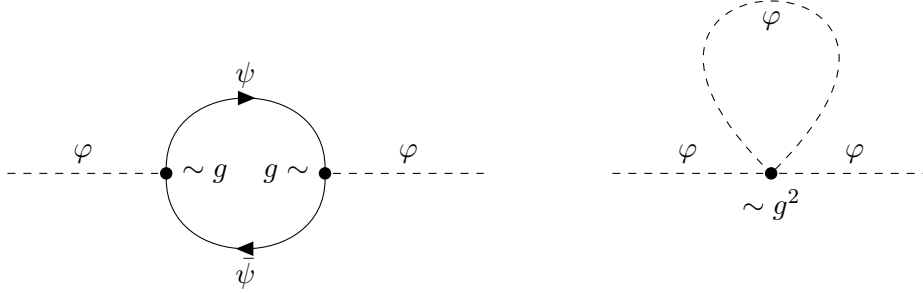


Figure 2.1: Scalar 1 loop corrections arising from the fermionic and scalar contributions.

$\Phi = \varphi$. We note that the Lagrangian for the F auxiliary field does not contain any derivative terms ($\sim \partial_\mu F$). Therefore the F field is not a propagating degree of freedom, and can be eliminated via the equations of motion ($F^* + \partial W / \partial \varphi = 0$ and its complex conjugate) and substituted into the Lagrangian (replacing the $F^* F$ and $((\partial W / \partial \varphi) F + \text{h.c.})$ terms), contributing to the scalar potential of φ as

$$V_F(\varphi) = - \left| \frac{\partial W}{\partial \varphi} \right|^2. \quad (2.98)$$

After eliminating the F field, from the form of the potential we note two main ideas:

- The masses of the scalar and the fermion are identical since their mass terms are dictated by the quadratic term of the superpotential and the 2nd derivative

$$m_\phi = m_\psi \sim m \sim \frac{\partial^2 W}{\partial \varphi^2}. \quad (2.99)$$

- The Yukawa coupling and the scalar self coupling are completely determined by the coefficient g

$$y_{\psi\varphi} \sim g(\varphi \bar{\psi} \psi), \quad \lambda_\varphi \sim g^2 |\varphi|^4. \quad (2.100)$$

In essence, this is the source of the SUSY cancellations present in the MSSM (shown in Fig. 2.1) which with an appropriate SUSY breaking scale solve the Hierarchy problem in the SM (see Sec. 2.8.1).

We now need to introduce vector fields. Starting with the *abelian* case, recalling from Sec. 2.6.1, we can introduce a vector field V such that the construct

$$K = \Phi^\dagger \exp(2qV) \Phi, \quad (2.101)$$

is invariant under the general gauge transformation $V \rightarrow V - \frac{i}{2} (\Lambda - \Lambda^\dagger)$. Note that this will now replace the Kähler potential in the WZ model since $\Phi^\dagger \Phi$ is not invariant under the gauge transform. Similarly in the WZ gauge we include the D-term of the Kähler potential, which in terms of fermionic and bosonic components is expressed as

$$\begin{aligned} \left(\Phi^\dagger \exp(2qV) \Phi \right) \Big|_D &= \partial^\mu \varphi^* \partial_\mu \varphi + i \bar{\psi} \bar{\sigma}^\mu \partial_\mu \psi + F^* F \\ &\quad + q V^\mu (\bar{\psi} \bar{\sigma}_\mu \psi + i \varphi^* \partial_\mu \varphi - i \varphi \partial_\mu \varphi^*) \\ &\quad + \sqrt{2} q (\varphi \bar{\lambda} \bar{\psi} + \varphi^* \lambda \psi) + q (D + q V_\mu V^\mu) |\varphi|^2 \end{aligned} \quad (2.102)$$

We still require a kinetic term for V , which is provided by the W_α construct from Sec. 2.6.1. Similarly to a non-SUSY theory the field strength term analogue is introduced via the superpotential W and has the form

$$W_{\text{kin}} = f(\Phi) (W_\alpha W^\alpha + \text{h.c.}), \quad (2.103)$$

where f is called the gauge kinetic function. The Lagrangian is renormalisable if $f(\Phi)$ is a constant. In the WZ gauge the F-term is included in the Lagrangian, which in terms of fermionic and bosonic components is expressed as

$$W_\alpha W^\alpha \Big|_F + \text{h.c.} = 2D^2 - F_{\mu\nu} F^{\mu\nu} - i \lambda \sigma^\mu \partial_\mu \bar{\lambda}. \quad (2.104)$$

For QED $f(\Phi)$ is chosen as $f = 1/4$.

Lastly, a $U(1)$ invariant SUSY theory admits an additional gauge invariant linear term in V called the Fayet-Iliopoulos (FI) term [44]

$$\mathcal{L}_{\text{FI}} = \xi V \Big|_D = \frac{1}{2} \xi D, \quad (2.105)$$

where the ξ term is a constant. Note that this term cannot appear in non-abelian theories since it would not form a gauge invariant object. The FI term in turn contributes to determining the auxiliary D field via the equations of motion. The D field is then eliminated and provides an additional negative contribution to the scalar potential

$$V_D(\varphi) = -\frac{1}{8} (\xi + 2q|\varphi|^2)^2. \quad (2.106)$$

We can summarise all of the above in a very neat fashion by writing the action as a super-space integral. Recalling that super-Minkowski was determined by the coset of super-Poincare and Lorentz we can write an invariant action S based on the supercoordinates $x^\mu, \theta, \bar{\theta}$. Additionally, we recall that Grassman variables obey

$$\int d^2\theta (\theta\theta) = 1, \quad \int d^2\theta \int d^2\bar{\theta} (\theta\theta)(\bar{\theta}\bar{\theta}) = 1, \quad (2.107)$$

which in turn provides us with a compact way of expressing the F and D terms. Putting all of this together, the most general action in superspace can be written as

$$S \left[K \left(\Phi_i^\dagger, \exp(2qV), \Phi_i \right); W(\Phi_i), f(\Phi_i), \xi \right] = \int d^4x \int d^4\theta (K + \xi D) \\ + \int d^4x \int d^2\theta (W + fW_\alpha W^\alpha + \text{h.c.}). \quad (2.108)$$

In the case of a non-abelian theory the above action no longer admits the FI term, and in addition requires an extra trace for the gauge field strength to keep it gauge invariant

$$W_\alpha W^\alpha \rightarrow \text{Tr} (W_\alpha W^\alpha). \quad (2.109)$$

2.8 The Minimal Supersymmetric Model (MSSM)

We are now prepared to write a minimal supersymmetric model which will contain the SM. Therefore we want to write a $SU(3)_C \times SU(2)_L \times U(1)_Y$ invariant theory that will then break down to $SU(3)_C \times U(1)_{\text{EM}}$. To this extent we will introduce:

- Abelian and non-abelian vector superfields corresponding to each of the unbroken gauge groups, which will contain the SM gauge bosons, along with their fermionic superpartners, i.e. the *gauginos*.
- Chiral superfields that will include 3 generations of quarks and leptons along with their superpartners, *squarks and sleptons*.
- To achieve $SU(2)_L \times U(1)_Y \rightarrow U(1)_{\text{EM}}$ breaking we require two chiral superfields which contain two scalar Higgs fields with opposite hypercharges (in order to avoid a gauge anomaly) along with the fermionic superpartners, the *higgsinos*.
- Finally, since supersymmetry is not a symmetry of the IR (since we do not observe degenerate mass SUSY partners for the SM fields), if it is present in nature it must be broken at a scale between the IR ($\sim 91\text{GeV}$) and UV ($\sim M_{\text{Pl}} \sim 10^{18}\text{GeV}$) that is consistent with our current experimental knowledge.

Superfield	Component Names	Spin $\frac{1}{2}$	Spin 1	G_{SM} rep.
\hat{G}^a	Gluinos, gluons	\tilde{G}^a	G^a	$(\mathbf{8}, 1, 0)$
\hat{W}^α	Winos, W bosons	$\tilde{W}^\pm, \tilde{W}^0$	W^\pm, W^0	$(1, \mathbf{3}, 0)$
\hat{B}	Binos, B boson	\tilde{B}	B	$(1, 1, 0)$

Table 2.3: Table summarising the gauge fields in the MSSM, where the columns contain the name of the containing superfield, the nomenclature of the components, the notations for the spin 1/2, 1 components, and their charges under the SM gauge group $G_{\text{SM}} = SU(3)_C \times SU(2)_L \times U(1)_Y$.

Superfield	Copies	Component Names	Spin 0	Spin $\frac{1}{2}$	G_{SM} rep.
Q	3 (fams.)	LH u, d s/quarks	$(\tilde{u}_L, \tilde{d}_L)$	(u_L, d_L)	$(\mathbf{3}, \mathbf{2}, \frac{1}{6})$
\bar{u}	3 (fams.)	RH u s/quarks	\tilde{u}_R^*	u_R^\dagger	$(\bar{\mathbf{3}}, 1, -\frac{2}{3})$
\bar{d}	3 (fams.)	RH d s/quarks	\tilde{d}_R^*	d_R^\dagger	$(\bar{\mathbf{3}}, 1, \frac{1}{3})$
L	3 (fams.)	LH s/leptons	$(\tilde{\nu}_L, \tilde{e}_L)$	(ν_L, e_L)	$(1, \mathbf{2}, -\frac{1}{2})$
\bar{e}	3 (fams.)	RH s/leptons	\tilde{e}_R^*	e_R^\dagger	$(1, 1, 1)$
H_u	1	u -type Higgs/inos	(H_u^\dagger, H_u^0)	$(\tilde{H}_u^\dagger, \tilde{H}_u^0)$	$(1, \mathbf{2}, \frac{1}{2})$
H_d	1	d -type Higgs/inos	(H_d^\dagger, H_d^0)	$(\tilde{H}_d^\dagger, \tilde{H}_d^0)$	$(1, \mathbf{2}, -\frac{1}{2})$

Table 2.4: Table summarising the matter fields in the MSSM, where the columns contain the name of the containing superfield, the number of copies of the superfield, the nomenclature of the components, the notations for the spin 0, 1/2 components, and their charges under the SM gauge group G_{SM} .

The gauge interactions are expressed via the D term of the Kähler potential, where we list the breakdown of the vector superfields in terms of spin and G_{SM} representations in Tab. 2.3.

The superpotential of the MSSM consists of

$$W_{\text{MSSM}} = \bar{u}y_uQH_u - \bar{d}y_dQH_d - \bar{e}y_eLH_d + \mu H_u H_d, \quad (2.110)$$

where we have suppressed the various indices (family, spin, colour, weak isospin), y_u, y_d, y_e are 3×3 Yukawa matrices in family space, μ is the SUSY analogue of the Higgs mass, H_u, H_d are Higgs chiral superfields, Q, \bar{u}, \bar{d} are the quark doublet, up type and down type quark superfields, and L, \bar{e} are the lepton doublet and electron singlet superfields. The breakdown of the superfields in terms of spin and G_{SM}

representations is outlined in Tab. 2.4.

We note that in contrast to the SM, the MSSM has two Higgs chiral supermultiplets which are introduced in order to avoid a gauge anomaly. In addition, due to the structure of the superpotential, we require a hypercharge $Y = 1/2$ chiral Higgs such that u type quarks can acquire masses, and another hypercharge $Y = -1/2$ chiral Higgs such that d type quarks can acquire masses.

Going back to the terms in the potential, we now look at the explicit statement of the indices. The $\bar{u}y_uQH_u$ term consists of

$$\bar{u}^{ia}(y_u)_i^j Q_{j\alpha a}(H_u)_\beta \varepsilon^{\alpha\beta}, \quad (2.111)$$

where $i = 1, 2, 3$ is the family index, a is the colour index, α, β are weak isospin indices, and $\varepsilon^{\alpha\beta}$ is the $SU(2)$ invariant anti-symmetric symbol. The $\bar{d}y_dQH_d, \bar{e}y_eLH_d$ terms have an analogous structure, and the $\mu H_u H_d$ holomorphic term is written out as

$$\mu(H_u)_\alpha(H_d)_\beta \varepsilon^{\alpha\beta}. \quad (2.112)$$

We also note, since the superpotential must be holomorphic in chiral superfields (i.e. doesn't admit terms of the form Φ^\dagger as specified in Eqn. (2.93)), Higgs terms of the form $H_u^*H_u$ and $H_d^*H_d$ are forbidden. Furthermore, the holomorphic argument also sets the need for two Higgs fields since we cannot use just one Higgs field (as we would in the SM) to simultaneously impart masses to all the fermionic matter fields without resorting to a term involving a conjugate, e.g. $\bar{u}QH_d^*$.

Regarding the Yukawa couplings, we note that post symmetry breaking in the MSSM, during which both H_u, H_d acquire VEVs, the Higgs fields are responsible for the masses of the various quarks, leptons and bosons along with the mixing angles in the CKM matrix.

If we look only at the 3rd generation, and assume the model is flavour diagonal to avoid the phenomenologically dangerous flavour changing neutral currents (FCNCs) (see Ref. [45]) with the Yukawas being 0 apart from the components relating to the top, bottom and tau $y_u \simeq (y_u)_{3,3} \equiv y_t; y_d \simeq (y_d)_{3,3} \equiv y_b; y_e \simeq (y_e)_{3,3} \equiv y_\tau$, we can write out the MSSM superpotential in terms of the constituent $SU(2)_L$ fields

$$\begin{aligned} Q_3 &= (t, b), & L_3 &= (\nu_\tau, \tau), & H_u &= (H_u^+, H_u^0), & H_d &= (H_d^+, H_d^0) \\ \bar{u}_3 &= \bar{t}, & \bar{d}_3 &= \bar{b}, & \bar{e}_3 &= \bar{\tau}. \end{aligned} \quad (2.113)$$

In the unbroken gauge eigenbasis the superpotential is then expressed as

$$W_{\text{MSSM}} = y_t (\bar{t}tH_u^0 - \bar{t}bH_u^+) - y_b (\bar{b}tH_d^- - \bar{b}bH_d^0) - y_\tau (\bar{\tau}\nu_\tau H_d^- - \bar{\tau}\tau H_d^0) + \mu (H_u^+ H_d^- - H_u^0 H_d^0). \quad (2.114)$$

Breaking the superpotential down in terms of the constituent bosonic and fermionic fields, we note that the Yukawa interactions will also specify the couplings between the Higgs fields, fermions and their superpartners. The Lagrangian terms have the general form $H\tilde{q}q, H\tilde{l}l$ which are $\mathcal{O}(y^1)$ with respect to the Yukawas, and result from the $\partial^2 W / \partial \varphi^2$ terms. In addition the $|\partial W / \partial \varphi|^2$ scalar potential will contribute with 4 point interactions of the form $\tilde{q}^* \tilde{q} H^* H$, and $\tilde{q}_L^* \tilde{q}_L \tilde{q}_R^* \tilde{q}_R$ which are $\mathcal{O}(y^2)$. We note that all these couplings are dimensionless; the dimensionful couplings are specified by the μ term which provide higgsino and Higgs squared mass terms

$$\mathcal{L}_{\text{Higgs}} = \mu (\tilde{H}_u^+ \tilde{H}_d^- - \tilde{H}_u^0 \tilde{H}_d^0) + \text{c.c.} + |\mu|^2 (|H_u^0|^2 + |H_u^+|^2 + |H_d^0|^2 + |H_d^-|^2). \quad (2.115)$$

We note that this potential is flat with the minimum lying at 0, i.e. we cannot achieve electro-weak symmetry breaking (EWSB) in the current state. This will be solved later on when we introduce soft-SUSY breaking terms which will trigger EWSB in addition to breaking supersymmetry. Finally we note that $\partial W / \partial H$ term combines the μ with the Yukawa couplings to yield the cubic scalar couplings

$$\mathcal{L}_{\phi^3} = \mu^* (\tilde{u}y_u \tilde{u}(H_d^0)^* + \tilde{d}y_d \tilde{d}(H_u^0)^* + \tilde{e}y_e \tilde{e}(H_u^0)^* + \tilde{u}y_u \tilde{d}(H_d^-)^* + \tilde{d}y_d \tilde{u}(H_u^+)^* + \tilde{e}y_e \tilde{\nu}(H_u^+)^*) + \text{c.c.}, \quad (2.116)$$

which determine the mixing of squarks, and sleptons.

One last closing remark before we move on to SUSY breaking, the MSSM is minimal in the sense that we haven't included any baryon (B) or lepton (L) violating terms. The most general such superpotential has the form

$$W_{\Delta L=1} = \frac{1}{2} \lambda^{ijk} L_i L_j \bar{e}_k + \lambda'^{ijk} L_i Q_j \bar{d}_k + \mu^i L_i H_u. \quad (2.117)$$

$$W_{\Delta B=1} = \frac{1}{2} \lambda''^{ijk} \bar{u}_i \bar{d}_j \bar{d}_k. \quad (2.118)$$

These in turn contribute to proton decay via diagrams of the form shown in Fig. 2.2.

This issue is dealt with in the MSSM by introducing matter parity defined via the $U(1)$ automorphism mentioned in Sec. 2.1, which is a discrete symmetry that

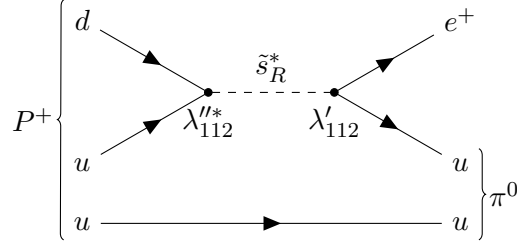


Figure 2.2: SUSY scalar B-L violating term contributing to the dimension 6 Feynman diagram for proton decay.

gives fields values based on their $B - L$ numbers

$$P_M = (-1)^{3(B-L)}. \quad (2.119)$$

This can be recast in terms of the field's spin s as $P_R = (-1)^{3(B-L)+2s}$, which is known as R-parity. This in turn has the effect of eliminating the B, L violating terms.

2.8.1 Soft SUSY Breaking in the MSSM

The supersymmetric theory has all been set up, we now only need to break supersymmetry and induce EWSB. We want to introduce terms that break SUSY explicitly, which for the aims of this discussion will have positive mass dimension terms also known as *soft SUSY breaking mass terms*. The most general soft SUSY breaking Lagrangian has the form

$$\mathcal{L}_{\text{soft}} = - \left(\frac{1}{2} M_a \lambda_a \lambda^a + \frac{1}{6} a^{ijk} \phi_i \phi_j \phi_k + \frac{1}{2} b^{ij} \phi_i \phi_j + t^i \phi_i \right) + \text{c.c.} \quad (2.120)$$

$$- (m^2)_j^i (\phi^j)^* \phi_i,$$

$$\mathcal{L}_{\text{maybe-soft}} = - \frac{1}{2} c_i^{jk} (\phi^i)^* \phi_j \phi_k + \text{c.c.}, \quad (2.121)$$

where the terms consist of gaugino masses M_a for each of the gauge groups, scalar masses $(m^2)_j^i, b^{ij}$, trilinear scalar couplings a^{ijk}, c^{ijk} , and tadpole couplings t^i . Note that including fermionic soft breaking mass terms such as $\mathcal{L} = -\frac{1}{2} m^{ij} \psi_i \psi_j + \text{c.c.}$ are neglected since it would be redundant; the fields and couplings can be reabsorbed into a redefinition of the superpotential and the terms $(m^2)_j^i, c_i^{jk}$. The Lagrangian in Eqn. (2.121) contains the general inclusion of the non-holomorphic scalar cubed couplings, which gets its namesake from the problematic nature associated with it. This consists of the possibility of the formally soft c^{ijk} terms causing quadratic

divergences, when the theory contains chiral supermultiplets that transform as singlets under any of the internal gauge symmetries. We note that this does not apply to the MSSM, since it does not contain any gauge singlet chiral supermultiplets. Moreover, the Lagrangian in Eqn. (2.121) is usually ignored, leaving Eqn. (2.120) as the general form of the soft supersymmetry breaking Lagrangian.

Following this general prescription, the MSSM soft SUSY breaking Lagrangian consists of

$$\begin{aligned} \mathcal{L}_{\text{soft}}^{\text{MSSM}} = & -\frac{1}{2} \left(M_3 \tilde{g} \tilde{g} + M_2 \tilde{W} \tilde{W} + M_1 \tilde{B} \tilde{B} + \text{c.c.} \right) \\ & - \left(\tilde{u} a_u \tilde{Q} H_u - \tilde{d} a_d \tilde{Q} H_d - \tilde{e} a_e \tilde{L} H_d + \text{c.c.} \right) \\ & - \left(\tilde{Q}^\dagger m_Q^2 \tilde{Q} + \tilde{L}^\dagger m_L^2 \tilde{L} + \tilde{u} m_u^2 \tilde{u}^\dagger + \tilde{d} m_d^2 \tilde{d}^\dagger + \tilde{e} m_e^2 \tilde{e}^\dagger \right) \\ & - \left(m_{H_u}^2 H_u^* H_u + m_{H_d}^2 H_d^* H_d + (b H_u H_d + \text{c.c.}) \right), \end{aligned} \quad (2.122)$$

where M_1, M_2, M_3 ($\sim M_a \lambda_a \lambda^a$) are the wino, bino and gluino terms; a_u, a_d, a_e ($\sim a^{ijk} \phi_i \phi_j \phi_k$) are the trilinear couplings which are 3×3 matrices in family space with mass dimension $[a_u] = M^1$ and have a 1-1 correspondence to the Yukawa matrices; $m_Q^2, m_L^2, m_u^2, m_d^2, m_e^2$ ($\sim (m^2)_j^i (\phi^j)^* \phi_i$) are the quark and lepton SUSY breaking matrices which are 3×3 complex hermitian matrices; and $m_{H_u}^2, m_{H_d}^2$ ($\sim (m^2)_j^i (\phi^j)^* \phi_i$), b ($\sim b^{ij} \phi_i \phi_j$) are Higgs soft breaking masses. In total these amount to 105 masses, phases and mixing angles that are not present in the SM Lagrangian [46].

Note, if we follow a naturalness argument we can infer the soft SUSY breaking scale m_{soft} (i.e. the scale of the soft parameters) by looking at the radiative corrections to the Higgs mass

$$\Delta m_H^2 \sim m_{\text{soft}}^2 \ln \frac{\Lambda_{\text{UV}}}{m_{\text{soft}}}, \quad (2.123)$$

where Λ_{UV} is the cutoff scale at which our formalism breaks down and some new physics becomes relevant. Taking this cutoff as the Planck scale (at which we expect quantum gravity to play a significant role) $\Lambda_{\text{UV}} \sim M_{\text{Pl}} \sim 10^{18} \text{GeV}$, in order for SUSY to be relevant to the Hierarchy problem we require $m_{\text{soft}}^2 \sim (\text{TeV})^2$.

So far we have introduced soft breaking masses that facilitate the breaking of supersymmetry. We now look at how this affects EW symmetry breaking. Including

the soft breaking masses the two Higgs doublet model has the structure

$$\begin{aligned}
V_{\text{Higgs}} = & (|\mu|^2 + m_{H_u}^2) (|H_u^0|^2 + |H_u^+|^2) + (|\mu|^2 + m_{H_d}^2) (|H_d^0|^2 + |H_d^-|^2) \\
& + [b (H_u^+ H_d^- - H_u^0 H_d^0)] \\
& + \frac{1}{8} (g^2 + g'^2) (|H_u^0|^2 + |H_u^+|^2 - |H_d^0|^2 - |H_d^-|^2) + \frac{1}{2} g^2 |H_u^+ H_d^0 + H_u^0 H_d^-|^2,
\end{aligned} \tag{2.124}$$

where g, g' are the $SU(2)_L$ and $U(1)_Y$ gauge couplings. The last line of terms arises from the kinetic part of $W_\alpha W^\alpha$ terms, more specifically the auxiliary D-fields, which in the non-abelian case have the generalised form $\frac{1}{2} \sum_a D^a D^a = \frac{1}{2} \sum g_a^2 (\phi T^a \phi)^2$. The Higgs fields are the only scalar fields that develop a VEV, since the other scalar terms in the potential involving squarks and sleptons have large positive squared masses leading to trivial vacuums for the respective fields.

Using the gauge freedom associated with $SU(2)_L$ we can rotate away a component of the VEV for one of the scalars, in this case $H_u^+ = 0$ at the minimum of the potential, which in turn implies that $H_d^- = 0$. Therefore we are left with the scalar potential

$$\begin{aligned}
V = & (|\mu|^2 + m_{H_u}^2) |H_u^0|^2 + (|\mu|^2 + m_{H_d}^2) |H_d^0|^2 - (b H_u^0 H_d^0 + \text{c.c.}) \\
& + \frac{1}{8} (g^2 + g'^2) (|H_u^0|^2 - |H_d^0|^2).
\end{aligned} \tag{2.125}$$

We can further simplify the b term by noting that we can reabsorb its complex phase into the definition of H_u^0, H_d^0 , which in turn allows us to take b as being real, $b \in \mathbb{R}$ with $b \geq 0$. Therefore, to develop a non-trivial minimum for the potential V we require that the product $\langle H_u^0 \rangle \langle H_d^0 \rangle$ be both real and positive, or equivalently that $\langle H_u^0 \rangle$ and $\langle H_d^0 \rangle$ have opposite phases. This can be done via a gauge transformation associated with the $U(1)_Y$ gauge freedom. In addition, we need to bound the potential from below, which in turn places the constraint on the soft-SUSY breaking masses

$$2b < 2|\mu|^2 + m_{H_u}^2 + m_{H_d}^2. \tag{2.126}$$

The holomorphic b term is now bounded from above, but to ensure the non-trivial minimum away from $H_u^0 = H_d^0 = 0$ we also require

$$b^2 > (|\mu|^2 + m_{H_u}^2) (|\mu|^2 + m_{H_d}^2). \tag{2.127}$$

With the constraints in place, we can now look at how EWSB works in the MSSM. First, we define the VEVs of the Higgs fields as

$$\nu_u \equiv \langle H_u^0 \rangle, \quad \nu_d \equiv \langle H_d^0 \rangle. \tag{2.128}$$

The two VEVs work together to set the electroweak scale via the mass of the Z^0 boson as

$$\nu_u^2 + \nu_d^2 = \nu^2 = \frac{2m_Z^2}{g^2 + g'^2} \sim (174\text{GeV})^2. \quad (2.129)$$

Note that we are using a slightly different convention than in Sec. 1.4, where in this case the definition of ν has the factor of $1/\sqrt{2}$ absorbed into its definition. A traditional parametrisation involves the ratio of the two VEVs, which is defined as

$$\tan \beta = \frac{\nu_u}{\nu_d}. \quad (2.130)$$

Furthermore, since $\nu_u, \nu_d \in \mathbb{R}$, we can make the identification $\nu_u = \nu \sin \beta$, $\nu_d = \nu \cos \beta$, which implies that $\beta \in [0, \pi/2]$. The minimum of the potential is determined by simultaneously solving the tadpole equations

$$\frac{\partial V}{\partial H_u^0} = \frac{\partial V}{\partial H_d^0} = 0, \quad (2.131)$$

which when expressed in the aforementioned parametrisation become

$$\begin{cases} m_{H_u}^2 + |\mu|^2 - b \cot \beta - \frac{1}{2}m_Z^2 \cos 2\beta = 0, \\ m_{H_d}^2 + |\mu|^2 - b \tan \beta - \frac{1}{2}m_Z^2 \cos 2\beta = 0. \end{cases} \quad (2.132)$$

As long as we are consistent with the parameter choices and bound constraints on b , the two tadpole equations have a solution. To make this consistent with SM experimental observations, we can recast the above, such that m_Z^2 and $\tan \beta$ become output parameters, dependent on the input parameters $m_{H_u}^2, m_{H_d}^2, \mu, b$, as

$$\sin 2\beta = \frac{2b}{m_{H_u}^2 + m_{H_d}^2 + 2|\mu|^2}, \quad m_Z^2 = \frac{|m_{H_d}^2 - m_{H_u}^2|}{\sqrt{1 - \sin(2\beta)}} - m_{H_u}^2 - m_{H_d}^2 - 2|\mu|^2. \quad (2.133)$$

This recasting gives us a more intuitive feel of the required values for $m_{H_u}^2, m_{H_d}^2, \mu, b$ to obtain a valid SM spectrum, and allows us to check if our parameter choices produce a valid Z^0 mass. In addition these equations highlight an issue with the MSSM, also known as the “ μ problem”. Namely, we have a mismatch in scales arising from the nature of μ which originates from a SUSY invariant term associated with high energies, whereas $m_{H_u}^2, m_{H_d}^2$ are soft-SUSY breaking parameters which should be of the order $\mathcal{O}(\text{TeV})$. Even with some mechanism that relates μ to the SUSY breaking scale there is still quite a bit of fine-tuning required to produce the right SM masses. We can see this expanding Eqn. (2.133) for large values of $\tan \beta$

$$m_Z^2 = -2(m_{H_u}^2 + |\mu|^2) + \frac{2}{\tan^2 \beta}(m_{H_d}^2 - m_{H_u}^2) + \mathcal{O}\left(\frac{1}{\tan^4 \beta}\right). \quad (2.134)$$

We note in order to get the right Z^0 mass, we require a small amount of fine tuning ($\sim 10\%$). Namely we need $m_{H_d}^2$ to be larger than $m_{H_u}^2$ and to conspire in such a way that their difference weighted by $2/\tan^2\beta$ partly cancels with $2(m_{H_u}^2 + |\mu|^2)$ to obtain m_Z^2 , all whilst maintaining $m_{H_u}, m_{H_d}, \mu, b > \mathcal{O}(\text{TeV})$. This mismatch between EW parameters and the new physics occurring at the TeV scale is known as “the little hierarchy problem”.

This effect becomes even worse when looking at the 1 loop calculation of the Higgs mass where we need to keep the top squarks light (which have their mass dictated by the overall scale of soft-SUSY breaking) which in turn feed into the running of $m_{H_u}^2$. One needs to include the loop corrections to the Higgs potential. Namely at one and two loop, the potential receives corrections ΔV of the form [47, 48] which in turn provide the corrected tadpole equations

$$\frac{\partial V}{\partial H_u} + \frac{\partial \Delta V}{\partial H_u} = 0, \quad \frac{\partial V}{\partial H_d} + \frac{\partial \Delta V}{\partial H_d} = 0. \quad (2.135)$$

These in turn provide corrections to $m_{H_u}^2, m_{H_d}^2$,

$$m_{H_u}^2 \rightarrow m_{H_u}^2 + \frac{1}{2\nu_u} \frac{\partial \Delta V}{\partial \nu_u}, \quad (2.136)$$

$$m_{H_d}^2 \rightarrow m_{H_d}^2 + \frac{1}{2\nu_d} \frac{\partial \Delta V}{\partial \nu_d}. \quad (2.137)$$

which in turn further complexify our fine-tuning problem.

2.8.2 Mass Spectrum of the MSSM - Higgs Sector

We now move on to the mass spectrum of the various fields present in the MSSM, where we start our discussion with the Higgs sector. The Higgs fields in the MSSM are two complex $SU(2)_L$ doublets, which consist of 8 real scalar degrees of freedom, which after EWSB form or contribute to the following mass eigenstates:

- G^0, G^\pm which are “swallowed up” by the Z^0, W^\pm and become longitudinal modes of the now massive gauge bosons.
- h^0, H^0 which are CP-even neutral scalars (where by convention h^0 is the lighter one).
- A^0 which is a CP-odd neutral pseudo-scalar.
- H^+, H^- which are charged $Q = +1$ and $Q = -1$ scalars.

The mass eigenstates can be expressed in terms of the gauge eigenstate fields (H_u^0, H_d^0) in a diagonal basis

$$\begin{pmatrix} H_u^0 \\ H_d^0 \end{pmatrix} = \begin{pmatrix} \nu_u \\ \nu_d \end{pmatrix} + \frac{1}{\sqrt{2}} R_\alpha \begin{pmatrix} h^0 \\ H^0 \end{pmatrix} + \frac{i}{\sqrt{2}} R_{\beta_0} \begin{pmatrix} G^0 \\ A^0 \end{pmatrix}, \quad (2.138)$$

$$\begin{pmatrix} H_u^+ \\ (H_d^-)^* \end{pmatrix} = R_{\beta_\pm} \begin{pmatrix} G^+ \\ H^+ \end{pmatrix}, \quad (2.139)$$

where by convention G^-, H^- are defined as $G^- = (G^+)^*, H^- = (H^+)^*$. The R_γ matrices ($\gamma \in \{\alpha, \beta_0, \beta_\pm\}$) are orthogonal rotation matrices

$$R_\alpha = \begin{pmatrix} \cos \alpha & \sin \alpha \\ -\sin \alpha & \cos \alpha \end{pmatrix}, R_{\beta_0} = \begin{pmatrix} \sin \beta_0 & \cos \beta_0 \\ -\cos \beta_0 & \sin \beta_0 \end{pmatrix}, R_{\beta_\pm} = \begin{pmatrix} \sin \beta_\pm & \cos \beta_\pm \\ -\cos \beta_\pm & \sin \beta_\pm \end{pmatrix}, \quad (2.140)$$

which are chosen such that the quadratic terms in the Higgs potential have diagonal masses

$$V = \frac{1}{2} m_{h^0}^2 (h^0)^2 + \frac{1}{2} m_{H^0}^2 (H^0)^2 + \frac{1}{2} m_{G^0}^2 (G^0)^2 + \frac{1}{2} m_{A^0}^2 (A^0)^2 \\ + m_{G^\pm}^2 |G^\pm|^2 + m_{H^\pm}^2 |H^\pm|^2 + \dots \quad (2.141)$$

The various accompanying tree level masses are determined by the VEVs ν_u, ν_d that minimise the potential (which reduce $\beta = \beta_0 = \beta_\pm$ and $m_{G^0}^2 = m_{G^\pm}^2 = 0$ in line with the longitudinal mode absorption), and are

$$m_{A^0}^2 = \frac{2b}{\sin(2\beta)} = 2|\mu|^2 + m_{H_u}^2 + m_{H_d}^2, \quad (2.142)$$

$$m_{h^0, H^0}^2 = \frac{1}{2} \left(m_{A^0}^2 + m_Z^2 \mp \sqrt{(m_{A^0}^2 - m_Z^2)^2 + 4m_Z^2 m_{A^0}^2 \sin^2(2\beta)} \right), \quad (2.143)$$

$$m_{H^\pm}^2 = m_{A^0}^2 + m_W^2. \quad (2.144)$$

The mixing angles α, β (by convention α is taken as negative) are then determined by the equations

$$\frac{\sin 2\alpha}{\sin 2\beta} = -\frac{m_{H^0}^2 + m_{h^0}^2}{m_{H^0}^2 - m_{h^0}^2}, \quad \frac{\tan 2\alpha}{\tan 2\beta} = \frac{m_{A^0}^2 + m_{Z^0}^2}{m_{A^0}^2 - m_{Z^0}^2}. \quad (2.145)$$

In addition the Higgs mass receives corrections at 1 loop, which are dominated by top quark/squark loops of the form

$$\Delta(m_h^2) = \text{---} h^0 \text{---} \text{---} + \text{---} h^0 \text{---} \text{---} + \text{---} h^0 \text{---} \text{---} . \quad (2.146)$$

Note that in order for SUSY to be relevant to the hierarchy problem and in line with naturalness we require that the stops \tilde{t} be light such that the fine tuning in Eqn. (2.146) is minimal. This has been a bit more worrisome with the LHC limits pushing the stop masses ever higher [49].

Within the MSSM, the quark masses and the mixing angles in the CKM matrix are determined by the Yukawa couplings in the super-potential, along with $\tan \beta$ parameter determining the up-type and down-type VEVs. At tree level, the masses of the 3rd generation of fermions are

$$m_t = y_t \sin \beta, \quad m_b = y_b \cos \beta, \quad m_\tau = y_\tau \cos \beta. \quad (2.147)$$

The Higgs couplings in the MSSM are similar to the ones present in the SM with an additional complexity introduced by the dependency on α, β . In addition to the SM couplings, the bosonic MSSM Higgs couplings have the additional terms

$$h^0 W^+ W^-, \quad h^0 Z^0 Z^0, \quad Z^0 H^0 A^0, \quad W^\pm H^0 H^\mp \quad \sim \sin(\beta - \alpha), \quad (2.148)$$

$$H^0 W^+ W^-, \quad H^0 Z^0 Z^0, \quad Z^0 h^0 A^0, \quad W^\pm h^0 H^\mp \quad \sim \cos(\beta - \alpha), \quad (2.149)$$

where the fermionic couplings have the accompanying factors

$$h^0 \bar{b} b, \quad h^0 \tau^+ \tau^- \quad \sim \sin(\beta - \alpha) - \tan \beta \cos(\beta - \alpha), \quad (2.150)$$

$$h^0 \bar{t} t \quad \sim \sin(\beta - \alpha) + \cot \beta \cos(\beta - \alpha), \quad (2.151)$$

$$H^0 \bar{b} b, \quad H^0 \tau^+ \tau^- \quad \sim \cos(\beta - \alpha) + \tan \beta \sin(\beta - \alpha), \quad (2.152)$$

$$H^0 \bar{t} t \quad \sim \cos(\beta - \alpha) - \cot \beta \cos(\beta - \alpha), \quad (2.153)$$

$$A^0 \bar{b} b, \quad A^0 \tau^+ \tau^- \quad \sim \tan \beta, \quad (2.154)$$

$$A^0 \bar{t} t \quad \sim \cot \beta. \quad (2.155)$$

In the “decoupling limit” $m_{A^0} \gg m_{Z^0}$ (in which we push the SUSY scale up with respect to the EW scale) α tends to $(\beta - \pi/2)$, where we can express the cosine and

sine terms as

$$\cos(\beta - \alpha) = \sin(2\beta) \cos(2\beta) \frac{m_Z^2}{m_{A^0}^2} + \mathcal{O}\left(\frac{m_{Z^0}^4}{m_{A^0}^4}\right), \quad (2.156)$$

$$\sin(\beta - \alpha) = 1 - \mathcal{O}\left(\frac{m_{Z^0}^4}{m_{A^0}^4}\right). \quad (2.157)$$

In the decoupling limit the lighter h^0 Higgs approaches the same couplings as those present in the SM. These couplings will be modified at one loop, but are not sufficient to cause a sizeable deviation from the SM-like couplings of the Higgs.

2.8.3 Mass Spectrum of the MSSM - Neutralinos & Charginos

Post electroweak symmetry breaking, the gauginos mix with the higgsinos that possess the same quantum numbers to form mass eigenstates, namely *charginos* and *neutralinos*. The charginos are $Q = \pm 1$ mass eigenstates that result from the mixing of the charged higgsinos $\tilde{H}_u^+, \tilde{H}_d^-$ with the corresponding winos \tilde{W}^+, \tilde{W}^- . The neutralinos result from the mixing of the neutral higgsinos $\tilde{H}_u^0, \tilde{H}_d^0$ with the neutral gauginos \tilde{W}^0, \tilde{B} .

To this extent, we label the neutralino states as \tilde{N}_i^0 , where $i = 1, 2, 3, 4$, and the chargino states as $\tilde{C}_1^+, \tilde{C}_2^-$, where we adopt the convention $m_{\tilde{N}_1} < m_{\tilde{N}_2} < m_{\tilde{N}_3} < m_{\tilde{N}_4}$ and $m_{\tilde{C}_1} < m_{\tilde{C}_2}$. \tilde{N}_1 is usually assumed to be the lightest supersymmetric particle (LSP) which makes it the most likely MSSM particle to be a suitable dark matter candidate when working under the assumption of R-parity conservation.

Starting with the neutralinos, in the gauge eigenstate basis $\psi^0 = (\tilde{B}, \tilde{W}^0, \tilde{H}_d^0, \tilde{H}_u^0)$, the Lagrangian containing the masses is expressed as

$$\mathcal{L}_{m_{\tilde{N}}} = -\frac{1}{2}(\psi^0)^T M_{\tilde{N}} \psi^0 + \text{c.c.}, \quad (2.158)$$

where $M_{\tilde{N}}$ is the mass matrix

$$M_{\tilde{N}} = \begin{pmatrix} M_1 & 0 & -g'v_d/\sqrt{2} & g'v_u/\sqrt{2} \\ 0 & M_2 & gv_d/\sqrt{2} & gv_u/\sqrt{2} \\ -g'v_d/\sqrt{2} & gv_d/\sqrt{2} & 0 & -\mu \\ g'v_u/\sqrt{2} & -gv_u/\sqrt{2} & -\mu & 0 \end{pmatrix}. \quad (2.159)$$

M_1, M_2 originate from the soft-SUSY breaking gaugino terms, the μ 's originate from the higgsino terms, and the g, g' terms come from the Higgs-higgsino-gaugino couplings where the Higgs fields are replaced by their respective VEVs. We can also

express this in the mass eigenstate basis by diagonalising $M_{\tilde{N}}$. This can be done via a unitary matrix N , which provides our new basis $\tilde{N}_i = N_{ij}\psi_j^0$ such that the mass matrix now reads

$$N^* M_{\tilde{N}} N^{-1} = \begin{pmatrix} m_{\tilde{N}_1} & 0 & 0 & 0 \\ 0 & m_{\tilde{N}_2} & 0 & 0 \\ 0 & 0 & m_{\tilde{N}_3} & 0 \\ 0 & 0 & 0 & m_{\tilde{N}_4} \end{pmatrix}. \quad (2.160)$$

The diagonal values are the eigenvalues of $M_{\tilde{N}}$, where $m_{\tilde{N}_1}, m_{\tilde{N}_2}, m_{\tilde{N}_3}, m_{\tilde{N}_4} \in \mathbb{R}$. Note that the convention is to take $\mu \in \mathbb{R}^+$ (this is to avoid possible phenomenological complications) along with $M_1, M_2, b, \langle \tilde{H}_u^0 \rangle, \langle \tilde{H}_d^0 \rangle \in \mathbb{R}^+$. Note that $\text{sign}(\mu)$ is undetermined at tree level.

A particular scenario which is relevant to our work, involves the case in which we have a supersymmetric grand unified theory (GUT), in which the gaugino masses are set by a common parameter at the GUT scale ($\sim 10^{16}(\text{GeV})$)

$$\frac{M_1}{g_1^2} = \frac{M_2}{g_2^2} = \frac{M_3}{g_3^2} = \frac{m_{1/2}}{g_U^2}. \quad (2.161)$$

$m_{1/2}$ is the unified gaugino mass and g_U is the unified gauge coupling. The renormalisation group equations (RGEs) of the MSSM then evolve each of the gaugino masses down to the EW scale such that one has the approximate prediction

$$M_1 \simeq \frac{5}{3} \tan^2 \theta_W M_2 \sim 0.5 M_2. \quad (2.162)$$

In this scenario EW symmetry breaking effects can be viewed as small perturbations to the neutralino mass matrix. More specifically M_1, M_2, μ are going to dominate the neutralino masses, and the terms arising from EW symmetry breaking will be small. Under the assumption that

$$m_Z^2 \ll |\mu \pm M_1|, |\mu \pm M_2|, \quad (2.163)$$

the neutralino masses are approximated, to a 1st order expansion in $m_Z/|\mu \pm M_{1,2}|$,

as

$$m_{\tilde{N}_1} = M_1 - \frac{m_Z^2 \sin^2 \theta_W (M_1 + \mu \sin 2\beta)}{\mu^2 - M_1^2} + \mathcal{O} \left(\left(\frac{m_Z^2}{\mu^2 - M_1^2} \right)^2 \right), \quad (2.164)$$

$$m_{\tilde{N}_2} = M_2 + \frac{m_W^2 (M_2 + \mu \sin 2\beta)}{\mu^2 - M_2^2} + \mathcal{O} \left(\left(\frac{m_Z^2}{\mu^2 - M_2^2} \right)^2 \right), \quad (2.165)$$

$$m_{\tilde{N}_3} = |\mu| + \frac{m_Z^2 (\text{sign}(\mu) - \sin 2\beta) (\mu + M_1 \cos^2 \theta_W + M_2 \sin^2 \theta_W)}{2(\mu + M_1)(\mu + M_2)} + \mathcal{O} \left(\left(\frac{m_Z^2}{2(\mu + M_1)(\mu + M_2)} \right)^2 \right), \quad (2.166)$$

$$m_{\tilde{N}_4} = |\mu| + \frac{m_Z^2 (\text{sign}(\mu) + \sin 2\beta) (\mu - M_1 \cos^2 \theta_W - M_2 \sin^2 \theta_W)}{2(\mu - M_1)(\mu - M_2)} + \mathcal{O} \left(\left(\frac{m_Z^2}{2(\mu - M_1)(\mu - M_2)} \right)^2 \right). \quad (2.167)$$

Again, in this limit the neutralino masses are dominated by the SUSY terms, which makes the mass eigenstates nearly “bino-like” ($\tilde{N}_1 \simeq \tilde{B}$), “wino-like” ($\tilde{N}_2 \simeq \tilde{W}^0$), and “higgsino-like” ($\tilde{N}_3, \tilde{N}_4 \simeq (\tilde{H}_u^0 \pm \tilde{H}_d^0)/\sqrt{2}$). Within this scenario the bino-like neutralino emerges as the LSP (as long as $|\mu| \gtrsim M_1$).

Moving on to the charginos, in the gauge-eigenstate basis $\psi^\pm = (\tilde{W}^\pm, \tilde{H}_u^\pm, \tilde{W}^\mp, \tilde{H}_d^\mp)$, the Lagrangian containing the chargino mass terms consists of

$$\mathcal{L}_{\psi^\pm} = -\frac{1}{2}(\psi^\pm)^T M_{\tilde{C}} \psi^\pm + \text{c.c.}, \quad (2.168)$$

where $M_{\tilde{C}}$ is a 4×4 matrix that can be expressed in block form

$$M_{\tilde{C}} = \begin{pmatrix} \mathbf{0} & \mathbf{X}^T \\ \mathbf{X} & \mathbf{0} \end{pmatrix} \quad \text{where} \quad \mathbf{X} = \begin{pmatrix} M_2 & g\nu_u \\ g\nu_d & \mu \end{pmatrix} = \begin{pmatrix} M_2 & \sqrt{2} \sin \beta m_W \\ \sqrt{2} \cos \beta m_W & \mu \end{pmatrix}. \quad (2.169)$$

Similarly to what we did in the neutralino case, we can rotate to the mass eigenstate basis via two unitary 2×2 matrices U, V such that

$$\begin{pmatrix} \tilde{C}_1^+ \\ \tilde{C}_2^+ \end{pmatrix} = V \begin{pmatrix} \tilde{W}^+ \\ \tilde{H}_u^+ \end{pmatrix}, \quad \begin{pmatrix} \tilde{C}_1^- \\ \tilde{C}_2^- \end{pmatrix} = U \begin{pmatrix} \tilde{W}^- \\ \tilde{H}_d^- \end{pmatrix}. \quad (2.170)$$

Note that the rotation matrix for the (+)-ve charged LH fermions is different from the one used for the (−)-ve charged LH fermions, and are chosen such that

$$U^* X V^{-1} = \begin{pmatrix} m_{\tilde{C}_1} & 0 \\ 0 & m_{\tilde{C}_2} \end{pmatrix}. \quad (2.171)$$

The two mass entries $m_{\tilde{C}_1}, m_{\tilde{C}_2}$ are real and positive, where their analytical form is

$$m_{\tilde{C}_1}^2, m_{\tilde{C}_2}^2 = \frac{1}{2} \left[(|M_2|^2 + |\mu|^2 + 2m_W^2) \mp \sqrt{(|M_2|^2 + |\mu|^2 + 2m_W^2)^2 - 4|\mu M_2 - m_W^2 \sin 2\beta|^2} \right]. \quad (2.172)$$

Similarly, in the case of a unified gaugino mass, in the EW limit, the charginos become “wino-like” ($\tilde{C}_1^\pm \sim \tilde{W}^\pm$) and “higgsino-like” ($\tilde{C}_2^\pm \sim \tilde{H}_u^\pm, \tilde{H}_d^\pm$) where the masses are

$$m_{\tilde{C}_1}^2 = M_2 - \frac{m_W^2 (M_2 + \mu \sin 2\beta)}{\mu^2 - M_2^2} + \mathcal{O} \left(\left(\frac{m_W^2}{\mu^2 - M_2^2} \right)^2 \right), \quad (2.173)$$

$$m_{\tilde{C}_2}^2 = |\mu| + \frac{\text{sign}(\mu) m_W^2 (\mu + M_2 \sin 2\beta)}{\mu^2 - M_2^2} + \mathcal{O} \left(\left(\frac{m_W^2}{\mu^2 - M_2^2} \right)^2 \right). \quad (2.174)$$

We note that the \tilde{C}_1 chargino is nearly degenerate in mass with the \tilde{N}_2 neutralino, where the loop corrections to the masses can have a significant effect [50–52]. Lastly, we mention the gluino which is an **8** coloured fermionic octet under $SU(3)_C$, which does not mix with any other particle in the MSSM. In the case of unified gaugino masses the gluino SUSY breaking parameter is related to the wino and bino mass parameters as

$$M_3 = \frac{\alpha_S}{\alpha} \sin^2 \theta_W M_2 = \frac{3}{5} \frac{\alpha_S}{\alpha} \cos^2 \theta_W M_1. \quad (2.175)$$

The above is valid at any RG scale, and in particular it implies a rough TeV prediction for the mass ratios of $M_3 : M_2 : M_1 \sim 6 : 2 : 1$. This in turn gives us a reasonable justification to suppose that the gluino is much heavier than the other neutralinos/charginos. Note that due to the Dynkin index associated with the **8** representation under QCD, the RGE flow of the gluino mass can be quite considerable at one loop, with small corrections ($\sim 1 - 2\%$) arising at two loop [53–55].

2.8.4 Mass Spectrum of the MSSM - Squarks and sleptons

The quark and lepton masses in the MSSM are determined by the Yukawa interactions in the superpotential, and have the additional dependency on $\tan \beta = \nu_u / \nu_d$ due to the different Higgs VEVs. The masses of the up-type, down-type quarks and electron-type leptons are

$$m_u = y_u \frac{\nu}{\sqrt{2}} \sin \beta, \quad m_d = y_d \frac{\nu}{\sqrt{2}} \cos \beta, \quad m_e = y_e \frac{\nu}{\sqrt{2}} \cos \beta. \quad (2.176)$$

We note that in the MSSM neutrinos are massless, which can be addressed by introducing additional fields.

We now move on to the scalar superpartners. There is a potential problem, in the fact that within the context of the full family structure of the MSSM, any scalars that possess the same quantum numbers can mix. More specifically with arbitrary soft SUSY breaking terms, the mass eigenstate basis is determined by diagonalising the three matrices corresponding to the 6 dimensional gauge eigenstates of the up-type and down-type squarks, charged sleptons and the 3 dimensional matrix corresponding to the sneutrino gauge eigenstates

$$\begin{aligned} (\tilde{u}_L, \tilde{c}_L, \tilde{t}_L, \tilde{u}_R, \tilde{c}_R, \tilde{t}_R), & \quad (\tilde{d}_L, \tilde{s}_L, \tilde{b}_L, \tilde{d}_R, \tilde{s}_R, \tilde{b}_R), \\ (\tilde{e}_L, \tilde{\mu}_L, \tilde{\tau}_L, \tilde{e}_R, \tilde{\mu}_R, \tilde{\tau}_R), & \quad (\tilde{\nu}_e, \tilde{\nu}_\mu, \tilde{\nu}_\tau). \end{aligned} \quad (2.177)$$

Fortunately, the mixing angles present in the superscalar partner sector are predicted to be small under the *flavour-blind soft hypothesis*. The flavour-blind soft hypothesis effectively states that supersymmetry breaking is “universal”, i.e. the limit in which the squark and slepton soft SUSY squared mass matrices are flavour blind, each proportional to the identity matrix

$$\mathbf{m}_Q^2 = m_Q^2 \mathbb{1}_3, \quad \mathbf{m}_U^2 = m_U^2 \mathbb{1}_3, \quad \mathbf{m}_D^2 = m_D^2 \mathbb{1}_3, \quad \mathbf{m}_L^2 = m_L^2 \mathbb{1}_3, \quad \mathbf{m}_E^2 = m_E^2 \mathbb{1}_3. \quad (2.178)$$

In addition if we require that the trilinear scalar cubed couplings $\mathbf{a}_u, \mathbf{a}_d, \mathbf{a}_e$ are each proportional to their corresponding Yukawa matrix

$$\mathbf{a}_u = A_{u0} \mathbf{y}_u, \quad \mathbf{a}_d = A_{d0} \mathbf{y}_d, \quad \mathbf{a}_e = A_{e0} \mathbf{y}_e, \quad (2.179)$$

then we also avoid the dangerous FCNCs present in SUSY models mentioned earlier, along with controlling the smallness of the mixing angles of the scalar superpartners.

Under the flavour blind hypothesis, we can now focus on the mass spectrum of the scalar particles. In addition to the squared soft-SUSY breaking masses, the scalar superpartners receive various contributions from either F terms of the MSSM superpotential or D terms of the Kähler potential. One of these corrections, that is universal for the scalars in discussion, is the contribution arising from the D term of the $SU(2)_L \times U(1)_Y$ scalar quartic interactions ($\sim \frac{1}{2} \sum_a D^a D^a = \frac{1}{2} \sum g_a^2 (\phi T^a \phi)^2$). This term arises post symmetry breaking after the Higgs fields have acquired their respective VEVs, and has the form

$$\Delta_\phi = \frac{1}{2} (T_{3\phi} g^2 - Y_\phi g'^2) (\nu_d^2 - \nu_u^2) = (T_{3\phi} - Q_q \sin^2 \theta_W) \cos 2\beta m_Z^2. \quad (2.180)$$

The corrections are determined by the field's third component of the weak isospin T_3 , and hypercharge Y . Equivalently, we can express this in terms of T_3 , the EM charge Q and the Weinberg angle $\sin \theta_W$.

We will now look at the top squark and highlight the contributions arising from the various supersymmetric contributions. First off we have squared terms in the potential of the form $\tilde{t}_L^* \tilde{t}_L$ and $\tilde{t}_R^* \tilde{t}_R$ whose coefficients are determined by the soft SUSY breaking masses and the aforementioned D term contributions

$$\tilde{t}_L^* \tilde{t}_L : \quad m_{Q_3}^2 + \Delta_{\tilde{u}_L}, \quad (2.181)$$

$$\tilde{t}_R^* \tilde{t}_R : \quad m_{u_3}^2 + \Delta_{\tilde{u}_R}. \quad (2.182)$$

Secondly, each one of the terms receives contributions of m_t^2 arising from the F terms of the Yukawa terms $\sim \left| \frac{\partial W}{\partial \tilde{t}_L^*} \right|^2, \left| \frac{\partial W}{\partial \tilde{t}_R^*} \right|^2$

$$\tilde{t}_L^* \tilde{t}_L : \quad m_{Q_3}^2 + \Delta_{\tilde{u}_L} + m_t^2, \quad (2.183)$$

$$\tilde{t}_R^* \tilde{t}_R : \quad m_{u_3}^2 + \Delta_{\tilde{u}_R} + m_t^2. \quad (2.184)$$

Thirdly, we have F term contributions arising from the $\sim \left| \frac{\partial W}{\partial H_u^0} \right|^2, \left| \frac{\partial W}{\partial H_d^0} \right|^2$ terms, which provide mixing terms of the form $\tilde{t}_L^* \tilde{t}_R, \tilde{t}_R^* \tilde{t}_L$, which post EW symmetry breaking have the explicit form

$$\tilde{t}_L^* \tilde{t}_R : \quad -\mu \nu y_t \cos \beta, \quad (2.185)$$

$$\tilde{t}_R^* \tilde{t}_L : \quad -\mu^* \nu y_t \cos \beta. \quad (2.186)$$

Lastly, the off diagonal terms receive contributions from the cubic scalar couplings arising from the trilinear soft SUSY breaking terms $\sim \tilde{u} a_u \tilde{Q} H_u$, which post symmetry breaking contribute to the mixing terms

$$\tilde{t}_L^* \tilde{t}_R : \quad -\mu \nu y_t \cos \beta + \nu a_t^* \sin \beta, \quad (2.187)$$

$$\tilde{t}_R^* \tilde{t}_L : \quad -\mu^* \nu y_t \cos \beta + \nu a_t \sin \beta. \quad (2.188)$$

Putting all of this together, the stop mass Lagrangian is given in the gauge eigen-basis by

$$\mathcal{L}_{\tilde{t}_L, \tilde{t}_R} = -(\tilde{t}_L^*, \tilde{t}_R^*) \begin{pmatrix} m_{Q_3}^2 + \Delta_{\tilde{u}_L} + m_t^2 & \nu(a_t^* \sin \beta - \mu y_t \cos \beta) \\ \nu(a_t \sin \beta - \mu^* y_t \cos \beta) & m_{u_3}^2 + \Delta_{\tilde{u}_R} + m_t^2 \end{pmatrix} \begin{pmatrix} \tilde{t}_L \\ \tilde{t}_R \end{pmatrix}, \quad (2.189)$$

which can be rotated in the mass eigenbasis $\sim (\tilde{t}_1^*, \tilde{t}_2^*)$ by diagonalising the hermitian mass matrix.

Along the same lines, we can perform an analogous set of calculations to obtain the sbottom and the stau mass Lagrangian in the gauge eigenbasis

$$\mathcal{L}_{\tilde{b}_L, \tilde{b}_R} = -(\tilde{b}_L^*, \tilde{b}_R^*) \begin{pmatrix} m_{Q_3}^2 + \Delta_{\tilde{d}_L} & \nu(a_b^* \cos \beta - \mu y_b \sin \beta) \\ \nu(a_b \cos \beta - \mu^* y_b \sin \beta) & m_{\tilde{d}_3}^2 + \Delta_{\tilde{u}_R} \end{pmatrix} \begin{pmatrix} \tilde{b}_L \\ \tilde{b}_R \end{pmatrix}, \quad (2.190)$$

$$\mathcal{L}_{\tilde{\tau}_L, \tilde{\tau}_R} = -(\tilde{\tau}_L^*, \tilde{\tau}_R^*) \begin{pmatrix} m_{L_3}^2 + \Delta_{\tilde{e}_L} & \nu(a_\tau^* \cos \beta - \mu y_\tau \sin \beta) \\ \nu(a_\tau \cos \beta - \mu^* y_\tau \sin \beta) & m_{\tilde{e}_3}^2 + \Delta_{\tilde{e}_R} \end{pmatrix} \begin{pmatrix} \tilde{\tau}_L \\ \tilde{\tau}_R \end{pmatrix}, \quad (2.191)$$

which can be brought to the mass eigenbasis $\sim (\tilde{b}_1^*, \tilde{b}_2^*), \sim (\tilde{\tau}_1^*, \tilde{\tau}_2^*)$ by diagonalising the mass matrices.

2.9 SUSY in GUTs

Having now reviewed the construction and particularities of the MSSM, we move on to explore how supersymmetry fits within grand unified theories, and look at how extra dimensional mechanisms can provide us with a structure and origin for the various soft SUSY breaking masses.

Orbifolds and Scherk-Schwarz breaking

The following chapter will look at a class of models known as orbifold grand unified theories (GUTs), along with their phenomenology in a variety of minimal and non-minimal settings. The chapter comprises of a series of sections reviewing the formalism used in extra dimensional GUTs, and how to build realistic models with the use of Scherk-Schwarz mechanism. We then examine the minimal $SU(5)$ models, rule them out, and proceed by extending them with an additional scalar field in the same gauge group or alternatively in a $SU(5) \times U(1)$ model. Finally we comment on the implications of a so called “natural” supersymmetry scenario, and look at higher dimensional alternatives.

3.1 Introduction

By formulating a supersymmetric GUT, we are now able to achieve gauge coupling and representation unification, along with solving the aforementioned Gildener hierarchy problem [13]. Therefore, for the remainder of this chapter, we choose to promote our theories to being supersymmetric.

Even though SUSY provides us with a mechanism to explain our GUT hierarchy (i.e. why are the W^\pm and Z^0 bosons so much more lighter than the X bosons introduced by unification $m_W \ll m_X$), we still need a mechanism to sort out the doublet-triplet splitting ($2-3$) problem. The $2-3$ problem effectively asks: “Since all of our Higgs fields are now contained in one single representation of the larger gauge group in question (e.g. $SU(5)$), how do we split the representation into a heavy coloured triplet and light weak doublet, such that proton decay is suppressed [56], [57]?” E.g. given the $H_{\bar{5}}$ as the $\bar{5}$ representation of $SU(5)$, how can we achieve the mass split

$$H_{\bar{5}} = (\underbrace{\phi^r, \phi^g, \phi^b}_{\text{Heavy}}, \underbrace{\phi^+, \phi^0}_{\text{Light}})? \quad (3.1)$$

In a 4 dimensional formalism there are some mechanisms on the market [58] - [59], which in general require a complicated or rather cumbersome Higgs sector, which can make them less desirable and to an extreme even unsatisfactory.

This issue can instead be approached from the point of view of theories with small compactified extra dimensions. In this class of models, heavy Kaluza - Klein modes naturally arise due to the compactified manifold [60]. Appropriate quantum number choices can then lead to a natural mechanism for $2 - 3$ splitting (as long as the reader accepts the premise that small extra dimensions are naturally occurring, but haven't yet been observed).

Furthermore, if supersymmetry is indeed a symmetry of the real world, it must be broken in order for it to correspond with our observations of nature. In addition to providing us with $2 - 3$ splitting, this class of models has another attractive feature, in that it can provide our theory with soft SUSY breaking masses via the Scherk-Schwarz (SS) mechanism [61], [62].

The work in this section will be based on Barbieri, Hall, and Nomura's model [63], [64], along with Nevzorov's E_6 inspired model [65], which we later modify to accommodate an additional singlet along with the Scherk-Schwarz mechanism.

The broad questions that we will be asking are: What spectrum does Barbieri, Hall and Nomura's original minimal model [63] produce? Is it ruled out by the LHC or dark matter constraints? If so, can we modify it to be viable along the lines of a next to minimal extension, such that it predicts the observed low energy spectrum of the SM?

Overall, we want to explore the idea of obtaining a "naturally" broken supersymmetry arising from the formalism, and asking if we are going to be able to see it at the TeV scale, with SUSY still being relevant to the hierarchy problem [66], [67].

3.2 Extra Dimensions, Compactifications, and SS Twists

In the following sections we will review the extra dimensional formalism along with the SS mechanism, by following the work in [68]. Note that in this chapter we are working within the context of a flat extra dimensional scenario, i.e. we are ignoring the tension of the branes and their potential implications. Here we are not considering a warped space-time as one would in a Randall-Sundrum model [69],

which will be the focus of the following chapters.

We start by working in $D = d + 4$ dimensions, where the d extra dimensions are spatial dimensions. We suppose the dimensionless action

$$S_D = \int d^D z \mathcal{L}[\phi(z^\mu)], \quad (3.2)$$

where z are the space-time coordinates, \mathcal{L} is the D dimensional Lagrangian dependent on generic fields ϕ . We now say a theory is compactified, if it is defined on a space which is a direct product of the form $\mathcal{M}_4 \times C$, where \mathcal{M}_4 is the usual flat Minkowski space-time and C is a compactified space. The product form of our defining space implies that we can “split” our description of the action in terms of the coordinates as

$$z^M = (x^\mu, y^m) = \begin{cases} x^\mu, & \mu = 0, 1, 2, 3 & \text{describes } \mathcal{M}_4 \\ y^m, & m = 1, \dots, d & \text{describes } C \end{cases}, \quad (3.3)$$

where the index M runs over both μ and m .

To connect this to our observable reality we have to obtain a 4D Lagrangian from our D dimensional action S_D in the low energy limit. Since we can split our description in terms of the coordinates of the non compact and the compact space, this is naturally achieved by integrating out the y^m coordinates leading to the 4D Lagrangian

$$\mathcal{L}_4 = \int d^d y \mathcal{L}_D[\phi(x^\mu, y^m)]. \quad (3.4)$$

Let us now look at the compact space and see what consequences its presence has on how we define our theory. We will reduce our discussion to just one extra dimension with coordinate y . In general, a compact manifold C is written out in terms of a non-compact manifold \mathcal{M} , which is “modded” out by a discrete group G , i.e. $C = \mathcal{M}/G$. What we mean by this, is that the discrete group G acts freely on the manifold \mathcal{M} via some operators τ_g as

$$\tau_g : \mathcal{M} \rightarrow \mathcal{M}, \quad g \in G, \quad (3.5)$$

where the τ_g ’s live in the representation space of G . The compact space is then obtained by identifying points y with points acted on by τ_g , which in turn define the same “orbit”

$$y \equiv \tau_g(y). \quad (3.6)$$

The identification must in turn be reflected by the physicality of our theory. I.e. the physics should no longer be dependent on individual points in y , but rather on

the orbits. In terms of the Lagrangian this becomes

$$\mathcal{L}_D[\phi(x^\mu, y)] = \mathcal{L}_D[\phi(x^\mu, \tau_g(y))]. \quad (3.7)$$

As a consequence of this restriction, we now have a constraint on how the fields must behave. Since we have essentially connected two points in our manifold, the fields defined on it will now have to satisfy some sort of periodicity constraint. We have a choice in what constraint the fields have to obey, where they can satisfy either

- A **sufficient** condition: $\phi(x^\mu, \tau_g(y)) = \phi(x^\mu, y)$.
- A **necessary and sufficient** condition: $\phi(x^\mu, \tau_g(y)) = T_g \phi(x^\mu, y)$, where T_g is a representation of G acting on field space.

We observe in the case of the latter that for the trivial choice $T_g = 1$ we recover the 1st case which is referred to as *ordinary compactification*. The non-trivial choice $T_g \neq 1$ is referred to as *Scherk-Schwarz compactification*.

In our formalism we will be working in $D = 5$ (i.e. $d = 1$ corresponding to y). We will be using the SS compactification and define our compact space in its initial phase as a circle $C = S^1$. We will see that the decomposition of the space in terms of a non-compact \times a compact space is defined by $\mathcal{M} = \mathbb{R}^1$, modded out by $G = \mathbb{Z}$ corresponding to the translational identification.

The action of the infinite discrete group modulo \mathbb{Z} , is given by the operators τ_n , acting on elements $y \in \mathbb{R}^1$ by mapping them onto

$$\tau_n(y) = y + 2n\pi R, \quad n \in \mathbb{Z}, \quad (3.8)$$

where R is the unit length in our operator action, which is identified as the radius of the circle S^1 . If we now perform the identification $y = \tau_n(y)$, diagrammatically we have taken the real number line \mathbb{R}^1 and “curled” it up, as shown in Fig. 3.1.

In terms of the definition domain, post identification, it has become $[y, y + 2\pi R]$. Note that without any loss of generality we have chosen $n = 1$ to reflect the transformation corresponding to the \mathbb{Z} generator $2\pi R$, and to eliminate the unnecessary redundancy caused by n . I.e. going around the circle once is equivalent to going around the circle n times in terms of the actual length of the circle.

Therefore the only generator of \mathbb{Z} , $\tau = 2\pi R$ will correspond to the only independent twist T , acting on fields ϕ as

$$\phi(x^\mu, \tau(y)) = \phi(x^\mu, y + 2\pi R) = T\phi(x^\mu, y). \quad (3.9)$$

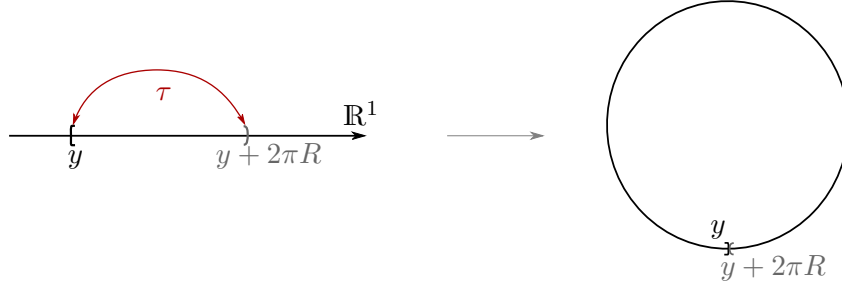


Figure 3.1: Identifying the circle S^1 as the manifold \mathbb{R}^1/\mathbb{Z} where the identification is performed by modding out the real number line \mathbb{R} via the action of the \mathbb{Z} modulo group.

Since the other operators are equivalent to the action of τ applied n times τ_n , the other elements defined by τ_n are given by

$$\phi(x^\mu, \tau_n(y)) = \phi(x^\mu, y + 2n\pi R) = (T)^n \phi(x^\mu, y). \quad (3.10)$$

In principle, we now have the necessary tools to write down a theory defined on $\mathcal{M}_4 \times S^1$. Even though this can produce stand-alone models, it has some problems, mainly the chirality problem [70]. Since our definition domain is a 5D space, the Lorentz algebra will be affected accordingly, making the Dirac spinor the fundamental spinorial representation, as opposed to the Weyl spinor. The chirality problem is then essentially overcoming the difficulties imposed by having to project the 5D Dirac spinors to the corresponding SM fermions in 4D [70].

This problem can be overcome, if we further mod out our circle into an interval. This is referred to as an *orbifold compactification*. We will now proceed to define it in an analogous manner to the Scherk-Schwarz compactification.

We start off with a compact manifold C , and introduce the discrete group H , which acts non-freely on C , where by non-freely we mean that some of the transformations acting on C have fixed points in C . It acts via the operators ξ_h as

$$\xi_h : C \rightarrow C, \quad h \in H, \quad (3.11)$$

where ξ_h lives in the representation space of H . Similarly to what we did in the SS case, we now identify points in $y \in C$ that differ by an amount dictated by the action of ξ_h as

$$y \equiv \xi_h(y). \quad (3.12)$$

Analogous to the SS case, this identification must reflect itself in the physicality of our system via the Lagrangian. To this extent we choose a necessary and sufficient condition, such that the fields ϕ obey

$$\phi(x^\mu, \xi_h(y)) = Z_h \phi(x^\mu, y), \quad (3.13)$$

where Z_h is a representation of H acting on field space.

The resulting manifold $O = C/H$ is no longer smooth, due to the non-free action of H , but now has *fixed points*, which are singularities (i.e at these points the tangent spaces are not well defined, and are identified with themselves). We refer to O as an *orbifold*.

Let us now proceed to “orbifold our circle”. In our case we start off with the circle as the compact space $C = S^1$, and mod it out by a \mathbb{Z}_2 symmetry, which results in the $O = S^1/\mathbb{Z}_2$ orbifold.

The action of the \mathbb{Z}_2 group is given by the unique non-trivial operator ξ , acting on $y \in S^1$ as

$$\xi(y) = -y. \quad (3.14)$$

We note that $\xi^2 = 1$, which is what we would expect as a result arising from a reflection. Depicting this diagrammatically, we are folding the circle in half as shown in Fig. 3.2. By performing the \mathbb{Z}_2 identification we get the two fixed points at $y = 0, \pi R$, and are left with the fundamental domain $y \in [0, \pi R]$.

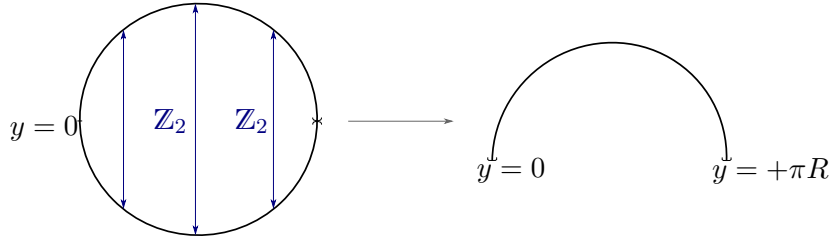


Figure 3.2: Modding S^1 by \mathbb{Z}_2 is done by identifying the opposite ends of the circle together resulting in the interval with fixed points at $y = 0, y = \pi R$

It is now worthwhile to pause before we move on to the field implications and anticipate our set-up. Our full space-time set up is now defined by the direct product $\mathcal{M}_4 \times S^1/\mathbb{Z}_2$. Within this construct, the fixed points correspond to a 4D manifold, also known as 4D *branes*. Our observable universe will consist of a brane, where we expect to retrieve the SM at low energies. Therefore we will have to “project”

down the 5D theory to the 4D branes, and see how the full UV theory defines our IR limits.

Back to the case at hand. Analogous to the SS compactification, the \mathbb{Z}_2 action is now reflected on the fields via the identification condition

$$\phi(x^\mu, \xi(y)) = \phi(x^\mu, (-y)) = Z\phi(x^\mu, y). \quad (3.15)$$

Z has eigenvalues ± 1 in some diagonal space, with $Z^2 = 1$. Along with the translation T , we now need to see how the two isometries T, Z affect each other. On this note, we can always think of G, H as subgroups of a larger discrete group J , where in general the operators do not commute

$$\tau_g \cdot \xi_h(y) \neq \xi_h \cdot \tau_g(y). \quad (3.16)$$

In essence, the above states that J is not necessarily the direct product of G and H , $J \neq G \otimes H$. Since we can think of both T, Z as being subgroups of J , it implies they have to obey some consistency condition. More specifically, T has to obey it since Z is already constrained within the larger group action by $Z^2 = 1$. This condition can be understood by looking at it from a diagrammatic point of view, in which definition domain $[0, 4\pi R]$ is depicted as a circle as shown in Figs. 3.3a, 3.3b. Note that this is the same as the modded interval, where we have performed the re-parametrisation $R \rightarrow 4R$.

The consistency condition on the fields can be seen as originating from the following geometrical argument. Starting at a point y , we apply a translation-reflection-translation to it, resulting in the $-y$ identification, which is equivalent to performing the $\xi(y)$ action. In terms of operators this is expressed as $\tau\xi\tau(y) = \xi(y)$, and we can view it diagrammatically by following the arrow flow shown in Fig. 3.3a.

Similarly, we can get a similar effect if we start off with a point y and apply a reflection-translation-reflection, resulting in the $y - 2\pi R$ identification, which is the same as $\tau^{-1}(y)$. In terms of operators this is expressed as $\xi\tau\xi(y) = \tau^{-1}(y)$ and we can view it diagrammatically by following the arrow flow shown in Fig. 3.3b.

Therefore the fields defined on S^1/\mathbb{Z}_2 , will also have to obey similar constraints via the general form of Z, T . To this extent, to have a consistent field picture we require

$$T Z T = Z \quad \leftrightarrow \quad Z T Z = T^{-1}. \quad (3.17)$$

Pausing our discussion for a second, it is worthwhile noting that if we look at the Fig. 3.3b, we notice that the combined transformation of $\tau\xi$ takes any point $-y$

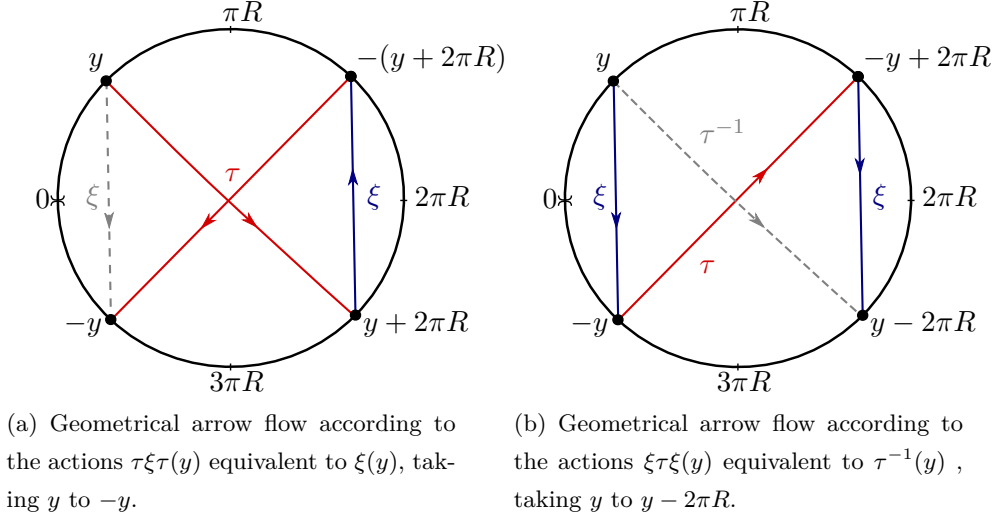


Figure 3.3: The two different ways of identifying y with $-y$ within S^1/\mathbb{Z}_2 . The red lines represent translation τ by $2\pi R$, the blue lines represent a reflection ξ around 0. The dotted grey lines represent the equivalent reflection/inverse translation that produces the same identification. Note that the open ended interval symbols at 0 denote this as just a depiction of the $[0, 4\pi R]$ interval, with the end points not being identified with each other.

and sends it to $-y + 2\pi R$, which can be viewed as a “vertical” reflection about πR . To that extent we can define a new reflection \mathbb{Z}'_2 defined by

$$\xi' = \tau\xi \quad \leftrightarrow \quad Z' = TZ, \quad (3.18)$$

where the consistency condition in Eqn. (3.17), now reduces to $(Z')^2 = 1$. This freedom in redefinition implies that we have an equivalent picture to the S^1/\mathbb{Z}_2 orbifold, i.e. the doubly modded real number line $\mathbb{R}^1/\mathbb{Z}_2 \times \mathbb{Z}'_2$. In terms of fields, this equivalence translates to the ability to change from the Z, T “eigenvalue basis” to the Z, Z' one depending on the situation.

Coming back to our discussion, to get a better intuition on what the constraint in Eqn. (3.17) entails, we write it out in a more detailed fashion. Since T corresponds to an operator expressing the local/global symmetry defined by G , and given that the action of the symmetry has a representation defined by its generators λ^a , we can write T as an exponentiated matrix

$$T = \exp(2\pi i \beta^a \lambda^a). \quad (3.19)$$

β^a are the symmetry parameters, and λ^a is an appropriately sized Hermitian matrix

$(\lambda^a)^\dagger = \lambda^a$. With the form of the above, we can rewrite the consistency condition for infinitesimal transformations. Keeping only the terms up to $\mathcal{O}(\beta^2)$, Eqn. (3.17) now becomes

$$\{\beta^a \lambda^a, Z\} = 0. \quad (3.20)$$

Effectively, we have recovered the fact that the two generators do not necessarily commute $\tau_g \cdot \xi_h(y) \neq \xi_h \cdot \tau_g(y)$, in terms of field space values. That is to say, in general T, Z do not commute.

We will now think a bit ahead and anticipate our models by looking at a theory that possesses a global $SU(2)$ symmetry, which contains fields ϕ transform under $SU(2)$ as doublets $\sim \mathbf{2}$. In this case, since $Z^2 = \mathbb{1}_2$, we will have two choices for the form of Z acting on the $SU(2)$ space, namely $Z = \sigma_3$ or $Z = \pm \mathbb{1}_2$ (where σ_i is the i th Pauli sigma matrix).

If we choose $Z = \pm \mathbb{1}$ we then get a singular solution to Eqn. (3.17), i.e. $T = \pm \mathbb{1}$, which is a special case when Z and T do commute. In this case we recover the trivial orbifolding.

Going along the path of the non-trivial choice of $Z = \sigma_3$, the general solution for T satisfying Eqn. (3.20) takes the form $T = \exp(2\pi i(\beta^1 \sigma^1 + \beta^2 \sigma^2 + \beta^3 \sigma^3))$. The latter has a singular solution for the parameter choice $(\beta^3 = 1/2, \beta^{1,2} = 0)$, reducing $T = \exp(i\pi \sigma^3) = \mathbb{1}$, which again brings us to the trivial case where $[T, Z] = 0$. Within the context of the non-trivial choice, we can use the residual $SU(2)$ symmetry and rotate away the σ^1 direction component $(\beta^1, \beta^2) \rightarrow (0, \alpha)$, leaving us with

$$Z = \sigma^3, \quad T = \exp(2\pi i \alpha \sigma^2). \quad (3.21)$$

The form of the above then determine how the different eigenvalues are assigned to the fields, and subsequently how these will affect our theory.

We now have the necessary tools to deal with the fields isometry assignments in the 5D formalism. We now move on to looking at how this impacts a supersymmetric theory, and the implication when taking the limit of a 4D action.

3.3 $5D \mathcal{N} = 1$ SUSY to $4D \mathcal{N} = 1$

In this section, we introduce a 5D supersymmetric Lagrangian and look at how it reduces to its corresponding 4D action. Formulating the 5D $\mathcal{N} = 1$ SUSY theory is based on the formalism introduced by Mirabelli and Peskin in [71]. As we briefly

mentioned in the previous chapter, the irreducible SUSY representations that we will be using are

- **Hypermultiplets** \mathcal{H} , which consists of the complex scalars A^i , $i = 1, 2$ and a Dirac spinor Ψ :

$$\mathcal{H} = (A^i, \Psi). \quad (3.22)$$

Note that Ψ can transform as a doublet under $SU(2)_R$ [72], the residual 5D $\mathcal{N} = 1$ symmetry that we introduced in the previous chapter.

- **Vector multiplets** \mathcal{V} , which consist of gauginos λ^i , $i = 1, 2$, the 5D gauge fields A_M , $M = 0, 1, 2, 3, 5$, and a real scalar Σ which transform under the adjoint representation of the gauge group

$$\mathcal{V} = (A_M, \lambda^i, \Sigma). \quad (3.23)$$

λ^i transforms as a doublet under $SU(2)_R$ [71], where λ^i are symplectic Majorana spinors which have the form

$$\lambda^i = \begin{pmatrix} \lambda_L^i \\ \epsilon_{ij} \bar{\lambda}_{jL} \end{pmatrix}, \quad \bar{\lambda}_{jL} \equiv -i\sigma^2 (\lambda_L^j)^*, \quad (3.24)$$

where λ_L^i is a left handed Weyl spinor.

This is within the context of 5D space-time defined on the $\mathcal{M}_4 \times S^1/\mathbb{Z}_2$ manifold, with a flat extra dimension that has the metric $\eta_{MN} = \text{diag}(1, -1, -1, -1, -1)$. We work in the chiral representation, under which we list the following useful matrices

$$\begin{aligned} \gamma^M &= \{\gamma^\mu, \gamma^5\}, & \gamma^5 &= \begin{pmatrix} -i & 0 \\ 0 & i \end{pmatrix} \otimes I_2, \\ \sigma^\mu &= (\mathbb{1}, \vec{\sigma}), & \bar{\sigma}^\mu &= (\mathbb{1}, -\vec{\sigma}). \end{aligned} \quad (3.25)$$

We start off with a 5D on-shell vector multiplet \mathcal{V} which is extended to off-shell, by adding a $SU(2)_R$ triplet of real valued auxiliary fields X^a , $a = 1, 2, 3$. The members of the multiplet are written out as matrices in the adjoint representation. Similarly, we extend the hypermultiplet \mathcal{H} by adding a complex doublet of auxiliary fields F^i , $i = 1, 2$, giving us the off-shell fields

$$\mathcal{V}_{\text{on-shell}} \sim (A_M, \Sigma, \lambda^i) \quad \rightarrow \quad \mathcal{V}_{\text{off-shell}} \sim (A_M, \Sigma, \lambda^i, X^a), \quad (3.26)$$

$$\mathcal{H}_{\text{on-shell}} \sim (A^i, \Psi) \quad \rightarrow \quad \mathcal{H}_{\text{off-shell}} \sim (A^i, \Psi, F^i). \quad (3.27)$$

The fields obey the supersymmetry transformation relations as presented in [68]. With the building blocks in place, we now need to ask how the SUSY fields behave in our S^1/\mathbb{Z}_2 orbifolded setup. In the S^1/\mathbb{Z}_2 orbifold case, we recall that we have two fixed points at $y = 0, \pi R$, which have attached two 4D branes. We will identify the $y = 0$ brane as the infrared (IR) brane which should contain in a low energy limit the SM.

Since we are dealing with an extra compactified dimension, from a kinetic point of view the theory will allow only certain momenta (analogous to wave-modes in a box) known as Kaluza - Klein (KK) momenta. The types of modes that we end up with, are also tied in with the isometries of the system, more specifically the reflection ξ and translation τ symmetries involved in orbifolding S^1/\mathbb{Z}_2 . Furthermore, it will turn out that since we require “massless” (also known as 0 modes) and “massive” modes in our theory, we will want to assign the corresponding field eigenvalues accordingly.

In line with this train of thought, we think slightly ahead and assign the modes for the fields that we want to be massless a $Z = +1$ eigenvalue and the massive modes $Z = -1$. This is our educated guess since the two assignments correspond to Dirichlet and von Neumann boundary conditions, of which only the first can produce 0 modes. Note that this has to be done in accordance with respecting the consistency conditions between Z, T as dictated by Eqn. (3.17). In the first stage we will talk about gauge preserving assignments and then move on to non-trivial gauge breaking structures.

In line with what we did earlier, recall that we have a non-trivial choice of $Z = \sigma^3$ as the reflection acting on the $SU(2)_R$ subspace. We start off by considering the vector multiplet and its components. With this choice of Z , the eigenvalue assignments for the fields (and the parameters) is

$$\begin{aligned} Z = +1 : & \quad A^M, \lambda_L^1, X^3; & \quad \xi_L^1, \\ Z = -1 : & \quad A^5, \Sigma, \lambda_L^2, X^{1,2}; & \quad \xi_L^2, \end{aligned} \tag{3.28}$$

where $\xi^i, i = 1, 2$ are the corresponding $5D \mathcal{N} = 1$ supersymmetry parameters, which are Symplectic Majorana spinors.

We now look at how the supersymmetric transformation behaves on the $y = 0$ brane. Since this is the future SM-like brane, we want it to possess “massless” modes. To this extent, we require that the fields that we wish to have 0 modes on the IR brane, have a $Z = +1$ parity assignment. Therefore ξ_L^1 will correspond to

the $\mathcal{N} = 1$ supersymmetric parameter that will preserve the Z assignments in the reduced 4D, $\mathcal{N} = 1$ SUSY transformation.

We pause now for a second and look at what impact the Z assignment has on the supersymmetry of the system. If we count the number of degrees of freedom in a $5D, \mathcal{N} = 1$ SUSY theory, we see that it has the same number as two $4D, \mathcal{N} = 1$ SUSY theories. What we are doing implicitly by assigning a $Z = \pm 1$ eigenvalue to the supersymmetric parameters, is effectively reducing from the 4 dimensional point of view $\mathcal{N} = 2$ SUSY (which is equivalent to a $5D, \mathcal{N} = 1$ SUSY) to a single allowed $\mathcal{N} = 1$ SUSY on the brane via the Z parity assignment in the orbifolding procedure.

After orbifolding, the states on the $y = 0$ brane will obey the reduced supersymmetric transformation, as shown in [68], of which we highlight

$$\left. \begin{aligned} \delta_\xi X^3 &= (\xi_L^1)^\dagger \bar{\sigma}^\mu \mathcal{D}_\mu - i(\xi_L^1)^\dagger \mathcal{D}_5 \bar{\lambda}_L^2 + \text{h.c.} \\ \delta_\xi (\partial_5 \Sigma) &= -i(\xi_L^2)^\dagger \mathcal{D}_5 \bar{\lambda}_L^2 + \text{h.c.} \end{aligned} \right\} \rightarrow \delta_\xi (X^3 - \partial_5 \Sigma) = \xi_L^1 \bar{\sigma}^\mu \mathcal{D}_\mu \lambda_L^1. \quad (3.29)$$

We note that the combined $X^3 - \partial_5 \Sigma$ term transforms as a total derivative, which can be used to write a SUSY invariant theory as discussed in the previous chapter. Even though Σ has a parity assignment of -1 , because of the derivative $\partial_5 \Sigma$, the $X^3 - \partial_5 \Sigma$ term transforms along with the supersymmetric brane parameter ξ_L^1 . The $\mathcal{N} = 1$ “projected” vector multiplet is given on the brane in the Wess-Zumino gauge by

$$(A^\mu, \lambda_L^1, D) \quad \text{where, } D = X^3 - \partial_5 \Sigma. \quad (3.30)$$

This is what we expected, since the 4D gauge components that “survive” on the brane and transform under the 4D $\mathcal{N} = 1$ SUSY, are the ones with the $Z = +1$ assignment.

Similarly with the hypermultiplet, starting of with the on shell version $\mathcal{H} = (A^i, \Psi, F^i)$, we give the components the following parity assignments

$$\begin{aligned} Z = +1 : & \quad A^1, \psi_L, F^1; & \xi_L^1, \\ Z = -1 : & \quad A^2, \psi_R, F^2; & \xi_L^2, \end{aligned} \quad (3.31)$$

where ψ_L, ψ_R are the components of the Dirac spinor Ψ . Analogous to the vector case, the hypermultiplet has a supersymmetry projection on the $y = 0$ brane generated by ξ_L^1 , where the components obey the reduced supersymmetric transformation

as shown in [68]. Similarly we highlight

$$\left. \begin{aligned} \delta_\xi F^1 &= i\sqrt{2}(\xi_L^1)^\dagger \bar{\sigma}^\mu \partial_\mu \psi_L + \sqrt{2}(\xi_L^1)^\dagger \partial_5 \psi_R \\ \delta_\xi(\partial_5 A^2) &= \sqrt{2}(\xi_L^1)^\dagger \partial_5 \psi_R \end{aligned} \right\} \rightarrow \partial_\xi(F^1 - \partial_5 A^2) = i\sqrt{2}(\xi_L^1)^\dagger \bar{\sigma}^\mu \partial_\mu \psi_L, \quad (3.32)$$

which transforms as a total derivative. Therefore the off-shell chiral supermultiplet on the $y = 0$ brane is formed by the $\mathcal{N} = 2 \rightarrow \mathcal{N} = 1$ projection, where

$$\mathcal{A} = (A^1, \psi_L, F) \quad \text{with, } F = F^1 - \partial_5 A^2. \quad (3.33)$$

We now have everything that we need in order to build a 5D theory and to project it down to the resulting 4D $\mathcal{N} = 1$ limit. To this extent, we start with a generic 5 dimensional action which has the form

$$S = \int d^4x dy \left\{ \mathcal{L}_5 + \sum_{i=1,2} \delta(y - y_i) \mathcal{L}_{4i} \right\}, \quad (3.34)$$

where \mathcal{L}_5 is the 5D bulk Lagrangian, and $\mathcal{L}_{4i}, i = 1, 2$ are 4D Lagrangians confined to the $y = 0, \pi R$ branes.

3.3.1 Gauge Lagrangian

The 5D gauge Lagrangian that we are using, is the standard 5D $\mathcal{N} = 1$ one used in the super Yang-Mills action

$$\mathcal{L}_5 = \text{Tr} \left\{ -\frac{1}{2} F_{MN}^2 + (\mathcal{D}_M \Sigma)^2 + i\bar{\lambda} \gamma^M \mathcal{D}_M \lambda + (X^a)^2 - \bar{\lambda} [\Sigma, \lambda] \right\}, \quad (3.35)$$

where the last term is the commutator between the λ, Σ fields, where $\text{Tr} [t^A t^B] = \delta^{AB}/2$ and t^A are gauge group generators.

In line with our supersymmetric transformation and our Z assignments, coupling the above to a hypermultiplet results in the 5D action. The $\mathcal{N} = 2 \rightarrow \mathcal{N} = 1$ identification determines the corresponding brane Lagrangian, which will have the standard form corresponding to a 4D chiral multiplet coupled to a $\mathcal{N} = 1$ gauge multiplet. For more detail we refer the reader to [68].

3.3.2 Matter Lagrangian

We note that we can now write a superpotential W that can connect the bulk and brane matter fields via the interaction of chiral superfields on the $y = 0$ brane

$$W = W(\Phi_0, \mathcal{A}), \quad (3.36)$$

where Φ_0 denotes any general 4D chiral superfield. The most general Lagrangian, for the bulk hypermultiplet \mathcal{H} components, ignoring the gauge couplings, is given by

$$\mathcal{L}_5 = |\partial_M A^i|^2 + i\bar{\psi}\gamma^M \partial_M \psi + |F^i|^2. \quad (3.37)$$

The projected brane Lagrangian involving matter interaction is then given by the F-term of the superpotential W , as

$$\mathcal{L}_4 = F^1 \frac{\partial W}{\partial A^1} + \text{h.c.} = (F^1 - \partial_5 A^2) \frac{\partial W}{\partial A^2} + \text{h.c.} \quad (3.38)$$

Integrating out the auxiliary field F^1 leaves us with the full 5D action

$$S = \int d^4x dy \left\{ |\partial_M A^i|^2 + i\bar{\psi}\gamma^M \partial_M \psi - \delta(y) \left[(\partial_5 A^2 \frac{\partial W}{\partial A^1} + \text{h.c.}) + \left| \frac{\partial W}{\partial A^1} \right|^2 \right] \right\}, \quad (3.39)$$

where we note the $\delta(y)$ term confining the superpotential terms to the brane. We will introduce the contact terms between the hypermultiplets and the gauge fields via the covariant derivative in the next section.

3.4 Breaking Symmetries

In the following section we will continue our review and see how the translational and reflection isometries built into the theory can be used to break supersymmetry, and gauge symmetry. This can in turn be used to build a GUT model that breaks down to give us a SM like theory at low energies.

3.4.1 SUSY Breaking

Let's now start and build the model presented in [73], where we start off by considering the simpler case when gauge symmetry is unaffected.

Consider a vector multiplet $\mathcal{V} = (A_M, \lambda^i, \Sigma)$ and two Higgs matter hypermultiplets $\mathcal{H} = (H_i^a, \Psi^a)$, $a = 1, 2$. Since the Higgs hypermultiplets have the same quantum numbers they transform under an accidental $SU(2)_H$ flavour symmetry. The 5D SUSY action will then be invariant under the $SU(2)_R \times SU(2)_H$ symmetry as dictated by the Lagrangian

$$\begin{aligned} \mathcal{L}_5 = & \frac{1}{g^2} \text{Tr} \left\{ -\frac{1}{2} F_{MN}^2 + (\mathcal{D}_M \Sigma)^2 + i\bar{\lambda}_i \gamma^M \mathcal{D}_M \lambda^i - \bar{\lambda}_i [\Sigma, \lambda^i] \right. \\ & + |\mathcal{D}_M H_i^a|^2 + \bar{\Psi}_a (i\gamma^M \mathcal{D}_M - \Sigma) \Psi^a - (i\sqrt{2} (H_i^a)^\dagger \bar{\lambda}_i \Psi^a + \text{h.c.}) \\ & \left. - (H_i^a)^\dagger \Sigma^2 H_i^a - \frac{g}{2} \left((H_i^a)^\dagger \bar{\sigma}_i^j T^A H_j^a \right)^2 \right\}. \end{aligned} \quad (3.40)$$

We draw attention to the following term

$$\mathcal{L}_{\text{int}} = - \left(i\sqrt{2}(H_i^a)^\dagger \bar{\lambda}_i \Psi^a + \text{h.c.} \right). \quad (3.41)$$

The above allows us to read off the transformation rules for the fields. Requiring invariance under $SU(2)_R \times SU(2)_H$ the gauginos transform as $\lambda^i \sim (\mathbf{2}_R, 1_H)$, the Dirac field transforms as $\Psi^a \sim (1_R, \mathbf{2}_H)$, and the Higgs doublet $H_i^a \sim (\mathbf{2}_R, \mathbf{2}_H)$, where the subscripts R, H refer to the $SU(2)_R$ residual 5D $\mathcal{N} = 1$ and $SU(2)_H$ Higgs flavour symmetries. Recalling from the previous section that we can choose the reflection form as the non-trivial $Z = \sigma^3$, this choice gives our fields the following parity assignments

$$\begin{aligned} Z = +1 : & \quad \lambda_L^1, V_\mu; \quad H_1^1, \psi_R^1; \quad H_2^2, \psi_L^2, \\ Z = -1 : & \quad \lambda_L^2, V_5, \Sigma; \quad H_2^1, \psi_L^1; \quad H_1^2, \psi_R^2. \end{aligned} \quad (3.42)$$

Under this parity assignment, the $Z = \pm 1$ fields will decompose into KK modes along the extra dimension y . The wave-profile, and implicitly the 4D masses of the modes are determined by the assignments as

$$\check{\phi}_+ = \phi^{(0)} + \sqrt{2} \sum_{n=1}^{\infty} \cos \frac{ny}{R} \phi_+^{(n)}, \quad (3.43)$$

$$\check{\phi}_- = \sqrt{2} \sum_{n=1}^{\infty} \sin \frac{ny}{R} \phi_-^{(n)}, \quad (3.44)$$

where we have denoted 5D fields generically as $\check{\phi}_\pm$, $\phi^{(0)}$ are the massless 4D modes, and $\phi_\pm^{(n)}$ are the various KK modes. We will review how these wave modes arise in detail in Chapter 4.

The parity operator acting on the fields, can be written out as the direct product between the individual operators acting on the $SU(2)_R$, and the $SU(2)_H$ subspaces as

$$Z = \pm(\sigma^3)_R \otimes (\sigma^3)_H \otimes i\gamma^5, \quad (3.45)$$

where $i\gamma^5$ acts on the spinor indices of the representations, and does not affect spin 0, 1 fields. With this form of Z , since T has to obey the consistency constraints specified in Eqn. (3.20), under the $SU(2)_R \times SU(2)_H$ subspace product, the form of T becomes

$$T = e^{2\pi i \alpha \sigma^2} \otimes e^{-2\pi i \gamma \sigma^2}. \quad (3.46)$$

α is the symmetry parameter corresponding to the $SU(2)_R$ symmetry, and γ the one corresponding to $SU(2)_H$. Note that we have introduced a $-$ sign for the $SU(2)_H$

parametrisation, which is a convention that will prepare us for soft SUSY breaking masses. This is allowed since the fields in our discussion transform as doublets $\mathbf{2}$ under $SU(2)$, and since the conjugate representation is equivalent $\bar{\mathbf{2}} = \mathbf{2}$.

Therefore under T , fields ϕ , have to obey boundary conditions dictated by Eqn. (3.9). To illustrate the argument we consider the action dictated by the $SU(2)_R$ field space, where the extension to $SU(2)_R \times SU(2)_H$ is trivial. The boundary condition now takes the explicit form

$$\phi(x^\mu, y + 2\pi R) = e^{2\pi i \alpha \sigma^2} \phi(x^\mu, y). \quad (3.47)$$

The above admits the trivial solution

$$\phi(x^\mu, y + 2\pi R) = e^{i\alpha \sigma^2 y/R} \check{\phi}(x^\mu, y), \quad (3.48)$$

where we have introduced $\check{\phi}(x^\mu, y + 2\pi R) = \check{\phi}(x^\mu, y)$ which is a periodic field in y , and R is the compactification radius. $\check{\phi}$ can be in turn expanded into KK modes according to each of the fields' Z assignments according to Eqns. (3.43), (3.44).

Putting all this together, and extending it to $SU(2)_R \times SU(2)_H$, we get the following solutions for our fields

$$\begin{aligned} \begin{pmatrix} \lambda_1 \\ \lambda_2 \end{pmatrix} &= e^{i\alpha \sigma^2 y/R} \begin{pmatrix} \check{\lambda}_1 \\ \check{\lambda}_2 \end{pmatrix}, & \begin{pmatrix} \Psi^1 \\ \Psi^2 \end{pmatrix} &= e^{-i\gamma \sigma^2 y/R} \begin{pmatrix} \check{\Psi}^1 \\ \check{\Psi}^2 \end{pmatrix}, \\ \begin{pmatrix} H_1^1 & H_2^1 \\ H_1^2 & H_2^2 \end{pmatrix} &= e^{i\alpha \sigma^2 y/R} \begin{pmatrix} \check{H}_1^1 & \check{H}_2^1 \\ \check{H}_1^2 & \check{H}_2^2 \end{pmatrix} e^{-i\gamma \sigma^2 y/R}, \end{aligned} \quad (3.49)$$

where the accompanying α and/or γ factors are dictated according to the fields' transformation law under $SU(2)_R \times SU(2)_H$.

Plugging in the above solutions into the Lagrangian specified in Eqn. (3.40), the ∂_5 derivative acts on the boundary conditions, giving us the effective 4D soft SUSY breaking masses as shown in [63]

$$\begin{aligned} \mathcal{L}_{\text{SUSY}} &= -\frac{1}{2} \frac{\alpha}{R} (\lambda_L^{1(0)} \lambda_L^{1(0)} + \text{h.c.}) \\ &\quad - \left(\frac{\alpha^2}{R^2} + \frac{\gamma^2}{R^2} \right) (|h_u|^2 + |h_d|^2) + \frac{2\alpha\gamma}{R^2} (h_u h_d + \text{h.c.}) \\ &\quad - \frac{\gamma}{R} (\bar{\psi}_h \psi_h + \text{h.c.}), \end{aligned} \quad (3.50)$$

where we have labeled the 0 modes of our solutions as $h_u = H_1^{1(0)}$, $h_d = H_2^{2(0)}$, $\bar{\psi}_h = \bar{\psi}_L^{2(0)}$, $\psi_h = \psi_R^{1(0)}$. We note that, this effective mass that was generated via the non-trivial Scherk-Schwarz compactification, is a shift in the mass modes induced

by the twist T . This is explicitly manifested if we look at how the non zero modes behave when plugged in the same ∂_5 kinetic term (see [68] for more details).

To summarise, the Scherk-Schwarz twist provides us with soft SUSY breaking masses via the kinetic terms in the Lagrangian. Before we move on to matter fields we now take a look on how one can achieve gauge symmetry breaking via the orbifolding action.

3.4.2 Gauge Breaking

We now look at the more complicated case, when the orbifolding action can affect the structure of gauge group being projected on the branes. This mechanism allows us to break a gauge group \mathcal{G} to a subgroup \mathcal{H} on the brane via the \mathbb{Z}_2 projection.

In this more general context, we extend the definition of the parity assignment acting on the fields with a non-trivial gauge structure as

$$A_M^A(x^\mu, -y) = \alpha^M \Lambda^{AB} A_M^B(x^\mu, y), \quad (3.51)$$

$$\Psi(x^\mu, -y) = \lambda_R \otimes (i\gamma^5) \Psi(x^\mu, y), \quad (3.52)$$

where $\alpha^M = \pm 1$ are the previously mentioned parity assignments, Λ^{AB} is an appropriately sized square matrix that obeys $\Lambda^2 = 1$, with eigenvalues ± 1 (since we need to maintain $Z^2 \phi \rightarrow \phi$), and λ_R is a hermitian matrix acting on the representation space of the field Ψ . Note that in the previous section we have implicitly assumed this generalised form of Z , but we worked under the assumption of the trivial structure where $\Lambda = 1, \lambda_R = 1$.

Since we want the bulk action to remain invariant under this assignment, we require that the field strength tensor F_{MN}^A obeys the same transformation rule as A_M^A under the action of \mathbb{Z}_2 , namely $F_{MN}^A \rightarrow \alpha^M \Lambda^{AB} F_{MN}^B$. If we require that the field strength tensor construct $F_{MN}^A (F^A)^{MN}$ remain invariant, then Λ has to satisfy

$$f^{ABC} = \Lambda^{AA'} \Lambda^{BB'} \Lambda^{CC'} f^{A'B'C'}, \quad (3.53)$$

where f^{ABC} are the structure constants of the gauge group. The above just states that the \mathbb{Z}_2 action on the Lie algebra must be an automorphism (i.e. a transformation of the form $T^A \rightarrow \Lambda^{AA'} T^{A'}$ that preserves the structure constants).

Now, since Λ has eigenvalues ± 1 , it can be written in a diagonal basis as $\Lambda^{AA'} = \delta^{AA'} \eta^{A'}$, where $\eta^{A'} = \pm 1$. In this basis, the above condition can be restated as

$$f^{ABC} = \eta^A \eta^B \eta^C f^{ABC}, \quad (3.54)$$

where we are not summing over repeated indices. Therefore we are free to choose whatever parity assignment we want for our fields, via the choice in the η^A 's, as long as it obeys the above constraint. This choice can be gauge preserving or gauge breaking. Note that setting all η^A 's to 1 recovers the trivial case of $\Lambda = 1, \lambda_R = 1$, thus maintaining gauge structure.

We can make our life easier, and choose the η^A 's such that the generators in the adjoint representation T^A are naturally split into unbroken T^a and broken generators $T^{\hat{a}}$.

- **Unbroken generators:** where the set of $\eta^a = +1$ corresponds to T^a 's such that the surviving gauge group has the associated generators $\mathcal{H} = \{T^a\}$. More explicitly, $\eta^a = +1$ implies that T^a transforms as $T^a \rightarrow \delta^{aa'} \eta^{a'} T^{a'} = T^a$. I.e under this assignment, the η choices obey the automorphism constraint, and the subgroup \mathcal{H} has its gauge structure preserved.
- **Broken generators:** where the set of $\eta^{\hat{a}} = -1$ corresponds to $T^{\hat{a}}$'s such that the broken group has the associated generators $\mathcal{K} = \mathcal{G}/\mathcal{H} = \{T^{\hat{a}}\}$. Again the $\eta^{\hat{a}} = -1$ choice implies that $T^{\hat{a}}$ transforms as $T^{\hat{a}} \rightarrow -T^{\hat{a}}$. More explicitly, the η assignment does not obey the automorphism constraint, and the modded out group contains the broken generators.

For example, suppose our gauge group is $\mathcal{G} = SU(2)$, and we choose the $\eta^a, \eta^{\hat{a}}$ assignment under the constraint of Eqn. (3.54), such that $a = \{1, 2, 3\}; \hat{a} = \{\emptyset\}$. I.e. this choice implies that we have no gauge breaking. If instead we would have chosen $a = \{3\}; \hat{a} = \{1, 2\}$, then the gauge group $SU(2)$ would be broken down to $U(1)$ via the action of the algebra automorphism.

The η assignment will also impact the fields that live in the gauge representation space. Since we require the bulk action be invariant, we also require the coupling

$$ig \bar{\Psi} \gamma^M A_M^A T^A \Psi, \quad (3.55)$$

to remain invariant. It can be shown that, in order for the above to maintain gauge invariance under the surviving gauge group, the λ_R matrix present in the fermionic assignment in Eqn. (3.52), must satisfy

$$\{\lambda_R, T_R^{\hat{a}}\} = 0, \quad [\lambda_R, T_R^a] = 0. \quad (3.56)$$

We can see that our choice in Λ , expressed via the choice in the η assignments, has also split our representation into two implicit subspaces, with the Z parity

assignment dictated by the above anticommutation and commutation relations. Furthermore, for rank preserving gauge breaking, it can be shown that orbifold breaking via the Lie algebra automorphism is restricted for the special unitary $SU(N)$ and special orthogonal $SO(N)$ groups as

$$\begin{aligned} SU(p+q) &\rightarrow SU(p) \otimes SU(q) \otimes U(1), \\ SO(p+q) &\rightarrow SO(p) \otimes SO(q), \quad \text{where } p \text{ or } q \text{ even,} \\ SO(2n) &\rightarrow SU(n) \otimes U(1). \end{aligned} \tag{3.57}$$

For example, let us look at our $SU(5)$ model. If we choose Λ such that $T^a \in G_{\text{SM}}$ and $T^{\hat{a}} \in SU(5)/G_{\text{SM}}$ (which is a valid assignment from the point of view of the Lie algebra automorphism of the surviving SM gauge group $SU(3)_C \times SU(2)_L \times U(1)_Y$), we have a consistent λ_R given as $\lambda_R = \text{diag}(+1, +1, +1, -1, -1)$. This effectively states that the fundamental $\mathbf{5} \sim SU(5)$ representation, splits under the \mathbb{Z}_2 action into $\mathbf{3} \oplus \mathbf{2}$ under G_{SM} . Since the surviving gauge group fields are able to have 0 modes, the model can then use the Higgs mechanism to undergo the usual SM electro-weak breaking. Furthermore since the projected out modes have $Z = -1$ the fields will have corresponding KK modes dictated by the decomposition in Eqn. (3.44) where $\sim \sin \frac{ny}{R}$, $n \geq 1$. When integrating out the 5th dimension to obtain the 4D theory, these modes acquire a naturally effective heavy mass of $\mathcal{O}(1/R)$ via the action ∂_5 derivative.

We noted in the Sec. 3.2, that we can combine our Z and T action to form another Z' , thus giving us the equivalent orbifold relationship between S^1/\mathbb{Z}_2 and $\mathbb{R}^1/\mathbb{Z}_2 \times \mathbb{Z}'_2$. The same argument that we presented here for the \mathbb{Z}_2 and the gauge structure breaking, can be followed in the same manner in the equivalent case of the $\mathbb{R}^1/\mathbb{Z}_2 \times \mathbb{Z}'_2$ orbifold, but with the \mathbb{Z}'_2 reflection having the gauge breaking effect instead of \mathbb{Z}_2 , which now has a trivial action on the gauge structure.

The reason we bring this up, is because we can express Z, T more easily since changing from one picture to another is equivalent with switching a “basis” between (Z, T) and (Z, Z') . If we now take $Z = \text{diag}(+, +, +, +, +)$ and Z' as the required $SU(5) \rightarrow G_{\text{SM}}$ breaking assignment, switching to the (Z, T) gives us the equivalent gauge breaking form

$$Z \sim \text{diag}(+, +, +, +, +), \quad T \sim \text{diag}(-, -, -, +, +). \tag{3.58}$$

By switching we have essentially transferred the gauge group breaking to our T action via the basis reinterpretation. The reason we do this, is to highlight

the situation when the $SU(2)_R \times SU(2)_H$ is implemented as a local symmetry. If this is the case it can be shown that the Scherk-Schwarz mechanism is the same as Hosotani breaking (or Wilson line breaking) [74–76]. In this case, the gauge breaking is expressed via the holonomy classes of the system, which are tied in with the translational symmetry. In essence we use the representation in Eqn. (3.58), since one can switch to the Hosotani picture where it can be easier to interpret its effect on gauge group representations. To summarise this section, the actions of our isometries acting on field space are defined by

$$Z = \pm(\sigma^3)_R \otimes (\sigma^3)_H \otimes \text{diag}(+, +, +, +, +), \quad (3.59)$$

$$T = e^{2\pi i \alpha \sigma^2} \otimes e^{-2\pi i \gamma \sigma^2} \otimes \text{diag}(-, -, -, +, +). \quad (3.60)$$

Due to the non-trivial nature of Scherk-Schwarz and orbifold compactification, in the model present in [63] the above will have the effect of breaking the 4D effective $\mathcal{N} = 2$ SUSY down to $\mathcal{N} = 1$, along with the Higgs flavour symmetry present in the bulk. Furthermore on the $y = 0$ brane the gauge structure is broken by restricting the gauge transformations allowed on the brane, where the only fields that transform under the surviving gauge group have 0 modes.

3.5 Fermionic Matter: Brane vs. Bulk

We are now just one puzzle piece away from being able to explore the model in [63], and further extend it via extra scalars/a gauge group extension. We now move on to fermionic matter in this category of models. We have a choice of where to put these fields dictated by Eqn. (3.34), either in the bulk as hypermultiplets via the 5D Lagrangian \mathcal{L}_5 , or on the brane as chiral multiplets via the 4D brane Lagrangians \mathcal{L}_{4i} . Their placement will impact the number of required multiplets to get the low energy SM fields. Not to lose track of what we are trying to do here, we are trying to recover the SM gauge structure and field content post identification on the IR brane at $y = 0$.

We start off with the simplest fermionic matter placement, brane matter. In this case we can just use the usual $\mathcal{N} = 1$ chiral multiplets from an ordinary $SU(5)$ SUSY model. This comes with the embedding of the supersymmetric SM fields U, D, Q, L, E within the $\mathbf{10} \sim SU(5)$ representation $T_{\mathbf{10}} \sim \mathbf{10} \supset \{Q, U, E\}$ and the $\bar{\mathbf{5}} \sim SU(5)$ representation as $F_{\bar{\mathbf{5}}} \sim \bar{\mathbf{5}} \supset \{D, L\}$. By putting these fields on the brane they are now coupled to the \mathbb{Z}_2 chiral projection of the Higgs hypermultiplets via the bulk superpotential W .

We note that, when projecting the bulk matter hypermultiplets on the brane, we form two chiral multiplets defined by the $Z = \pm 1$ eigenvalues. To maintain gauge invariance in the bulk as dictated by the Lagrangian in Eqn. (3.40), the components of the hypermultiplet must transform appropriately. More specifically the components contained in the $Z = +1$ chiral multiplet will transform as the fundamental of the group, where the $Z = -1$ one will transform as the conjugate, which we denote with a superscript c . E.g for an arbitrary matter hypermultiplet $\mathcal{A} = (A^i, \Psi_a)$, within the context of the $SU(5)$ gauge structure, the \mathbb{Z}_2 identification produces the 4D chiral multiplets

$$\mathcal{A} = (A^1, \psi_R^A) \sim \mathbf{5}, \quad \mathcal{A}^c = (A^2, \psi_L^A) \sim \bar{\mathbf{5}}. \quad (3.61)$$

Therefore, using the usual $SU(5)$ superfield prescription, the IR brane Lagrangian is expressed in term of the superspace action as

$$S_{\text{Matter}} = \int d^4x \, dy \, \delta(y) \left[\int d^2\theta \sum_{j,k=1}^3 (y_1)_{jk} T_{\mathbf{10}_j} T_{\mathbf{10}_k} H_{\mathbf{5}}^c + (y_2)_{jk} T_{\mathbf{10}_j} F_{\bar{\mathbf{5}}_k} H_{\bar{\mathbf{5}}} + \text{h.c.} \right], \quad (3.62)$$

where $H_{\mathbf{5}} = (H_1^1, \psi_R^1)$, $H_{\bar{\mathbf{5}}} = (H_2^2, \psi_L^2)$, and we have introduced 3 generations of matter denoted by the j, k indices.

After the SS and orbifolding mechanisms perform their various attributes, the $H_{\mathbf{5}}, H_{\bar{\mathbf{5}}}$ suffer gauge breaking and automatically acquire a 2 – 3 splitting. The rest of the model's phenomenology is then analogous to the usual supersymmetric $SU(5)$ GUT.

If on the other hand, we put our matter fields as components of bulk hypermultiplets, we run into a small issue. Since all the bulk hypermultiplets will automatically undergo the 2 – 3 splitting induced by the T action, putting just one of the chiral analogs $\mathcal{T}_{\mathbf{10}}, \mathcal{T}_{\bar{\mathbf{5}}}$, would suffer from having some of the states in the SM spectrum projected out. This means that we will not be able to recover the correct 0 mode spectrum in order to recreate the SM.

In order to get around this, we put in two copies of each of the $SU(5)$ fermionic matter hypermultiplet, where we assign them opposite Z assignments with respect to each other. I.e. we introduce 4 matter hypermultiplets $\mathcal{T}_{\mathbf{10}} = \{T_{\mathbf{10}}, T_{\mathbf{10}}^c\}$, $\mathcal{T}'_{\mathbf{10}} = \{T'_{\mathbf{10}}, T'^c_{\mathbf{10}}\}$, $\mathcal{T}_{\bar{\mathbf{5}}} = \{F_{\bar{\mathbf{5}}}, F_{\bar{\mathbf{5}}}^c\}$, $\mathcal{T}'_{\bar{\mathbf{5}}} = \{F'_{\bar{\mathbf{5}}}, F'^c_{\bar{\mathbf{5}}}\}$, to which we assign the Z assignments

$$\begin{aligned} \{T_{\mathbf{10}}, T_{\mathbf{10}}^c\} &\rightarrow \{(+T_{\mathbf{10}}, (-)T_{\mathbf{10}}^c\}, \\ \{T'_{\mathbf{10}}, T'^c_{\mathbf{10}}\} &\rightarrow \{(-)T'_{\mathbf{10}}, (+)T'^c_{\mathbf{10}}\}. \end{aligned} \quad (3.63)$$

The assignments for $\mathcal{F}_{\overline{5}}, \mathcal{F}'_{\overline{5}}$ are analogous. With these assignments laid out, we have now fully described the model introduced in [63].

However with this matter placement we have another added complexity in the sense that now, the individual hypermultiplets transform under the residual $SU(2)_R$ symmetry. Note that we assume a trivial flavour action on \mathcal{T}, \mathcal{F} . After orbifolding, the non-trivial SS conditions will provide us with squark soft SUSY breaking masses via the kinetic part of the Lagrangian in Eqn. (3.40), along with a contribution to the trilinear squark coupling A_0 via the $\partial_5 Q^2$ term in Eqn. (3.39).

3.6 Models

We now want to examine the full UV model, and see if the resulting spectrum matches the 4D SM along with ensuring that it is phenomenologically consistent with the current experimental observation. This is done by fully specifying the low scale model encapsulating the SM that would result from a UV SUSY theory, along with its renormalisation group equations (RGEs). We then connect to the high scale UV model to the IR one by imposing gauge coupling unification along with the soft SUSY breaking masses dictated by the SS mechanism, which are then run down from the GUT scale to the IR scale via the RGEs. Throughout this chapter, we refer to gauge coupling unification and the soft SUSY breaking masses at the GUT scale, as high scale boundary conditions. We will now go through all the bits and pieces that we have laid out and summarise them here for convenience.

The first model we consider is the $SU(5)$ GUT in 5D, compactified on the S^1/Z_2 orbifold, presented in [63]. The 4D model that we obtain post SS breaking and orbifolding will consist of the MSSM. The matter content of the model consists of a vector hypermultiplet $\mathcal{V} = (A_M, \lambda^i, \Sigma)$, and two Higgs hypermultiplets $\mathcal{H}^a = (H^a, \Psi^a)$, $a = 1, 2$. The 5D action is invariant under the aforementioned $SU(2)_R \times SU(2)_H$ symmetry where the fields have the representations $\lambda^i \sim (\mathbf{2}_R, \mathbf{1}_H)$, $\Psi^a \sim (\mathbf{1}_R, \mathbf{2}_H)$, $H_i^a \sim (\mathbf{2}_R, \mathbf{2}_H)$. The extra dimension is compactified at a scale $M_{\text{GUT}} = 1/R = 10^{16}$ GeV to break both the $SU(5)$ symmetry and the supersymmetry. The form of the T, Z actions is the one specified earlier, namely

$$Z = (\sigma^3)_R \otimes (\sigma^3)_H \otimes \text{diag}(+, +, +, +, +), \quad (3.64)$$

$$T = e^{2\pi i \alpha \sigma^2} \otimes -e^{2\pi i \gamma \sigma^2} \otimes \text{diag}(+, +, +, -, -), \quad (3.65)$$

where the final matrix is acting on the $SU(5)$ space. Note that in the above T

has an explicit minus sign in front of the flavour action, in contrast to Eqn. (3.60), which is compensated by the diagonal gauge matrix.

The ∂_5 derivative acts on the boundary conditions giving us effective 4D soft SUSY breaking terms [63] of the form

$$\begin{aligned} \mathcal{L}_{\text{SUSY}} = & -\frac{1}{2} \frac{\alpha}{R} (\lambda_L^{1(0)} \lambda_L^{1(0)} + \text{h.c.}) - \left(\frac{\alpha^2}{R^2} + \frac{\gamma^2}{R^2} \right) (|h_u|^2 + |h_d|^2) + \frac{2\alpha\gamma}{R^2} (h_u h_d + \text{h.c.}) \\ & - \frac{\gamma}{R} (\bar{\psi}_h \psi_h + \text{h.c.}), \end{aligned} \quad (3.66)$$

where we've labeled the zero-modes as $h_u = H_1^{1(0)}$, $h_d = H_2^{2(0)}$, $\bar{\psi}_h = \bar{\psi}_L^{2(0)}$, $\psi_h = \psi_R^{1(0)}$. From the point of view of the MSSM, the SS twists have generated universal gaugino breaking terms ($m_0 = \hat{\alpha}$), and holomorphic Higgs terms ($m_{H_u}^2 = m_{H_d}^2 = \hat{\alpha}^2$, $\mu = \hat{\gamma}$, $\mu B = -2\hat{\alpha}\hat{\gamma}$) via the $\hat{\alpha} \equiv \alpha/R$, $\hat{\gamma} \equiv \gamma/R$ parameters controlling the $SU(2)_R \times SU(2)_H$ breaking.

As previously discussed, we may still choose where to place our fermionic matter fields. We may either keep them restricted to the $y = 0$ brane or allow them to propagate in the 5D bulk. Restricting them to the brane results in the MSSM at low energies with supersymmetry breaking masses given by

$$\begin{aligned} m_{1/2} &= \hat{\alpha}, & \mu &= \hat{\gamma}, \\ m_{h_u, h_d}^2 &= \hat{\alpha}^2, & \mu B &= -2\hat{\alpha}\hat{\gamma}, \end{aligned} \quad (3.67)$$

and

$$m_{\tilde{q}, \tilde{u}, \tilde{d}, \tilde{l}, \tilde{e}}^2 = 0, \quad A_0 = -\hat{\alpha}, \quad (3.68)$$

where the above are defined at the compactification scale ($\sim M_{\text{GUT}}$). Note that with the brane matter placement the trilinear A_0 still gets a contribution from the $\partial_5 H^2(dW/dH^1)$ term in Eqn. (3.39).

If we instead place the fermionic matter in the bulk, we gain extra contributions to A_0 and the squark soft SUSY breaking masses which arise from their non-trivial transformation under the $SU(2)_R$ symmetry. The higgs and gaugino soft breaking masses remain the same as shown in Eqn. (3.67), but now have

$$m_{\tilde{q}, \tilde{u}, \tilde{d}, \tilde{l}, \tilde{e}}^2 = \hat{\alpha}^2, \quad A_0 = -3\hat{\alpha}. \quad (3.69)$$

3.6.1 Methodology

The RGE running is performed using the FlexibleSUSY [v.2.0.1] [77, 78] spectrum generator which uses numerical routines generated by SOFTSUSY [79, 80] and with

two-loop RGEs provided by SARAH [v.4.12.2] [81–84]. SARAH also provides the electroweak tadpole conditions.

In principle, the electroweak tadpole equations could set our final low energy observables, the ratio of vacuum expectation values (VEVs) of the two Higgs doublets, $\tan\beta$, and the Z -boson mass. However, for technical reasons it is easier to assign these values at the low scale. To this extent we temporarily relax some of our high scale relations between the soft SUSY breaking parameters and the model inputs. We choose to allow our choice of $\tan\beta$ to fix $\hat{\gamma}$ and leave μB unfixed. At the end of the process we check if $\mu B = -2\hat{\alpha}\hat{\gamma}$ as required by SS compactification. We will refer to this as the “Scherk-Schwarz condition”. Due to the uncertainties arising from the RGE running, we insist that the Scherk-Schwarz condition is obeyed with 95% confidence. This is reflected via a χ_{SS}^2 contribution as

$$\chi_{\text{SS}}^2 = \frac{\left(\left(\frac{\mu B}{\mu} + 2\hat{\alpha}\right) - 0\right)^2}{\sigma_c^2}, \quad (3.70)$$

where $\sigma_c^2 = (\mu B)^2 \sigma_\mu^2 / \mu^4 + \sigma_{\mu B}^2 / \mu^2$ is the combined uncertainty on the constraint arising from the RGE running uncertainties in $\mu, \mu B$. The $\sigma_\mu, \sigma_{\mu B}$ uncertainties are taken in line with the 95% confidence bound. We stress that in principle, this is no different than forcing the relation at high energies and searching for values of $\tan\beta$ that satisfy the tadpole equations.

To explore the parameter space we employ a ‘seeded random walk’ scanning algorithm. The scanning procedure consists of two stages to minimize computing time and explore relevant sections of the subspace.

Stage 1: This stage is a random sampling of the parameter space. Here we define our parameter space, and then define the relevant limits of each parameter. After this the algorithm picks a random point within the bounds and then runs FlexibleSUSY with the point’s parameters to check if the conditions produce EWSB, and does not output non-perturbative runnings and tachyons. If the point produces a valid electroweak spectrum we keep it. We stop when we deem that we’ve “populated” the phase space (somewhere around 5000 - 10000 points).

Stage 2: Now, after we have populated the phase space we want to inspect regions that come close or satisfy the imposed experimental bounds and constraints. To this extent we define and evaluate the χ_i^2 ’s associated with the constraints (excluding the SS condition), which are then added together to form a global χ^2 mea-

sure

$$\chi^2 = \sum_{i=1}^n \chi_i^2. \quad (3.71)$$

Following this we then deem what points are phenomenologically relevant, by inspecting if they come close to satisfying our required constraints, with ‘closeness’ being defined by the global χ^2 value. If the point is deemed as relevant, then the scan performs a random walk around the point, until it finds another one with a smaller χ^2 value. This is repeated until we find a point that agrees with the required constraints (if it exists). The search is abandoned if computation time exceeds a preset limit. This provides us with points that are theoretically well behaved but may still be experimentally excluded. We therefore then must check LHC and Dark Matter constraints.

We apply LHC bounds and constraints from the ATLAS and CMS collaborations:

1. We insist on a Higgs mass in the range $123 \leq m_H \leq 127$ GeV, where we’ve assumed a 2 GeV theoretical uncertainty dominates those from the experimental measurement [85, 86].
2. We require a gluino mass $m_{\tilde{g}} \geq 2$ TeV [87, 88].
3. We require a lightest neutralino and chargino masses to be outside the exclusion contour provided by Fig. 13 of Ref. [89], which in particular combines the exclusions from [90, 91].
4. The stop quark $m_{\tilde{t}}$ should be heavier than 1 TeV [49].
5. Any extra gauge boson must have mass $m_{Z'} \geq 2.4$ TeV [92].

For scenarios that pass the LHC constraints and satisfy the Scherk-Schwarz constraint, we apply constraints on the Dark Matter relic density. We use the measurement from Planck [93],

$$\Omega_c h^2 = 0.1157 \pm 0.0023, \quad (3.72)$$

and include a further 10% uncertainty arising from the mass difference from MicrOmegas [94–96] and FlexibleSUSY. We therefore accept points with a Dark Matter relic density smaller than $\Omega_c h^2 = 0.1275$ to allow for the possibility of other sources of Dark Matter.

3.6.2 Barbieri, Hall and Nomura $SU(5)$: Brane and Bulk

We start off by considering the aforementioned minimal $SU(5)$ flat extra dimensional model which will result in the minimal supersymmetric model at low energies (MSSM). When considering fermionic matter on the brane, we will have soft SUSY breaking masses and couplings resulting from the SS and orbifolding procedure as per the original model. Reiterating for convenience, in the case of brane fermionic matter, from the perspective of the MSSM, the soft SUSY breaking masses are given at the GUT scale by

$$\begin{aligned} m_{1/2} &= \hat{\alpha} \equiv \alpha/R, \\ m_{h_u, h_d}^2 &= \hat{\alpha}^2, \quad m_{\tilde{q}, \tilde{u}, \tilde{d}, \tilde{l}, \tilde{e}}^2 = 0, \quad A_0 = -\hat{\alpha}, \\ \mu &= \hat{\gamma} \equiv \gamma/R, \quad \mu B = -2\hat{\alpha}\hat{\gamma}, \end{aligned} \quad (3.73)$$

where we take the GUT scale M_{GUT} as the compactification scale $M_{\text{GUT}} = 1/R = 10^{16}$ GeV. Similarly, for the bulk case, we have the high scale soft SUSY breaking masses

$$\begin{aligned} m_{1/2} &= \hat{\alpha} \equiv \alpha/R, \\ m_{h_u, h_d}^2 &= \hat{\alpha}^2, \quad m_{\tilde{q}, \tilde{u}, \tilde{d}, \tilde{l}, \tilde{e}}^2 = \hat{\alpha}^2, \quad A_0 = -3\hat{\alpha}, \\ \mu &= \hat{\gamma} \equiv \gamma/R, \quad \mu B = -2\hat{\alpha}\hat{\gamma}. \end{aligned} \quad (3.74)$$

As pointed out in the original paper, the model has a fine tuning problem. Note that all the presented masses are given at the GUT scale $1/R \sim 10^{16}$ GeV. In order for supersymmetry to be a relevant solution to the hierarchy problem, the effective parameters $\hat{\alpha}, \hat{\gamma}$ which dictate the scale at which supersymmetry is broken, must be of the same order of the weak scale. Therefore the SS twist α, γ parameters must be of the order of $\mathcal{O}(10^{-13})$. We end up with a “natural” (in the sense that SS twists provide an organising principle in introducing soft SUSY masses) supersymmetry falling out of the theory, but it comes at the cost of introducing the question of why are the parameters so small, and can they be dictated by a more UV complete theory such as string theory.

Throughout this chapter we will therefore restrict ourselves to models with a reasonably low supersymmetry breaking scale so that the hierarchy problem itself is not an issue. Therefore we make the restriction that $\hat{\alpha}$ be less than 10^4 GeV. Similarly, we allow $\tan\beta$ to vary from 1 to 40. Once our low energy scenarios are generated in FlexibleSUSY we then confront them with the Scherk-Schwarz condition and the experimental constraints outlined in the previous section.

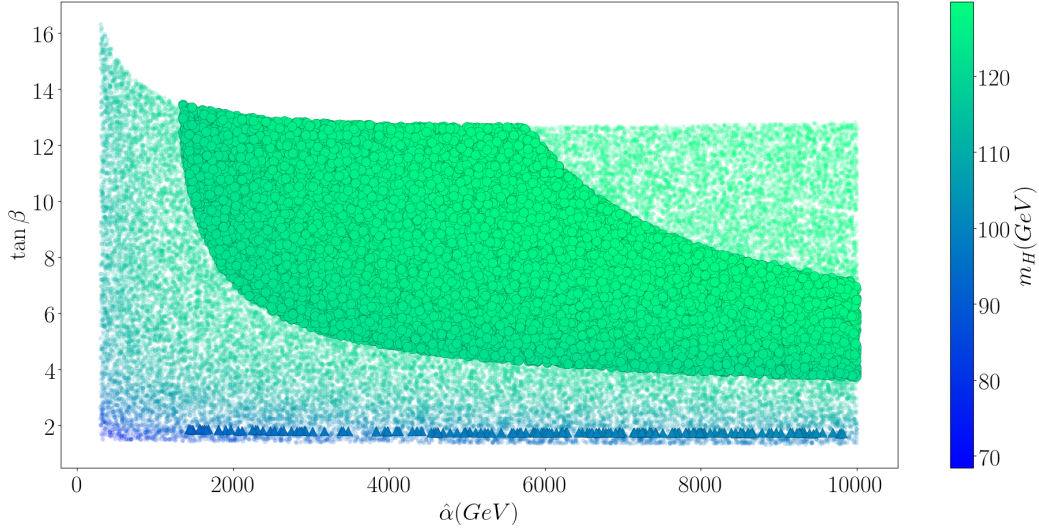


Figure 3.4: Points from the Barbieri, Hall and Nomura $SU(5)$ model with brane fermionic matter. Circles denote points that have passed the experimental constraints and have the desired Higgs mass, triangles show points that obey the Scherk-Schwarz constraint. Fainter points in the background fail these constraints but are otherwise well behaved. The x axis represents the soft SUSY scale parameter $\hat{\alpha}$, the y axis shows the corresponding value for $\tan\beta$ and the colour axis represent the value of the Higgs mass.

Recalling that we have allowed $\tan\beta$ to fix $\hat{\gamma}$, our only input parameters are $\hat{\alpha}$ and $\tan\beta$. We show generated scenarios in the $\hat{\alpha}$ - $\tan\beta$ plane in Figs. 3.4 and 3.5. The colour bar represents the mass of the lightest Higgs boson which we would like to identify with the discovered 125 GeV resonance. Points denoted with a circle have passed the LHC and DM constraints, and have the desired Higgs mass. In contrast, points that pass the Scherk-Schwarz constraint are denoted by triangles. The fainter points in the background are points that fail these constraints (but are otherwise well behaved). Fig. 3.4 shows scenarios where the matter is kept on the $y = 0$ brane, while Fig. 3.5 allows matter to propagate in the bulk.

From the two cases we can see that the subset of points corresponding to the correct Higgs mass and LHC/DM constraints do not overlap with the ones obeying the SS constraint. In essence, the Scherk-Schwarz condition prohibits a heavy enough lightest Higgs boson. However, we note that the Higgs boson mass is not too far from its measured value, particularly when matter is allowed to propagate in the bulk, which warrants exploration in next to minimal scenarios. We also note that

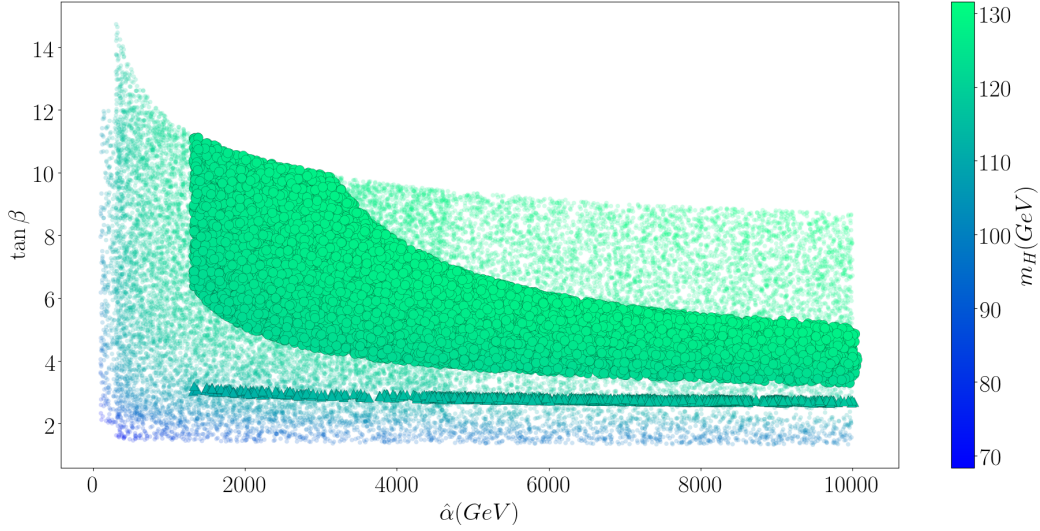


Figure 3.5: Points from the Barbieri, Hall and Nomura SU(5) Model with bulk matter. We use the same conventions for the points as in Fig. 3.4.

the points with acceptable Higgs mass allow lower $\tan \beta$ as $\hat{\alpha}$ is increased, so there may still be room for agreement with the SS constraint in theories of High Scale or Split Supersymmetry which allow higher values of $\hat{\alpha}$ (see for example Ref. [97]).

It is difficult to provide a definitive explanation of why the Scherk-Schwarz condition requires such a low value of $\tan \beta$, since $\tan \beta$ is a low energy parameter arising from electroweak symmetry breaking involving parameters that are evolved from the high scale. Nevertheless we can obtain some insights into the patterns arising in Figs. 3.4, 3.5, by examining the leading order tadpole equations. When analysing these, we temporarily make the assumption that the supersymmetry breaking parameters do not evolve between the UV and IR. Then $m_{H_u}^2$, $m_{H_d}^2$, μ and μB keep their values in terms of $\hat{\alpha}$ and $\hat{\gamma}$ seen in Eqn. (3.67). Plugging these into the leading-order tadpoles gives

$$\hat{\alpha}^2 + \hat{\gamma}^2 - 2\hat{\alpha}\hat{\gamma}\frac{1}{\tan \beta} - \frac{1}{8}\nu^2(g_1^2 + g_2^2)\frac{1 - \tan^2 \beta}{1 + \tan^2 \beta} = 0, \quad (3.75)$$

$$\hat{\alpha}^2 + \hat{\gamma}^2 - 2\hat{\alpha}\hat{\gamma}\tan \beta + \frac{1}{8}\nu^2(g_1^2 + g_2^2)\frac{1 - \tan^2 \beta}{1 + \tan^2 \beta} = 0. \quad (3.76)$$

The sum of these has a solution $\tan \beta = \hat{\alpha}/\hat{\gamma}$, while the difference leads to $\hat{\alpha} = \hat{\gamma}$. Therefore at leading order and with no running, we would always expect $\tan \beta = 1$. Clearly the supersymmetry breaking parameters *do* run, and our tadpole equations

are taken beyond leading order,

$$\frac{\partial V}{\partial \phi_i} + \frac{\partial \Delta V}{\partial \phi_i} = 0, \quad (3.77)$$

where the corrections are stated in [98]. The actual results deviate from this expectation, but this provides a rough justification for why the Scherk-Schwarz boundary conditions lead to a low value of $\tan \beta$.

3.6.3 $SU(5)$ with an additional scalar

This subsection will explore our extension of the original model via a next to minimal approach. Since we have seen that the Higgs masses produced by the points that obey the SS constraint are not sufficiently large enough in the basic $SU(5)$ model, we move on to a next to minimal extension. This will comprise of introducing a $SU(5)$ scalar singlet that couples to the Higgs field, resulting in a general low energy NMSSM rather than the MSSM.

Again, we have two ways of introducing the scalar, either as a chiral multiplet scalar singlet on the brane $S = (s, \psi_s)$, or as a hypermultiplet $\mathcal{S} = \{s^i, \Psi_S\}$ coupled to the Higgs fields. Note that we will only couple the scalar to the Higgs and to itself, which results in 4 cases when considering brane/bulk fermionic matter.

The most general next to minimal superpotential that will result in either of the scalar/matter combinations at the low energy, has the form

$$W = W_{\text{Higgs-Fermions}} + \mu H_u H_d + \lambda H_u H_d S + \frac{1}{3} \kappa S^3 + L S + \frac{1}{2} M_S S^2, \quad (3.78)$$

where λ, κ, L, M_S are constants. Note that we have kept an explicit $\mu H_u H_d$ term in favour of the traditional \mathbb{Z}_3 invariant NMSSM, since the model produces an effective μ via the ∂_5 derivative, resulting in \mathbb{Z}_3 violating terms. Using a shift symmetry we now set the linear term to $L = 0$ and $M_S = 0$, not to be confused with m_S^2 the soft SUSY breaking mass for the scalar superfield.

We also note that our holomorphic terms arise as a combination of the Scherk-Schwarz $SU(2)_H$ flavour breaking along with a component arising from the VEV of S

$$\mu_{\text{eff}} = \mu + \frac{1}{\sqrt{2}} \lambda \langle S \rangle, \quad (3.79)$$

$$\mu B_{\text{eff}} = \mu B + \frac{1}{\sqrt{2}} T_\lambda \langle S \rangle + \frac{1}{2} \kappa \lambda \langle S \rangle^2, \quad (3.80)$$

where T_λ is the trilinear coupling arising from the $\lambda H_u H_d S$ term in the superpotential. Furthermore, we assume that the only soft SUSY breaking masses and mass

terms arise from the Scherk-Schwarz mechanism, therefore extending our parameter space by λ, κ .

We first introduce our scalar S as a brane confined chiral supermultiplet along with the same type of matter. Computing the soft breaking masses and trilinears, we get the following soft SUSY breaking masses

$$\begin{aligned} m_{1/2} &= \hat{\alpha}, \\ m_{h_u, h_d}^2 &= \hat{\alpha}^2, \quad m_{\tilde{q}, \tilde{u}, \tilde{d}, \tilde{l}, \tilde{e}}^2 = 0, \quad A_0 = -\hat{\alpha}, \\ \mu &= \hat{\gamma}, \quad \mu B = -2\hat{\alpha}\hat{\gamma}, \\ m_S^2 &= 0, \quad T_\lambda = -2\lambda\hat{\alpha}, \quad T_\kappa = 0. \end{aligned} \tag{3.81}$$

Similarly for a brane chiral multiplet S , and bulk fermions we have

$$\begin{aligned} m_{1/2} &= \hat{\alpha}, \\ m_{h_u, h_d}^2 &= \hat{\alpha}^2, \quad m_{\tilde{q}, \tilde{u}, \tilde{d}, \tilde{l}, \tilde{e}}^2 = \hat{\alpha}^2, \quad A_0 = -3\hat{\alpha}, \\ \mu &= \hat{\gamma}, \quad \mu B = -2\hat{\alpha}\hat{\gamma}, \\ m_S^2 &= 0, \quad T_\lambda = -2\lambda\hat{\alpha}, \quad T_\kappa = 0. \end{aligned} \tag{3.82}$$

The results of the parameter scans in the above cases are given in Figs. 3.6, 3.7. Note that we are using the same convention for the points as in the previous figures.

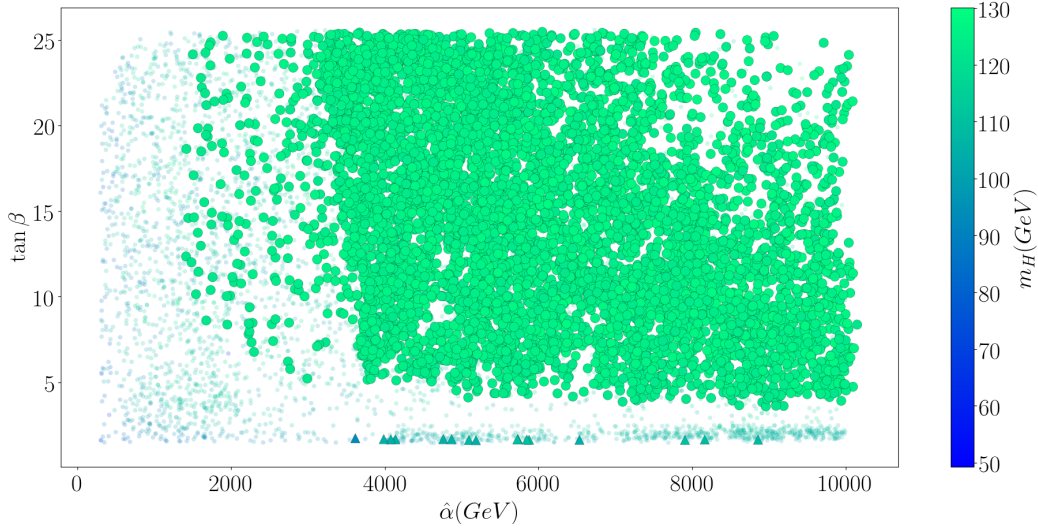


Figure 3.6: Points for the $SU(5)$ model with an additional scalar S on the brane, and brane matter. We use the same conventions for the points as in Fig. 3.4.

In the case of the brane scalar S we see that both the fermionic matter placements produce an appropriate low energy SM spectrum with the appropriate Higgs mass,

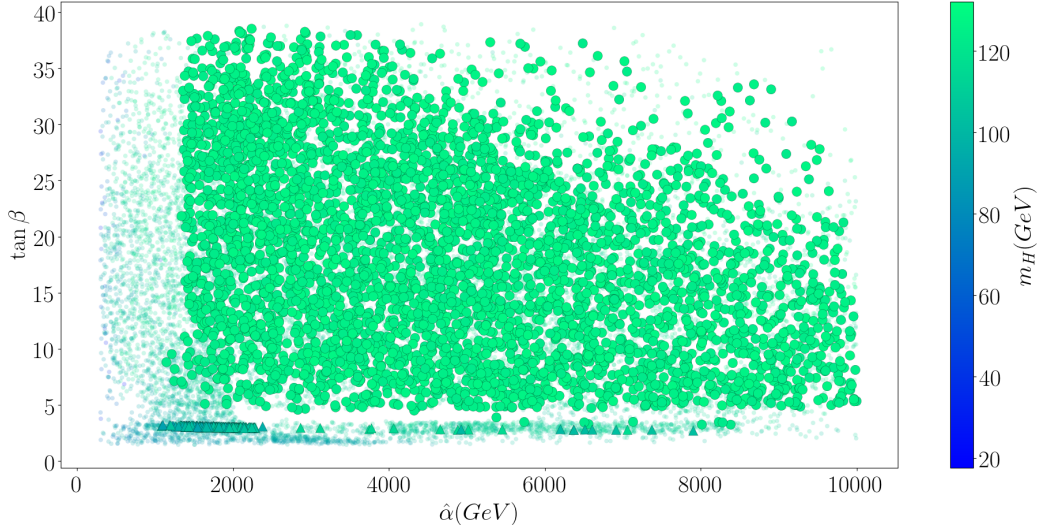


Figure 3.7: Points for the $SU(5)$ model with an additional scalar S on the brane, and bulk matter. We use the same conventions for the points as in Fig. 3.4.

with the main difference being in the range of $\tan\beta$ values that the model allows for EWSB.

It is interesting to note that all the SM like Higgs points reside in a region where \hat{a} is roughly greater than 2 TeV, with fairly high $\tan\beta$ values, which is to say that if SUSY is broken via SS as per this set of models it will ‘naturally’ fall in the $\mathcal{O}(1 - 10)\text{TeV}$ scale.

Similar to what happened in the “vanilla” $SU(5)$ case, the points that pass the SS constraint do not overlap or are in a close region to those which pass Higgs and LHC constraints. This is a recurrent theme that we’ll see all through the chapter, namely the points that would originate from the SS breaking of $SU(2)_H, SU(2)_R$, can’t seem to produce a large enough Higgs mass and/or pass LHC constraints. This is much clearer and stronger in the brane/brane case than the brane/bulk one. The closeness in the second case is where a closer look is needed with regard to the points obeying the SS constraint. What could be happening is that we’ve been overly conservative with our error estimates for $\mu, \mu B$, where their relaxation would result in an overlap. For example, the maximum Higgs mass for the Scherk-Schwarz points is $m_H \approx 116.9\text{ GeV}$, which is close enough to provide some doubt.

Alternatively, we can try a bulk scalar placement, where we introduce the $SU(5)$ singlet hypermultiplet $\mathcal{S} = \{s^i, \Psi_s\}$, $\Psi_s = (\psi_L^s, \psi_R^s)$, $i = 1, 2$, which transforms non-trivially under the $SU(2)_R$ residual supersymmetry. Analogous to what we have

done so far, we assign the following Z parities to the hypermultiplet

$$Z = +1 : \quad s^1, \psi_L^s, \quad (3.83)$$

$$Z = -1 : \quad s^2, \psi_R^s. \quad (3.84)$$

The assignment then projects the S chiral multiplet with its corresponding 0 modes, which are then coupled in the same way as shown in Eqn. (3.78). Furthermore under T , the fields transform as

$$\begin{pmatrix} s^1 \\ s^2 \end{pmatrix} = e^{i\alpha\sigma^2 y/R} \begin{pmatrix} \tilde{s}^1 \\ \tilde{s}^2 \end{pmatrix}. \quad (3.85)$$

Due to this transformation the ∂_5 term will in turn produce a soft SUSY breaking mass for the scalar m_S^2 . Therefore, in the case of a bulk scalar hypermultiplet \mathcal{S} and brane fermionic matter we have the following soft SUSY breaking masses

$$\begin{aligned} m_{1/2} &= \hat{\alpha}, \\ m_{h_u, h_d}^2 &= \hat{\alpha}^2, \quad m_{\tilde{q}, \tilde{u}, \tilde{d}, \tilde{l}, \tilde{e}}^2 = 0, \quad A_0 = -\hat{\alpha}, \\ \mu &= \hat{\gamma}, \quad \mu B = -2\hat{\alpha}\hat{\gamma}, \\ m_S^2 &= \hat{\alpha}^2, \quad T_\lambda = -3\lambda\hat{\alpha}, \quad T_\kappa = -\kappa\hat{\alpha}. \end{aligned} \quad (3.86)$$

Similarly in the case of a bulk scalar hypermultiplet \mathcal{S} , and bulk fermionic matter:

$$\begin{aligned} m_{1/2} &= \hat{\alpha}, \\ m_{h_u, h_d}^2 &= \hat{\alpha}^2, \quad m_{\tilde{q}, \tilde{u}, \tilde{d}, \tilde{l}, \tilde{e}}^2 = \hat{\alpha}^2, \quad A_0 = -3\hat{\alpha}, \\ \mu &= \hat{\gamma}, \quad \mu B = -2\hat{\alpha}\hat{\gamma}, \\ m_S^2 &= \hat{\alpha}^2, \quad T_\lambda = -3\lambda\hat{\alpha}, \quad T_\kappa = -\kappa\hat{\alpha}. \end{aligned} \quad (3.87)$$

Performing the same analysis as before and running the constraints we obtain the plots in Figs. 3.8, 3.9. Again the story seems to repeat itself similar to the brane scalar S . Unfortunately, the same applies as the previous case when comparing the two constraints, the points in the different regions do not overlap. The gap is much more pronounced for brane matter than bulk matter, where the gap looks almost absent in Fig. 3.9. To be clear that there is indeed no overlap in this latter case, we have also plotted the data of Fig. 3.9 as $2\hat{\alpha} + \mu B/\mu$ against m_H , with $\tan\beta$ as the point's colour in Fig. 3.10. The SS condition is exactly realised for points at $2\hat{\alpha} + \mu B/\mu = 0$ and the spread of points around this value is due to uncertainties. One can clearly see that these points have no overlap with the correct Higgs mass

region. Even when we artificially inflate our uncertainties by a factor of 10 (not shown), we do not find an overlap, though the Higgs mass becomes significantly better. So unfortunately once again we cannot reconcile this model and Scherk-Schwarz breaking with the Higgs mass and experimental constraints.

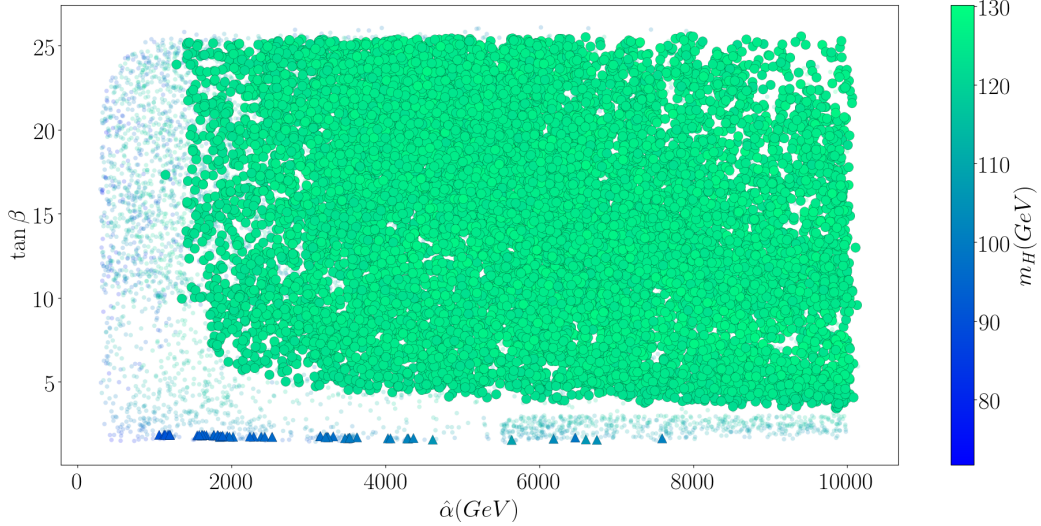


Figure 3.8: Points for the $SU(5)$ model with an additional bulk scalar \mathcal{S} , and brane matter. We use the same conventions for the points as in Fig. 3.4.

We also consider a more similar version of the \mathbb{Z}_3 invariant NMSSM, namely

$$W = W_{\text{Higgs-Fermions}}(\mu = 0) + \lambda H_u H_d S + \frac{1}{3} \kappa S^3 + LS + \frac{1}{2} M_S S^2. \quad (3.88)$$

To avoid breaking the \mathbb{Z}_3 symmetry, we assume trivial Higgs flavour symmetry breaking by setting $\hat{\gamma} = 0$. In other words the low energy $\mu, \mu B$ terms are purely determined by the scalar VEV as

$$\mu_{\text{eff}} = \frac{1}{\sqrt{2}} \lambda \langle S \rangle, \quad (3.89)$$

$$\mu B_{\text{eff}} = \frac{1}{\sqrt{2}} T_\lambda \langle S \rangle + \frac{1}{2} \kappa \lambda \langle S \rangle^2. \quad (3.90)$$

Since we have set $\hat{\gamma} = 0$, the Scherk-Schwarz constraint is effectively absent and electroweak symmetry breaking proceeds just like in the NMSSM with freedom to choose $\tan \beta$. However, this has extremely constrained supersymmetry breaking parameters since $\hat{\alpha}$ is the only input at high energies.

Unfortunately, we now find that we are unable to simultaneously satisfy this restrictive high scale boundary condition and the electroweak tadpole constraints, irrespective of our choice of brane/bulk scalars or brane/bulk fermions. The model

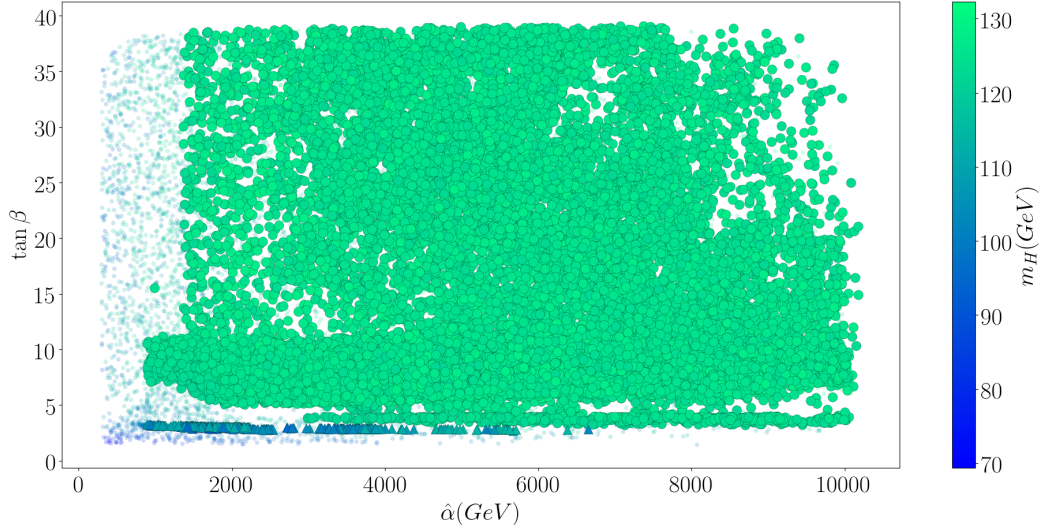


Figure 3.9: Points for the $SU(5)$ model with an additional bulk scalar \mathcal{S} , and bulk matter. We use the same conventions for the points as in Fig. 3.4.

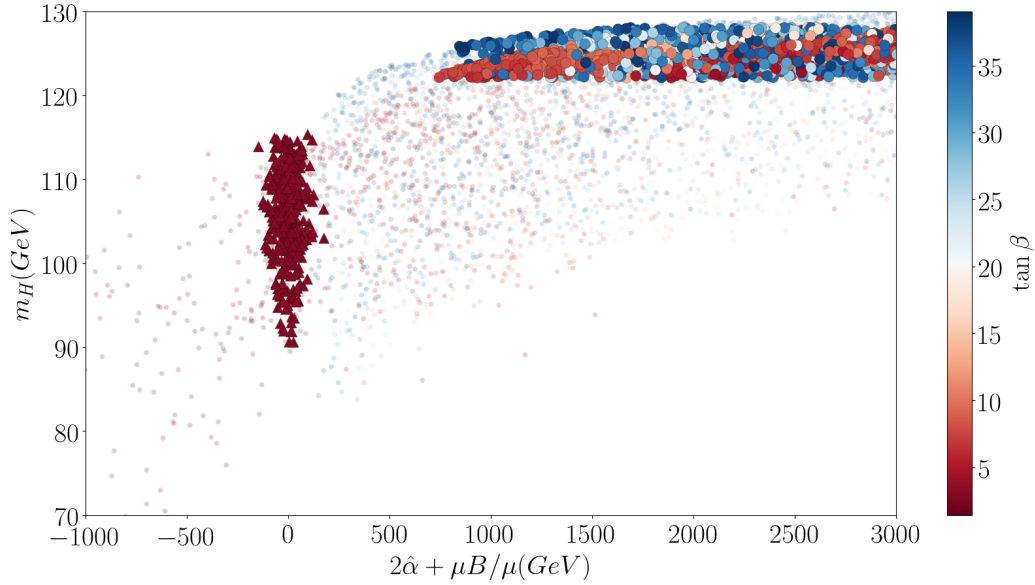


Figure 3.10: Points for the $SU(5)$ model with an additional bulk scalar \mathcal{S} , and bulk matter. We use the same conventions for the points as in Fig. 3.4, but this time we have plotted the deviation from the Scherk-Schwarz condition vs. the Higgs mass m_H .

is too constrained and is not viable. One could imagine introducing an additional scalar mass M_S and associated B_{M_S} to increase the freedom of the model, possibly allowing the correct pattern of electroweak symmetry breaking, but this is beyond

the philosophy of our study because it introduces additional supersymmetry breaking by hand, separate from the SS mechanism.

Since the explored non-trivial extensions have failed to produce an acceptable spectrum in line with the SS high scale constraints, we now move on to the next level of complexity where we extend our GUT group with an additional $U(1)$ symmetry. This in turn will provide us with the freedom of potentially embedding the model inside a higher dimensional $SO(10)$ or E_6 model. The infrared theory will now be that of the UMSSM, and come with its own particularities as we will see in the next section.

3.6.4 $SU(5) \times U(1)$ via $SO(10)$ and E_6

Moving on to the low energy modified UMSSM, the superpotential is identical to the one in Eqn. (3.78), with the added complexity of the low energy gauge group being extended to $G_{SM} \times U(1)$. With this extension we now break the $U(1)$ group at the SUSY scale via the brane scalar (projected or placed), prior to which we assign our fields appropriate charges that correspond to either a E_6 or a $SO(10)$ inspired breaking chain. Again, this is in line with the idea of further UV completion.

Starting with the E_6 charge assignment, the 5D bulk gauge structure is assumed to be $SU(5) \times U(1)_N$. Analogously to what we have done so far, leaving our Z, T unchanged we now break the bulk gauge group on the brane down to $G_{SM} \times U(1)_N$, resulting in the aforementioned UMSSM-like low energy theory. The E_6 inspired charges under the $U(1)_N$ gauge group are [65]

$$\begin{aligned} Q_q &= \frac{1}{\sqrt{40}}, & Q_l &= \frac{2}{\sqrt{40}}, & Q_d &= \frac{2}{\sqrt{40}}, & Q_u &= \frac{1}{\sqrt{40}}, & Q_e &= \frac{1}{\sqrt{40}}, \\ Q_{H_d} &= -\frac{3}{\sqrt{40}}, & Q_{H_u} &= -\frac{2}{\sqrt{40}}, & Q_S &= \frac{5}{\sqrt{40}}. \end{aligned} \quad (3.91)$$

From the point of view of the high scale boundary conditions, everything remains the same as the $SU(5)$ model with an extra scalar, with the same scalar/matter brane/bulk combinations and soft SUSY breaking masses. The difference in the spectra will come from the presence of the extra $U(1)_N$ which will modify the structure of the RGEs. In addition, the breaking of $U(1)_N$ will produce a Z' boson, where we exclude points that violate the ATLAS exotics bounds [92].

We employ the same scanning technique as in the previous sections, starting with the scalar as a brane chiral multiplet S , and brane/bulk fermionic matter which provide the spectra in Figs. 3.11, 3.12.

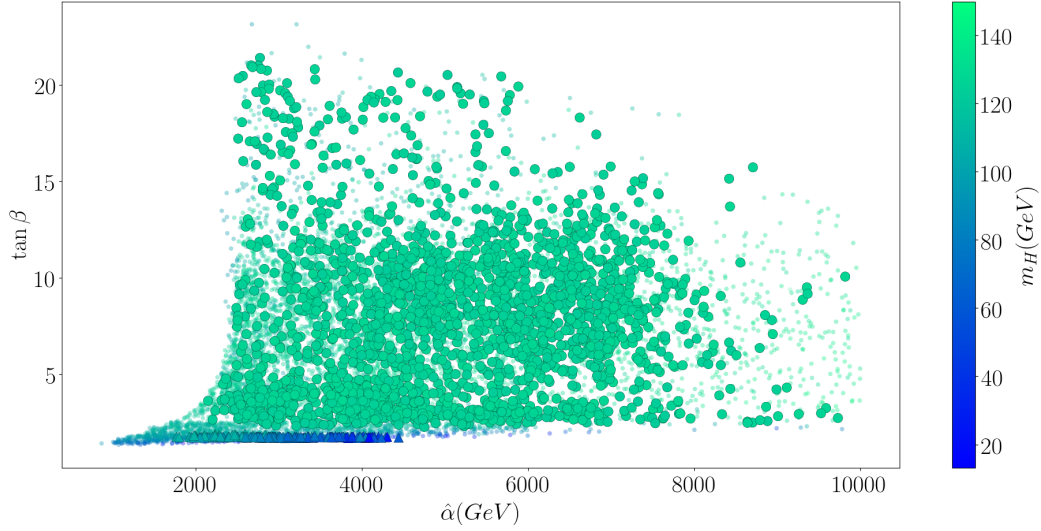


Figure 3.11: Points for the $SU(5) \times U(1)$ model with the additional scalar S and fermions both on the brane. We use the same conventions for the points as in Fig. 3.4.

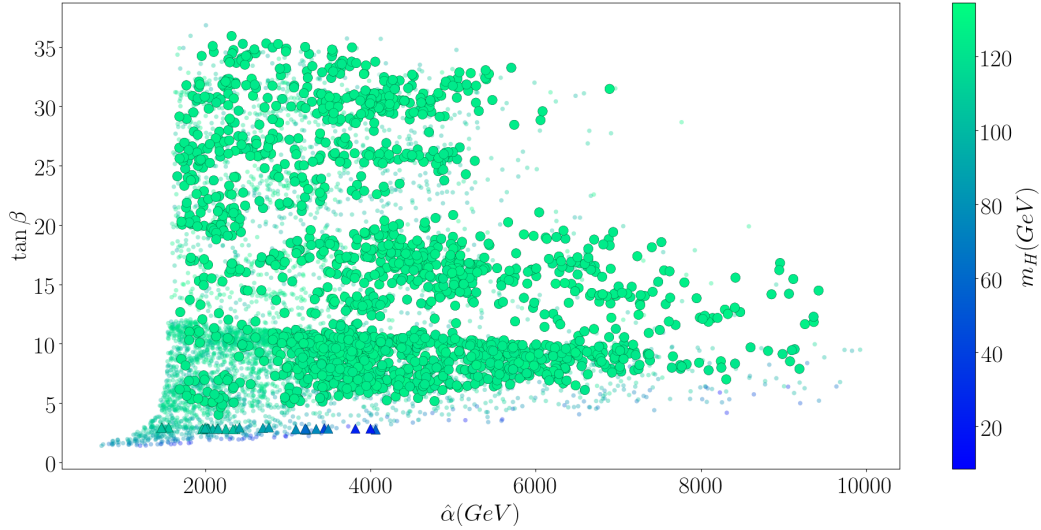


Figure 3.12: Points for the $SU(5) \times U(1)$ model with the additional scalar S on the brane and fermions in the bulk. We use the same conventions for the points as in Fig. 3.4.

Similar to what we saw in the previous case the scan produces a multitude of regions that pass LHC/DM constraints, but again the ones passing the SS constraint do not overlap. This is more pronounced for the brane/brane placement, but are closer for the brane/bulk case, unfortunately being excluded by the LHC

constraints.

Moving on to the bulk scalar \mathcal{S} , performing the scan with brane/bulk matter we get the spectra of Figs. 3.13, 3.14.

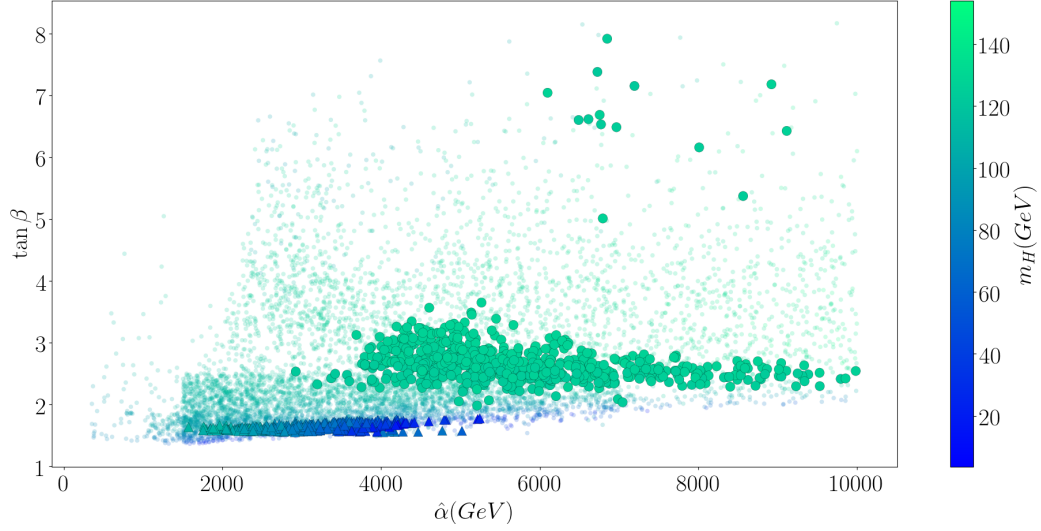


Figure 3.13: Points for the $SU(5) \times U(1)_N$ model with the additional scalar \mathcal{S} in the bulk and fermions on the brane. We use the same conventions for the points as in Fig. 3.4.

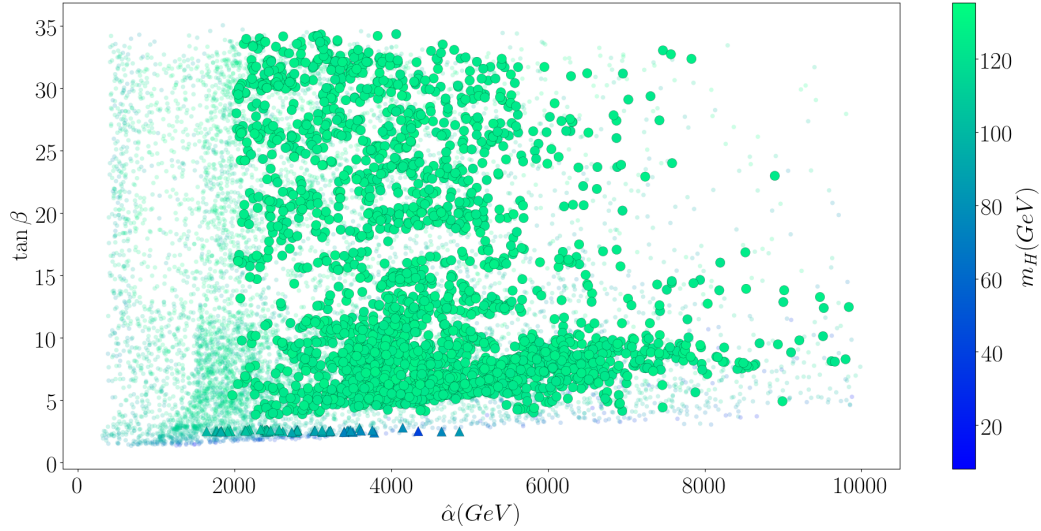


Figure 3.14: Points for the $SU(5) \times U(1)$ model with the additional scalar \mathcal{S} and fermions both in the bulk. We use the same conventions for the points as in Fig. 3.4.

Again the story repeats itself, similar to the UMSSM with brane scalar S . The two constraint regions do not overlap, with the difference that now the points seem

to favour a lower value for $\tan \beta$. Similarly, we implemented a version of the UMSSM without the holomorphic μ term by trivialising the Higgs flavour breaking with $\hat{\gamma} = 0$. Unfortunately none of the possible scenarios produce EWSB.

The setting of our $U(1)$ charges need not follow the pattern of E_6 , as the $U(1)$ may be of some completely different origin. Another case that we look at is considering $U(1)_X$ as a remnant of $SO(10)$, in which case the charge assignments would be [99]

$$\begin{aligned} Q_q = -1, \quad Q_l = 3, \quad Q_d = 1, \quad Q_u = 3, \quad Q_e = -5, \\ Q_{H_d} = -2, \quad Q_{H_u} = 2, \quad Q_S = 10. \end{aligned} \quad (3.92)$$

For this charge assignment none of the possible bulk/brane combinations, with or without a non-trivial holomorphic term μ produce EWSB.

3.6.5 An E_6 Model

The keen observer might have already noticed that this modified UMSSM isn't really the proper low scale energy remnant of an E_6 model, but rather a restricted subset of the usual fields. If this was the case, it would imply that part of the traditionally low energy spectrum had been lifted if we are to believe that the UMSSM with the previously mentioned $U(1)_N$ charges originates from a more complete E_6 UV theory.

To put this into context, a low energy model denoted as the E_6 SSM, which can originate from an E_6 orbifold GUT, as presented in [65, 100–103], has the general form of the superpotential

$$\begin{aligned} W_{E_6SSM} = & W_{MSSM}(\mu = 0) + \lambda H_u H_d S + \lambda_{\alpha\beta} S(H_\alpha^d)(H_\beta^u) + \kappa_{ij} S(D_i \bar{D}_j) \\ & + \tilde{f}_{\alpha\beta} S_\alpha(H_\beta^d H_u) + f_{\alpha\beta} S_\alpha(H_d H_\beta^u) + g_{ij}^D(Q_i L_4) \bar{D}_j \\ & + h_{i\alpha}^E e_i^c(H_\alpha^d) + \mu_L L_4 \bar{L}_4, \end{aligned} \quad (3.93)$$

where $\alpha, \beta = 1, 2, 3$ and $i, j = 1, 2$ are different generation indices. Applying the SS high scale boundary conditions to the model presented [65], where we have placed the **27**, $\overline{\mathbf{27}}$ in the bulk, provides the soft SUSY breaking masses

$$\begin{aligned} m_{1/2} &= \hat{\alpha}, \\ m_{h_u, h_d}^2 &= \hat{\alpha}^2, \quad m_{\tilde{q}, \tilde{u}, \tilde{d}, \tilde{l}, \tilde{e}}^2 = \hat{\alpha}^2, \quad A_0 = -3\hat{\alpha}, \\ m_S^2 &= \hat{\alpha}^2, \quad T_\xi = -3\xi\hat{\alpha}, \\ m_{H_\alpha^u, H_\beta^d, D_i, \bar{D}_j, S_\alpha, L_4, \bar{L}_4}^2 &= \hat{\alpha}^2, \end{aligned} \quad (3.94)$$

where $\xi \in \{\lambda, \kappa_{ij}, \lambda_{\alpha\beta}, \tilde{f}_{\alpha\beta}, f_{\alpha\beta}, g_{ij}^D, h_{i\alpha}^E\}$. During our scans we let μ_L vary independently, and set the values of $m_{H_d}^2$, $m_{H_u}^2$, m_S^2 during EWSB. We would then have to check for a new Scherk-Schwarz condition to make sure the full boundary conditions are obeyed. Unfortunately, even without enforcing this new Scherk-Schwarz condition, we find that the boundary conditions on the other parameters at the high scale are so restrictive that we can find no valid low energy scenarios.

We note that the implementation of this model is somewhat different from those described earlier because the Higgs bosons themselves are in the **27** and $\overline{\mathbf{27}}$. Therefore the $SU(2)_H$ symmetry should be enlarged to encompass the full **27** and $\overline{\mathbf{27}}$. However, here we have taken the simplest route, ignoring this enlarged symmetry and allowing the holomorphic $\mu_L L_4 \overline{L}_4$ term to arise from some another unknown mechanism altogether (that is, allowing it to vary). It is possible that a more non-minimal implementation, where the **27** and $\overline{\mathbf{27}}$ symmetry is fully incorporated would have more success in producing a viable phenomenology, but this is beyond the scope of this work.

3.7 Conclusions

In this chapter we have examined models of Scherk-Schwarz orbifold compactification. In these scenarios, the extra dimension of a 5D space is given periodic boundary conditions and rolled-up to a radius $R \sim 1/M_{\text{GUT}}$; the space is folded to provide an orbifold with fixed points in the standard fashion. Scherk-Schwarz compactification differs from standard orbifold compactification in that it allows non-trivial transformations of the fields under the orbifolding symmetries. This Scherk-Schwarz orbifolding allows for the breaking of both supersymmetry and the GUT symmetry.

We apply this compactification to several models of Grand Unification, including $SU(5)$ unification, $SU(5)$ with an additional singlet, $SU(5) \times U(1)$, and an E_6 inspired model, all with several variations. The Scherk-Schwarz mechanism provides severe constraints on the supersymmetry breaking parameters at the unification scale. We apply these constraints and use Renormalisation Group equations to evolve the theory down to the electroweak scale, where they are confronted with low energy constraints from the LHC, the Dark Matter relic density and the Higgs mass.

We find that these boundary conditions are very difficult to combine with a

125 GeV Higgs boson. Generally, these models prefer a lighter Higgs boson and rather low $\tan\beta$, and despite an exhaustive scan and variations in the models we were unable to find parameter choices which simultaneously obeyed all low scale measurement constraints. In cases where the Higgs mass was in the correct range, for example in the $SU(5)$ models with an extra singlet when an effective Higgs-higgsino mass term was entirely generated by the Scherk-Schwarz breaking, the models were ruled out by other low energy constraints such as LHC chargino exclusions.

Although we studied several models with lots of variations, this work does not claim to rule out the Scherk-Schwarz compactification in general. One could imagine having more complicated gauge groups and extra-dimensional geometry which would change the unification constraints on the supersymmetry breaking masses. Indeed, we saw in the implementation of the E_6 gauge group that one has additional freedom in allowing an alternative treatment of the large representations that now include the Higgs. However, we are confident in making the claim that Scherk-Schwarz compactification of $SU(5)$ models, $SU(5)$ models with an extra singlet, and $SU(5) \times U(1)$ models where the extra dimension is compactified on S^1/\mathbb{Z}_2 are not compatible with electroweak scale observations.

3.7.1 Back to the Gildener Problem

In lieu of the various pitfalls and problems associated with supersymmetry, we now turn our attention to another class of extra dimensional GUT models that solves the Gildener problem and eliminates the need for supersymmetry. This class involves radiative symmetry breaking via the Hosotani mechanism, which bypasses the Gildener problem by not requiring an interconnected VEV structure to achieve the multiple gauge symmetry breakdowns. The latter are in turn implemented by the extra dimensional parity assignments, along with the non-trivial holonomies associated with the Wilson line phases in the extra dimension/s. These are in turn identified as the Higgs field. In the following chapters we will review the Hosotani mechanism, along with examining in more detail the extra dimensional equations of motion, after which we proceed to examine a 6D $SO(11)$ model that recreates the SM at low energies.

The Hosotani Mechanism

The following chapter will look at how non-trivial holonomies arising within the context of an extra dimensional orbifolded theory can induce spontaneous symmetry breaking via the Hosotani mechanism. The chapter is based on Refs. [104–108].

4.1 Introduction

Defining a quantum field theory (QFT), with an underlying space-time resulting as a direct product between Minkowski space and a multiply connected manifold introduces new subtleties and complexities. Among them, is that one can impose boundary conditions to affect the symmetry of the theory. In the previous chapter we introduced gauge breaking via orbifolding, but one aspect we did not touch on was that we can project out degrees of freedom in the theory via Wilson lines associated with the non-simply connected manifolds. It turns out, this can be achieved when the effective potential associated with the Wilson line phases, acquires a global minimum at a non-trivial configuration.

4.2 Orbifolds, Boundary Conditions & the Hosotani Mechanism

Similar to the previous chapter we will be working with the 5D compactified space-time $\mathcal{M}_4 \times (S^1/\mathbb{Z}_2)$, described by the coordinates (x^μ, y) . Under the compactification, S^1 has a radius R , and we perform the identifications

$$S^1 : \quad y \rightarrow y + 2\pi R, \tag{4.1}$$

$$\mathbb{Z}_2 : \quad y \rightarrow -y, \tag{4.2}$$

which restricts y to the fundamental domain $y \in [0, \pi R]$. We now want to build a generic Lagrangian by requiring it be single valued, and gauge invariant on $\mathcal{M}_4 \times (S^1/\mathbb{Z}_2)$.

Suppose we have an internal gauge group G . Under a gauge transformation, the periodicity of S^1 requires that each field must return to its original value (up to a global transformation in G) after a full rotation. We refer to this as the S^1 *boundary condition*, and denote its matrix form as U . Under this boundary condition, a gauge field A_M transforms as

$$U : \quad A_M(x^\mu, y + 2\pi R) = U A_M(x^\mu, y) U^\dagger. \quad (4.3)$$

Similarly, the \mathbb{Z}_2 orbifolding is specified by the P_0, P_1 parity matrices, which describe a reflection around $y = 0$, and $y = \pi R$ respectively. The A_M gauge fields transform as:

$$P_0 : \begin{cases} A_\mu(x^\mu, -y) = P_0 A_\mu(x^\mu, y) P_0^\dagger \\ A_y(x^\mu, -y) = -P_0 A_y(x^\mu, y) P_0^\dagger \end{cases}, \quad (4.4)$$

$$P_1 : \begin{cases} A_\mu(x^\mu, \pi R - y) = P_1 A_\mu(x^\mu, \pi R + y) P_1^\dagger \\ A_y(x^\mu, \pi R - y) = -P_1 A_y(x^\mu, \pi R + y) P_1^\dagger \end{cases}. \quad (4.5)$$

Note that the $(-)$ signs accompanying the A_y component transformations arise from requiring that we simultaneously maintain gauge covariance in both the $F_{\mu 5}$ and $F_{\mu\nu}$ via the 5D action

$$S = \int d^4 x dy \operatorname{Tr} \left[-\frac{1}{4} F_{\mu\nu} F^{\mu\nu} - \frac{1}{2} F_{\mu 5} F^{\mu 5} \right]. \quad (4.6)$$

Moving on to \mathbb{Z}_2 , since a repeated transform must bring back a generic field ϕ to its original value, it follows that P_0 must be an element of the centre of the group G (the elements of the centre of an arbitrary group G , commute with all the elements of G). For $SU(N)$ the centre is denoted as $Z(SU(N))$, and consists of

$$Z(SU(N)) = \left\{ e^{i\theta} \mathbf{1}_N \mid \theta = \frac{2k\pi}{N}, \quad k = 0, \dots, N-1 \right\}. \quad (4.7)$$

Therefore we can set $P_0^2 = 1$ with $P_0^\dagger = P_0$, where the analogous argument can be made for P_1 . We note that not all U, P_0, P_1 are independent of each other. Since a reflection around πR ($\pi R + y \rightarrow \pi R - y$) is equivalent to a reflection around $y = 0$ followed by a translation by $2\pi R$ ($(\pi R + y) \rightarrow -(\pi R + y) \rightarrow \pi R - y$), it follows that in field space

$$U = P_0 P_1. \quad (4.8)$$

For the rest of this discussion, we will specify the reflection conditions and then derive the S^1 condition.

So far we have specified the boundary conditions for a general gauge field. Moving on to scalars and fermions, a generic scalar field ϕ transforms under the boundary conditions as

$$\begin{cases} \phi(x, -y) = \pm T_\phi[P_0]\phi(x, y) \\ \phi(x, \pi R - y) = \pm e^{i\pi\beta_\phi} T_\phi[P_1]\phi(x, \pi R + y) \\ \phi(x, y + 2\pi R) = e^{i\pi\beta_\phi} T_\phi[U]\phi(x, y) \end{cases} \quad , \quad (4.9)$$

where we note that the P_0 does not have a phase factor due to the consistency condition and the freedom of absorbing it into P_1 's phase, and $T_\phi[P_0], T_\phi[P_1], T_\phi[U]$ are appropriate representation matrices in field space, where $T_\phi[U] = T_\phi[P_0]T_\phi[P_1]$.

To be more explicit about what we mean by ‘‘appropriate representations’’, below we have the examples of a scalar that transforms under the fundamental and the adjoint of the gauge group G , and the respective forms for $T_\phi[U]$

$$\phi \in \text{fundamental of } G \quad \Rightarrow \quad T_\phi[U]\phi \quad \text{is} \quad U\phi, \quad (4.10)$$

$$\phi \in \text{adjoint of } G \quad \Rightarrow \quad T_\phi[U]\phi \quad \text{is} \quad U\phi U^\dagger. \quad (4.11)$$

Furthermore, if we impose that $P_i^2 = 1$, it follows that the gauge phase factor $e^{i\pi\beta_\phi}$ must be either $+1$ or -1 (i.e. $\beta_\phi = 0, 1$).

Similarly for the Dirac fields, gauge invariance of the kinetic term in the 5D Dirac action, demands:

$$\begin{cases} \psi(x, -y) = \pm T_\psi[P_0]\gamma_5\psi(x, y) \\ \psi(x, \pi R - y) = \pm e^{i\pi\beta_\psi} T_\psi[P_1]\gamma_5\psi(x, \pi R + y) \\ \psi(x, y + 2\pi R) = e^{i\pi\beta_\psi} T_\psi[U]\gamma_5\psi(x, y) \end{cases} \quad . \quad (4.12)$$

Similarly requiring that $P_i^2 = 1$ the phase factors reduce to ± 1 , i.e. $\beta_\psi = 0, 1$. We note that the γ_5 matrices arise in the reflection conditions as a consequence of the 5D action, which contains γ_5 as part of the Lorentz algebra

$$\begin{aligned} S &= \int d^4x dy \left(i\bar{\psi} \mathcal{D}_M \Gamma^M \psi \right) \\ &= \int d^4x dy \left(i\bar{\psi} \mathcal{D}_\mu \psi - \bar{\psi} \gamma_5 \partial^5 \psi + i g \bar{\psi} A^5 \gamma_5 \psi \right), \end{aligned} \quad (4.13)$$

where $\Gamma^M = \{\gamma^\mu, -i\gamma_5\}$. At a first glance, the fact that the phases have naturally been trivialised is a bit worrisome since the premise of the previous chapter was that

within SS Higgs breaking the phase parameter was free to take any value dictated by the UV complete theory. The subtlety comes from the non-commutative nature of the flavour or multiplet structure we previously encountered. I.e. if we have several multiplets in the same gauge group, e.g. say ϕ^A (where A is an arbitrary flavour index), then the generalised twisting including flavour space, takes the following form for the S^1 condition

$$\phi^A(x, y + 2\pi R) = \{ \exp(i\pi\beta_F M) \}_B^A T_\phi[U] \phi^B(x, y), \quad (4.14)$$

where M is a matrix in flavour space. In this SS case, if we assign a non-trivial breaking to the \mathbb{Z}_2 parity relating to flavour space, and if M anti-commutes with the \mathbb{Z}_2 assignment, then β_F can take any value.

4.3 Residual Gauge Invariance of the Boundary Conditions

In the previous chapter we mentioned briefly that the theory possesses some residual gauge invariance on the branes after gauge symmetry breaking. This is determined fully by the specified boundary conditions (P_0, P_1, U, β) . Under a general gauge transformation $\Omega(x, y)$, generic boson, fermion and scalar fields transform as

$$A_M \rightarrow A'_M = \Omega A_M \Omega^\dagger - \frac{i}{g} \Omega \partial_M \Omega^\dagger, \quad (4.15)$$

$$\phi \rightarrow \phi' = T_\phi[\Omega] \phi, \quad (4.16)$$

$$\psi \rightarrow \psi' = T_\psi[\Omega] \psi. \quad (4.17)$$

The gauge transformation also affects the boundary conditions, producing a new set. Leaving the fermions and the scalars aside for a second, the new gauge fields A'_M now obey

$$A'_M(x, y + 2\pi R) = U' A'_M(x, y) (U')^\dagger - \frac{i}{g} U' \partial_M (U')^\dagger, \quad (4.18)$$

$$\begin{pmatrix} A'_\mu(x, -y) \\ A'_y(x, -y) \end{pmatrix} = P'_0 \begin{pmatrix} A'_\mu(x, y) \\ -A'_y(x, y) \end{pmatrix} (P'_0)^\dagger - \frac{i}{g} P'_0 \begin{pmatrix} \partial_\mu \\ -\partial_y \end{pmatrix} (P'_0)^\dagger, \quad (4.19)$$

$$\begin{pmatrix} A'_\mu(x, \pi R - y) \\ A'_y(x, \pi R - y) \end{pmatrix} = P'_1 \begin{pmatrix} A'_\mu(x, \pi R + y) \\ -A'_y(x, \pi R + y) \end{pmatrix} (P'_1)^\dagger - \frac{i}{g} P'_1 \begin{pmatrix} \partial_\mu \\ -\partial_y \end{pmatrix} (P'_1)^\dagger, \quad (4.20)$$

where the new set of boundary conditions (U', P'_0, P'_1) are related to the old set via the gauge transformations

$$U' = \Omega(x, y + 2\pi R)U\Omega^\dagger(x, y), \quad (4.21)$$

$$P'_0 = \Omega(x, -y)P_0\Omega^\dagger(x, y), \quad (4.22)$$

$$P'_1 = \Omega(x, \pi R - y)P_1\Omega^\dagger(x, \pi R + y). \quad (4.23)$$

Analogously, the gauge transformed fermionic and scalar fields ψ', ϕ' satisfy similar conditions to their previous ones. E.g. the gauge transformed scalar fields obey $\phi'(x, y + 2\pi R) = e^{i\pi\beta\phi}T_\phi[U']\phi'(x, y)$.

With this being said, the residual gauge invariance in the theory is given by the subset of gauge transformations that preserve boundary conditions and implicitly the structure of the theory. I.e. the theory has a residual symmetry defined by $\Omega \in G_R$, where the Ω 's satisfy the preservation requirements

$$U' = U, \quad P'_0 = P_0, \quad P'_1 = P_1, \quad (4.24)$$

or equivalently

$$\begin{aligned} \Omega(x, y + 2\pi R)U &= U\Omega(x, y), \\ \Omega(x, -y)P_0 &= P_0\Omega(x, y), \\ \Omega(x, \pi R - y)P_1 &= P_1\Omega(x, \pi R + y). \end{aligned} \quad (4.25)$$

In general, the residual gauge symmetry G_R will differ from the physical symmetry of the theory since it may change due to radiative corrections arising from the Hosotani mechanism. This will be covered in detail in the following sections.

4.4 Wilson Line Phases

The following section will look at how Wilson lines can cause symmetry breaking within the context of a non simply connected manifold. Before that, we review the geometrical significance of gauge invariance, along with how holonomies affect KK spectra.

4.4.1 Geometry of Gauge Invariance

Suppose we want to build a $U(1)$ gauge invariant theory containing fermions that transform non-trivially under the gauge group. Suppose we have a Dirac field $\psi(x)$. Therefore we want the theory to be invariant under a local phase rotation

$$\psi \rightarrow e^{i\alpha(x)}\psi(x), \quad (4.26)$$

where $\alpha(x)$ varies at each point in space-time. We can easily write down a mass term $m\bar{\psi}\psi$ that is invariant under this transformation, but the theory falls apart when we try introducing a derivative in the n^μ direction. E.g. suppose we define the usual derivative construct where

$$n^\mu \partial_\mu \psi = \lim_{\epsilon \rightarrow 0} \frac{1}{\epsilon} [\psi(\epsilon n + x) - \psi(x)]. \quad (4.27)$$

With the form of the above, the difference in the square brackets no longer has a simple transformation law under $\psi \rightarrow e^{i\alpha(x)}\psi(x)$ and loses any geometrical significance.

Therefore we need to introduce a factor that compensates for the difference from one point to another. To this extent, we introduce a scalar quantity $U(y, x)$, that depends on two points in space time y, x . Furthermore, we require that under a local gauge transform at x, y it has the transformation law

$$U(y, x) \rightarrow e^{i\alpha(y)}U(y, x)e^{-i\alpha(x)}. \quad (4.28)$$

Along these lines we define $U(y, y) = 1$ and can further request that $U(y, x)$ consists of a pure phase term $U(y, x) = \exp(i\phi(y, x))$.

With this new quantity we can now define a derivative that has a geometrical interpretation, namely the covariant derivative

$$n^\mu \mathcal{D}_\mu \psi = \lim_{\epsilon \rightarrow 0} \frac{1}{\epsilon} [\psi(x + \epsilon n) - U(x + \epsilon n, x)\psi(x)]. \quad (4.29)$$

We can in turn Taylor expand $U(x + \epsilon n, x)$ in powers of ϵ , and take the $\epsilon \rightarrow 0$ limit for the infinitesimal displacement

$$U(x + \epsilon n, x) = 1 - ie\epsilon n^\mu A_\mu(x) + \mathcal{O}(\epsilon^2). \quad (4.30)$$

In the above we have introduced an arbitrary constant e , and the coefficient of the ϵn^μ displacement $A_\mu(x)$, which we identify as the vector field (or similarly the affine connection). Plugging this in the limit in Eqn. (4.29) gives us the well known form of the covariant derivative

$$\mathcal{D}_\mu \psi = \partial_\mu \psi + ieA_\mu \psi. \quad (4.31)$$

Furthermore, since the comparator $U(y, x)$ transforms as dictated by Eqn. (4.28), plugging in the Taylor expansions, the transformation law for the vector field follows

$$A_\mu \rightarrow A_\mu - \frac{1}{e} \partial_\mu \alpha(x). \quad (4.32)$$

To complete the construction of the Lagrangian we still need a kinetic term for A_μ . One way of doing this, which gives us some geometric insight into what this term represents, is to use the comparator. First off, we notice that $U^\dagger(x, y) = U(y, x)$, which can in turn be used to parametrise a comparator between an infinitesimal separation ϵ in the n^μ direction as

$$U(x + \epsilon n, x) = \exp \left\{ -i \epsilon n^\mu A_\mu(x + \epsilon n/2) + \mathcal{O}(\epsilon^3) \right\}. \quad (4.33)$$

For the purposes of illustration we will now look at a two dimensional (space dimensions) case, which we denote as the $(\hat{1}, \hat{2})$ plane. We now consider the following construct, where we go around a square in the $(\hat{1}, \hat{2})$ plane in increments of ϵ as shown in Fig. 4.1. With this in mind, we now define $\mathbf{U}(x)$ as the product of the

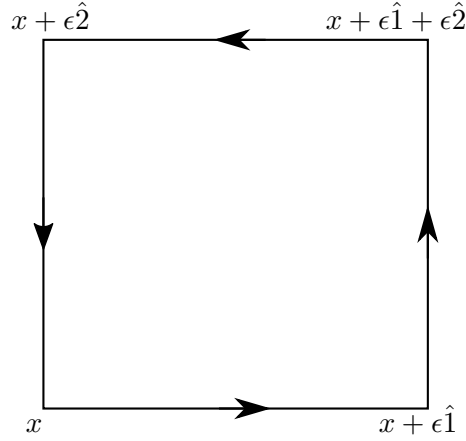


Figure 4.1: Wilson loop $\mathbf{U}(x)$ around a square of size ϵ in $\{\hat{1}, \hat{2}\}$, where we start off at x and consecutively make ϵ increments in the $\hat{1}$ and $\hat{2}$ dimensions to form a square along the flow of the arrows.

four comparators around the square

$$\begin{aligned} \mathbf{U}(x) \equiv & U(x, x + \epsilon \hat{2}) \\ & \cdot U(x + \epsilon \hat{2}, x + \epsilon \hat{2} + \epsilon \hat{1}) \\ & \cdot U(x + \epsilon \hat{2} + \epsilon \hat{1}, x + \epsilon \hat{1}) \\ & \cdot U(x + \epsilon \hat{1}, x). \end{aligned} \quad (4.34)$$

Under the $U(1)$ gauge transformation, $\mathbf{U}(x)$ is by construction invariant, since the end of each comparator will cancel out with its adjacent one. Therefore $\mathbf{U}(x)$ can serve as an appropriate ansatz for our search of a kinetic invariant construct

for A_μ . Introducing the Taylor expansions for the comparators and keeping terms up to $\mathcal{O}(\epsilon)$ gives us the infinitesimal form of

$$\mathbf{U}(x) = 1 - \epsilon^2 e [\partial_1 A_2(x) - \partial_2 A_1(x)] + \mathcal{O}(\epsilon^3). \quad (4.35)$$

Since $\mathbf{U}(x)$ is invariant under the underlying $U(1)$, the structure $F_{12} = [\partial_1 A_2(x) - \partial_2 A_1(x)]$ is locally invariant. Therefore we can identify $F_{\mu\nu}$ as the familiar electromagnetic field strength.

We note that \mathbf{U} is not trivial, in the sense that it differs from unity by a term proportional to the field strength and the area of the square. This is in turn a particular case of a more general conclusion, that the comparator between two points x, y at finite separation depends on the path. To get to this conclusion, we can perform the inverse argument, by starting off with the connection A_μ and imposing the transformation law $A_\mu \rightarrow A_\mu - \frac{1}{e} \partial_\mu \alpha(x)$ under the $U(1)$. We now construct the comparator $W(z, y)$ as a function of A_μ around a path \mathcal{P} running from $y \rightarrow z$ as

$$W(z, y) = \exp \left\{ -ie \int_{\mathcal{P}} dx^\mu A_\mu(x) \right\}. \quad (4.36)$$

We refer to this construct as a Wilson line. If \mathcal{P} is a closed path, we then obtain a Wilson loop

$$W(y, y) = \exp \left\{ -ie \oint_{\mathcal{P}} dx^\mu A_\mu(x) \right\}, \quad (4.37)$$

which, similar to the comparator square, is by construction gauge invariant.

We can now move on to the non-abelian case. Promoting our gauge field to the non-abelian case introduces a couple of complexities. Namely, suppose we have a gauge group G with $V(x)$ an appropriate representation matrix of the symmetry group, under which the fermionic field ψ , and the gauge field $A_\mu(x) = A_\mu^a(x) t^a$ (t^i are the generators of G) transform as

$$\psi(x) \rightarrow V(x) \psi(x), \quad (4.38)$$

$$A_\mu(x) \rightarrow V(x) A_\mu(x) V^\dagger(x) + \frac{i}{2g} V(x) (\partial_\mu V^\dagger(x)). \quad (4.39)$$

Therefore, the comparator, and by extension the Wilson line $W(y, x)$, are now promoted to a matrix structure and transform as

$$W(y, x) \rightarrow V(y) W(y, x) V^\dagger(x). \quad (4.40)$$

To make the mathematics consistent, one further needs to parametrise the path in the Wilson line \mathcal{P} via a parameter $s \in [0, 1]$ where $s = 0$ is at y , and $s = 1$ is

at z . Furthermore we have to introduce path ordering $\mathcal{P}\{\}$ such that the Wilson line is now defined as the power series expansion of the exponential, with the gauge matrices in each term ordered such that the higher value of s stands to the left. The Wilson line is then written as

$$W(z, y) = \mathcal{P} \left\{ \exp \left[ig \int_0^1 ds \frac{dx^\mu}{ds} A_\mu^a(x(s)) t^a \right] \right\}. \quad (4.41)$$

As for the Wilson loop, in addition, we now have to trace over it to maintain gauge invariance

$$W(y, y) \rightarrow \text{Tr } W(y, y). \quad (4.42)$$

4.4.2 Wilson Line Phases on Multiply Connected Manifolds

Within the context of gauge theories, non-simply connected manifolds can have an extra complexity associated with their behaviour, namely that the theory can develop multiple degrees of freedom associated with a Wilson line around a non-contractable loop.

Throughout this review we will be working in a regime of vanishing field strength, $\langle F_{\mu\nu} \rangle = 0$, which is analogous to $\langle A_\mu \rangle = -\frac{i}{g} V^\dagger \partial_\mu V$. A vanishing field strength is not equivalent to a non-trivial Wilson line configuration.

Firstly we look at how a non-trivial holonomy can affect the spectrum of a theory. Suppose that we have a theory defined on a manifold resulting from the direct product of Minkowski space-time and a circle of radius R , $\mathcal{M}_4 \times S^1$. We denote the extra dimensional spatial coordinate as $y \in [0, 2\pi R]$. Similarly, we impose an internal gauge group $G = SU(2)$. For simplicity's sake, we take the gauge field to lie purely in the 3rd isospin direction

$$A(y) = A^3(y) \frac{1}{2} \tau^3. \quad (4.43)$$

Without any loss of generality, by gauge transforming, we can turn A^3 into a constant $A^3(y) \rightarrow \langle A^3 \rangle$ (see [105]).

Holonomy T , measures the extent to which parallel transport across a smooth manifold changes a geometrical quantity. With a constant background field, holonomy is non-trivial and expressed as

$$T = \exp \left(i \oint_{S^1} dy \langle A^3 \rangle \frac{1}{2} \tau^3 \right) = \exp (i \langle A^3 \rangle \pi R \tau^3), \quad (4.44)$$

where $\tau^3 = \frac{1}{2} \sigma^3$, and σ^3 is the 3rd Pauli matrix. Since we now have a non-trivial holonomy, or equivalently a non-trivial transport function, this in turn affects the

5D equation of motion. More specifically, it acts through the modification of the y covariant derivative as

$$\mathcal{D}_y \mathcal{D}^y \phi \rightarrow (\partial_y - i \frac{1}{2} \langle A^3 \rangle \tau^3)^2 \phi. \quad (4.45)$$

This in turn affects the 4D tower Kaluza-Klein (KK) decomposition, where we recall that ϕ can be decomposed into a tower of KK modes as $\sim \phi_{(n)} \exp(iny/R)$. The covariant derivative modification results in a mass shift for the modes

$$m_n = \left| \frac{n}{R} - \frac{1}{2} \langle A^3 \rangle \tau^3 \right|. \quad (4.46)$$

Similarly the gauge fields are affected, and the allowed 0 modes become massive. One can argue, that if we gauge away $\langle A^3 \rangle$ via a gauge transform of the form

$$U(y) = \exp \left(-\frac{i}{2} \langle A^3 \rangle \tau^3 y \right), \quad (4.47)$$

which in turn produces a simple mode equation

$$\mathcal{D}_M \mathcal{D}^M \phi = -\partial_y^2 \phi = m_{\text{KK}}^2 \phi, \quad (4.48)$$

that the fields no longer incur the shift in their KK modes. In this case, we note that the fields are subject to periodic boundary conditions that transform under the gauge transformation. With the modified boundary conditions, ϕ now obeys

$$\phi(y + 2\pi R) = \exp(-i\pi \langle A^3 \rangle \tau^3 R) \phi(y = 0). \quad (4.49)$$

This in turn affects the KK mode decomposition as

$$\phi_{(n)}(y) = \exp \left\{ i \left(\frac{n}{R} - \frac{1}{2} \langle A^3 \rangle \tau^3 \right) y \right\}, \quad (4.50)$$

where we have recovered the mode mass shift. Therefore, the non-trivial holonomy represents physical degrees of freedom that *cannot be gauged away*. The difference in the orbifold case is that the holonomy is represented via the Wilson line, which allows for non-smooth manifolds. We refer to these as non-integrable Wilson line phases of WU .

Let us now consider a Wilson line along a non-contractable loop of S^1/\mathbb{Z}_2 from $y \rightarrow y + 2\pi R$:

$$W(x, y) = \mathcal{P} \exp \left\{ ig \int_y^{y+2\pi R} dy' A_y(x, y') \right\}. \quad (4.51)$$

The first consequence of the Wilson line being along a non-contractable loop, is that $W(x, y)$ no longer transforms covariantly, according to Eqn. (4.40).

Rather, in the orbifold case, this is replaced by the construction WU which transforms as

$$W(x, y)U \rightarrow \Omega(x, y)W(x, y)U\Omega^\dagger(x, y), \quad (4.52)$$

which can be derived using the relations in Eqn. (4.25). The expectation values of the Wilson line phases are now determined at the quantum level such that the effective potential for the lines is minimised.

On the $\mathcal{M}_4 \times S^1/\mathbb{Z}_2$ orbifold, the Wilson line phases correspond to the x, y independent “0 modes” of A_y . Given the generators $\lambda^a/2$ of the gauge group, we define the anti-commuting set \mathcal{H}_W as

$$\mathcal{H}_W = \left\{ \frac{\lambda^{\hat{a}}}{2} \mid \{\lambda^{\hat{a}}, P_0\} = \{\lambda^{\hat{a}}, P_1\} = 0 \right\}. \quad (4.53)$$

where P_0, P_1 are the reflection matrices defined by the \mathbb{Z}_2 action, and \hat{a} just denotes the simultaneously anticommuting generators. The anti-commuting gauge components of A_y that are specified by the above are the “0 modes” that can acquire an expectation value, breaking or restoring the gauge symmetry imposed by the boundary conditions. This depends on the effective potential associated with the respective A_y modes, which is determined by the matter content of the theory. The Wilson line phases associated with A_y are defined as $\{\theta^{\hat{a}} = g\pi R A_y^{\hat{a}}, \hat{a} \in \mathcal{H}_W\}$.

4.4.3 Caveat

Our theory is specified by boundary conditions which can be quite arbitrary. As we will see the Hosotani mechanism ensures that certain theories with different boundary conditions can be physically equivalent.

Since an arbitrary gauge choice should not affect the physics, we want to make sure that our theory is gauge independent. To this extent, we say that two sets of boundary conditions (U, P_0, P_1) and (U', P'_0, P'_1) , which are related by a gauge transformation Ω , are equivalent if

$$\partial_M U' = 0, \quad \partial_M P'_0 = 0, \quad \partial_M P'_1 = 0, \quad (4.54)$$

$$(P'_0)^\dagger = P_0, \quad (P'_1)^\dagger = P_1. \quad (4.55)$$

The first row effectively states, that the new gauge fields A'_M determined by the Ω transform, obey the same boundary conditions as the previous ones, i.e. without the pure gauge component. The second row states the requirement that the new boundary conditions maintain hermiticity. Whenever we have two sets of boundary

conditions that are equivalent we write $(U, P_0, P_1) \sim (U', P'_0, P'_1)$. The entire set of equivalence relationships define the equivalence class of the respective boundary conditions.

For example, suppose that we have a $SU(2)$ theory with the explicit boundary conditions $(U, P_0, P_1) = (1, \tau^3, \tau^3)$, and we perform a gauge transformation along the 1st isospin direction τ^1 by an amount α . This in turn produces a new set of equivalent boundary conditions that can be shown to take the form

$$(1, \tau^3, \tau^3) \sim (e^{i\alpha\tau^3}, \tau^3, e^{i\alpha\tau^1}\tau^3). \quad (4.56)$$

Clearly the two boundary conditions are different, but the physics are guaranteed to be the same due to the Hosotani mechanism.

4.5 The Hosotani Mechanism

The Hosotani Mechanism [74–76] is present in gauge theories defined on multiply connected manifolds, and consists of 5 parts:

1. Wilson line phases $\theta^{\hat{a}}$ along non-contractable loops become physical degrees of freedom. The Wilson line phases are determined by the boundary conditions and cannot be gauged away. They yield vanishing field strengths such that they appear as degenerate vacua at the classical level.
2. In general the degeneracy is lifted by radiative corrections which are determined by the matter content via the effective potential V_{eff} . The effective potential for Wilson line phases has a non-trivial dependence on $\theta^{\hat{a}}$. The physical vacuum of the theory is given by the θ configuration that minimises V_{eff} .
3. If the effective potential is minimised at a non-trivial configuration of Wilson line phases then the gauge symmetry is either spontaneously broken or restored by radiative corrections. Non-vanishing expectation values of the Wilson line phases “give masses” to the gauge fields in lower dimensions (some matter fields also acquire masses).
4. A non-trivial minimum also implies that the extra dimensional components of the gauge fields become massive. The masses of which are given by $\partial^2 V_{\text{eff}} / \partial \theta_a^2$.
5. Two sets of boundary conditions are physically equivalent if they can be related via a gauge transformation such that Eqns. (4.54), (4.55) are satisfied.

The physical symmetry of the theory is determined by the combination of the boundary conditions and the expectation values of Wilson line phases.

With the Hosotani mechanism outlined, let's look at how the physical symmetry of the theory is established. Again, we are working with a theory defined on $\mathcal{M}_4 \times S^1/\mathbb{Z}_2$, with an arbitrary set of boundary conditions (U, P_0, P_1) . Suppose that the effective potential is minimised at a non-trivial minimum set by the Wilson line phases θ_a with the parametrisation

$$\langle A_y \rangle = \frac{1}{2\pi g R} \sum_a \theta_a \lambda^a, \quad a \in \mathcal{H}_W, \quad (4.57)$$

where g is the 5D gauge coupling, R is the size of the extra dimension. Note that form in Eqn. (4.57), is just a parametrisation of the general form of $\langle A_y \rangle$, namely $-\frac{i}{g} V^\dagger \partial_\mu V$. The associated Wilson line is then defined as

$$W \equiv \exp \{i 2\pi g R \langle A_y \rangle\} = \exp \left\{ i \sum_a \theta_a \lambda^a \right\}. \quad (4.58)$$

We can now use the residual gauge symmetry of the theory to bring $\langle A_y \rangle \rightarrow 0$ via a gauge transformation $\Omega = V$, whose explicit general form is

$$\Omega(y; \gamma) = \exp \left\{ i \left(\frac{y}{2\pi R} + \gamma \right) \sum_{a \in \mathcal{H}_W} \theta_a \lambda^a \right\}, \quad (4.59)$$

where γ is an arbitrary constant. Along these lines we introduce the notation

$$\Omega(y; \gamma) = S \left(\frac{y}{2\pi R} + \gamma \right), \quad (4.60)$$

where $S(z)$ is defined as

$$S(z) = \exp \left\{ i z \sum_{a \in \mathcal{H}_W} \theta_a \lambda^a \right\}. \quad (4.61)$$

Note that $W = S(1)$. One can check that after performing the Ω transform, we indeed have a vanishing $\langle A_y \rangle$. Therefore, V_{eff} is now minimised at a trivial configuration. But, by performing the gauge transformation we also change the boundary conditions to

$$P_0^{\text{sym}} \equiv P'_0 \Omega(-y; \gamma) P_0 \Omega^\dagger(y, \gamma) = S(\gamma) P_0 S^\dagger(\gamma), \quad (4.62)$$

$$P_1^{\text{sym}} \equiv P'_1 \Omega(\pi R - y; \gamma) P_0 \Omega^\dagger(\pi R + y, \gamma) = S(\gamma) W P_1 S^\dagger(\gamma), \quad (4.63)$$

$$U^{\text{sym}} \equiv U' \Omega(y + 2\pi R; \gamma) U \Omega^\dagger(y, \gamma) = W U. \quad (4.64)$$

One can check that the new boundary conditions satisfy the relations in Eqns. (4.54), (4.55), which imply the equivalence relation

$$(U, P_0, P_1, \beta) \sim (U^{\text{sym}}, P_0^{\text{sym}}, P_1^{\text{sym}}, \beta), \quad (4.65)$$

where β is the phase accompanying the fermionic transformation that is stated for completeness.

Since the new gauge rotates out our VEV, this results in a trivial Wilson line configuration $\langle W \rangle$. Therefore the physical symmetry of the theory \mathcal{H}^{sym} , is fully specified by the boundary conditions, and more specifically, it is spanned by the generators λ^a which simultaneously commute with $(U^{\text{sym}}, P_0^{\text{sym}}, P_1^{\text{sym}})$ as

$$\mathcal{H}^{\text{sym}} = \left\{ \frac{\lambda^a}{2} \mid [\lambda^a, P_0^{\text{sym}}] = [\lambda^a, P_1^{\text{sym}}] = 0 \right\}. \quad (4.66)$$

\mathcal{H}^{sym} is the surviving unbroken symmetry of the theory. We also note that even though $P_0^{\text{sym}}, P_1^{\text{sym}}$ depend on γ , \mathcal{H}^{sym} does not.

Therefore, if we have a boundary condition equivalence, the Hosotani mechanism ensures that the different theories have the same physical symmetry. As we will see later on, this is partly due to the non-trivial dependence of the effective potential on the boundary conditions and the Wilson lines.

4.6 Orbifolds in $SU(5)$ Gauge Theory

Analogous to what we did in the Scherk-Schwartz discussion, we suppose that we have gauge bosons $A_M(x, y)$ that live in the 5D bulk space-time obeying a $SU(5)$ gauge symmetry which we break down to G_{SM} via a non-trivial \mathbb{Z}_2 assignment, acting as an algebra automorphism.

The $SU(5) \rightarrow G_{\text{SM}}$ breaking can be achieved at the classical level via two \mathbb{Z}_2 parity assignments

$$C1 : \begin{cases} P_0 = \pm \text{diag}(+, +, +, +, +), \\ P_1 = \pm \text{diag}(+, +, +, -, -), \\ U = \text{diag}(+, +, +, -, -), \end{cases} \quad (4.67)$$

$$C2 : \begin{cases} P_0 = \pm \text{diag}(+, +, +, -, -), \\ P_1 = \pm \text{diag}(+, +, +, -, -), \\ U = \text{diag}(+, +, +, +, +). \end{cases} \quad (4.68)$$

If we assume the assignments in $C1$, there are no 0 modes for A_y . The $SU(5)$ gauge symmetry is fully broken by the orbifold condition at $y = \pi R$, and no Hosotani breaking occurs since the Wilson line configuration is trivial. I.e. \mathcal{H}_W is empty since there aren't any generators $\lambda^a \in SU(5)$ that simultaneously anti commute with the reflection matrices $\{P_0, \lambda^a\} = \{P_1, \lambda^a\} = 0$.

In $C2$, the boundary conditions still cause the breaking $SU(5) \rightarrow G_{\text{SM}}$, but \mathcal{H}_W is no longer empty. In this case the Wilson line phases are determined by

$$\mathcal{H}_W = \left\{ \frac{\lambda^a}{2}; \quad a = 13 \sim 24 \right\}, \quad (4.69)$$

where the generators correspond to the coset $SU(5)/G_{\text{SM}}$. Note that the coset in $C1$ is the same, but the generators do not simultaneously anti-commute with the forms of P_0, P_1 from $C1$.

Therefore in the 2nd case, the 0 modes of A_y^a where $(a \in \mathcal{H}_W)$ give non trivial Wilson line phases. As we will see in the next section quantum effects will give A_y^a finite masses via the respective effective potential $V_{\text{eff}}(A_y^a)$. As prescribed by the Hosotani mechanism, this in turn results in a physical symmetry \mathcal{H}^{sym} different from the G_{SM} dictated by the boundary conditions.

4.7 Effective Potentials

We will now quickly go over the important attributes of computing the effective potential in the background field method. We start off with a pure Yang-Mills 5D theory which is described by the Lagrangian

$$\mathcal{L}_{\text{gauge}} = -\frac{1}{2} \text{Tr} (F_{MN} F^{MN}) - \frac{1}{\alpha} \text{Tr} (F^2[A]) - \text{Tr} \left(\bar{\eta} \frac{\delta F[A]}{\delta A_M} \mathcal{D}^M \eta \right), \quad (4.70)$$

where α is the gauge fixing parameter that for the rest of the discussion is set to 1, $F[A]$ is the gauge fixing condition and $\eta, \bar{\eta}$ are ghost fields. Extending the above, we add matter fields via the Lagrangian

$$\mathcal{L}_{\text{matter}} = i\bar{\psi}\gamma_M \mathcal{D}^M \psi + |\mathcal{D}_M \phi|^2 - V[\phi, \psi], \quad (4.71)$$

where ϕ, ψ are generic matter scalar and fermion fields, $\mathcal{D}_M \equiv \partial_M + ig\Gamma^a A_M^a$ is the 5D covariant derivative, and $V[\phi, \psi]$ is an arbitrary interaction potential.

With the Lagrangians established, we move on to the schematic of the computation of the effective potential for A_M . We split A_M into a background field A_M^0 that satisfies the classical equations of motion, and the quantum fluctuation A_M^q .

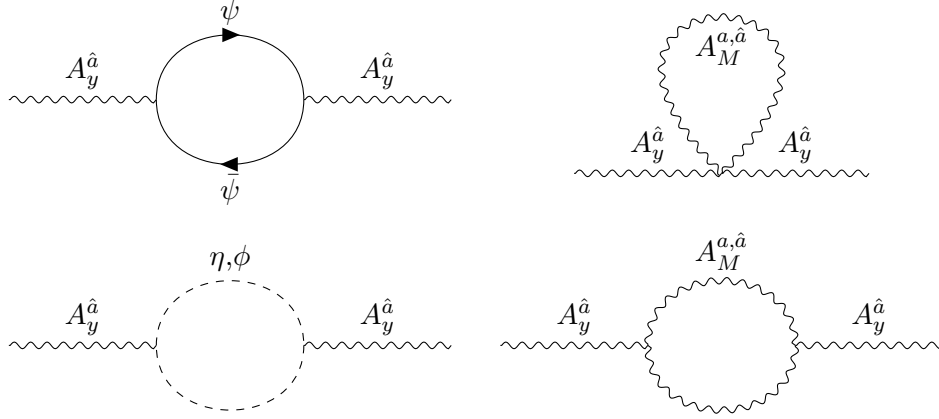


Figure 4.2: One loop contributions to $V_{\text{eff}}(A_y^{\hat{a}})$ arising from fermions ψ , boson couplings $A_M^{a,\hat{a}}$, scalars ϕ , and ghosts η . The hat index $\hat{a} \in \mathcal{H}_W$ denotes the gauge components that transform under the broken coset, where the rest denote the ones transforming under the gauge symmetry imposed by $[\lambda^a, P_0] = [\lambda^a, P_1]$

At the same time, A_M^q is the variable of integration in the path-integral formalism. With the split in place, we choose the gauge fixing condition

$$F[A] = \mathcal{D}_M(A^0)A^{qM} = \partial_M A^{qM} + ig[A_M^0, A^{qM}] = 0. \quad (4.72)$$

Note that our theory still possesses a residual gauge invariance Ω , under which the newly defined classical and quantum fields transform as

$$A_M^0 \rightarrow A_M'^0 = \Omega A_M^0 \Omega^\dagger - \frac{i}{g} \Omega \partial_M \Omega^\dagger, \quad (4.73)$$

$$A_M^q \rightarrow A_M'^q = \Omega A_M^q \Omega^\dagger, \quad (4.74)$$

$$\psi \rightarrow \psi' = T_\psi[\Omega]\psi, \quad (4.75)$$

$$\phi \rightarrow \phi' = T_\phi[\Omega]\phi. \quad (4.76)$$

By integrating out the fields $A_M^q, \bar{\eta}, \eta, \psi, \phi$ we can find the one loop effective potential for A_y^a . This is equivalent to computing the generic loop corrections corresponding to the Feynman diagrams shown in Fig. 4.2.

On the same note, one can show that the effective potential of $V_{\text{eff}}[A^0]$ depends on the boundary condition parameters

$$V_{\text{eff}}[A^0] = V_{\text{eff}}[A^0; P_0, P_1, U, \beta]. \quad (4.77)$$

Therefore, if we perform a residual gauge transformation $\sim \Omega$, that has the effect of transforming (P_0, P_1, U) to the gauge equivalent set (P'_0, P'_1, U') defined

by Eqns. (4.54), (4.55), one can check that the action remains invariant. More specifically the effective potential $V_{\text{eff}}[A_y^0]$ is also invariant, where

$$V_{\text{eff}}[A^0; P_0, P_1, U, \beta] = V_{\text{eff}}[A'^0; P'_0, P'_1, U', \beta]. \quad (4.78)$$

We saw in the previous section, that we can choose a gauge transformation Ω such that we bring $\langle A \rangle \rightarrow 0$. Recalling that $A^0 = \langle A \rangle$, and that Ω has the effect of changing the boundary conditions to $(P_0^{\text{sym}}, P_1^{\text{sym}}, U^{\text{sym}})$, one can show that

$$V_{\text{eff}}[\langle A \rangle; P_0, P_1, U, \beta] = V_{\text{eff}}[\langle A \rangle = 0; P_0^{\text{sym}}, P_1^{\text{sym}}, U^{\text{sym}}, \beta]. \quad (4.79)$$

The above allows to switch from viewing the problem as a theory possessing a set of imposed boundary conditions with a non-trivial VEV, to an equivalent scenario where the theory possesses a trivial Wilson line configuration with the physical symmetry fully specified by $(P_0^{\text{sym}}, P_1^{\text{sym}}, U^{\text{sym}})$.

Coming back to our $SU(5)$ example, let us see how the mechanism works in the 2nd case $C2$ when we have a non-trivial Wilson line configuration. The Wilson lines are given by the $SU(5)/G_{\text{SM}}$ coset $\mathcal{H}_W = \{\frac{\lambda^a}{2}, a = 13 \sim 24\}$, where we parametrise the corresponding extra dimensional modes A_y^0 as

$$A_y^0 = \frac{1}{2\pi R} \begin{pmatrix} 0 & \Theta \\ \Theta^\dagger & 0 \end{pmatrix}. \quad (4.80)$$

$g_4^2 = g^2/\pi R$ is the 4D gauge coupling, and Θ is a 3×2 complex matrix parametrising the gauge transformation under the broken coset.

Note that the particular matrix structure of A_y^0 and implicitly of Θ , is in line with the generic form specified in Eqn. (4.57) which states the form for a vanishing field strength. Θ possesses $8+3+1$ degrees of freedom, corresponding to the residual G_{SM} symmetry groups, which come in the form of 6 complex variables. Under the residual gauge symmetry, Θ transforms as

$$\Theta \rightarrow \Theta' = e^{i\alpha} \Omega_3 \Theta \Omega_2^\dagger, \quad (4.81)$$

where $e^{i\alpha} \in U(1)$, $\Omega_2 \in SU(2)$, $\Omega_3 \in SU(3)$. We can use this gauge freedom to simplify the form of Θ . Using the residual gauge invariance, we can bring Θ into a “diagonal” form

$$\Theta = \begin{pmatrix} \alpha & \gamma \\ 0 & \beta \\ 0 & 0 \end{pmatrix}, \quad \alpha, \gamma \in \mathbb{C}, \quad \beta \in \mathbb{R}. \quad (4.82)$$

Furthermore, under a G_{SM} transformation we can form two subgroup invariants, namely

- $SU(2) \times U(1)$ invariant: $\Theta\Theta^\dagger \xrightarrow{G_{\text{SM}}} \Omega_3\Theta\Theta^\dagger\Omega_3^\dagger$.
- $SU(3) \times U(1)$ invariant: $\Theta^\dagger\Theta \xrightarrow{G_{\text{SM}}} \Omega_2\Theta^\dagger\Theta\Omega_2^\dagger$.

Using the diagonal form of θ , the two invariants take the form

$$\Theta\Theta^\dagger = \begin{pmatrix} |\alpha|^2 + |\gamma|^2 & \beta\gamma & 0 \\ \beta\gamma^* & \beta^2 & 0 \\ 0 & 0 & 0 \end{pmatrix}, \quad \Theta^\dagger\Theta = \begin{pmatrix} |\alpha|^2 & \gamma\alpha^* \\ \gamma^*\alpha & \beta^2 + |\gamma|^2 \end{pmatrix}. \quad (4.83)$$

The above have the eigenvalues 0, λ_+ , λ_- , and λ_+ , λ_- , where one finds

$$\lambda_\pm = \frac{1}{2} \left(\beta^2 + |\alpha|^2 + |\gamma|^2 \pm \sqrt{(\beta^2 + |\alpha|^2 + |\gamma|^2)^2 - 4|\alpha|^2\beta^2} \right). \quad (4.84)$$

With this in mind, we note that the effective potential $V_{\text{eff}}(A_y^a)$ depends on θ according to the invariant constructs $\Theta\Theta^\dagger$ and $\Theta^\dagger\Theta$. Therefore $V_{\text{eff}}(A_y^a)$ is a function of the eigenvalues $V_{\text{eff}}(\lambda_+, \lambda_-)$. Furthermore since λ_\pm depend only on the absolute value of the parameters, we can further simplify the situation via the parameter choice

$$\alpha = a \in \mathbb{R}, \quad \beta = b \in \mathbb{R}, \quad \gamma = 0, \quad (4.85)$$

such that $\lambda_\pm = a^2, b^2$. Putting this all together, we evaluate V_{eff} with a Θ parameter choice of the form

$$\Theta = \begin{pmatrix} a & 0 \\ 0 & b \\ 0 & 0 \end{pmatrix}, \quad (4.86)$$

and we adopt the convention $V_{\text{eff}}(a, b)$ that refers to the eigenvalue dependency $V_{\text{eff}}(\sqrt{\lambda_+}, \sqrt{\lambda_-})$.

4.8 Non-SUSY $SU(5)$ Theory

To find the Wilson line configuration we now need to compute V_{eff} and then find the minimum of the potential. To this extent we remind ourselves that the shape of the potential is determined by the matter content of the theory. One can then show, that the generic form of an effective potential for the Wilson lines in a theory that contains in addition to the bulk gauge bosons, scalar bulk fields, and fermions is given as

$$V_{\text{eff}}(a, b) = -C \left\{ N_A [f_5(a) + f_5(b)] + N_B [f_5(a+b) + f_5(a-b)] + \frac{3}{2} [f_5(2a) + f_5(2b)] \right\}. \quad (4.87)$$

In the above $C = \frac{3}{64\pi^7 R^5}$, the N_A, N_B constants are determined by the number of scalar and fermion bulk fields, and the f_5 functions are related to the KK decomposition as

$$\begin{aligned} f_D(x) &= \sum_{m=1}^{\infty} \frac{\cos m\pi x}{m^D} = f_D(x+2) = f_D(-x), \\ f_D(0) &= \zeta_R(D), \quad f_D(1) = -(1-2^{1-D})\zeta_R(D), \end{aligned} \quad (4.88)$$

where ζ_R is the Riemann zeta function and $D = 5$. Note that f_D is equivalent to the polylogarithm sum

$$f_D(x) = \frac{1}{2} \left(\text{Li}_D(e^{-i\pi x}) + \text{Li}_D(e^{i\pi x}) \right), \quad (4.89)$$

where the polylogarithm Li_s is defined for a arbitrary complex order s and variable z as

$$\text{Li}_s(z) = \sum_{k=1}^{\infty} \frac{z^k}{k^s}. \quad (4.90)$$

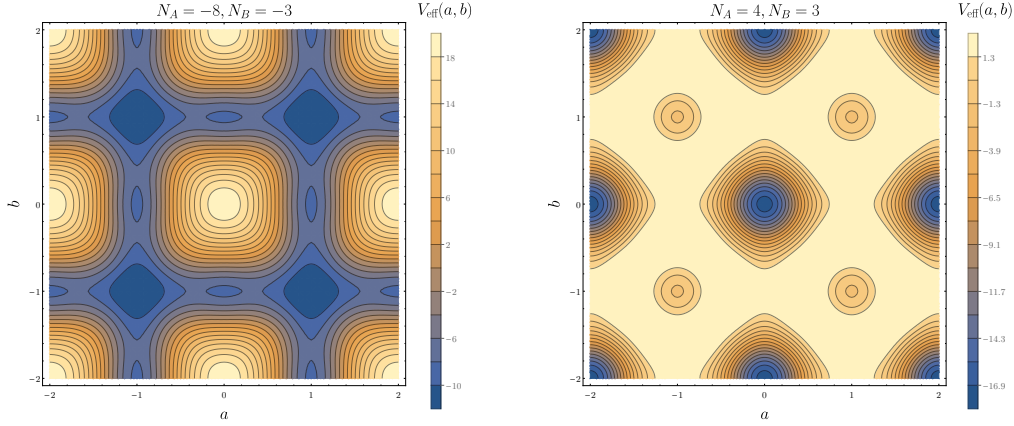
Within the $SU(5)$ model, the constants are given by the number of massless scalar fields $N_h^{\mathbf{5}}$ in the $\mathbf{5}$ representation, and the number of massless fermion fields $N_f^{\mathbf{5}}, N_f^{\mathbf{10}}$ in the $\mathbf{5}, \mathbf{10}$ representations

$$N_A \equiv 3 + N_h^{\mathbf{5}} - 2N_f^{\mathbf{5}} - 2N_f^{\mathbf{10}}, \quad (4.91)$$

$$N_B \equiv 3 - 2N_f^{\mathbf{10}}. \quad (4.92)$$

To highlight how the matter content of the theory impacts the Wilson line configuration via the effective potential, we consider the case of brane matter (i.e. $N_h = 1, N_f^{\mathbf{5}} = N_f^{\mathbf{10}} = 0$ which is equivalent to $N_A = 4, N_B = 3$), and bulk matter (i.e. $N_h = 1, N_f^{\mathbf{5}} = N_f^{\mathbf{10}} = 3$ which is equivalent to $N_A = -8, N_B = -3$), where the Higgs field lives in the bulk. The two cases are sufficient in recreating the SM spectrum, see e.g. Refs. [63, 64].

We plot the effective potential for the two cases in Fig. 4.3. For the brane case, $V_{\text{eff}}(a, b)$ has a trivial global minimum at $(0, 0)$, i.e. we have no dynamical symmetry breaking via the Hosotani mechanism. In contrast for the bulk case $V_{\text{eff}}(a, b)$ has a non-trivial global minimum at $(1, 1)$, i.e. we have dynamical symmetry breaking. Therefore the presence of bulk fermions changes the physical symmetry of the theory when we're considering boundary conditions as in C2. Note that since the potential is periodic, it exhibits degenerate global minima which provide equivalent physical scenarios.



(a) Effective potential with bulk matter $N_h^5 = 1, N_f^5 = N_f^{10} = 3$

(b) Effective potential with brane matter $N_h^5 = 1, N_f^5 = N_f^{10} = 0$

Figure 4.3: Effective potential contour plots for the cases of bulk and fermionic brane matter. The color bar represents the value of the potential $V_{\text{eff}}(a, b)$, and the x, y axis represent the Wilson line phases a, b . Note that the potential is periodic, where in the case of bulk matter the global minimum lies at a non-trivial point away from the origin, whereas in the brane matter case the minimum is trivial.

For the brane matter case, since we have a trivial minimum at $(0, 0) \Rightarrow \langle A_y \rangle = 0$, this means that the physical symmetry of the theory is the one imposed by the boundary conditions (P_0, P_1, U) , namely G_{SM} . Even though we do not have any spontaneous symmetry breaking via the Hosotani mechanism, the extra dimensional gauge components $A_y^a (a = 13 \sim 24)$ still have 0 modes, and acquire a common mass M_A via the second derivative of the effective potential

$$M_A^2 = (gR)^2 \frac{\partial^2 V_{\text{eff}}(a, b)}{\partial a^2} \Big|_{a=b=0} = \frac{3g_4^2}{4\pi^4 R^2} \zeta_R(3). \quad (4.93)$$

Note that if we took the partial derivative with respect to b , we would obtain the same result since $V_{\text{eff}}(a, b) = V_{\text{eff}}(b, a)$. Therefore the 0 modes of A_y^a have acquired a large mass $\mathcal{O}(\frac{g_4}{R})$ generated via loop corrections. Even though the fermions do not acquire masses directly via the Hosotani mechanism or via the Higgs mechanism, their masses can be subject to large radiative corrections from A_y^a , which implies a large degree of fine tuning.

In the second case of bulk fermions we have seen that the potential develops a non-trivial minimum at $(1, 1)$. Therefore the Wilson lines develop non-vanishing

VEVs. More explicitly, $(a, b) = (1, 1)$ corresponds to the Θ matrix structure

$$\Theta = \begin{pmatrix} 1 & 0 \\ 0 & 1 \\ 0 & 0 \end{pmatrix} \Rightarrow \hat{w} = 2\pi R \langle A_y \rangle = \pi \begin{pmatrix} 0 & 0 & 0 & 1 & 0 \\ 0 & 0 & 0 & 0 & 1 \\ 0 & 0 & 0 & 0 & 0 \\ 1 & 0 & 0 & 0 & 0 \\ 0 & 1 & 0 & 0 & 0 \end{pmatrix}, \quad (4.94)$$

which corresponds to the Wilson line

$$W = e^{i\hat{w}} = \text{diag}(-, -, +, -, -). \quad (4.95)$$

As we have previously discussed, we want to gauge transform to the trivial VEV configuration such that the theory is now fully specified by the boundary conditions. This gauge is known as the twisted gauge. To bring $\langle A_y \rangle \rightarrow 0$, we perform a gauge transformation of the form

$$\Omega(y) = \exp \left\{ i \frac{y}{2\pi R} \hat{w} \right\}. \quad (4.96)$$

This in turn provides us with the new boundary conditions specified via the transformation laws in Eqns. (4.62), (4.63), which have the explicit forms

$$\begin{aligned} P_0^{\text{sm}} &= S(\gamma) P_0 S^\dagger(\gamma) \Big|_{\gamma=0} = P_0 = \text{diag}(-, -, -, +, +), \\ P_1^{\text{sym}} &= S(\gamma) W P_1 S^\dagger(\gamma) \Big|_{\gamma=0} = W P_1 = \text{diag}(+, +, -, -, -). \end{aligned} \quad (4.97)$$

Since the physical symmetry of the theory is now fully encapsulated by $H^{\text{sym}} = \{\lambda^a, [\lambda^a, P_0^{\text{sym}}] = [\lambda^a, P_1^{\text{sym}}] = 0\}$, one needs to find the simultaneously commuting generators with the forms specified in Eqns. (4.97). Performing the latter, one finds that the Hosotani mechanism has caused the $SU(3)$ group to spontaneously break down to $SU(2) \times U(1)$, resulting in the $H^{\text{sym}} = SU(2) \times SU(2) \times U(1) \times U(1)$ physical symmetry of the theory.

4.8.1 Equivalence Classes

The Hosotani mechanism also guarantees that theories within the same equivalence class have the same physical symmetry.

We can generate some equivalence relations by acting on the $SU(2)$ invariant subspace of the exemplified relations. One can then check that these boundary conditions are indeed related via appropriate residual gauge transformations. We

now proceed to list the following boundary conditions that correspond to the same equivalence class

$$\begin{aligned} \text{BC1 : } \quad P_0 &= (-, -, -, +, +), \quad P_1 = (-, -, -, +, +), \quad U = (+, +, +, +, +), \\ G_{\text{BC}}^{(1)} &= SU(3) \times SU(2) \times U(1), \end{aligned} \quad (4.98)$$

$$\begin{aligned} \text{BC2 : } \quad P_0 &= (-, -, -, +, +), \quad P_1 = (-, +, -, +, -), \quad U = (+, -, +, +, -), \\ G_{\text{BC}}^{(2)} &= SU(2) \times [U(1)]^3, \end{aligned} \quad (4.99)$$

$$\begin{aligned} \text{BC3 : } \quad P_0 &= (-, -, -, +, +), \quad P_1 = (+, +, -, -, -), \quad U = (-, -, +, -, -), \\ G_{\text{BC}}^{(3)} &= [SU(2)]^2 \times [U(1)]^2, \end{aligned} \quad (4.100)$$

$$\begin{aligned} \text{BC4 : } \quad P_0 &= (-, -, -, +, +), \quad U = P_0 P_1, \\ P_1 &= \begin{pmatrix} -\cos \pi p & 0 & 0 & -i \sin \pi p & 0 \\ 0 & -\cos \pi q & 0 & 0 & -i \sin \pi q \\ 0 & 0 & -1 & 0 & 0 \\ i \sin \pi p & 0 & 0 & \cos \pi p & 0 \\ 0 & i \sin \pi q & 0 & 0 & \cos \pi q \end{pmatrix}, \\ G_{\text{BC}}^{(4)} &= [U(1)]^3, \end{aligned} \quad (4.101)$$

where $G_{\text{BC}}^{(i)}$ denotes the residual gauge invariance of the theory.

We saw in the previous section that the matter content of the theory can result in different physical symmetries post Hosotani breaking. Namely for brane matter case, the resulting physical symmetry was $H^{\text{sym}} = G_{\text{BC}}^{(1)}$, whereas for the bulk matter case we had $H^{\text{sym}} = G_{\text{BC}}^{(3)}$. Since the cases are part of an equivalence class, as long as the matter content is identical between them, the physical picture remains the same.

Let's look at $BC(2)$, where according to $G_{\text{BC}}^{(2)}$, we have $3 + 1 + 1 + 1$ degrees of freedom, which are reflected in the Wilson lines via $A_y^0 \in SU(5)/G_{\text{BC}}^{(2)}$

$$A_y^0 = \frac{1}{2gR} \begin{pmatrix} 0 & \Theta \\ \Theta & 0 \end{pmatrix}, \quad \Theta = \begin{pmatrix} \alpha & 0 \\ 0 & \beta \\ \gamma & 0 \end{pmatrix}, \quad \alpha, \beta, \gamma \in \mathbb{C}. \quad (4.102)$$

By using the residual gauge symmetry, we can simplify the above to the parameter choice $\alpha = a, \beta = b, \gamma = 0$. Note that is the same form for Θ as we had in the exemplified case.

We can now find the explicit form for the effective potential. With the same matter content one can prove that the current effective potential is equivalent to the previous one shifted by

$$V_{\text{eff}}^{BC2}(a, b) = V_{\text{eff}}^{BC1}(a, b - 1). \quad (4.103)$$

Completely analogous for $BC3$, we have $3 + 3 + 1 + 1$ degrees of freedom corresponding to the explicit form

$$A_y^0 = \frac{1}{2gR} \begin{pmatrix} 0 & & \Theta \\ & 0 & \\ \Theta^\dagger & & 0 \end{pmatrix}, \quad \Theta = \begin{pmatrix} \alpha & \delta \\ \gamma & \beta \end{pmatrix}, \quad \alpha, \beta, \delta, \gamma \in \mathbb{C}, \quad (4.104)$$

which can be simplified to the parameter choice $\alpha = a, \beta = b, \gamma = \delta = 0$. Similarly, due to the equivalence class, the change in boundary conditions, can now be traced to a shift relating to the effective potential to the one in $BC1$ as

$$V_{\text{eff}}^{BC3}(a, b) = V_{\text{eff}}^{BC1}(a - 1, b - 1). \quad (4.105)$$

Therefore we can see on an intuitive level how the Hosotani mechanism operates, in the sense that the potential for equivalent boundary conditions is identical but shifted to account for either the breaking or enhancing of the symmetry.

We can go a step further with this exercise and look at the most general conditions in this equivalence class, namely $BC4$. Note that all the previously discussed ones are subcases of the latter. Completely analogous we have the same form for Θ with a, b , and where the effective potential shift is now

$$V_{\text{eff}}^{BC4}(a, b) \equiv V_{\text{eff}}^{(p,q)}(a, b) = V_{\text{eff}}^{BC1}(a - p, b - q). \quad (4.106)$$

The global minimum is located at $(a, b) = (p, q)$ for brane matter, and at $(a, b) = (p - 1, q - 1)$ for bulk matter. We can showcase the generality of the Hosotani mechanism by bringing the non-trivial Wilson line configuration to $\langle A_y \rangle \rightarrow 0$ via a gauge transformation $\Omega(y; p, q)$ of the form

$$\Omega(y; p, q) = \exp \left\{ i \frac{y}{2R} (p\lambda_{13} + q\lambda_{19}) \right\}. \quad (4.107)$$

In the case of brane matter, the gauge transformation $\Omega(y; p, q)$ brings $\langle A_y \rangle \rightarrow 0$ and gives us the physical boundary conditions and symmetry of the theory

$$P_0^{\text{sym}} = \text{diag}(-, -, -, +, +), \quad (4.108)$$

$$P_1^{\text{sym}} = \text{diag}(-, -, -, +, +), \quad (4.109)$$

$$U^{\text{sym}} = \text{diag}(+, +, +, +, +), \quad (4.110)$$

$$\therefore \mathcal{H}^{\text{sym}} = SU(3) \times SU(2) \times U(1). \quad (4.111)$$

Similarly in the case of bulk matter, the gauge transformation $\Omega(y; p-1, q-1)$ brings $\langle A_y \rangle \rightarrow 0$ and gives us the physical boundary conditions and symmetry of the theory:

$$P_0^{\text{sym}} = \text{diag}(-, -, -, +, +), \quad (4.112)$$

$$P_1^{\text{sym}} = \text{diag}(+, +, -, -, -), \quad (4.113)$$

$$U^{\text{sym}} = \text{diag}(-, -, +, -, -), \quad (4.114)$$

$$\therefore \mathcal{H}^{\text{sym}} = SU(2) \times SU(2) \times U(1) \times U(1). \quad (4.115)$$

In both cases the physical symmetry of the theory is independent of (p, q) , further emphasising the equivalence conditions and their relation to the Hosotani mechanism. Therefore the matter content and the boundary condition equivalence class specify the physical symmetry of the theory.

4.9 Conclusions

Throughout this chapter we have reviewed the concepts and the implementation behind the Hosotani mechanism. We have seen that the non-simply connected nature of orbifolds can manifest itself in non-trivial ways via Wilson lines, which depending on the matter content and placement of the theory can have non-trivial configurations. This can impact the physical symmetry via the effective potential causing either a dynamical breakdown or a restoration of the symmetry. We have also seen that some of the arbitrariness of the boundary conditions is eliminated via the different theory analogues specified by the equivalence classes within the Hosotani mechanism.

In preparation of the phenomenological exploration of a realistic orbifold GUT model that incorporates the Hosotani mechanism, the next chapter will review the equations of motion for fields defined within the context of flat and warped extra dimensional models.

Flat & Warped Extra Dimensions

The following chapter reviews the Bessel equation, and how this relates to fermionic and bosonic equations of motion (EOM) in 5D warped space time backgrounds AdS_5 . In doing so we will review how the EOMs arise in flat dimensional models, and how we can assign consistent parity assignments to the various fields defined in these scenarios. We then review how to write the EOMs and the 4D decompositions in terms of basis functions dependent on the boundary conditions within the flat/warped extra dimension.

5.1 Extra Dimensions: Equations of Motion

The following section will review the equations of motion (EOMs) for fields defined within the context of a flat and a warped extra dimension. We start off with the simpler case of the flat extra dimension to get an intuitive understanding of what is going on, and then move on to the warped case. The following is based on [109–114].

5.1.1 Fermions in a Flat Extra Dimension

Whenever we deal with $D > 4$ space-time dimensions the Clifford algebra of the corresponding Lorentz group representation automatically includes the traditional γ^5 (to exemplify and simplify our discussion we will be working with $D = 4 + 1$ where 4 refers to the usual Minkowski space-time dimensions). The inclusion of γ^5 in the Lorentz algebra implies that the simplest irreducible representation that we can formulate in the 5D space, that then breaks consistently under the 4D Lorentz subgroup, is $(0, \frac{1}{2}) \oplus (\frac{1}{2}, 0)$ i.e. a Dirac spinor $\Psi(x, y)$. This is due to the extension of the Clifford algebra which prohibits defining a “ γ^5 analogue”. In turn the theory no longer possess representations of definite chirality (see Ref [40]). Therefore, when we will build our 5D theory, we are forced to use Dirac spinors rather than Weyl

as the fundamental building blocks. This constitutes a problem in recovering a 4D chiral theory which is solved by orbifolding.

We start by looking at the flat extra dimensional case for a theory defined on the $\mathcal{M}_4 \times S^1/\mathbb{Z}$ orbifold (\mathcal{M}_4 is the 4D Minkowski spacetime, and S^1/\mathbb{Z}_2 is the modded circular extra dimension). The minimal 5D Lagrangian consists of a bulk gauge field $A_M(x, y)$ coupled to a spinor field $\Psi(x, y)$, and has the general form

$$S = \int d^5x \left(\frac{i}{2} (\bar{\Psi} \Gamma^M \partial_M \Psi - \partial_M \bar{\Psi} \Gamma^M \Psi) - m \bar{\Psi} \Psi \right), \quad (5.1)$$

where $M \in \{0, 1, 2, 3, 5\}$ is the index accounting for both the Minkowski coordinates $\mu \in \{0, 1, 2, 3\}$ and the extra dimensional coordinate $y = 5$.

Under the 4D Lorentz subgroup, the Dirac field $\Psi = \begin{pmatrix} \chi_\alpha \\ \bar{\psi}^{\dot{\alpha}} \end{pmatrix} \sim \begin{pmatrix} \chi_L \\ \bar{\psi}_R \end{pmatrix}$ decomposes into two Weyl spinors $\chi_L, \bar{\psi}_R$ where \dot{a}, a denote RH /LH fields, with $(\psi_a)^\dagger = \psi_a^\dagger$. With a bit of foresight, we prepare the introduction of the boundary conditions on the interval by rewriting the Lagrangian in it's symmetric form

$$S = \int d^5x \left(-i\bar{\chi} \bar{\sigma}^\mu \partial_\mu \chi - i\psi \sigma^\mu \partial_\mu \bar{\psi} + \frac{1}{2} \left(\psi \overset{\leftrightarrow}{\partial}_5 \chi - \bar{\chi} \overset{\leftrightarrow}{\partial}_5 \bar{\psi} \right) + m(\psi \chi + \bar{\chi} \bar{\psi}) \right), \quad (5.2)$$

where $\psi \overset{\leftrightarrow}{\partial}_5 \chi = \psi \partial_5 \chi - (\partial_5 \psi) \chi$. Performing the variation of the 5D action, and imposing that $\delta S = 0$, we get the *5D bulk equations of motion for the 4D Weyl spinors*

$$\begin{aligned} -i\bar{\sigma}^\mu \partial_\mu \chi(x, y) - \partial_5 \bar{\psi}(x, y) + m\bar{\psi}(x, y) &= 0, \\ -i\sigma^\mu \partial_\mu \bar{\psi}(x, y) + \partial_5 \chi(x, y) + m\chi(x, y) &= 0. \end{aligned} \quad (5.3)$$

With the respective equations of motion now in place, we want to see what are the possible boundary conditions that are consistent with the action and the orbifold. We will find that the two Weyl spinors χ, ψ are going to be fully specified by a single boundary condition rather than the naive assumption of two separate ones.

We look at the variation of the action containing derivatives along the extra dimension. After integrating by parts along with the extra dimension, we have the consistency condition

$$\delta S = \int d^4x \left(-\delta\psi \chi + \psi \delta\chi + \delta\bar{\chi} \bar{\psi} - \bar{\chi} \delta\bar{\psi} \right) \Big|_0^L = 0, \quad (5.4)$$

where we have imposed the 0 variation requirement at both ends of the extra dimensional interval $0, L$. The simplest boundary condition that can be written down,

consists of setting one of the spinors to vanish at the end points. E.g. if we wanted to impose this for ψ , the analytical form is

$$\psi(y=0) = \psi(y=L) = 0, \quad (5.5)$$

which is equivalent to specifying Dirichlet (D) boundary conditions at the ends of the interval. By imposing this we automatically insure that $\delta\psi|_{0,L} = 0$. Therefore if we look at the bulk equations of motion, we note that we have effectively ensured the boundary conditions for χ

$$(\partial_5 + m)\chi \Big|_0^L = 0. \quad (5.6)$$

In the massless limit $m \rightarrow 0$ the above becomes $\partial_5\chi|_{0,L} = 0$, which is a von Neumann (N) boundary condition.

Summing this all up, if one imposes a (\pm) boundary condition (Dirichlet / von Neumann) on the LH/ RH projection χ/ψ , then the other will have the opposite sign (\mp) (von Neumann / Dirichlet) as a result.

We now come back to the bulk equations of motion. The 5D Dirac spinors can be written out in terms of their 4D Weyl decompositions as wave modes with the extra dimensional component factorised out,

$$\chi(x, y) = \sum_{n=0}^{\infty} g_n(y) \chi_n(x), \quad (5.7)$$

$$\psi(x, y) = \sum_{n=0}^{\infty} f_n(y) \psi_n(x). \quad (5.8)$$

The $\chi_n(x), \psi_n(x)$ are the 4D towers of fermions that are present in the effective 4D theory, and as such will obey the 4D Dirac equation with a corresponding mass m_n to be determined shortly,

$$-i\bar{\sigma}^\mu \partial_\mu \chi_n(x) + m_n \bar{\psi}_n(x) = 0, \quad (5.9)$$

$$-i\bar{\sigma}^\mu \partial_\mu \bar{\psi}_n(x) + m_n \chi_n(x) = 0. \quad (5.10)$$

Plugging all of this in the bulk equations of motion in Eqns. (5.3) we get the corresponding mode equations,

$$\frac{\partial g_n(y)}{\partial y} + m g_n(y) - m_n f_n = 0, \quad (5.11)$$

$$\frac{\partial f_n(y)}{\partial y} - m f_n(y) + m_n g_n = 0, \quad (5.12)$$

which can be combined into two second order wave equations,

$$\frac{\partial^2 g_n(y)}{\partial y^2} + (m_n^2 - m^2)g_n = 0, \quad (5.13)$$

$$\frac{\partial^2 f_n(y)}{\partial y^2} + (m_n^2 - m^2)f_n = 0. \quad (5.14)$$

Eqns. (5.13), (5.14) have a set of solutions determined by $\omega_n = (m_n^2 - m^2)$, which have the general form

$$f_n(y) = C_n \sin(m_n^2 - m^2)^{\frac{1}{2}} y + D_n \cos(m_n^2 - m^2)^{\frac{1}{2}}, \quad (5.15)$$

$$g_n(y) = A_n \sin(m_n^2 - m^2)^{\frac{1}{2}} y + B_n \cos(m_n^2 - m^2)^{\frac{1}{2}}. \quad (5.16)$$

Plugging in the general solution in the original 1st order equations, we find the relationship between the coefficients

$$mC_n - (m_n^2 - m^2)^{\frac{1}{2}} D_n - m_n A_n = 0, \quad (5.17)$$

$$(m_n^2 - m^2)^{\frac{1}{2}} C_n + mD_n - m_n B_n = 0. \quad (5.18)$$

After we have imposed the corresponding boundary conditions, the values of the remaining coefficients are determined by the wave-mode normalisation conditions $\int_0^L f_n(y) dy = 1$.

Taking the $m \rightarrow 0$ limit along with plugging in the forms of the general solutions in the original ODEs along with evaluating them at the boundaries $(0, L)$, gives us the mass quantisation condition for a flat extra dimension

$$m_n^2 = \frac{n^2}{L^2}. \quad (5.19)$$

Furthermore, once we impose the boundary conditions on either the LH χ or RH component ψ , the other is fully determined. E.g. imposing that the LH component transforms under \mathbb{Z}_2 as $\mathbb{Z}_2(\chi) \rightarrow (+)\chi$, determines the RH component's transformation as $\mathbb{Z}_2(\psi) \rightarrow (-)\psi$. With this choice of boundary conditions, the general solutions reduce to either a sine or a cosine, leaving us with the fermion tower equations

$$\chi(x, y) = \sum_{n=0}^{\infty} B_n \cos \frac{ny}{L} \chi_n(x), \quad (5.20)$$

$$\psi(x, y) = \sum_{n=1}^{\infty} C_n \sin \frac{ny}{L} \psi_n(y). \quad (5.21)$$

As previously mentioned, this allows for a trivial 0 mode for the LH component (i.e. a massless mode), while the RH component starts at $n = 1$ inducing the mass separation of $\sim 1/L$. In essence, orbifolding has allowed us to obtain a chiral theory from an intrinsically non-chiral one.

5.1.2 Fermions in a Warped Extra Dimension

First off, we introduce the AdS₅ metric and the general form of an action written within this background. The AdS₅ metric that satisfies Einstein's equations, has the general form

$$ds^2 = e^{-2\sigma} \eta_{\mu\nu} dx^\mu dx^\nu + dy^2, \quad (5.22)$$

where $\sigma = k|y|$ is the warp factor, $1/k$ is the AdS₅ curvature radius, $\eta_{\mu\nu} = \text{diag}(-, +, +, +)$ is the 4D Minkowski space-time metric, and x^μ are the 4D coordinates along with y which is the 5th dimensional coordinate. This can be recast in terms of the *conformal coordinate* z , which is defined as

$$z = e^{ky}, \quad (5.23)$$

under the equivalent domain $z \in [1, z_L] \equiv [1, e^{kL}]$. Using the conformal coordinate form, the AdS₅ metric takes the form

$$ds^2 = \frac{1}{z^2} \left(\eta_{\mu\nu} dx^\mu dx^\nu + \frac{dz^2}{k^2} \right). \quad (5.24)$$

Preparing our AdS₅ action, we note that in contrast with the flat extra dimensional case, the fermionic warped action has an additional piece consisting of the spin-connection, which is manifest via the covariant derivative

$$D_\mu \Psi = \left(\partial_\mu + \frac{1}{4z} \gamma_\mu \gamma_5 \right) \Psi. \quad (5.25)$$

γ^μ, γ^5 are the usual 4D Dirac matrices in the chiral representation, and $D_5 \Psi = \partial_5 \Psi$. In addition we have another complexity arising from the gamma matrices in warped space Γ^M required to form a 5D Lorentz invariant with the covariant derivative D_M . These are related to their 4D counterparts via the vielbeins e_a^M ,

$$\Gamma^M = e_a^M \gamma^a, \quad (5.26)$$

which relate the flat space metric to the curved AdS₅ metric via $e_a^M \eta^{ab} e_b^N = g^{MN}$. One can show that the vielbeins can be expressed as $e_a^M = \delta_a^M / z$ [109]. With this in

mind we move on to writing down the symmetric action for a 5D fermion in warped space. The most general expression is

$$S = \int d^5x \sqrt{g} \left(\frac{i}{2} \bar{\Psi} \Gamma^M D_M \Psi - \frac{i}{2} D_M \bar{\Psi} \Gamma^M \Psi - m \bar{\Psi} \Psi \right). \quad (5.27)$$

where we've introduced a 5D mass term m , and the action is weighted by the metric determinant $\sqrt{g} = 1/(z)^5$. Plugging in the explicit forms of the vielbeins, and expressing everything in terms of the conformal coordinate, we get the form of the action

$$S = \int d^5x \left(\frac{1}{z} \right)^4 \bar{\Psi} \left(i \not{\partial} + i \gamma^5 k \left(\partial_z - \frac{2}{z} \right) - \frac{c}{z} k \right) \Psi, \quad (5.28)$$

where we've introduced $c = m/k$, and $\partial_5 = \partial_y = kz \partial_z$. To derive the equations of motion for ψ, χ , we can perform an analogy to the flat dimensional case, and rewrite the action in terms of the Weyl components

$$S = \int d^5x \frac{1}{z^4} \left(-i \bar{\chi} \bar{\sigma}^\mu \partial_\mu \chi - i \psi \sigma^\mu \partial_\mu \bar{\psi} + \frac{k}{2} \left(\psi \overset{\leftrightarrow}{\partial}_z \chi - \bar{\chi} \overset{\leftrightarrow}{\partial}_z \bar{\psi} \right) + \frac{c}{z} k (\psi \chi + \bar{\chi} \bar{\psi}) \right), \quad (5.29)$$

where $\partial_{\bar{z}} = \partial_z - 2/z$. Note that this time around we have the conformal coordinate z present in the mass term, which will get an additional contribution from the $2/z$ arising from the extra dimensional derivative. Performing the variation of the action we get the warped AdS₅ bulk equations of motion

$$\begin{aligned} -i \bar{\sigma}^\mu \partial_\mu \chi(x, z) - k \partial_z \bar{\psi}(x, z) + k \frac{c+2}{z} \bar{\psi}(x, y) &= 0, \\ -i \sigma^\mu \partial_\mu \bar{\psi}(x, z) + k \partial_z \chi(x, z) + k \frac{c-2}{z} \chi(x, z) &= 0. \end{aligned} \quad (5.30)$$

Analogous to the flat dimensional case we expand the bulk fields as a sum of 4D eigenmodes,

$$\chi(x, z) = \sum_{n=1}^{\infty} g_n(z) \chi(x), \quad \bar{\psi}(x, z) = \sum_{n=1}^{\infty} f_n(z) \bar{\psi}(x), \quad (5.31)$$

which in turn will satisfy the corresponding 4D Dirac equations of motion,

$$\begin{aligned} -i \bar{\sigma}^\mu \partial_\mu \chi_n(x) + m_n \bar{\psi}_n(x) &= 0, \\ -i \bar{\sigma}^\mu \partial_\mu \bar{\psi}_n(x) + m_n \chi_n(x) &= 0. \end{aligned} \quad (5.32)$$

Substituting in the eigenmode decomposition into the bulk equations of motion we get our profile equations for the LH, and RH towers,

$$\begin{aligned} \frac{\partial f_n(z)}{\partial z} + \frac{m_n}{k} g_n - \frac{c-2}{z} f_n &= 0, \\ \frac{\partial g_n(z)}{\partial z} - \frac{m_n}{k} f_n + \frac{c+2}{z} g_n &= 0. \end{aligned} \quad (5.33)$$

We now take the 2nd derivative, perform the corresponding substitutions and in turn decouple the two into Bessel equations (see Appendix A.1 for an overview). These in turn can be written in the standard form of Eqn. (A.16) as

$$\begin{aligned} \frac{\partial^2 f_n}{\partial z^2} + \frac{1 - 2 \cdot \frac{5}{2}}{z} \frac{\partial f_n}{\partial z} + \left\{ \left(\frac{m_n}{k} \cdot 1 \cdot z^{1-1} \right)^2 + \frac{\left(\frac{5}{2} \right)^2 - 1 \cdot \left(c - \frac{1}{2} \right)^2}{z^2} \right\} f_n &= 0, \\ \frac{\partial^2 g_n}{\partial z^2} + \frac{1 - 2 \cdot \frac{5}{2}}{z} \frac{\partial g_n}{\partial z} + \left\{ \left(\frac{m_n}{k} \cdot 1 \cdot z^{1-1} \right)^2 + \frac{\left(\frac{5}{2} \right)^2 - 1 \cdot \left(c + \frac{1}{2} \right)^2}{z^2} \right\} g_n &= 0. \end{aligned} \quad (5.34)$$

Therefore the above admit the general solutions

$$f_n(z) = z^{5/2} \left[A_n J_{(c-\frac{1}{2})} \left(\frac{m_n}{k} z \right) + B_n Y_{(c-\frac{1}{2})} \left(\frac{m_n}{k} z \right) \right], \quad (5.35)$$

$$g_n(z) = z^{5/2} \left[C_n J_{(c+\frac{1}{2})} \left(\frac{m_n}{k} z \right) + D_n Y_{(c+\frac{1}{2})} \left(\frac{m_n}{k} z \right) \right]. \quad (5.36)$$

We note that by performing the $c - 1/2 \rightarrow c + 1/2$ transformation for g_n we recover f_n , and therefore only focus on the latter. We can reparametrize f_n as

$$f_n(z) = \frac{z^{5/2}}{N_n} \left[J_{(c-\frac{1}{2})}(\lambda_n z) + b_{(c-\frac{1}{2})}(\lambda_n) Y_{(c-\frac{1}{2})}(\lambda_n z) \right], \quad (5.37)$$

where we've introduced the notation $\lambda_n = m_n/k$, and we've traded A_n, B_n in favour of the normalisation constants N_n and $b_{(c-\frac{1}{2})}(\lambda_n)$. In this form, N_n is now fully determined by the extra dimensional normalisation condition $\int \frac{dz}{z} \chi_n \chi_m = \delta_{nm}$ as,

$$N_n^2 = \int_1^{z_L} dz z^2 \left[J_{(c-\frac{1}{2})}(\lambda_n z) + b_{(c-\frac{1}{2})}(\lambda_n) Y_{(c-\frac{1}{2})}(\lambda_n z) \right]^2. \quad (5.38)$$

Similarly, the form of $b_{(c-\frac{1}{2})}(\lambda_n)$ is determined by the boundary conditions at $z = 1, z_L$. For example, suppose that $\bar{\psi}$ obeys Dirichlet boundary conditions at both ends of the interval. This implies $f_n = 0|_{z=1, z_L}$, and more specifically $b_{(c-\frac{1}{2})}(\lambda_n)$ at $z = 1$ takes the form

$$b_{(c-\frac{1}{2})}(\lambda_n) = -\frac{J_{(c-\frac{1}{2})}(\lambda_n)}{Y_{(c-\frac{1}{2})}(\lambda_n)}. \quad (5.39)$$

Plugging it all back into f_n and requiring $f_n = 0|_{z=z_L}$, we now get the quantisation condition for λ_n

$$Y_{(c-\frac{1}{2})}(\lambda_n) J_{(c-\frac{1}{2})}(\lambda_n z_L) - Y_{(c-\frac{1}{2})}(\lambda_n z_L) J_{(c-\frac{1}{2})}(\lambda_n) = 0. \quad (5.40)$$

The above therefore determines *the mass spectrum* for $\bar{\psi}$. The mass quantisation of the KK towers is therefore determined by the zeros of Eqn. (5.40), where the n th mode has a mass $m_n = \lambda_n k$. Similarly, for a fermion obeying a von Neumann

boundary condition, the above holds with the only difference arising in $b_{(c-\frac{1}{2})}(\lambda_n)$ which now becomes

$$b_{(c-\frac{1}{2})}(\lambda_n) = -\frac{(c-\frac{1}{2})J_{(c-\frac{1}{2})}(\lambda_n) + \lambda_n J'_{(c-\frac{1}{2})}(\lambda_n)}{(c-\frac{1}{2})Y_{(c-\frac{1}{2})}(\lambda_n) + \lambda_n Y'_{(c-\frac{1}{2})}(\lambda_n)}. \quad (5.41)$$

We can approach the entire problem in a similar, more efficient way, along the lines outlined by the method in [115]. We start off by performing the redefinition $\hat{\Psi} = z^{-2}\Psi$, which allows us to rewrite the AdS₅ fermion action as

$$S = \int d^4x \int_1^{z_L} \frac{dz}{k} \begin{pmatrix} \bar{\hat{\chi}} & \hat{\psi} \end{pmatrix} \begin{pmatrix} -kD_{z-}(c) & \sigma^\mu \partial_\mu \\ \bar{\sigma}^\mu \partial_\mu & -kD_{z+}(c) \end{pmatrix} \begin{pmatrix} \hat{\chi} \\ \hat{\psi} \end{pmatrix}, \quad (5.42)$$

where we have expressed everything in terms of the chiral representation of γ_5 , and we've defined $D_{z\pm}(c) = \pm \frac{d}{dz} + \frac{c}{z}$. The bulk equations of motion now take the form

$$-kD_{z-}(c)\bar{\hat{\psi}}(x, z) + \sigma^\mu \partial_\mu \hat{\chi}(x, z) = 0, \quad (5.43)$$

$$-kD_{z+}(c)\hat{\chi}(x, z) + \sigma^\mu \partial_\mu \bar{\hat{\psi}}(x, z) = 0. \quad (5.44)$$

After plugging in the appropriate 4D Dirac decomposition relationships, we obtain the analogous 1st order coupled equations of motion

$$D_{z-}(c)\hat{f}_n(z) = \frac{m_n}{k}\hat{g}_n(z), \quad (5.45)$$

$$D_{z+}(c)\hat{g}_n(z) = \frac{m_n}{k}\hat{f}_n(z), \quad (5.46)$$

where in contrast to Eqns. (5.33), the factor of $-2/z$ is missing due to our field redefinition. The above can be treated as a set of coupled eigenvalue equations with boundary conditions at $z = 1, z_L$. We can postulate a basis function ansatz based on their \pm boundary conditions at z_L , and then choose the appropriate functions based on the actual fields in the theory and their concrete transformation properties under \mathbb{Z}_2 . The ansatz can be formulated based on the form of the solutions that we've previously derived. Namely we define the auxiliary function

$$F_{\alpha,\beta}(u, v) = J_\alpha(u)Y_\beta(v) - Y_\alpha(u)J_\beta(v), \quad (5.47)$$

that is the foundation of our ansatz. To this extent we define 4 basis functions corresponding to LH/RH spinors that obey either von Neumann or Dirichlet boundary conditions. Depending on the handedness of the fermionic field, we label functions that obey von Neumann boundary conditions as $C_{L,R}$, and Dirichlet as $S_{L,R}$. The

basis functions are then defined in line with the authors in [115], and have the form

$$\begin{aligned}
C_L(z; \lambda, c) &= (+) \frac{\pi}{2} \lambda \sqrt{z z_L} F_{c+\frac{1}{2}, c-\frac{1}{2}}(\lambda z, \lambda z_L), \\
S_L(z; \lambda, c) &= (-) \frac{\pi}{2} \lambda \sqrt{z z_L} F_{c+\frac{1}{2}, c+\frac{1}{2}}(\lambda z, \lambda z_L), \\
C_R(z; \lambda, c) &= (-) \frac{\pi}{2} \lambda \sqrt{z z_L} F_{c-\frac{1}{2}, c+\frac{1}{2}}(\lambda z, \lambda z_L), \\
S_R(z; \lambda, c) &= (-) \frac{\pi}{2} \lambda \sqrt{z z_L} F_{c-\frac{1}{2}, c-\frac{1}{2}}(\lambda z, \lambda z_L).
\end{aligned} \tag{5.48}$$

It can be shown that the ansatz solutions, at $z = z_L$, obey the relations

$$C_L(z) = C_R(z) = 1 \Big|_{z=z_L}, \quad S_L(z) = S_R(z) = 0 \Big|_{z=z_L}, \tag{5.49}$$

and transform under the action of the covariant derivative as

$$D_{z+}(c) \begin{pmatrix} C_L \\ S_L \end{pmatrix} = \lambda_n \begin{pmatrix} S_R \\ C_R \end{pmatrix}, \quad D_{z-}(c) \begin{pmatrix} C_R \\ S_R \end{pmatrix} = \lambda_n \begin{pmatrix} S_L \\ C_L \end{pmatrix}. \tag{5.50}$$

We note, that this is effectively the formalised version of the previously derived general solution with the boundary conditions at z_L automatically incorporated, and adapted for the different boundary conditions corresponding to either LH/ RH modes. Lastly we note, that the explicit power of z in this derivation is different, since we have absorbed a factor of z^2 in our redefinition of the fields.

5.2 Stepping Stones

We now have all the necessary tools in order to analyse the 6D $SO(11)$ GHGUT presented in [116, 117]. This will entail exploring and enlarging the viable parameter space via evolutionary algorithms. We will then examine the Higgs and exotic phenomenology of the model, along with checking the consistency between the UV to the IR phases of the theory via renormalisation group equation runnings within 4D and 5D approximations.

$SO(11)$ GHGUT - The Model

The following chapter is a review of the model presented in Refs. [116, 117]. We will briefly look at the torus compactification, and move on to examine the 6D hybrid space time of the model, consisting of extra warped and flat dimensions.

We then proceed to discuss the overall layout of the model consisting of the matter content and placement within the branes or bulk, the symmetry breaking mechanisms and the determination of the effective potential via the various extra dimensional equations of motion. We finish off by highlighting the relevant relations for our analysis in Chapter 7.

6.1 6D Orbifold Compactification

In the following section we will briefly review the construction of the T^2/\mathbb{Z}_2 orbifold, following the prescription outlined in [73]. We start off with our extra dimensional space. With two extra dimensions, the simplest obtainable compactification is a torus T^2 . The torus can be described by a complex variable $z \in \mathbb{C}$ as

$$z = x_5 + ix_6, \quad (6.1)$$

where x_5, x_6 are the coordinates along the two \vec{e}_1, \vec{e}_2 directions.

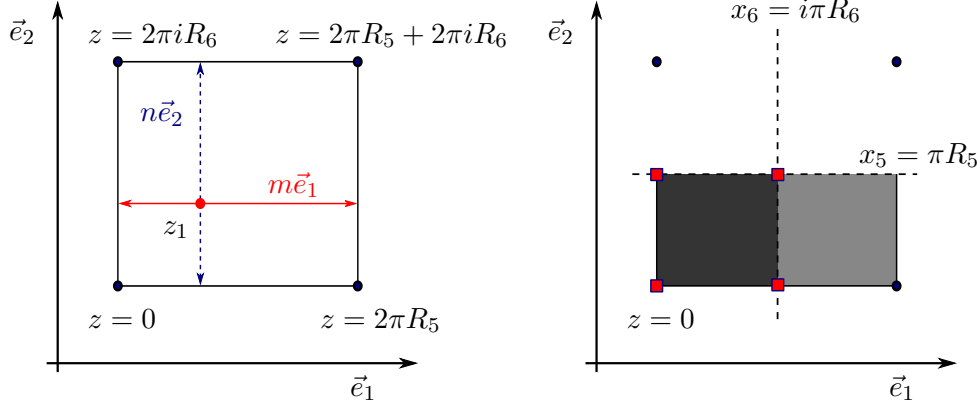
To form the torus, analogous to the circle, we can compactify two dimensions, by identifying points under the two corresponding translations $\mathcal{T}_1, \mathcal{T}_2$ associated with \vec{e}_1, \vec{e}_2 . Under the two, we identify a point z_1 with z_2 as

$$z_1 \rightarrow z_2 = z_1 + m\vec{e}_1 + n\vec{e}_2, \quad (6.2)$$

where $m, n, \in \mathbb{N}$. We can now “unfold” the torus, making it topologically equivalent with a rectangular lattice with the ends identified with each other. To this extent, we normalise the unit vectors to

$$|\vec{e}_1| = 2\pi R_5, \quad |\vec{e}_2| = 2\pi R_6, \quad (6.3)$$

where R_5, R_6 are the radii of the torus (see Fig. 6.1a).



(a) Rectangular lattice view of the torus T^2 , where the edges and corners are identified with each other. The length of each side is given by the respective unit vectors $|\vec{e}_1| = 2\pi R_5, |\vec{e}_2| = 2\pi i R_6$. A torus identification $z_1 \rightarrow z_1 + m\vec{e}_1 + n\vec{e}_2$ is equivalent with the red rod identifying itself where the translations correspond to m, n integral lattice translations.

(b) The \mathbb{Z}_2 identification of the T^1 torus results in the T^1/\mathbb{Z}_2 orbifold. The identification is performed by “folding” the lattice along the two directions \vec{e}_1, \vec{e}_2 in line with the complex identification $z \rightarrow -z$. The resulting manifold is equivalent to a pillow (dark shaded grey area) with fixed points denoted by the red squares.

Figure 6.1: Diagrammatic views of the torus as a lattice, and the orbifolding procedure resulting in T^2/\mathbb{Z}_2 .

To form the T^2/\mathbb{Z}_2 orbifold, we perform the \mathbb{Z}_2 identification

$$z_1 \rightarrow -z_2, \quad (6.4)$$

or equivalently in the (x_5, x_6) plane $x_5 \rightarrow -x_5, x_6 \rightarrow -x_6$. The orbifolding procedure is shown diagrammatically in Fig. 6.1b, and it transforms our lattice into a “pillow” with fixed points at

$$\{z = 0, z = \pi R_5, z = i\pi R_6, z = \pi R_5 + i\pi R_6\}. \quad (6.5)$$

Similar to the 5D case, we impose consistency conditions between the translations and reflections. These in turn carry over to the fields, and define how they transform. This is specified by the forms of the translational and reflection matrices U_1, U_2, Z , as

$$U_1 Z = Z U_1^{-1}, \quad U_2 Z = Z U_2^{-1}, \quad U_1 U_2 = U_2 U_1. \quad (6.6)$$

Analogous to the 5D case, since \mathbb{Z}_2 is a reflection, we require $Z^2 = 1$. We note that we can break down the reflection in terms of the x_5, x_6 coordinates, and can combine them with each of the translational directions to form reflections around the mid points. Therefore we can form four parity transformations $P_j, j = 0, 1, 2, 3$, linked by a consistency constraint. This in turn allows us to treat the two dimensions separately, which will prove useful as we will see in the next section.

6.2 6D Spacetime and Gauge Symmetry

The model we are going to explore in this Chapter was introduced in [116], and is formulated on a hybrid 6D compactified space. The 6D space-time in the model is described by the generalised Randall-Sundrum metric [117, 118]

$$ds^2 = e^{-2\sigma(y)}(\eta_{\mu\nu}dx^\mu dx^\nu + d\nu^2) + dy^2, \quad (6.7)$$

which is defined in terms of the two compactified coordinates ν, y , the warp factor along the 5th dimension $e^{-2\sigma(y)}$, and the flat 4D Minkowski space-time metric $\eta_{\mu\nu} = \text{diag}(-1, +1, +1, +1)$. The two compactified coordinates are identified as the Electroweak (EW) coordinate $y \in [0, L_5]$, and the GUT coordinate $\nu \in [0, 2\pi R_6]$. Note that both compactified dimensions are defined on the circle S^1 , where L_5, R_6 are the respective radii. We further note that L_5 has factor of 2π absorbed into its definition.

The warp factor $\sigma(y) = k|y|$ is subject to the periodic boundary conditions and obeys the end interval conditions

$$\sigma(y) = \sigma(-y) = \sigma(y + 2L_5), \quad (6.8)$$

where we have introduced the AdS_5 curvature k .

We identify two spacetime points via a \mathbb{Z}_2 transformation as $(x^\mu, y, \nu) \rightarrow (x^\mu, -y, -\nu)$, under which the defining manifold of the theory has the topology of the $\mathcal{M}_4 \times (T^2/\mathbb{Z}_2)$ orbifold. This space-time has two fixed points at $y = \{0, L_5\}$, with an anti-de-Sitter bulk and a cosmological constant of $\Lambda = -10k^2$. At the fixed points, we have 5D branes with a $\mathcal{M}_4 \times S^1$ topology. We depict the orbifold in Fig. 6.2, along with the various gauge breaking assignments.

We can rewrite the metric in terms of the conformal coordinate z defined as

$$z = e^{ky}, \quad (6.9)$$

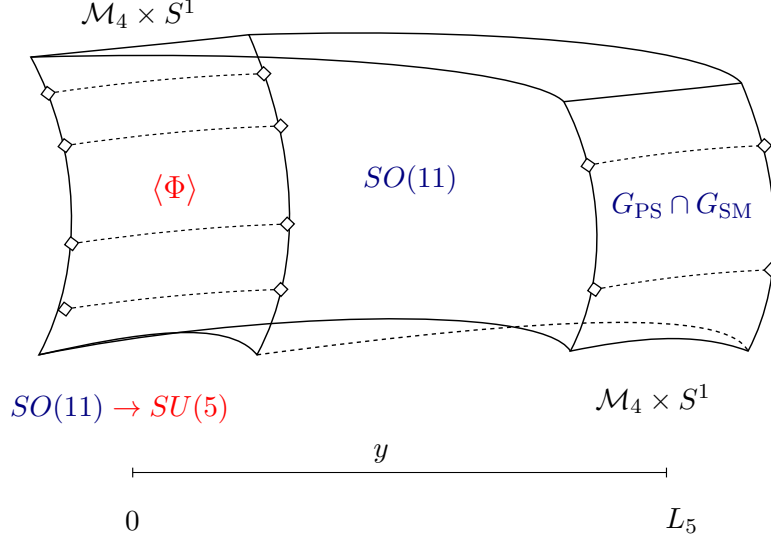


Figure 6.2: $\mathcal{M}_4 \times (T^2/\mathbb{Z}_2)$ orbifold with 5D branes with a $\mathcal{M}_4 \times S^1$ topology at $y = 0, L_5$. y corresponds to the warped coordinate, and the 5D branes have the extra dimensional flat coordinate corresponding to $\nu \in [0, 2\pi R_6]$. The blue labels represent the $SO(11)$ symmetry in the 6D bulk, the same manifest UV brane symmetry, and with the effective Pati-Salam (PS) projection that results from the parity assignments intersection $G_{\text{PS}} \sim SO(6) \times SO(4) = SO(10) \cap SO(7) \times SO(4)$. The red labels represent the 5D $SO(11)$ spinor scalar field $\Phi_{\mathbf{32}}$ that breaks the UV brane symmetry down to $SU(5)$ via a Higgs mechanism, which in turn project the IR brane PS symmetry down to the SM.

where z has the definition domain of $z \in [1, z_L]$ defined by $z_L = e^{kL_5}$. In terms of the conformal coordinate, the 6D metric now becomes

$$ds^2 = \frac{1}{z^2} \left(\eta_{\mu\nu} dx^\mu dx^\nu + d\nu^2 + \frac{dz^2}{k^2} \right). \quad (6.10)$$

In terms of the new compactified coordinates z, ν , we have two associated mass scales

$$m_{\text{KK}_5} = \frac{\pi k}{z_L - 1}, \quad m_{\text{KK}_6} = \frac{1}{R_6}, \quad (6.11)$$

which are defined in terms of the 1st non-zero solution of the photon tower and the 1st non-zero mass mode along the GUT coordinate. Since m_{KK_5} is associated with

the EW scale, it will be of the order a few TeV, and m_{KK_6} will define the GUT scale M_{GUT} . The mass scales for the different fields will be set by their various parity assignments along either z or ν . Throughout this work we assume that there is a large mass gap between the two with $m_{\text{KK}_6} \gg m_{\text{KK}_5}$, where for a rough qualitative measure we take $M_{\text{GUT}} \sim 10^{16}$ GeV.

Moving on to the parity transformations, on the T^2/\mathbb{Z}_2 orbifold, we can define four reflections P_j , $j = \{0, 1, 2, 3\}$. We note that out of the four, only three are independent, where they obey the consistency constraint

$$P_3 = P_2 P_0 P_1 = P_1 P_0 P_2. \quad (6.12)$$

In addition, in line with the authors in Ref. [116], we adopt the following simplification,

$$P_0 = P_1, \quad P_2 = P_3, \quad (6.13)$$

which is introduced to avoid the presence of light exotic fermions. Note that this was an issue with an early attempt at formulating a $SO(11)$ model in a AdS_5 background[115].

The forms of orbifold boundary conditions P_j act to reduce the $SO(11)$ gauge symmetry as

$$SO(11) \xrightarrow{P_0=P_1} SO(4) \times SO(7), \quad (6.14)$$

$$SO(11) \xrightarrow{P_2=P_3} SO(10). \quad (6.15)$$

The explicit form of the parity assignment acting on the vector representation of $SO(11)$ is

$$P_0^{\text{vec}} = P_1^{\text{vec}} = \text{diag}(\mathbb{1}_4, -\mathbb{1}_7), \quad P_2^{\text{vec}} = P_3^{\text{vec}} = \text{diag}(\mathbb{1}_{10}, -\mathbb{1}_1). \quad (6.16)$$

Similarly from of the parity transformations acting on the spinorial representations P_j^{sp} is expressed as the outer products

$$P_0^{\text{sp}} = P_1^{\text{sp}} = \mathbb{1}_2 \otimes \sigma^3 \otimes \mathbb{1}_8, \quad P_2^{\text{sp}} = P_3^{\text{sp}} = \mathbb{1}_{16} \otimes \sigma^3. \quad (6.17)$$

Note that in order to achieve the desired symmetry breaking pattern, the forms of P_i are chosen such that the surviving gauge symmetry is dictated by $[T^a, P_i] = \{T^{\hat{a}}, P_i\} = 0$, where T^a represent the generators of the unbroken symmetry and $T^{\hat{a}}$ represent the broken generators. To find the spinorial forms of P_j^{sp} , one needs the appropriate generator representations T_{sp}^a which analogously define the same relations $[T_{\text{sp}}^a, P_i^{\text{sp}}] = \{T_{\text{sp}}^{\hat{a}}, P_i^{\text{sp}}\} = 0$.

A useful tool that we will use to inspect the symmetry breaking, consists of the 5D, and 6D translations U_5 , and U_6 which are related to the parity transformations via the consistency conditions

$$U_5 = P_0 P_1 = P_3 P_2, \quad U_6 = P_2 P_0 = P_3 P_1. \quad (6.18)$$

6.3 Matter Content

The matter content of the model consists of 6D and 5D fields. The following section will be an overview of what fields are present in the model along with their transformation rules and decompositions under the different boundary conditions specified by the isometries.

6.3.1 6D Fields

Starting of with the $SO(11)$ bulk gauge bosons $A_M(x, y, \nu)$, they transform under P_j as the adjoint representation, as

$$\begin{pmatrix} A_\mu \\ A_y \\ A_\nu \end{pmatrix} (x, y_j - y, \nu_j - \nu) = P_j^{\text{vec}} \begin{pmatrix} A_\mu \\ A_y \\ A_\nu \end{pmatrix} (x, y_j + y, \nu_j + \nu) (P_j^{\text{vec}})^{-1}. \quad (6.19)$$

Next, we have a set of $SO(11)$ bulk Dirac spinors in the **32** spinorial representation $\Psi_{\mathbf{32}}^\alpha(x, y, \nu)$ where $\alpha = \{1, 2, 3, 4\}$ corresponds to a generational index. The index corresponds to two subsets $\alpha = \{1, 2, 3\}$ and $\alpha = \{4\}$, which contain the three generations of the SM quarks and leptons, with the latter being introduced to ensure 6D anomaly cancellation, and will show up phenomenologically as a “dark fermion multiplet”. Note that this is analogous to its namesake counterpart presented in the $SO(5) \times U(1)$ gauge-Higgs unification model in [119].

The $\Psi_{\mathbf{32}}^\alpha(x, y, \nu)$ spinor fields transform under the boundary conditions P_j as

$$\begin{aligned} \Psi_{\mathbf{32}}^\alpha(x, y_j - y, \nu_j - \nu) &= \eta_j^\alpha (-i\gamma^5 \gamma^6) P_j^{\text{sp}} \Psi_{\mathbf{32}}^\alpha(x, y_j + y, \nu_j + \nu) \\ &\equiv \eta_j^\alpha (\bar{\gamma}) P_j^{\text{sp}} \Psi_{\mathbf{32}}^\alpha(x, y_j + y, \nu_j + \nu) \\ &= \eta_j^\alpha (\gamma_{4D}^5 \gamma_{6D}^7) P_j^{\text{sp}} \Psi_{\mathbf{32}}^\alpha(x, y_j + y, \nu_j + \nu) \\ &= \eta_j^\alpha (\gamma_{6D}^7 \gamma_{4D}^5) P_j^{\text{sp}} \Psi_{\mathbf{32}}^\alpha(x, y_j + y, \nu_j + \nu), \end{aligned} \quad (6.20)$$

where $\eta_j^\alpha = \pm 1$ are the parity assignments that are used to ensure anomaly cancellation, $\gamma^a, a = \{1, \dots, 6\}$ are the 6D Dirac matrices, which satisfy the Clifford

algebra anticommutation relations related to the 6D flat Minkowski metric as

$$\{\gamma^a, \gamma^b\} = 2\eta^{ab} = 2 \text{diag}(-\mathbf{1}_1, \mathbf{1}_5), \quad (6.21)$$

and we have introduced $\gamma_{4D}^5 = \mathbf{1}_2 \otimes \sigma^3 \otimes \mathbf{1}_2$, $\gamma_{6D}^7 = \mathbf{1}_4 \otimes \sigma^3$ which determine the parity even/odd decomposition eigenmodes.

To ensure anomaly cancellation, we have $\eta_j^{1,2} = -1$, $\eta_j^3 = +1$, and $\eta_{0,2}^4 = -\eta_{1,3}^4 = 1$, which leads to the parity assignment for 4D LH and RH modes in Ref. [116]. This assignment corresponds to the ‘‘Weyl condition’’, which translates to ± 1 eigenvalues corresponding to γ_{6D}^7 for $\alpha = 1, 2$ and $\alpha = 3, 4$ respectively. These resulting fields are referred to as ‘‘6D Weyl fields’’ which is a bit improper since for $D = d+4$, $d \geq 1$ the lowest irreducible representation for the Lorentz algebra is no longer the chiral Weyl spinor but rather the Dirac spinor. This is due to the automatic inclusion of γ^5 in the Lorentz algebra for $d \geq 1$. In other words all bulk fields need to come as Dirac rather than Weyl, but for all intents and purposes we can treat them as ‘‘bulk Weyl’’ after we’ve made the γ_{6D}^7 identification. To this extent, the $SO(11)$ Dirac spinor representation $\Psi_{\mathbf{32}}$ decomposes under $SO(10)$ and has the following $\gamma(\pm)$ decomposition

$$\Psi_{\mathbf{32}_D} = \begin{pmatrix} \psi_{\mathbf{16}_D} \\ \bar{\psi}_{\mathbf{16}_D} \end{pmatrix}, \quad \gamma(+): \begin{pmatrix} \psi_{\mathbf{16}_D} \\ 0 \end{pmatrix} \sim \begin{pmatrix} \mathbf{16}_L \\ \mathbf{16}_R \\ 0 \\ 0 \end{pmatrix}, \quad \gamma(-): \begin{pmatrix} 0 \\ \bar{\psi}_{\mathbf{16}_D} \end{pmatrix} \sim \begin{pmatrix} 0 \\ 0 \\ \bar{\mathbf{16}}_R \\ \bar{\mathbf{16}}_L \end{pmatrix}. \quad (6.22)$$

Next off, we have the 6D $SO(11)$ vector $\mathbf{11}$ bulk Dirac fermions $\Psi_{\mathbf{11}}^\beta(x, y, \nu)$, $\Psi_{\mathbf{11}}^{\prime\beta}(x, y, \nu)$, where $\beta = 1, 2, 3$ is a generational index. Under the aforementioned boundary conditions the vector fields transform as

$$\Psi_{\mathbf{11}}^{(\prime)\beta}(x, y_j - y, \nu_j - \nu) = \eta_j^{(\prime)\beta} (-i\gamma^5 \gamma^6) P_j^{\text{vec}} \Psi_{\mathbf{11}}^{(\prime)\beta}(x, y_j + y, \nu_j + \nu), \quad (6.23)$$

where the η parity assignments are $\eta_{0,1}^\beta = -\eta_{2,3}^\beta = -1$ for $\Psi_{\mathbf{11}}^\beta$, and similarly $\eta_{0,1}^{\prime\beta} = -\eta_{2,3}^{\prime\beta} = -1$ for $\Psi_{\mathbf{11}}^{\prime\beta}$. Under $SO(10)$, the $SO(11)$ vector representation $\mathbf{11}$ decomposes as

$$\mathbf{11} \stackrel{SO(10)}{\sim} \mathbf{10} \oplus \mathbf{1}. \quad (6.24)$$

Note that these fields are introduced to ensure that the mass degeneracy between the various fermionic fields arising from the GUT structure is lifted (which will be achieved via brane interactions between the 6D bulk fields and brane confined 5D fields), along with ensuring the 6D anomaly cancellation.

6.3.2 5D Fields

In addition to the 6D bulk fields we have 5D fields, which are confined on the 5D UV brane at $y = 0$. First off, we have the $SO(11)$ scalar $\Phi_{\mathbf{32}}(x, \nu)$ in the $\mathbf{32}$ spinorial representation, which transforms only under $P_{0,2}^{\text{sp}}$, since it is confined on the UV brane on which the parity assignment associated with the GUT direction acts on. The form of the transformation is

$$\Phi_{\mathbf{32}}(x, \nu_j - \nu) = \eta_j P_j^{\text{sp}} \Phi_{\mathbf{32}}(x, \nu_j + \nu), \quad (6.25)$$

where the η assignments are $\eta_0 = -\eta_2 = -1$.

Note that the role of the $\Phi_{\mathbf{32}}$ field is to introduce the $SO(11) \rightarrow SU(5)$ breaking on the UV brane by developing a non-trivial VEV along the $SU(5)$ direction. This in turn will reduce $G_{\text{PS}} \rightarrow G_{\text{SM}}$ on the IR brane via the introduction of effective Dirichlet boundaries. We will review this in further detail in a following section.

Finally, we have the $SO(11)$ brane symplectic Majorana fermions $\chi_{\mathbf{1}}^\beta(x, \nu)$, where $\beta = 1, 2, 3$ is a generational index. The fields transform under the aforementioned boundary conditions as

$$\chi_{\mathbf{1}}^\beta(x, \nu_j - \nu) = (-i\gamma^5\gamma^6)\chi_{\mathbf{1}}^\beta(x, \nu_j + \nu). \quad (6.26)$$

In addition $\chi_{\mathbf{1}}^\beta$ satisfy the 5D symplectic Majorana condition $\chi^C = \tilde{\chi}, \tilde{\chi} \equiv i\bar{\gamma}\chi$ where $\bar{\gamma} \equiv \gamma_{4D}^5\gamma^6$.

Note that the purpose of $\chi_{\mathbf{1}}^\beta$ is to implement the extra dimensional see-saw mechanism presented in [117].

6.4 Parity Assignments

In the following section we review the field parity assignments relevant for our analysis. For a complete listing of the fields' parity assignments see Tabs.1-4 in Ref. [116]. Out of them we mention the component decomposition under G_{PS} that have 0 modes related to the 6th dimension and/or the 5th.

6.4.1 Gauge Fields

The boundary conditions are chosen such that $(P_0, P_2) = (P_1, P_3)$, and the translational parity assignments $U_{5,6}$ are defined by the consistency conditions as

$$U_5 = P_1 P_0 = P_3 P_2 = P_0^2 = \mathbb{1}, \quad \text{and} \quad U_6 = P_2 P_0 = P_3 P_1. \quad (6.27)$$

Since $U_5 = 1$ is trivial, the 0 modes along the 5th dimension are fully specified by the P_0, P_2 parity assignments, where the eigenvalues correspond to either von Neumann (N) or Dirichlet (D) boundary conditions. For the 6th dimension, since $U_6 = P_2 P_0$ we can check if a component has 0 modes by inspecting if the product U_6 is even or odd.

E.g. suppose we have a set fields that we attribute the following assignments $(+, +), (-, +), (-, -)$ under $(P_0, P_2) = (P_1, P_3)$. Then:

- $(+, +)$ has 0 modes in both directions since both parity assignments are $(+)$.
- $(-, +)$ doesn't have a 0 mode along the 6th dimension since $P_2 P_0 = P_3 P_1 = (-) \times (+) = (-)$, and does not have a 0 mode along the 5th dimension since it has mixed boundary conditions $(P_0, P_2) = (P_1, P_3) \sim D, N$.
- $(-, -)$ has 0 modes along the 6th dimension since $P_2 P_0 = P_3 P_1 = (-) \times (-) = (+)$ but does not have any along the 5th dimension since it has Dirichlet boundary conditions $(P_0, P_2) = (P_1, P_3) \sim D, D$.

Under the boundary conditions specified in Sec. 6.2, the following gauge fields have 0 modes along the 5th and 6th dimensions. Note that this is in the absence of brane mass terms. The final towers are fully determined after Φ_{32} acquires a VEV and causes $SO(11) \rightarrow SU(5)$ symmetry breaking on the UV brane. We list the gauge fields in terms of their x^μ, y, ν components, that arise from the various gauge decompositions originating from the original $SO(11)$ gauge bosons.

- A_μ components: Under $G_{PS} = SU(4)_C \times SU(2)_L \times SU(2)_R$, the following decompositions have 0 modes:

$$(\mathbf{1}, \mathbf{3}, \mathbf{1}), \quad (\mathbf{1}, \mathbf{1}, \mathbf{3}), \quad (\mathbf{15}, \mathbf{1}, \mathbf{1}). \quad (6.28)$$

Note that in the original paper the authors have chosen to label G_{PS} as $SU(2)_L \times SU(2)_R \times SU(4)_C$, which under our convention translates as the right-permutation of the original notation.

- A_y components: Under G_{PS} , the following components have 0 modes:

$$(\mathbf{1}, \mathbf{2}, \mathbf{2}). \quad (6.29)$$

The above is identified as the Higgs that results from the Hosotani mechanism. It is responsible for the $G_{SM} \rightarrow SU(3)_C \times U(1)_{EM}$ EW symmetry

breaking. Within the Hosotani breaking mechanism, the Higgs corresponds to the Wilson line phase in the extra dimension which has its gauge symmetry determined by the coset $(SO(11)/G_{\text{PS}}) \sim (SO(5)/SO(4))$. The $(\mathbf{1}, \mathbf{2}, \mathbf{2})$ representation transforms under the coset symmetry as a $SU(2)$ isodoublet. Note that throughout this report we refer to the warped component as either A_y or A_z , where the latter corresponds to the conformal coordinate notation.

- A_ν components: Under G_{PS} , the $(\mathbf{1}, \mathbf{2}, \mathbf{2})$ field has 0 modes for both the 6th and 5th dimension. Note that even though this is identical to the A_y component in terms of the gauge group behaviour, it gains a large mass correction from its coupling to the brane VEV $\langle \Phi_{\mathbf{32}} \rangle$. This in turn gives the A_ν components masses of order $\mathcal{O}(M_{\text{GUT}})$, leaving only the A_y field to be identified as the Higgs.

6.4.2 Spinor Fields

Moving on to the spinor fields. Under $\eta_j^\alpha \bar{\gamma} P_j^{\text{sp}}$, for $\alpha = 1, 2, 3, 4$ and $j = 0, 1, 2, 3$ the spinor fields have a set of parity assignments dictated by

$$\begin{pmatrix} P_2^{\text{sp}} & P_3^{\text{sp}} \\ P_0^{\text{sp}} & P_1^{\text{sp}} \end{pmatrix}, \quad (6.30)$$

where the matrix placement is just a choice in notation and has no intrinsic structure or symmetry. The transformation laws under \mathbb{Z}_2 are determined by the values of η_j^α along with $(P_0^{\text{sp}}, P_2^{\text{sp}}) = (P_1^{\text{sp}}, P_3^{\text{sp}})$. These discriminate between $\alpha = 1, 2, 3$ and $\alpha = 4$, giving the \tilde{P}_j “effective projections”

$$\text{For } \alpha = 1, 2, 3 \quad \begin{pmatrix} \tilde{P}_2 & \tilde{P}_2 \\ \tilde{P}_0 & \tilde{P}_0 \end{pmatrix} \quad \text{where } \tilde{P}_2 = \eta_j^\alpha \bar{\gamma} P_2 \quad \tilde{P}_0 = \eta_j^\alpha \bar{\gamma} P_0, \quad (6.31)$$

$$\text{For } \alpha = 4 \quad \begin{pmatrix} \tilde{P}_2 & -\tilde{P}_2 \\ \tilde{P}_0 & -\tilde{P}_0 \end{pmatrix} \quad \text{where } \tilde{P}_2 = \eta_0^4 \bar{\gamma} P_2 \quad \tilde{P}_0 = \eta_0^4 \bar{\gamma} P_0. \quad (6.32)$$

Since the combination of P_i ’s reduce the $SO(11)$ down to G_{PS} on the IR brane, the ± 1 parity assignments determine the G_{PS} spinorial decomposition, which will in turn provide the parity assignment for the fields under the G_{SM} decomposition.

E.g. for the $\gamma(+)$ assignment, the decomposition of $\Psi_{\mathbf{32}}$ Dirac spinor under $SO(11) \rightarrow SO(10) \rightarrow G_{\text{PS}} \rightarrow G_{\text{SM}}$ breaking chain follows

$$\begin{aligned}
\mathbf{32}_D \rightarrow \begin{pmatrix} \mathbf{16}_D \\ \overline{\mathbf{16}}_D \end{pmatrix} \xrightarrow{\gamma^{(+)}_{\sim}} \begin{pmatrix} \mathbf{16}_L \\ \mathbf{16}_R \\ 0 \\ 0 \end{pmatrix} \rightarrow \begin{pmatrix} \begin{pmatrix} (\mathbf{4}, \mathbf{2}, 1)_L \\ \oplus \\ (\overline{\mathbf{4}}, 1, \mathbf{2})_L \end{pmatrix} \\ \begin{pmatrix} (\overline{\mathbf{4}}, \mathbf{2}, 1)_R \\ \oplus \\ (\mathbf{4}, 1, \mathbf{2})_R \end{pmatrix} \\ 0 \\ 0 \end{pmatrix} \rightarrow \begin{pmatrix} \begin{pmatrix} (1, \mathbf{2}, -\frac{1}{2}) = \begin{pmatrix} \nu \\ e \end{pmatrix}_L \\ \oplus \\ (\mathbf{3}, \mathbf{2}, \frac{1}{6}) = \begin{pmatrix} u \\ d \end{pmatrix}_L \end{pmatrix} \\ \begin{pmatrix} (\overline{\mathbf{3}}, 1, \frac{1}{3}) \\ \oplus \\ (\overline{\mathbf{3}}, 1, -\frac{2}{3}) \end{pmatrix} = \begin{pmatrix} \hat{d} \\ \hat{u} \end{pmatrix}_L \\ \begin{pmatrix} (1, 1, 1) \\ \oplus \\ (1, 1, 0) \end{pmatrix} = \begin{pmatrix} \hat{e} \\ \hat{\nu} \end{pmatrix}_L \\ \vdots \end{pmatrix} \quad (6.33)
\end{aligned}$$

Following the above chain, by inspecting how the $\eta_j^\alpha \bar{\gamma} P_j^{\text{sp}}$ act on the Pati-Salam subspace, we get the same parity assignment for the SM subspace as the Pati-Salam states. E.g. in the above $(\mathbf{4}, \mathbf{2}, 1)_L$ has a (+)ve assignment under P_0, P_1, P_2, P_3 , which implies $\begin{pmatrix} \nu \\ e \end{pmatrix}_L, \begin{pmatrix} u \\ d \end{pmatrix}_L$ have (+)ve assignments under P_0, P_1, P_2, P_3 . Similarly, $(\overline{\mathbf{4}}, 1, \mathbf{2})_L$ has a (-)ve assignment under P_0, P_1 , and a (+)ve assignment under P_2, P_3 which implies $\begin{pmatrix} \hat{d} \\ \hat{u} \end{pmatrix}_L, \begin{pmatrix} \hat{e} \\ \hat{\nu} \end{pmatrix}_L$ have (-) under P_0, P_1 , and (+) under P_2, P_3 .

Note that the RH spinors have the opposite assignments to the ones assigned to the LH spinors, since ∂_5, ∂_6 transform as $-\partial_5, -\partial_6$ under the corresponding parity transforms (see Chap. 5).

To check if a decomposition has 0 modes along either the 5th or the 6th dimension we employ a similar method that we used to determine the gauge field decompositions. We have an additional complexity arising from the addition of the η 's, where we have to check for the y direction by multiplying the effective parity assignments instead of the raw assignments, since they no longer trivially commute.

E.g. suppose we have a set of fields which have the “effective” assignments $\begin{pmatrix} + & + \\ + & + \end{pmatrix}, \begin{pmatrix} - & - \\ - & - \end{pmatrix}, \begin{pmatrix} + & + \\ - & - \end{pmatrix}$ and $\begin{pmatrix} - & + \\ - & + \end{pmatrix}$, then:

- $\begin{pmatrix} + & + \\ + & + \end{pmatrix}$ has 0 modes along the 5th dimension, and the 6th.
- $\begin{pmatrix} - & - \\ - & - \end{pmatrix}$ has 0 modes along the 6th dimension, and does not have 0 modes along the 5th dimension since it has Dirichlet boundary conditions.
- $\begin{pmatrix} + & + \\ - & - \end{pmatrix}$ has 0 modes along the 5th dimension since $(+) \cdot (+) = (-) \cdot (-) = (+)$, and does not have 0 modes along the 6th dimension since $(+) \cdot (-) = (-) \cdot (+) = (-)$.
- $\begin{pmatrix} - & + \\ - & + \end{pmatrix}$ does not have 0 modes along the 5th dimension since $(-) \cdot (+) = (-) \cdot (+) = (-)$, but has 0 modes along the 6th dimension since $(-) \cdot (-) = (+) \cdot (+) = (+)$.

Under the aforementioned boundary conditions the following G_{PS} components have 0 modes along both the 5th and 6th dimensions (a priori to the brane interactions) that originate from the Ψ_{32}^α fields

$$(\mathbf{4}, \mathbf{2}, 1)_{L,R}, \quad (\mathbf{4}, 1, \mathbf{2})_{L,R}, \quad (6.34)$$

where for $\alpha = 1, 2, 3$.

Similarly, the following components have 0 modes along the 6th dimension but not along the 5th (i.e. $\text{mass} \sim \mathcal{O}(m_{\text{KK}_5})$)

$$(\mathbf{4}, \mathbf{2}, 1)_{L,R}, \quad (\mathbf{4}, 1, \mathbf{2})_{L,R}, \quad (6.35)$$

where the above are all contained in Ψ_{32}^4 .

6.4.3 Vector Fields

The $\Psi_{11}^\beta, \Psi_{11}'^\beta$ Dirac vector fermions have the parity assignments $\eta_j^\beta \bar{\gamma} P_j^{\text{vec}}$, and $\eta_j'^\beta \bar{\gamma} P_j^{\text{vec}}$. Again we have the effective projections \tilde{P}_j defined via $P_0^{\text{vec}} = P_1^{\text{vec}}, P_2^{\text{vec}} = P_3^{\text{vec}}$ and the η assignments,

$$\text{For } \Psi_{11}^\beta, \beta = 1, 2, 3 \quad (\tilde{P}_0, \tilde{P}_2) \quad \text{where } \tilde{P}_0 = \eta_0^\beta \bar{\gamma} P_0^{\text{vec}}, \quad \tilde{P}_2 = \eta_2^\beta \bar{\gamma} P_2^{\text{vec}}, \quad (6.36)$$

$$\text{For } \Psi_{11}'^\beta, \beta = 1, 2, 3 \quad (\tilde{P}_0', \tilde{P}_2') \quad \text{where } \tilde{P}_0' = \eta_0'^\beta \bar{\gamma} P_0^{\text{vec}}, \quad \tilde{P}_2' = \eta_2'^\beta \bar{\gamma} P_2^{\text{vec}}. \quad (6.37)$$

Completely analogous to the spinorial case the right handed assignments have the signs flipped, and if we wanted to check which decomposition has 0 modes along the 5th and/or 6th dimension, we perform the same check as with the gauge fields.

Under the aforementioned boundary conditions the following G_{PS} components of $\Psi_{11}^\beta, \Psi'_{11}^\beta$ have 0 modes along the 5th and 6th dimensions (a priori to brane interactions):

$$(\mathbf{6}, 1, 1)_R^{(+)}, \quad (\mathbf{6}, 1, 1)_L^{(-)} \subset \Psi_{11}^\beta, \quad (6.38)$$

$$(1, \mathbf{2}, \mathbf{2})_L^{(+)}, \quad (1, \mathbf{2}, \mathbf{2})_R^{(-)}, \quad (1, 1, 1)_R^{(+)}, \quad (1, 1, 1)_L^{(-)} \subset \Psi'_{11}^\beta. \quad (6.39)$$

Note that the \pm sign in the headers of the parity tables refer to the $\gamma(\pm)$ eigenmodes.

6.5 Lagrangians

The matter fields interact via a set of bulk and brane Lagrangians. In the following section we review the structure of the theory and highlight the relevant interactions.

6.5.1 Bulk Lagrangian

We start off with the gauge sector, which has the usual form for a Yang-Mills theory, accompanied by a gauge fixing term and a ghost Lagrangian

$$S_{\text{Bulk}}^{\text{Gauge}} = \int d^6x \sqrt{-\det G} \left\{ -\text{Tr} \left(\frac{1}{4} F^{MN} F_{MN} + \frac{1}{2\xi} (f_{\text{gf}})^2 + \mathcal{L}_{\text{ghost}} \right) \right\}, \quad (6.40)$$

where $\sqrt{-\det G} = \frac{1}{kz^6}$ is expressed in terms of the conformal coordinate $z = e^{ky}$, where $M, N = \{0, 1, 2, 3, 5, 6\}$, and $F_{MN} \equiv \partial_M A_N - \partial_N A_M - ig[A_M, A_N]$.

Using the background gauge method, the gauge field A_M is split into a classical and a quantum component as $A_M = A_M^c + A_M^q$ which are used to compute the effective potential for the Wilson line phases. In addition, in line with the authors in [116], we use the following gauge fixing and ghost terms

$$f_{\text{gf}} = z^2 \left(\eta^{\mu\nu} \mathcal{D}_\mu^c A_\nu^q + \mathcal{D}_6^c A_6^q + \xi k^2 z^2 \mathcal{D}_z^c \left(\frac{A_z^q}{z^2} \right) \right), \quad (6.41)$$

$$\mathcal{L}_{\text{gf}} = \bar{c} \left(\eta^{\mu\nu} \mathcal{D}_\mu^c \mathcal{D}_\nu^{c+q} + \mathcal{D}_6^c \mathcal{D}_6^{c+q} + \xi k^2 z_L^2 \mathcal{D}_z^c \frac{1}{z^2} \mathcal{D}_z^{c+q} \right) c. \quad (6.42)$$

ξ is the gauge fixing parameter, $\eta^{\mu\nu} = \text{diag}(-1, 1, 1, 1)$ is the 4D Minkowski metric and we have defined

$$\begin{aligned} \mathcal{D}_M^c B &= \partial_M B - ig[A_M^c, B], \\ \mathcal{D}_M^{c+q} B &= \partial_M B - ig[A_M, B], \end{aligned} \quad \text{where} \quad B \in \left\{ A_\mu^q, \frac{1}{z^2} A_z^q, A_6^q, c \right\}. \quad (6.43)$$

Moving on to the fermionic fields, the general action for a 6D Dirac fermion is given by

$$S = \int d^6x \sqrt{-\det G} \bar{\Psi} [\mathcal{D}(c)_M + ick\gamma^6] \Psi, \quad (6.44)$$

where the covariant derivative is dependent on the vielbeins e_a^M , the spin connection ω_{Mbc} , and the bulk mass parameter c , and has the explicit form

$$\mathcal{D}(c) = \gamma^a e_a^M \left(\partial_M + \frac{1}{8} \omega_{Mbc} [\gamma^b, \gamma^c] - igA_M \right) - c\sigma'(y). \quad (6.45)$$

Plugging in the fermionic fields $\Psi_{32}^\alpha(x, y, \nu)$, $\Psi_{11}^\beta(x, y, \nu)$ and $\Psi_{11}'^\beta(x, y, \nu)$ we have the resulting action

$$S_{\text{Bulk}}^{\text{Ferm}} = \int d^6x \sqrt{-\det G} \left\{ \sum_{\alpha=1}^4 \bar{\Psi}_{32}^\alpha \mathcal{D}(c_{\Psi_{32}^\alpha}) \Psi_{32}^\alpha + \sum_{\beta=1}^3 \bar{\Psi}_{11}^\beta \mathcal{D}(c_{\Psi_{11}^\beta}) \Psi_{11}^\beta + \sum_{\beta=1}^3 \bar{\Psi}_{11}'^\beta \mathcal{D}(c_{\Psi_{11}'^\beta}) \Psi_{11}'^\beta \right\}, \quad (6.46)$$

where we've introduced the bulk mass parameters $c_{\Psi_{32}^\alpha}$, $c_{\Psi_{11}^\beta}$, $c_{\Psi_{11}'^\beta}$ corresponding to the Dirac fermions in their respective representation along with the generational index. Using the explicit form of the vielbeins, the covariant derivative becomes

$$\mathcal{D}(c) = z \left(\gamma^\mu D_\mu + \gamma^6 D_6 - \frac{5}{2z} \sigma' \gamma^5 + \sigma' \gamma^5 D_z + i \frac{c}{z} \sigma' \gamma^6 \right). \quad (6.47)$$

To more conveniently discuss the fermion mass spectra, we redefine our fields to absorb powers of z as

$$\check{\Psi} \equiv \frac{1}{z^{5/2}} \Psi. \quad (6.48)$$

Plugging in the explicit form of $\sqrt{-\det G}$, along with the above field redefinition and the explicit form of the covariant derivative from Eqn. (6.47) into Eqn. (6.46) gives the simplified version of the fermion action

$$S_{\text{Bulk}}^{\text{Ferm}} = \int d^4x \int_0^{2\pi R_6} d\nu \int_1^{z_L} \frac{dz}{k} \left[\bar{\check{\Psi}}_{32}^\alpha \left(\gamma^\mu D_\mu + \gamma^6 D_6 + \sigma' \gamma^5 D_z + i \frac{c_{\Psi_{32}^\alpha}}{z} \sigma' \gamma^6 \right) \check{\Psi}_{32}^\alpha + \bar{\check{\Psi}}_{11}^\beta \left(\gamma^\mu D_\mu + \gamma^6 D_6 + \sigma' \gamma^5 D_z + i \frac{c_{\Psi_{11}^\beta}}{z} \sigma' \gamma^6 \right) \check{\Psi}_{11}^\beta + \bar{\check{\Psi}}_{11}'^\beta \left(\gamma^\mu D_\mu + \gamma^6 D_6 + \sigma' \gamma^5 D_z + i \frac{c_{\Psi_{11}'^\beta}}{z} \sigma' \gamma^6 \right) \check{\Psi}_{11}'^\beta \right]. \quad (6.49)$$

6.5.2 Brane Lagrangians

The physical symmetry of the low energy theory on the IR brane is shaped by the parity assignments, along with the Planck brane interactions between the $\Phi_{\mathbf{32}}$ scalar field and the bulk gauge bosons which in turn affect the various mode decompositions. In addition we have the interactions between the brane symplectic Majorana fermions that aim to recreate the neutrino spectrum. To this extent we now review the UV brane actions, which either consists of couplings between the 5D fields or between 5D and 6D fields.

First off, we have the action of the 5D spinor scalar $\Phi_{\mathbf{32}}(x, \nu)$ which is confined to the 5D UV brane. Since the UV brane possesses a manifest $SO(11)$ invariance, the action for $\Phi_{\mathbf{32}}(x, \nu)$ consists of the usual Higgs-like scalar potential

$$S_{\text{Scalar}}^{\text{Brane}} = \int d^6x \delta(y) \left\{ -(D_\mu \Phi_{\mathbf{32}})^\dagger (D^\mu \Phi_{\mathbf{32}}) - (D_\nu \Phi_{\mathbf{32}})^\dagger (D^\nu \Phi_{\mathbf{32}}) - \lambda (\Phi_{\mathbf{32}}^\dagger \Phi_{\mathbf{32}} - |w|^2)^2 \right\}, \quad (6.50)$$

where $|w|$ is the quartic coupling strength, and λ is the quadratic coupling strength.

We want to break the $SO(11)$ gauge symmetry down to $SU(5)$ such that we induce 'effective Dirichlet' boundary conditions for bulk fields. This has the consequence of preventing the fields that transform under the broken set of generators from having 0 modes on the IR brane. The physical symmetry on the IR brane will be dictated by the generators contained in both $SU(5)$ and G_{PS} , i.e. $SU(5) \cap G_{\text{PS}} = G_{\text{SM}}$. Note that this is valid in the pre-Hosotani breaking phase.

To this extent one can break $SO(10) \rightarrow SU(5)$ via $\mathbf{1}_{+5} \sim SU(5) \times U(1)_Z$ which is contained in $(\bar{\mathbf{4}}, \mathbf{1}, \mathbf{2}) \sim G_{\text{PS}}$. This in turn is contained in $\mathbf{16} \sim SO(10)$ which finally, is contained in $\mathbf{32} \sim SO(11)$. This has a spinorial decomposition under $SO(10)$ that goes as $\mathbf{32} \rightarrow \mathbf{16} \oplus \bar{\mathbf{16}}$. To this extent the VEV structure of the $\Phi_{\mathbf{32}}(x, \nu)$ Higgs mechanism is

$$\langle \Phi_{\mathbf{32}} \rangle = \begin{pmatrix} \langle \Phi_{\mathbf{16}} \rangle \\ \langle \Phi_{\bar{\mathbf{16}}} \rangle \end{pmatrix}, \quad \langle \Phi_{\mathbf{16}} \rangle = \begin{pmatrix} 0_4 \\ 0_4 \\ \nu_4 \\ 0_4 \end{pmatrix}, \quad \nu_4 = \begin{pmatrix} 0 \\ 0 \\ 0 \\ w \end{pmatrix}, \quad \text{and} \quad \langle \Phi_{\bar{\mathbf{16}}} \rangle = 0. \quad (6.51)$$

Since we are working with a complex Higgs field, we want to introduce couplings between the scalar field and the bulk fermions, which also will entail couplings involving the conjugate representation of Φ . These entail couplings of the form

$(\Gamma^a \xi_a)^*$, where ξ_a stands for a field in a generic spinorial representation, and Γ^a is the matrix representation of the $SO(11)$ Clifford algebra $\{\Gamma^a, \Gamma^b\} = 2\delta^{ab}\mathbb{1}_{32}$. Regarding the Clifford algebra, we note that we can define the conjugate Gamma matrices, and the R matrix as

$$(\Gamma^a)^* = (-1)^{a+1}\Gamma^a = -R\Gamma^a R, \quad (6.52)$$

$$R = \Gamma^2 \Gamma^4 \Gamma^6 \Gamma^8 \Gamma^{10} = -\sigma_2 \otimes \sigma_3 \otimes \sigma_2 \otimes \sigma_3 \otimes \sigma_2 \equiv -\hat{R} \otimes \sigma_2. \quad (6.53)$$

To this extent we introduce the ‘ R transformed’ spinor scalar field $\tilde{\Phi}_{\mathbf{32}}$:

$$\tilde{\Phi}_{\mathbf{32}} \equiv iR\Phi_{\mathbf{32}}^* = \begin{pmatrix} -\hat{R}\Phi_{\mathbf{16}}^* \\ \hat{R}\Phi_{\mathbf{16}}^* \end{pmatrix}, \quad (6.54)$$

which in turn has the VEV structure

$$\hat{R}\langle\tilde{\Phi}_{\mathbf{16}}\rangle = \begin{pmatrix} 0_4 \\ 0_4 \\ 0_4 \\ \tilde{\nu}_4 \end{pmatrix}, \quad \tilde{\nu}_4 = \begin{pmatrix} 0 \\ 0 \\ w^* \\ 0 \end{pmatrix} \quad \text{and} \quad \hat{R}\langle\Phi_{\mathbf{16}}^*\rangle = 0. \quad (6.55)$$

On the same 5D brane, we have the brane symplectic Majorana fermions $\chi_1^\beta(x, \nu)$, $\beta = \{1, 2, 3\}$, which are introduced to produce the 6D seesaw mechanism [117]. Their self interaction is given as

$$S_{\text{Majorana}}^{\text{brane}} = \int d^6x \delta(y) \left\{ \frac{1}{2} \bar{\chi}_1^\beta (\gamma^\mu \partial_\mu + \gamma^6 \partial_\nu) \chi_1^\beta - \frac{1}{2} M^{\beta\beta'} \bar{\chi}_1^\beta \chi_1^{\beta'} \right\}, \quad (6.56)$$

where $M^{\beta\beta'}$ is a constant matrix.

Finally, we have the Lagrangians that specify the coupling between the bulk 6D fermions and the 5D fields on the $SO(11)$ brane which as previously mentioned, induce the effective Dirichlet boundary conditions, and lift the mass degeneracy of the quark and lepton sector on the IR brane. To this extent, the action consists of

$$S_{\Psi\Phi\chi}^{\text{brane}} = \int d^6x \sqrt{-\det G} \cdot \delta(y) \left\{ \sum_{i=1}^8 \mathcal{L}_i \right\}, \quad (6.57)$$

which contains all the allowed couplings between $\Phi_{\mathbf{32}}$, $\Psi_{\mathbf{32}}$, $\Psi_{\mathbf{11}}$ which are consistent with gauge symmetry, parity assignments and keeping the action dimensionless. We will now list the interactions.

For $i = \{3, 6\}$ we have vector-vector interactions of the form

$$\mathcal{L}_i = -2\xi_i^{\beta\beta'} (\bar{\Psi}_{\mathbf{11}}^i)^\beta (\Psi_{\mathbf{11}}^i)^{\beta'}, \quad (6.58)$$

where $\xi_i^{\beta\beta'} = \{\mu_{11}^{\beta\beta'}, \mu_{11}'^{\beta\beta'}\}$ are dimensionless couplings, and $\Psi_{11}^i = \{\Psi_{11}, \Psi_{11}'\}$.

Next up, for $i = \{1, 2, 4, 5\}$ up we have spinor - scalar - vector interactions of the form

$$\mathcal{L}_i = -\zeta_i^{\alpha\beta} (\overline{\Psi_{32}^i})^\alpha \Gamma^a \Phi_{32}^i (\Psi_{11}^i)_a^\beta - (\zeta_i^{\alpha\beta})^* (\overline{\Psi_{11}^i})^\beta (\Phi_{32}^i)^\dagger \Gamma^a (\Psi_{32}^i)^\alpha, \quad (6.59)$$

where $\zeta_i^{\alpha\beta} = \{\kappa^{\alpha\beta}, \tilde{\kappa}^{\alpha\beta}, \kappa'^{\alpha\beta}, \tilde{\kappa}'^{\alpha\beta}\}$ are couplings with mass dimension M^{-1} , $\Psi_{11}^i = \{\Psi_{11}, \Psi_{11}', \Psi_{11}'', \Psi_{11}'''\}$, $\Psi_{32}^i = \{\Psi_{32}, \Psi_{32}', \Psi_{32}'', \Psi_{32}'''\}$, $\Phi_{32}^i = \{\Phi_{32}, \tilde{\Phi}_{32}, \Phi_{32}', \tilde{\Phi}_{32}'\}$. The i index specifies the field from each set, e.g. for $i = 1$ we have the term $\kappa^{\alpha\beta} (\overline{\Psi_{32}})^\alpha \Gamma^a \Phi_{32} (\Psi_{11})_a^\beta$.

Finally for $i = \{7, 8\}$ we have the Majorana - scalar - spinor interactions

$$\mathcal{L}_i = -\iota^{\alpha\beta} \overline{\chi_1}^\beta (\Phi_{32}^i)^\dagger (\Psi_{32})^\alpha - (\iota_i^{\alpha\beta})^* (\overline{\Psi_{32}})^\alpha \Phi_{32}^i \chi_1^\beta, \quad (6.60)$$

where $\iota^{\alpha\beta} = \{\tilde{\kappa}_1^{\alpha\beta}, \kappa_1^{\alpha\beta}\}$ are couplings with mass dimension M^{-1} , and $\Phi_{32}^i = \{\tilde{\Phi}_{32}, \Phi_{32}\}$.

We have mentioned that these couplings are responsible for lifting the mass degeneracy which comes as a consequence of the gauge unification. The lifting is due to the couplings on the $SO(11)$ brane, which show up in the equations of motion via a $\delta(y)$ function which indicates their confinement to the brane. The brane interactions affect the boundary conditions at $y = 0$, which in turn show up in the mass equations that determine the effective masses of the 0 mode in the twisted gauge (will be covered in the Higgs section).

We now move on to describing the full symmetry breaking mechanism along with how the VEV $\langle \Phi_{32} \rangle$ changes the physical spectrum on the IR brane by inducing large masses to the components of $SO(11)/SU(5)$.

6.6 Symmetry Breaking

The model's symmetry breaking consists of 3 stages which act to break $SO(11)$ down to $SU(3)_C \times U(1)_{EM}$ on the IR brane. They act in the following order:

- 1) Symmetry breaking via orbifold parity assignments, which reduces the $SO(11)$ gauge symmetry to G_{PS} on the IR brane.
- 2) Symmetry breaking via 5D brane interactions between the bulk gauge fields and $\langle \Phi_{32} \rangle$, which reduce the $SO(11)$ symmetry down to $SU(5)$ on the UV

brane. This in turn alters boundary conditions from von Neumann to effective Dirichlet which restricts the 0 mode spectrum on the IR brane to the intersection $SU(5) \cap G_{\text{PS}} = G_{\text{SM}}$.

- 3) Hosotani breaking which acts as the electroweak symmetry breaking mechanism, reducing G_{SM} down to $SU(3)_C \times U(1)_{\text{EM}}$.

6.6.1 Orbifold Breaking

As previously mentioned in Sec. 6.2, we have two parity assignments, which break the $SO(11)$ gauge symmetry down to two subgroups (corresponding to the maximal subalgebras) as

$$P_0 = P_1 \quad \text{break} \quad SO(11) \rightarrow SO(10), \quad (6.61)$$

$$P_2 = P_3 \quad \text{break} \quad SO(11) \rightarrow SO(7) \times SO(4). \quad (6.62)$$

The 5D brane at $y = 0$ possesses the intact full $SO(11)$ symmetry, where the brane at $y = L_5$ has its symmetry dictated by the intersection of the breaking assignments $SO(10) \cap SO(7) \times SO(4) = SO(6) \times SO(4) \simeq G_{\text{PS}}$ (in effect due to consistency conditions of the two translations). The Venn diagram of the common symmetry group generator intersections is presented in Fig. 6.3.

The unbroken generators lie within the blue shaded region in Fig. 6.3 and are fully determined by G_{PS} generators. The broken generators are contained in the white regions. These consist of

$$SO(11)/SO(10) = \left\{ \begin{array}{c} SO(11)/(SO(10) \cup (SO(7) \times SO(4))) \\ \oplus \\ SO(7) \times SO(4)/G_{\text{PS}} \end{array} \right\} \simeq \left\{ \begin{array}{c} SO(5)/SO(4) \\ \oplus \\ SO(7)/SO(6) \end{array} \right\}, \quad (6.63)$$

$$SO(10)/G_{\text{PS}}. \quad (6.64)$$

In terms of the G_{PS} components of the $SO(11)$ adjoint representation **55**, the parity assignments classify the components as either broken or unbroken as follows

$$\begin{aligned} \text{Broken:} \quad & (\mathbf{6}, 1, 1) \sim SO(7)/SO(6), \\ & (1, \mathbf{2}, \mathbf{2}) \sim SO(5)/SO(4), \\ & (\mathbf{6}, \mathbf{2}, \mathbf{2}) \sim SO(10)/G_{\text{PS}}, \end{aligned} \quad (6.65)$$

$$\text{Unbroken:} \quad (1, \mathbf{3}, 1) \oplus (1, 1, \mathbf{3}), \oplus (\mathbf{15}, 1, 1) \sim G_{\text{PS}}. \quad (6.66)$$

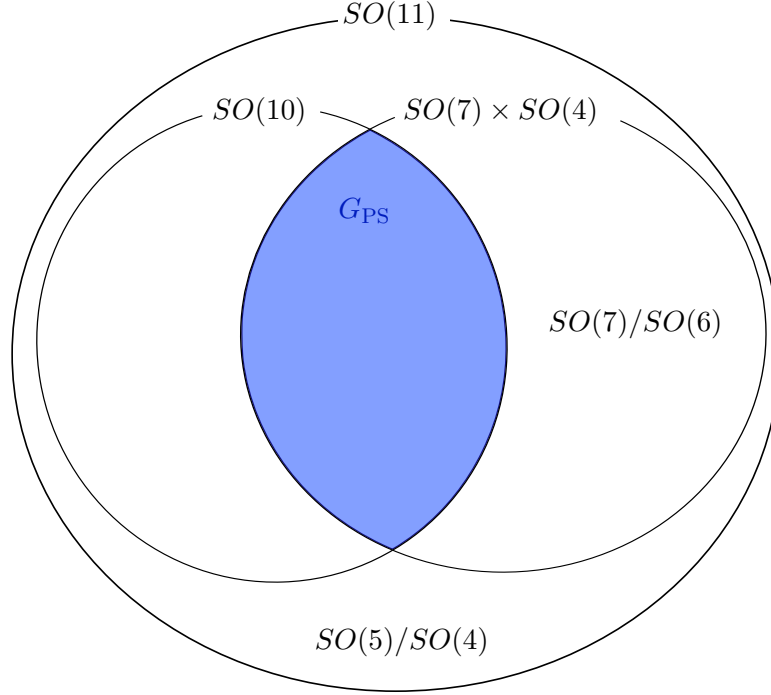


Figure 6.3: $SO(11)$ breaking diagram depicting the maximal subgroups $SO(10)$ and $SO(7) \times SO(4)$, their intersection $SO(10) \cap SO(7) \times SO(4) = SU(4)_C \times SU(2)_L \times SU(2)_R \equiv G_{PS}$ highlighted in blue, and the different cosets $SO(7)/SO(6)$, $SO(5)/SO(4)$ originating from the subgroup breaking.

The broken representations have parity assignments $(-, +), (-, -), (+, -)$ for the A_μ components whereas the unbroken ones have $(+, +)$. Note that the A_ν, A_y components have opposite signs with respect to their A_μ counterparts under the \mathbb{Z}_2 transformations.

6.6.2 Brane gauge breaking via $\langle \Phi_{32} \rangle$

The purpose of the second stage of symmetry breaking is to reduce the Pati-Salam symmetry down to the SM on the IR brane. This consists of introducing a Higgs mechanism on the 5D UV brane and giving the 5D scalar field $\Phi_{32}(x, \nu)$ a VEV along the $SU(5)$ direction, which in turn achieves the $SO(11) \rightarrow SU(5)$ breaking on the UV brane. The breaking induces heavy masses on the UV brane, effectively inducing Dirichlet boundary conditions for the $SO(11)/SU(5)$ bulk gauge bosons on the UV brane. This in turn affects the KK decomposition of the IR brane,

reducing the 0 mode spectrum to the intersection $SU(5) \cap G_{\text{SM}}$.

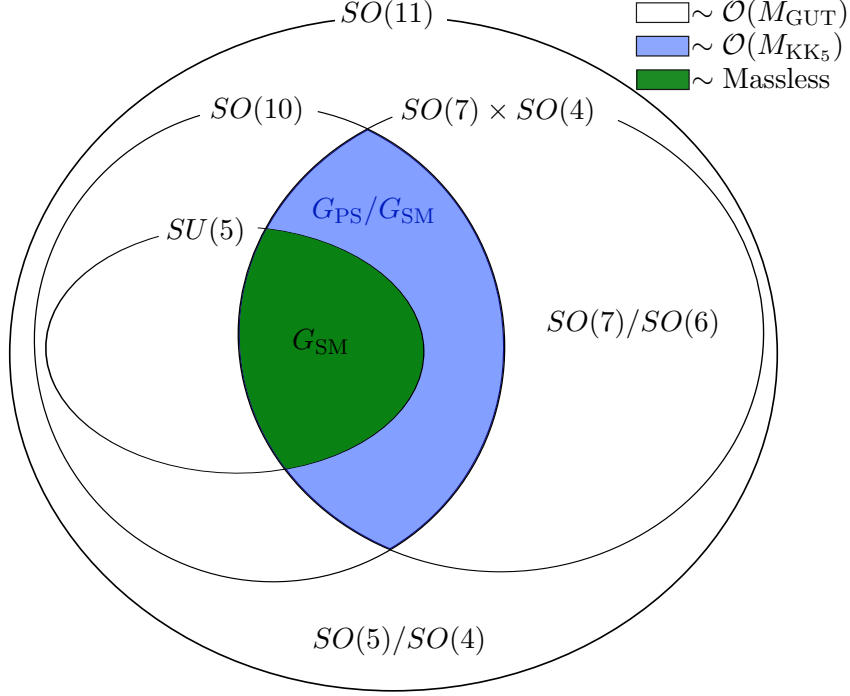


Figure 6.4: $SO(11)$ breaking diagram after the introduction of the $SU(5)$ UV brane breaking. Fields invariant under G_{SM} (represented as the green shaded region) have massless modes, those corresponding to the coset $G_{\text{PS}}/G_{\text{SM}}$ have masses of order $\mathcal{O}(M_{\text{KK}_5})$ (represented as the blue shaded region), and all the rest have masses of order $\mathcal{O}(M_{\text{GUT}})$ (represented as the white region).

We can express the parity assignments for the gauge fields A_M along the z coordinate in terms of von Neumann (N) and Dirichlet (D) boundary conditions, as

$$N : \quad \frac{\partial}{\partial z} A_\mu = \frac{\partial}{\partial z} \left(\frac{1}{z^2} A_z \right) = \frac{\partial}{\partial z} A_\nu = 0, \quad (6.67)$$

$$D : \quad A_\mu = A_z = A_\nu = 0, \quad (6.68)$$

which are valid at $z = 1, z = z_L$.

The VEV on the UV 5D brane induces mass terms of the form $|gA_\mu \langle \Phi_{\mathbf{32}} \rangle^2|$, and $|gA_\nu \langle \Phi_{\mathbf{32}} \rangle^2|$ along the $SU(5)$ direction which gives mass to all $SO(11)/SU(5)$ 5D gauge bosons, to the A_μ, A_ν components. Writing the bulk equation of motion for either of the gauge field components, we see that the breaking induces a $\delta(y)$

function weighted by the VEV component w of $\langle \Phi_{32} \rangle$

$$\left\{ \mathcal{D}(\mu, y, \nu) - \frac{g^2 w^2}{2} \delta(y) \right\} A_\mu - \left(1 - \frac{1}{\xi}\right) \partial_\mu (\partial^\nu A_\nu + \partial_\nu A_\nu) = \left(\sum \text{Interaction Terms} \right), \quad (6.69)$$

where $\mathcal{D}(\mu, y, \nu) = \partial_\mu \partial^\mu + e^{\sigma(y)} \frac{\partial}{\partial y} \left(e^{-3\sigma(y)} \frac{\partial}{\partial y} \right) + \frac{\partial^2}{\partial \nu^2}$.

Suppose we have an even parity assignment for some A_μ^a component,

$$A_\mu^a(x, -y, -\nu) = (+) A_\mu^a(x, y, \nu). \quad (6.70)$$

Under this parity assignment it follows that the ν component A_ν^a has odd parity, and $\partial^\nu A_\nu^a$ has even parity. With this in mind, we now want to find the A_μ^a component behaviour close to $y = 0$ (due to our introduction of the $\delta(y)$). This is done by integrating Eqn. (6.69) along dy from $[-\epsilon, \epsilon]$, and taking the limit $\epsilon \rightarrow 0$. This results in the new modified boundary condition at $y = 0$

$$\lim_{\epsilon \rightarrow 0} \frac{\partial A_\mu^a}{\partial y} \Big|_{y=\epsilon} = \frac{g^2 w^2}{4} A_\mu^a \Big|_{y=0}. \quad (6.71)$$

Equivalently in terms of the conformal coordinate, as we approach $z = 1$ from the positive direction, the above becomes

$$\left(\frac{\partial}{\partial z} - \mathbf{w} \right) A_\mu^a = 0 \Big|_{z=1^+}, \quad \mathbf{w} = \frac{g^2 w^2}{4k}. \quad (6.72)$$

Since the mass dimensions of g, w are $[g] = M^{-1}, [w] = M^{3/2}$, where g is a 6D gauge coupling, it implies in terms of natural scales that $g \sim \sqrt{R_6/k} \cdot g_{4D}$. Similarly w is the VEV of a 5D field confined on $\mathcal{M}_4 \times S^1$, with its scale being set as $w \sim 1/(R_6^{3/2})$. Therefore \mathbf{w} is dimensionless and is of order $\mathcal{O}((M_{\text{GUT}})^2/k^2)$. In the regime $M_{\text{GUT}} \gg k$, \mathbf{w} then acts as the infinite limit in which the above effectively recreates a Dirichlet condition [109, 120, 121].

Therefore, by introducing the VEV $\langle \Phi_{32} \rangle$ we have effectively modified the A_μ^a gauge field component from a von Neumann boundary condition to an effective Dirichlet condition (denoted as D_{eff}). As a consequence the corresponding gauge components, when projected to the 4D IR brane, no longer have a massless 0 mode but have a low lying mode dictated by the z coordinate of the order $\mathcal{O}(M_{\text{KK}_5})$.

In terms of the A_μ components that interest us, we have induced an effective breaking that gives masses of the order $\mathcal{O}(M_{\text{KK}_5})$ to fields with gauge components transforming under the coset $G_{\text{PS}}/G_{\text{SM}}$. After this process, the only gauge fields with allowed 0 modes for the μ components are those which are invariant under

G_{SM} (see Fig. 6.4 for a diagrammatic summary on the broken groups and their mass scales).

In terms of the A_ν components that interest us, we've given effective Dirichlet conditions to the fields invariant under $SO(5)/SO(4)$ which will no longer have a massless 0 mode along the z dimension. This in turn has the effect that the IR Higgs field will be fully identified as the A_z component arising from Hosotani breaking.

6.6.3 Hosotani EW Breaking

The last stage of symmetry breaking, consisting of $G_{\text{SM}} \rightarrow SU(3)_C \times U(1)_{\text{EM}}$, as reviewed in Chapter 1, is induced by the Hosotani mechanism [122–124], and more specifically by the A_z component $(1, \mathbf{2}, \mathbf{2}) \sim G_{\text{PS}}$. From the point of view of the gauge symmetry it behaves as the traditional Higgs $SU(2)_L$ iso-doublet since it possesses non-trivial quantum numbers under the Pati-Salam group [125]. Note that the A_ν component with the same quantum numbers does not factor in the Hosotani mechanism due to its different boundary conditions (see Tab. 5 in [116]) and due to the radiative corrections it receives.

The $A_z^{a,11} \in SO(5)/SO(4)$ components are physical degrees of freedom which cannot be gauged away. The full 6D KK expansion for $A_z^{a,11}$, $a = \{1, 2, 3, 4\}$ is that of a scalar field (see Ref. [112] for details) with $(+, +)$ boundary conditions

$$A_z^{a,11} = \frac{1}{\sqrt{2\pi R_6}} \left(u_H(z) \cdot \phi_H^{a(0)}(x) + \sum_{n=1}^{\infty} \phi_H^{a(n)} h_n^{(+,+)}(z) \right), \quad (6.73)$$

where $u_H(z) = \sqrt{\frac{3}{k(z_L^3 - 1)}} z^2$. $h_n^{(+,+)}(z)$ are the basis functions expressed in terms of Bessel functions (see Appendix A.2 in [116]), which obey the orthonormality conditions

$$\int_1^{z_L} dz \frac{k}{z} h_n(z) h_l(z) = \delta_{nl}. \quad (6.74)$$

$\phi_H^{a(0)}$ is identified as the EW Higgs doublet, where $\phi_H^{1,2,3(0)}$ are the degrees of freedom absorbed by the W^\pm, Z^0 bosons and $\phi_H^{4(0)}$ plays the role of the dynamical Higgs. The symmetry breaking is radiatively determined via the corresponding Wilson line's non-trivial effective potential $V_{\text{eff}}(\theta_H)$.

Using the residual gauge invariance on the brane we can now perform a gauge transformation that has the effect of inducing $\langle \theta_H \rangle = 0$. This in turn transforms the boundary conditions $P_i \rightarrow \tilde{P}_i$, which reflects the physical symmetry of the theory via the simultaneously commuting generators T^a and the modified boundary conditions \tilde{P}_i .

To this extent, we perform the gauge transform $\Omega(y)$ that has the effect of rotating the Wilson line phase θ_H expectation value to $\langle \theta_H \rangle \rightarrow 0$, along with inducing the new boundary conditions

$$P_i \rightarrow \Omega P_i \Omega^\dagger. \quad (6.75)$$

Ω is quantified as (see Ref. [115])

$$\Omega(y) = \exp \left[i \frac{g \theta_H f_H}{\sqrt{4\pi R_6}} \int_y^L dy \tilde{u}_H(y) T^{4,11} \right] = \exp \{ i \theta_H(z) T_{4,11} \}, \quad (6.76)$$

where $T_{4,11}$ is the corresponding $SO(11)$ generator, $\tilde{u}_H(y) = k z u_H(z)$, $f_H = \frac{\sqrt{6}}{g} \sqrt{\frac{2\pi R_6 k}{z_L^3 - 1}}$ and $\theta_H(z) = \theta_H \frac{z_L^3 - z^3}{z_L^3 - 1}$, for $z \in [1, z_L]$. We refer to this as the twisted gauge, under which the new boundary condition matrices become

$$\tilde{P}_j = \exp \{ 2\pi i \theta_H T^{4,11} \} P_j, \quad j = 0, 2, \quad (6.77)$$

$$\tilde{P}_k = P_k, \quad k = 0, 2. \quad (6.78)$$

Therefore, $\tilde{P}_{0,2} = \tilde{P}_{1,3}$ act nontrivially on the 4 – 11 subspace via the θ_H exponentiated matrix, where the boundary conditions for the vector subspace have the explicit form,

$$\tilde{P}_0^{\text{vec}} = \begin{cases} \begin{pmatrix} \cos \theta_H & -\sin \theta_H \\ -\sin \theta_H & -\cos \theta_H \end{pmatrix} & \text{acting on the 4-11 subspace} \\ \mathbb{1}_3 & \text{acting on the 1, 2, 3 subspace} \\ -\mathbb{1}_6 & \text{acting on the 5, ..., 10 subspace} \end{cases} \quad (6.79)$$

$$\tilde{P}_2^{\text{vec}} = \begin{cases} \begin{pmatrix} \cos \theta_H & -\sin \theta_H \\ -\sin \theta_H & -\cos \theta_H \end{pmatrix} & \text{acting on the 4-11 subspace} \\ \mathbb{1}_9 & \text{otherwise} \end{cases}. \quad (6.80)$$

Similarly, these are expressed in the spinorial representation as

$$\tilde{P}_0^{\text{sp}} = \begin{pmatrix} \pm \cos \frac{\theta_H}{2} & -i \sin \frac{\theta_H}{2} \\ i \sin \frac{\theta_H}{2} & \mp \cos \frac{\theta_H}{2} \end{pmatrix}, \quad \tilde{P}_2^{\text{sp}} = \begin{pmatrix} \cos \frac{\theta_H}{2} & \mp i \sin \frac{\theta_H}{2} \\ \pm i \sin \frac{\theta_H}{2} & -\cos \frac{\theta_H}{2} \end{pmatrix}, \quad \text{acting on } \begin{Bmatrix} \psi \\ \hat{\psi} \end{Bmatrix}, \quad (6.81)$$

where $\begin{pmatrix} \psi \\ \hat{\psi} \end{pmatrix}$ refers to the $SO(10)$ spinor decomposition **16** under G_{PS} , and the upper signs of $(\pm), (\mp)$ in the explicit forms act on the ψ components, where the lower signs act on $\hat{\psi}$.

6.7 EOMs, $V_{\text{eff}}(\theta_H)$ & the Parameter Space

The following section will review the relevant fields to our analysis (those that possess 6D $n = 0$ modes), along with highlighting some of the equations of motion to showcase how the UV brane dynamics impact the spectrum decomposition on the IR brane. We finish off by enumerating the relevant towers that contribute to the Higgs effective potential.

6.7.1 Boson Equations of Motion

We now review the equations of motion for some of the relevant G_{SM} towers, and how they relate to the post electroweak breaking $SU(3)_C \times U(1)_{\text{EM}}$ via the twisted gauge imposed via the Hosotani mechanism. Throughout this subsection we will only be looking at fields that have 6D $n = 0$ modes. To this extent we ignore the GUT coordinate y in their decomposition. For a full treatment we refer the reader to the original discussion in Ref. [116].

First off, the gauge fields A_M are expressed under the twisted gauge as,

$$\tilde{A}_M = \Omega(z) A_M \Omega^{-1}(z) + \frac{i}{g} \Omega(z) \partial_M \Omega^{-1}(z), \quad (6.82)$$

where $\Omega(z) = \exp(i\theta_H(z)T_{4,11})$. In essence the twisted gauge has the effect of mixing the $\{k, 4\}$ (for $k \neq 4$), $\{k, 11\}$ (for $k \neq 11$), and $\{4, 11\}$ subspaces, via the Wilson line phase θ_H as

$$\begin{cases} A_M^{k,4} = \cos \theta_H(z) \tilde{A}_M^{k,4} - \sin \theta_H(z) \tilde{A}_M^{k,11}, & \text{for } k \neq 4, 11 \\ A_M^{k,11} = \sin \theta_H(z) \tilde{A}_M^{k,4} + \cos \theta_H(z) \tilde{A}_M^{k,11}, & \text{for } k \neq 4, 11 \\ A_z^{4,11} = \tilde{A}_z^{4,11} - \frac{\sqrt{2}}{g} \partial_z \theta_H(z) = \tilde{A}_z^{4,11} + \frac{3\sqrt{2}}{g} \frac{z^2}{z_L^3 - 1} \theta_H \end{cases} \quad (6.83)$$

Since the surviving symmetry is given in terms of the broken groups $SU(3)_C \times U(1)_{\text{EM}}$, we want to look at that subset of gauge fields, along with the coset $SU(2)_L \times U(1)_Y / U(1)_{\text{EM}}$ required to get the W^\pm, Z^0 tower equations.

The W^\pm tower originates from A_μ^{aL} , $a = 1, 2$ where $A_\mu^{1L} = \frac{1}{2}(A_\mu^{2,3} + A_\mu^{1,4})$, $A_\mu^{2L} = \frac{1}{2}(A_\mu^{3,1} + A_\mu^{2,4})$ (see Appendix A in Ref. [115]). We only look at $a = 1$ since the 2nd set of equations are completely identical, showcasing the degeneracy between W^+, W^- . Expressing this in the twisted gauge, we have

$$A_\mu^{1L} = \tilde{A}_\mu^{2,3} + \cos \theta_H(z) \tilde{A}_\mu^{1,4} - \sin \theta_H(z) \tilde{A}_\mu^{1,11}. \quad (6.84)$$

Plugging the above into the respective boundary condition equation, provides us with one of the 3 equations necessary to determine the masses. Therefore we need to look at the two other fields that involve the sub-components. By symmetry, another comes from the W_R tower originating from A_μ^{aR} , $a = 1, 2$ where $A_\mu^{1R} = \frac{1}{2}(A_\mu^{2,3} - A_\mu^{1,4})$, $A_\mu^{2R} = \frac{1}{2}(A_\mu^{3,1} - A_\mu^{2,4})$. Writing A_μ^{1R} in terms of the twisted gauge we have,

$$A_\mu^{1R} = \tilde{A}_\mu^{2,3} + \cos \theta_H(z) \tilde{A}_\mu^{1,4} + \sin \theta_H(z) \tilde{A}_\mu^{1,11}. \quad (6.85)$$

Examining the two EOMs, we see that $\tilde{A}_\mu^{1,4}, \tilde{A}_\mu^{1,11}$ mix together to form $A^{1,11}$ in the twisted gauge,

$$A_\mu^{1,11} = \sin \theta_H(z) \tilde{A}_\mu^{1,4} + \cos \theta_H(z) \tilde{A}_\mu^{1,11}. \quad (6.86)$$

Therefore we have the 3 EOMs required to deduce the $\tilde{A}_\mu^{2,3}, \tilde{A}_\mu^{1,4}, \tilde{A}_\mu^{1,11}$ component EOMs in the twisted gauge. Since we are only interested in 0 modes along the ν dimension, the boundary conditions along the z axis are determined by the parity assignments, and are

$$\left. \frac{\partial}{\partial z} A_\mu^{1L} \right|_{z=1^+} = 0, \quad \left(\frac{\partial}{\partial z} - \mathbf{w} \right) A_\mu^{1R} = 0 \Big|_{z=1^+}, \quad A_\mu^{1,11} = 0. \quad (6.87)$$

Plugging in the expressions for the twisted gauge, we can therefore express the fields as

$$\tilde{A}_\mu^{2,3} = \alpha_{2,3} C(z; \lambda) A_\mu(x), \quad \tilde{A}_\mu^{1,4} = \alpha_{1,4} C(z; \lambda) A_\mu(x), \quad \tilde{A}_\mu^{1,11} = \alpha_{1,11} S(z; \lambda) A_\mu(x), \quad (6.88)$$

where the basis functions $C(z; \lambda), S(z; \lambda)$ are defined in Appendix B.4. Plugging in the corresponding forms in their boundary conditions, we get the mass equation

$$2C'(1; \lambda) (S(1; \lambda) C'(1; \lambda) + \lambda \sin^2 \theta_H) - \mathbf{w} C(1; \lambda) (2S(1; \lambda) C(1; \lambda) + \lambda \sin^2 \theta_H) = 0. \quad (6.89)$$

Since we are working in the regime where $w \gg (m_{\text{KK}_5})^{3/2}$, the 2nd term dominates. In this limit, we identify the parenthesis as the tower equation for W^+ (since $SU(2)_L$ is affected by the Hosotani breaking), and the prefactor as the tower equation for the W_R tower

$$W^+ : \quad 2S(1; \lambda_W) C(1; \lambda_W) + \lambda_W \sin^2 \theta_H = 0, \quad (6.90)$$

$$W_R^1 : \quad C(1; \lambda_{W_R}) = 0. \quad (6.91)$$

After we have found the dynamical value for θ_H , we numerically find the n th roots λ_n of the above, which gives us the mass towers for each of the fields $m_n = k\lambda_n$.

Similarly, the same set of equations applies for W^- , W_R^2 . Analogously we can perform the same arguments for the Z^0 , photon γ and Z^R towers which are determined by

$$A_\mu^{3L}, \quad B_\mu^Y = \sqrt{\frac{3}{5}}A_\mu^{3R} - \sqrt{\frac{2}{5}}A_\mu^{0C}, \quad C_\mu = \sqrt{\frac{2}{5}}A_\mu^{3R} + \sqrt{\frac{3}{5}}A_\mu^{0C}, \quad (6.92)$$

which is due to the breaking chain $SU(4)_C \times SU(2)_R \rightarrow SU(3)_C \times U(1)_Y$. E.g. the hypercharge field B_μ^Y consists of the 3rd normalised $SU(2)_R$ generator and the 0th normalised $SU(4)_C$ field $A_\mu^{0C} = \frac{1}{\sqrt{3}}(A_\mu^{5,6} + A_\mu^{7,8} + A_\mu^{9,10})$.

Performing the same analysis as before, one finds the tower equations

$$\gamma : \quad C'(1; \lambda_\gamma) = 0, \quad (6.93)$$

$$Z^0 : \quad 5S(1; \lambda_{Z^0})C(1; \lambda_{Z^0}) + 4\lambda_{Z^0} \sin^2 \theta_H = 0, \quad (6.94)$$

$$Z^R : \quad C(1; \lambda_{Z^R}) = 0. \quad (6.95)$$

Regarding the μ component, there are a couple of other towers that are noteworthy, namely the $A_\mu^{4,11}$, gluon G_μ , and the X-gluon $X_\mu \sim G_{\text{PS}}/G_{\text{SM}}$ towers,

$$A_\mu^{4,11} : \quad S(1; \lambda_{A^{4,11}}) = 0, \quad (6.96)$$

$$G_\mu : \quad C'(1, \lambda_G) = 0, \quad (6.97)$$

$$X_\mu : \quad C(1, \lambda_X) = 0. \quad (6.98)$$

Note that the gluon tower has the same solution as the photon tower, which is a reflection of the surviving gauge symmetry, $SU(3)_C \times U(1)_{\text{EM}}$.

Similarly we note that the z gauge component towers have a similar behaviour where we mention $A_z^{a,4}, A_z^{a,11}$, $a = 1, 2, 3$ which are absorbed by the W^\pm, Z^0 towers via the Hosotani breaking mechanism. We also note that the Higgs tower $A_z^{4,11}$ has solutions identical to its $A_\mu^{4,11}$ counterpart, and $A_z^{a,b}, 1 \leq a < b \leq 3$, $A_z^{j,k}, 5 \leq j < k \leq 10$ which have modes given by $C'(1, \lambda) = 0$.

Finally we ignore the ν components due to their loop corrections of order $\mathcal{O}(1/(gR_6))$ which make them irrelevant to our analysis.

Out of all the aforementioned tower equations, the ones that are relevant to our analysis (i.e. have masses $\sim M_{\text{KK}_5}$, see Appendix B.5 for discussion), are the photon, gluon, and W^\pm, Z^0 towers. The only contributions to the effective potential come from the W^\pm, Z^0 towers (since they are the only ones with explicit θ_H contributions). In line with the authors in Ref. [116], we rewrite the Z equation

to showcase the dependence of the Weinberg angle at the GUT scale, as

$$W^\pm : \quad 2S(1; \lambda_W)C(1; \lambda_W) + \lambda_W \sin^2 \theta_H = 0, \quad (6.99)$$

$$Z^0 : \quad 2S(1; \lambda_Z)C(1; \lambda_Z) + \frac{1}{\cos^2 \theta_W} \Big|_{M_{\text{GUT}}} \lambda_Z \sin^2 \theta_H = 0. \quad (6.100)$$

$\cos \theta_W|_{M_{\text{GUT}}} = 1 - \frac{3}{8}$, is the $SU(5)$ prediction for the Weinberg angle. For the purposes of exploring the phase space we set the Weinberg angle to its electroweak value of $(\sin^2 \theta_W)_{\text{EW}} = 0.2312$. We will then proceed to analyse the RGE runnings to see if this value is consistent with the above GUT prediction for the valid points in parameter space.

To summarise, the *bosonic sector* contributions to the effective potential $V_{\text{eff}}(\theta_H)$ come from,

$$\begin{cases} W^\pm : & 2S(1; \lambda_W)C(1; \lambda_W) + \lambda_W \sin^2 \theta_H = 0, \\ Z^0 : & 2S(1; \lambda_Z)C(1; \lambda_Z) + \frac{1}{1 - (\sin^2 \theta_W)_{\text{EW}}} \lambda_Z \sin^2 \theta_H = 0. \end{cases} \quad (6.101)$$

To this extent, the free parameters in the theory that contribute to the parameter space consist of

$$\{k, z_L\}, \quad (6.102)$$

where we note the implicit Bessel function dependence on the warp factor z_L , and the mass spectra being determined by the AdS curvature k .

Note that we also have the z component towers $A_z^{a,4}, A_z^{a,11}$, which are absorbed by the massive modes and have a contribution of,

$$S(1; \lambda)C'(1; \lambda) + \lambda \sin^2 \theta_H = 0. \quad (6.103)$$

Throughout this paper we'll be working in the $R_\xi = 0$ gauge (see Ref. [116]) which will set their contribution to the effective potential to 0. Note, this is a sign that the z components are absorbed by the massive towers.

6.7.2 Fermion Equations of Motion

In line with the authors in Ref. [116], we will be assuming that the theory is flavour diagonal and will only be working with the 3rd generation of matter. To this extent, the bulk $SO(11)$ fermion masses are relabelled as

$$c_{\Psi_{32}^\beta} = c_0, \quad c_{\Psi_{11}^\beta} = c_1, \quad c_{\Psi_{11}^{\prime\beta}} = c_2, \quad c_{\Psi_{32}^4} = c'_0, \quad (6.104)$$

where we assume the 3rd generation is present, along with the others providing negligible contributions. In addition for the neutrino sector we set the neutrino mass matrix to a diagonal constant $M^{\beta\beta'} = M\mathbf{1}_3$, and only look at the 3rd generation. Note that we will only be presenting the tower equation derivation in a schematic fashion, and refer the reader to Refs. [115, 116] for more details on a complete overview, since this is beyond the scope of this work.

The SM fields result as a superposition of the eigenstates originating from the various fields with the same Q_{EM} charge assignment.

We look at the simplest example, i.e the up type quark ($Q_{\text{EM}} = +2/3$). The SM field results from the equations of motion of $u \subset (\mathbf{4}, \mathbf{2}, 1) \sim G_{\text{PS}}$ and $u' \subset (\bar{\mathbf{4}}, 1, \mathbf{2}) \sim G_{\text{PS}}$ which are obtained by identifying the corresponding $Q_{\text{EM}} = +2/3$ sub-representations of the respective $\gamma_{6\text{D}}^7 = +1$ assignments. In this case the EOMs are purely determined by the bulk action, and are expressed as

$$-i\delta \begin{pmatrix} u_{+L}^\dagger \\ u_{+L}'^\dagger \end{pmatrix} : \quad \left(-k\hat{D}_-(c_0) + i\partial_\nu\right) \begin{pmatrix} \tilde{u}_{+R} \\ \tilde{u}_{+R}' \end{pmatrix} + \sigma^\mu \partial_\mu \begin{pmatrix} \tilde{u}_{+L} \\ \tilde{u}_{+L}' \end{pmatrix} = 0, \quad (6.105)$$

$$-i\delta \begin{pmatrix} u_{+R}^\dagger \\ u_{+R}'^\dagger \end{pmatrix} : \quad \bar{\sigma}^\mu \partial_\mu \begin{pmatrix} \tilde{u}_{+R} \\ \tilde{u}_{+R}' \end{pmatrix} + \left(-k\hat{D}_+(c_0) + i\partial_\nu\right) \begin{pmatrix} \tilde{u}_{+L} \\ \tilde{u}_{+L}' \end{pmatrix} = 0, \quad (6.106)$$

where $\hat{D}_\pm(c_0) = \pm(\partial_z + i\theta_H(z)T_{4,11}) + c_0/z$ is the conformal derivative acting on the 4, 11 spinorial subspace. Note that we are working with the “ z redefined” fields, which contain the absorbed z factor $u = 1/(z^{(5/2)})\tilde{u}$.

With our choice of the twisted gauge Ω , the fields are expressed as \tilde{u}, \tilde{u}' , where

$$\begin{pmatrix} \tilde{u} \\ \tilde{u}' \end{pmatrix} = \begin{pmatrix} \cos \frac{1}{2}\theta_H(z) & -i\sin \frac{1}{2}\theta_H(z) \\ -i\sin \frac{1}{2}\theta_H(z) & \cos \frac{1}{2}\theta_H(z) \end{pmatrix} \begin{pmatrix} \tilde{\tilde{u}} \\ \tilde{\tilde{u}}' \end{pmatrix}. \quad (6.107)$$

Applying the corresponding parity boundary conditions for the LH and RH fields

$$\tilde{u}_L, \tilde{u}_L' \sim \begin{pmatrix} \tilde{P}_2 & \tilde{P}_3 \\ \tilde{P}_0 & \tilde{P}_1 \end{pmatrix} = \begin{pmatrix} + & + \\ + & + \end{pmatrix}, \quad \tilde{u}_R, \tilde{u}_R' \sim \begin{pmatrix} \tilde{P}_2 & \tilde{P}_3 \\ \tilde{P}_0 & \tilde{P}_1 \end{pmatrix} = \begin{pmatrix} - & - \\ - & - \end{pmatrix}, \quad (6.108)$$

we can decompose the fields along the GUT dimension, where we only look at the 6D $n = 0$ modes $\tilde{u}_{0L}, \tilde{u}_{0L}', \tilde{u}_{0R}, \tilde{u}_{0R}'$. To this extent we can express the resulting \tilde{u}, \tilde{u}' fields in terms of the corresponding basis functions along the warped dimension as

$$\begin{pmatrix} \tilde{u}_{0R} \\ \tilde{u}_{0R}' \end{pmatrix} = \begin{pmatrix} \alpha_R^u S_R(z; \lambda, c_0) \\ \alpha_R'^u C_R(z; \lambda, c_0) \end{pmatrix} f_R(x), \quad \begin{pmatrix} \tilde{u}_{0L} \\ \tilde{u}_{0L}' \end{pmatrix} = \begin{pmatrix} \alpha_L^u C_L(z; \lambda, c_0) \\ \alpha_L'^u S_L(z; \lambda, c_0) \end{pmatrix} f_L(x), \quad (6.109)$$

where S_L, S_R, C_L, C_R are basis function defined in terms of Bessel functions as specified in Appendix B.4. Plugging the above in the bulk EOMs in Eqns. (6.105), (6.106), one finds that the tower equation of up type quarks is then determined by,

$$S_L(1; \lambda, c_0)S_R(1; \lambda, c_0) + \sin^2 \frac{\theta_H}{2} = 0. \quad (6.110)$$

The mass of the n -th mode is $m_n = k\lambda_n$, where λ_n is a root of the above.

The more complicated fields such as the down type quarks, have additional challenges in their derivation introduced by the UV brane masses. In this case, the SM field with $Q_{\text{EM}} = -1/3$ results from the EOMs of $d \subset (\mathbf{4}, \mathbf{2}, 1) \sim G_{\text{PS}}$, $d' \subset (\bar{\mathbf{4}}, 1, \mathbf{2}) \sim G_{\text{PS}}$, $\mathcal{D}, \mathcal{D}' \subset (\mathbf{6}, 1, 1) \sim G_{\text{PS}}$. In addition to the pure bulk EOMs, we now have the brane masses weighting the delta functions $\delta(y)$. The EOMS for the aforementioned fields are

$$-i\delta \begin{pmatrix} d_{+L}^\dagger \\ d_{+L}'^\dagger \end{pmatrix} : \quad \left(-k\hat{D}_-(c_0) + i\partial_\nu\right) \begin{pmatrix} \check{d}_{+R} \\ \check{d}_{+R}' \end{pmatrix} + \sigma^\mu \partial_\mu \begin{pmatrix} \check{d}_{+L} \\ \check{d}_{+L}' \end{pmatrix} = 0, \quad (6.111)$$

$$-i\delta \begin{pmatrix} d_{+R}^\dagger \\ d_{+R}'^\dagger \end{pmatrix} : \quad \bar{\sigma}^\mu \partial_\mu \begin{pmatrix} \check{d}_{+R} \\ \check{d}_{+R}' \end{pmatrix} + \left(-k\hat{D}_+(c_0) + i\partial_\nu\right) \begin{pmatrix} \check{d}_{+L} \\ \check{d}_{+L}' \end{pmatrix} = 2\mu_1 \delta(y) \begin{pmatrix} 0 \\ \check{\mathcal{D}}_{-L} \end{pmatrix}, \quad (6.112)$$

$$-i\delta \mathcal{D}_{+L}^\dagger : \quad \left(-k\hat{D}_-(c_1) + i\partial_\nu\right) \check{\mathcal{D}}_{+R} + \sigma^\mu \partial_\mu \check{\mathcal{D}}_{+L} = 0, \quad (6.113)$$

$$i\delta \mathcal{D}_{+R}^\dagger : \quad \bar{\sigma}^\mu \partial_\mu \check{\mathcal{D}}_{+R} + \left(-k\hat{D}_+(c_1) + i\partial_\nu\right) \check{\mathcal{D}}_{+L} = 2\mu_{11} \delta(y) \check{\mathcal{D}}_{-L}, \quad (6.114)$$

$$-i\delta \mathcal{D}_{-L}^\dagger : \quad \left(k\hat{D}_+(c_1) - i\partial_\nu\right) \check{\mathcal{D}}_{-R} + \sigma^\mu \partial_\mu \check{\mathcal{D}}_{-L} = \delta(y) [2\mu_{11} \check{\mathcal{D}}_{+R} + 2\mu_1 \check{d}_{+R}'], \quad (6.115)$$

$$i\delta \mathcal{D}_{-R}^\dagger : \quad \bar{\sigma}^\mu \partial_\mu \check{\mathcal{D}}_{-R} + \left(k\hat{D}_-(c_1) - i\partial_\nu\right) \check{\mathcal{D}}_{-L} = 0. \quad (6.116)$$

We note the 5D mass term c_0 is present for the fields that originate from $\Psi_{\mathbf{32}}$, whereas c_1 shows up for the fields originating from $\Psi_{\mathbf{11}}$. Analogously to the up type quarks, by expanding along the extra dimensions, and imposing the corresponding boundary conditions, we are left with the tower equation for down type quarks,

$$S_L(1; \lambda, c_0)S_R(1; \lambda, c_0) + \sin^2 \frac{\theta_H}{2} = - \frac{\mu_1^2 S_R(1; \lambda, c_0)C_R(1; \lambda, c_0)S_L(1; \lambda, c_1)C_R(1; \lambda, c_1)}{\mu_{11}^2 (C_R(1; \lambda, c_1))^2 - (S_L(1; \lambda, c_1))^2}, \quad (6.117)$$

where μ_1, μ_{11} are localised 5D UV brane couplings. Performing the same analysis for the electron type lepton, the neutrino sector and the dark fermion multiplet

arising from $\Psi_{\mathbf{32}}^4$, and gathering them all together give us the *fermionic sector* contributions to the effective potential,

$$\left\{ \begin{array}{l} S_L(1; \lambda_t, c_0)S_R(1; \lambda_t, c_0) + \sin^2 \frac{\theta_H}{2} = 0, \\ S_L(1; \lambda_b, c_0)S_R(1; \lambda_b, c_0) + \sin^2 \frac{\theta_H}{2} = \\ \quad - \frac{\mu_1^2 S_R(1; \lambda_b, c_0)C_R(1; \lambda_b, c_0)S_L(1; \lambda_b, c_1)C_R(1; \lambda_b, c_1)}{\mu_{11}^2 (C_R(1; \lambda_b, c_1))^2 - (S_L(1; \lambda_b, c_1))^2}, \\ S_L(1; \lambda_\tau, c_0)S_R(1; \lambda_\tau, c_0) + \sin^2 \frac{\theta_H}{2} = \\ \quad - \frac{\tilde{\mu}_2^2 S_L(1; \lambda_\tau, c_0)C_L(1; \lambda_\tau, c_0)S_R(1; \lambda_b, c_2)C_L(1; \lambda_\tau, c_2)}{\mu_{11}'^2 (C_L(1; \lambda_\tau, c_2))^2 - (S_R(1; \lambda_\tau, c_2))^2}, \\ -\frac{k\lambda_\nu + M}{m_B} \left[S_L(1; \lambda_\nu, c_0)S_R(1; \lambda_\nu, c_0) + \sin^2 \frac{\theta_H}{2} \right] \\ \quad - \frac{m_B}{2k} S_R(1; \lambda_\nu, c_0)C_R(1; \lambda_\nu, c_0) = 0, \\ S_L(1; \lambda_\psi, c'_0)S_R(1; \lambda_\psi, c'_0) + \cos^2 \frac{\theta_H}{2} = 0. \end{array} \right. \quad (6.118)$$

$\lambda_t, \lambda_b, \lambda_\tau, \lambda_\nu, \lambda_\psi$ refer to the solutions for the top, and bottom quark, the tau lepton, the neutrino and the dark fermion multiplet.

Therefore, the free parameter set in charge of controlling the solution space consists of

$$\mathcal{P} = \{k, z_L, c_0, c_1, c_2, c'_0, \mu_1, \tilde{\mu}_2, \mu_{11}, \mu_{11}', M, m_B\}. \quad (6.119)$$

$\mu_1, \tilde{\mu}_2, \mu_{11}, \mu_{11}'$ are the localised 5D UV brane couplings (at $y = 0$ in Fig. 6.2) between the 5D scalar $\Phi_{\mathbf{32}}$ and the bulk fermion fields $\Psi_{\mathbf{32}}^\alpha, \Psi_{\mathbf{11}}^\beta, \Psi_{\mathbf{11}}^{\prime\beta}$, and M, m_B are the 5D Majorana masses confined to the UV brane. Note that we include the 2nd neutrino sector mass equations and their effective potential contribution, but neglect including them in the parameter space analysis. Throughout this chapter note that we have set m_B, M to the sample values stated by the authors in the original paper, $M = -10^7$ GeV, $m_B = 1.145 \cdot 10^{12}$ GeV, which is done to simplify the analysis and ensure the correct order of magnitude for neutrino masses (i.e. < 0.1 eV). These will determine, along with the bosonic contributions, the dynamical value of $\theta_H = \langle \theta_H \rangle$.

6.7.3 The Effective Higgs Potential $V_{\text{eff}}(\theta_H)$

The form of one loop effective potential resulting from the KK tower contributions with mass $m_n(\theta_H)$ is given by,

$$V_{\text{eff}}(\theta_H) = \pm \frac{1}{2} \int_0^\infty \frac{d^4 p}{(2\pi)^4} \sum_n \ln(p^2 + m_n(\theta_H)), \quad (6.120)$$

where the \pm sign accounts for either the fermion or bosonic contributions. The above can be recast by rewriting the mass spectra equations in the form,

$$1 + \tilde{Q}(\lambda_n)f(\theta_H) = 0, \quad (6.121)$$

where $f(\theta_H)$ is some arbitrary function purely dependent on θ_H and $Q(q) = \tilde{Q}(iqz_L^{-1})$. This in turn gives the effective potential contribution in the form of $V_{\text{eff}}(\theta_H) = \pm I[Q(q); f(\theta_H)]$, where

$$I[Q(q); f(\theta_H)] = \frac{(kz_L^{-1})}{(4\pi)^2} \int_0^\infty dq q^3 \ln(1 + Q(\lambda_n)f(\theta_H)). \quad (6.122)$$

To be able to find the mass spectra of the model we need to compute the minimum of the potential $\langle \theta_H \rangle$. This is done via numerical integration of the various contributions using Mathematica's inbuilt numerical integration [126].

To be a bit more explicit, we give an example and look at the top quark contribution. Its equation of motion can be cast in the aforementioned form as,

$$1 + \frac{\sin^2(\theta_H/2)}{S_L(1, iqz_L^{-1}, c_0)S_R(1, iqz_L^{-1}, c_0)} = 0, \quad (6.123)$$

where we identify $f(\theta_H) = \sin^2(\theta_H/2)$, and

$$Q_0(q) = \frac{1}{S_L(1, iqz_L^{-1}, c_0)S_R(1, iqz_L^{-1}, c_0)}. \quad (6.124)$$

Therefore the top quark effective potential contribution has the explicit form

$$V_{\text{eff}}^{\text{Top}}(\theta_H) = -\frac{(kz_L^{-1})^4}{(4\pi)^2} \int_0^\infty dq q^3 \ln \left(1 + \frac{1}{S_L(1, iqz_L^{-1}, c_0)S_R(1, iqz_L^{-1}, c_0)} \sin^2 \frac{\theta_H}{2} \right). \quad (6.125)$$

Similarly $Q_0(q)$ can be rewritten in terms of the modified Bessel function basis $\hat{F}_c^{\pm\pm}(q)$ presented in Appendix B.4.

The rest of the contributions are computed in an analogous way, where we use the same effective potential as in the original paper. The contributions are expressed in the $R_\xi = 0$ gauge, and come from all the fields that have 0 modes for both the 5th and 6th dimension and have an explicit θ_H dependence,

$$\begin{aligned} V_{\text{eff}}^{\text{Bosons}}(\theta_H) &= V_{\text{eff}}^{W^\pm} + V_{\text{eff}}^{Z^0} + V_{\text{eff}}^{A_z^{a,4}, A_z^{a,11}}, \\ V_{\text{eff}}^{\text{Fermi}}(\theta_H) &= V_{\text{eff}}^{\text{Top}} + V_{\text{eff}}^{\text{Bottom}} + V_{\text{eff}}^{\text{Tau}} + V_{\text{eff}}^{\text{Neutrino - 1}} + V_{\text{eff}}^{\text{Neutrino - 2}} + V_{\text{eff}}^{\text{Dark Multiplet}}, \\ V_{\text{eff}}(\theta_H) &= V_{\text{eff}}^{\text{Bosons}} + V_{\text{eff}}^{\text{Fermions}}. \end{aligned} \quad (6.126)$$

For the explicit form of the effective potential we refer the reader to Sec.5 in Ref. [116].

Furthermore, the Higgs mass is then given by the 2nd derivative of the effective potential,

$$m_H^2 = \frac{1}{f_H^2} \frac{dV_{\text{eff}}(\theta_H)}{d\theta_H^2} \Big|_{\theta_H=\langle\theta_H\rangle}, \quad (6.127)$$

where f_H is the warp factor that ensures the right dimensionality,

$$f_H^2 = \frac{\sqrt{6}}{(e/\sin\theta_W)} \frac{k}{\sqrt{(1-z_L^{-1})(z_L^3-1)}}. \quad (6.128)$$

Similarly, the trilinear coupling of the Higgs τ_H , consists of the third derivative of the Higgs effective potential, which is then weighted by an appropriate power of f_H ,

$$\tau_H = \frac{1}{6} \frac{1}{f_H^3} \frac{d^3 V_{\text{eff}}(\theta_H)}{d\theta_H^3} \Big|_{\theta_H=\langle\theta_H\rangle}. \quad (6.129)$$

Note that the Higgs potential is flat at tree level and is fully determined by the 1-loop radiative contributions.

6.8 A Brief Pause

With all the tools now in place, the following chapter will go through the parameter space and phenomenological exploration of the model. This is done numerically via directed random techniques: a random sample of the parameter space is selected, the corresponding contributions and global minimum to the effective potential are then determined. From this, we find the relevant mass spectra by solving the individual tower equations. Having explored and extended the parameter space, we look at the model's Higgs and exotic phenomenology along with checking the consistency between the UV and the IR pictures of the theory.

$SO(11)$ GHGUT - RGEs & spectra

The following chapter is an exploration of the model introduced in Refs. [116, 117] and reviewed in Chapter 6. The content is organised as follows.

We detail our scan methodology to connect the UV picture with concrete phenomenological implications at the TeV scale. We then move on to exploring the di-Higgs physics for viable parameter choices. On the basis of LHC (and FCC-hh) projections of di-Higgs measurements and our scan results, we identify exotic states that will allow us to directly constrain this scenario in the near future.

Finally we look at the consistency between the UV and IR by evolving the model’s renormalisation group equations. More specifically we analyse at how the Weinberg angle evolves from its predicted GUT value to the EW value, which can then be used as a tool for future model building. This entails approximating our theory within 4D and 5D regimes and performing a piecewise RGE evolution based on the resultant spectra.

7.1 Scanning Algorithm

We now move on to the exploration of the model’s low energy effective theory. This is done in a stochastic fashion, by randomly sampling the parameter space, finding the corresponding effective Higgs potential’s minimum, which is then used to numerically solve the tower equations. The parameter space exploration strategy that we have chosen, consists of two stages in the following order:

- 1) A “vetted” random sampling of the phase space.
- 2) A differential evolution minimisation algorithm based on a global χ_G^2 measure.

We have adopted this strategy to maximise our limited computational power, along with trying to ensure the exploration of the most interesting regions of the

phase space. We now go through the two stages and explain their functioning and implementation. Note that in the original paper (Ref. [116]) the strategy employed by the authors serves to find a reasonable number of solutions for the $\theta_H \sim 0.15$ value of the Higgs potential minimum. What we are trying to achieve via our method, is to dynamically determine the minimum and more thoroughly explore the parameter space. This also comes with the added benefit of deriving a general exploration methodology which can in turn be applied for any other set of BSM models.

Given our set of controlling parameters $\mathcal{P} = \{p^i\}$ defined in Eqn. (6.119), along with the definition bounds $\mathcal{P}_{\text{bounds}} = \{(p_i^{\min}, p_i^{\max})\}$ (where $p^i \in [p_i^{\min}, p_i^{\max}]$), we pick a point at random in parameter space. We then pass it through our “mathematical apparatus” (consisting of all the stages required to obtain the mass spectra) and extract the outputted masses and couplings which are then compared to the relevant experimental SM constraints.

The issue with uniform sampling arises when a point’s passing through the “mathematical apparatus” requires a large amount of computational resources and time. Combine this with having most of the points being non physical or undefined within the random bounds, and the computational cost of finding solutions consistent with the SM, quickly spirals out of control.

To reconcile this, at least in part, it turns out to be convenient to split the parameter set into two stages

$$\mathcal{P}_1 = \{k, z_L\}, \quad \mathcal{P}_2 = \{c_0, c_1, c_2, c'_0, \mu_1, \tilde{\mu}_2, \mu_{11}, \mu'_{11}\}. \quad (7.1)$$

This choice enables us to pre-sample points, that directly reflect experimental constraints on the Kaluza Klein mass scale of 4.1 TeV [127]

$$m_{\text{KK}_5} = \frac{\pi k}{z_L - 1} \geq 4.1 \text{ TeV}. \quad (7.2)$$

The scan over the remaining parameters \mathcal{P}_2 is then performed within their respective boundaries.

In first instance, we define a set of general bounds

$$\begin{aligned} \mathcal{P}_{\text{bounds}} = \Big\{ & k \in [10^3 \text{ GeV}, 10^7 \text{ GeV}], z_L \in [10, 2500], \\ & c_0 \in [0, 1], c'_0 \in [0, 1], c_1 \in [0, 2], c_2 \in [-3, 3] \\ & \mu_1 \in [0, 50], \tilde{\mu}_2 \in [0, 50], \mu_{11} \in [0, 50], \mu'_{11} \in [0, 50] \Big\}. \end{aligned} \quad (7.3)$$

Similarly, we define the more restricted parameter range $\mathcal{P}_{\text{bounds}}^{\text{extSol}}$ which is obtained by forming an appropriate extension from the sample solutions' parameters presented in Ref. [116]

$$\begin{aligned} \mathcal{P}_{\text{bounds}}^{\text{extSol}} = \Big\{ & k \in [10^5 \text{GeV}, 5 \cdot 10^5 \text{GeV}], z_L \in [30, 60], \\ & c_0 \in [0, 0.8], c'_0 \in [0.1, 0.8], c_1 \in [0, 0.4], c_2 \in [-1.5, -0.2] \\ & \mu_1 \in [9, 15], \tilde{\mu}_2 \in [0, 3.5], \mu_{11} \in [0, 2.5], \mu'_{11} \in [0, 2.5] \Big\}. \end{aligned} \quad (7.4)$$

The choice of the latter is due to the high dimensionality of the parameter space and the optimisation choice of meta-parameters required for the differential evolution algorithm used in the next stage. In particular, we consider wide z, k intervals. The latter criteria give rise to an adequate number of trial solutions. However, most of these are phenomenologically ruled out as they typically do not reproduce the SM mass spectrum, predominantly due to $\langle \theta_H \rangle \simeq 0$ and periodic solutions. This behaviour is well-known from composite Higgs scenarios [128–133] (which are dual to the $D > 4$ formulation in the sense of the AdS/CFT correspondence [134–136]) where some fine-tuning is required to lift the Higgs mass and create a large mass gap between the electroweak scale and the UV composite scale. Yet, through the use of adapted techniques we can approach physically viable solutions for large ad-hoc parameter windows.

To identify the phenomenologically acceptable solutions we employ differential evolution [137, 138] based on a global χ_G^2 that parametrises the goodness of fit of the generated points given the experimental observations. χ_G^2 is defined as the unweighted sum of χ_i^2 terms

$$\chi_G^2 = \sum_{i \in \mathcal{C}} \chi_i^2, \quad \text{with} \quad \chi_i^2 \equiv \frac{(m_i - m_i^{\text{Gen}})^2}{((\sigma_i^{\text{Exp}})^2 + (\sigma_i^{\text{Th}})^2)}, \quad (7.5)$$

where $\mathcal{C} = \{H, W^\pm, t, b, \tau\}$ for our purposes. m_i is the central value of the masses being probed, m_i^{Gen} is the generated mass given the parameter input, σ_i^{Exp} are the experimental uncertainties. We also introduce a “theoretical uncertainty” σ_i^{Th} of 1%, see Tab. 7.1, to account for the RGE and threshold effects in the masses that we neglect. We also do not consider electroweak radiative corrections that affect input parameter relations. Both effects are usually small, see e.g. Ref. [1, 139–141]. We note that in the context of GUTs a special role is played by the Weinberg angle that we use as theoretical input to our scan (from which follows the Z mass through SM relations). We will explore the implications of the Weinberg angle and associated RGE effects in the next section.

state	mass m [GeV]	σ_H^{Exp} [GeV]	σ_H^{Th} [GeV]
H	125.18	0.016	1.25
W^\pm	80.379	0.012	0.8037
t	172.44	0.9	1.724
τ	1.776	0.00012	0.01776
b	4.18	0.04	0.0418

Table 7.1: Parameter values for the definition of χ_G^2 . The experimental uncertainties are the most recent bounds [22] for the Higgs boson H [9], the W^\pm bosons, the top quark t , the bottom quark b , and the tau lepton τ . We include a “theoretical” error to widen the parameter windows to discuss the phenomenological outcome in more detail below. The Z mass is obtained through the Weinberg angle, which we use as an input.

From the point of view of the infrared theory, in addition to the constrained SM masses, we need to reflect exclusion constraints from existing LHC searches that are relevant for the low energy spectrum of the model. As the most limiting searches, we include exotic quark searches [142], Z' searches [92] as well as exotic charged lepton searches [143] to constrain the first non-SM KK states. By taking the aforementioned exclusion constraints at face value, if a parameter choice is in conflict with any of these searches, we reject the point directly.

We deem a point as “SM-like” when its χ_G^2 falls within the 95% confidence limit bound for our degrees of freedom which selects a region

$$\chi_G^2 \leq 20.52. \quad (7.6)$$

This bound is obtained by solving Eqn. (7.7) numerically for χ_B^2

$$0.95 = \frac{1}{\Gamma(10/2)} \int_0^{\chi_B^2/2} t^{10/2-1} e^{-t} dt. \quad (7.7)$$

The bound is set by the cumulative distribution function for a χ^2 distribution with 10 degrees of freedom.

We can now interpret χ_G^2 as a cost function, and look for points in the parameter space that minimise it. In addition, the χ_G^2 evaluation can be time-consuming and can suffer from numerical singularities which makes the minimisation non-trivial. To more efficiently explore the parameter space, and find relevant solutions, we employ the differential evolution algorithm introduced by Storn and Price in Ref. [137]

(see also [138]). The algorithm uses the initial set of trial points described above to generate points that iteratively minimise the χ_G^2 cost function. The stochastic algorithm consists of four stages: initialisation, mutation, recombination, and selection. It is designed as a parallelisable algorithm based on selection via a so-called “greedy criterion”. Mutation, recombination and selection are then performed until we sufficiently minimise the cost function. Performing these routines is then referred to, as going through a generation, where we label the generation number with G . We outline the algorithm as follows:

- In the initialisation stage we randomly partition our initial population into subsets consisting of N_P points. Each subpopulation is then treated separately, enabling (pseudo-)parallelisation of the algorithm. Each of the points has associated a $|\mathcal{P}| = 10$ dimensional parameter vector \mathbf{p}^G , formed by the corresponding point’s parameter values.
- During the mutation stage we aim to generate a new parameter vector which will be used to generate a new point with smaller χ_G^2 value. In this stage, we cycle through the points of the partition picking a random target point alongside three other distinct parameter points called “donor points”. We label the target point parameter vector as \mathbf{p}_t^G , and the donor points parameter vectors as $\mathbf{p}_{d_1}, \mathbf{p}_{d_2}, \mathbf{p}_{d_3}$. From the 3 points we then form a “mutation” \mathbf{p}_m^G by combining the parameter vectors,

$$\mathbf{p}_m^G = \mathbf{p}_{d_1}^G + F \cdot (\mathbf{p}_{d_2}^G - \mathbf{p}_{d_3}^G) \quad (7.8)$$

where $F \in [0, 2]$ is a constant amplification factor to be set by the user.

- Recombination then aims to keep successfully minimised solutions of the current generation and improve on them by combining the target and the mutated points. The combination works as follows: To ensure that we have at least one component arising from the mutation vector we pick one parameter of the mutated vector \mathbf{p}_m^G at random. The remaining parameters are adopted from the target vector \mathbf{p}_t^G , however we replace the i th component with the corresponding mutated entry with a uniform probability steered by a tunable decision factor C_R . This results in a combined parameter vector \mathbf{p}_c^G .
- In the last stage, selection, we compare the target \mathbf{p}_t^G and the candidate point \mathbf{p}_c^G by evaluating and comparing their respective cost function values.

We admit to the new generation $G + 1$ the point with the lowest cost function value. This is the admission via the “greedy criterion”.

Mutation, recombination and selection are performed until we have treated all points within a generation as a target, which in turn determines the next generation. We keep iterating through generations until the cost function hits the threshold of a point being SM-like like, specified by Eqn. (7.6), or abort the process if no viable solution is obtained. This numerically minimises the cost function.

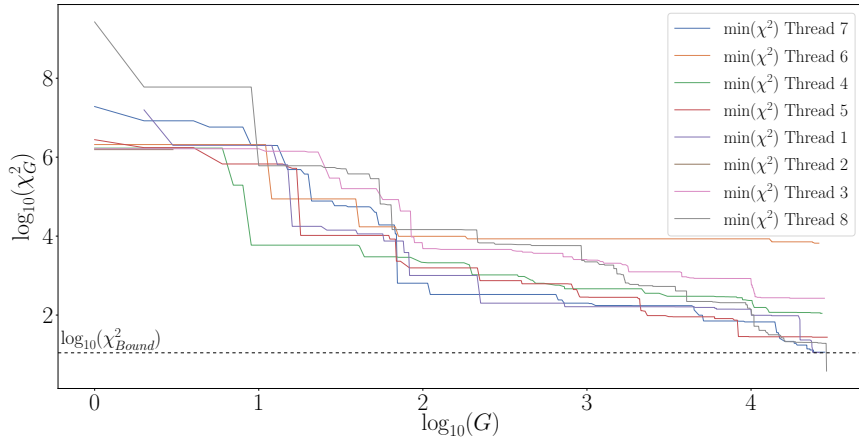


Figure 7.1: Log-log sample runs of the differential evolution outlined in the text, showing the χ_G^2 value as a function of the generation number G . Note that each run (shown in different colours and denoted as “thread” specifies a parallel run) contains a population $N_P = 12$. The horizontal dotted line represents the \log_{10} value of the SM like lower bound in Eqn. (7.6), after which we terminate the thread. Note that this run was ended prematurely for Threads 5, 4, 3, 6, leading to non-SM solutions.

In obtaining results, the differential evolution parameters N_P, F, C_R play important roles for convergence and its speed. Tuning F, C_R to the problem at hand needs to be balanced against the population number N_P . By optimising these meta-parameters we can obtain adequate mutation and recombination rates which enables reliable convergence. For the extended parameter range $\mathcal{P}_{\text{bounds}}^{\text{extSol}}$, the choices

$$N_P = 12, \quad C_R = 0.2368, \quad F = 0.6702, \quad (7.9)$$

are appropriate (see also Ref. [144]). We obtain $\chi_G^2 \lesssim 20$ from an initial value of $\sim 10^7$ using on average $\sim 10^4$ generations (see Fig. 7.1).

7.2 Mass Spectra

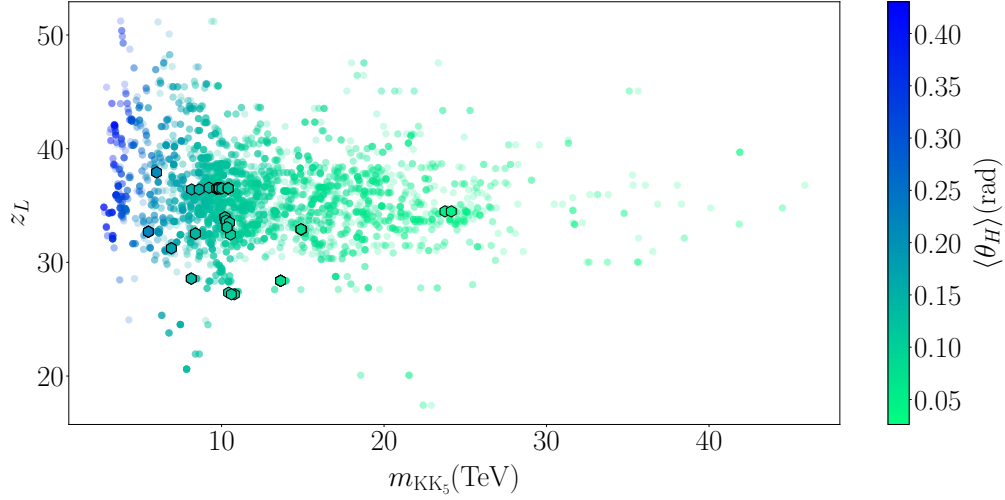


Figure 7.2: Scatter plot of representative parameter space points for the $SO(11)$ model before and after differential evolution as functions of the KK scale m_{KK_5} and warp factor z_L . The color reflects the order parameter $\langle \theta_H \rangle$. Points highlighted as hexagons are the points that are SM-like (i.e. they obey the bound set in Eqn. (7.6)). Faded points are excluded on the basis of falling short of the χ_G^2 measure bound.

Employing the algorithm detailed in the previous section we can produce the consistent mass spectrum depicted in Fig. 7.2. Direct LHC searches and our χ_G^2 measure then reduce the viable solution space to the points highlighted as hexagons in Fig. 7.2, which serve as the basis of our discussion. From this we observe values of the order parameter $\langle \theta_H \rangle \lesssim 0.2$, which ensure minimal deviations from the SM phenomenological values (see [145]). Given that we require consistency with the observed Higgs mass, the theory cannot approach the decoupling limit. In other words, the AdS/CFT dual of the symmetry-breaking Wilson loop becomes a Goldstone field if we send the UV cut-off to infinity. Therefore, a large mass gap between the KK scale and the Higgs mass is also not straightforward to achieve, which provides another motivation to implement the targeted numerical techniques detailed above. The differential evolution converges to solutions with a relatively low KK scale M_{KK_5} for which the points are not yet excluded.

7.3 Low Energy Phenomenology Implications

7.3.1 Di-Higgs Physics

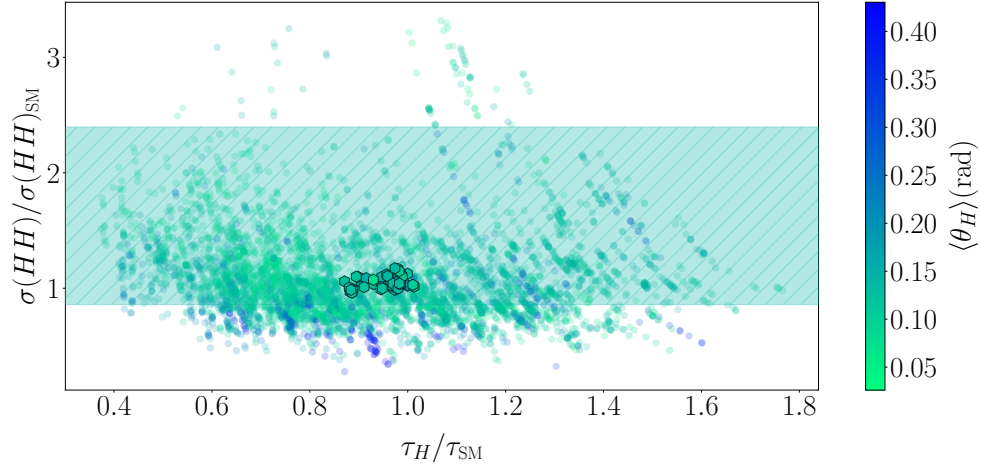
We turn to the discussion of the low energy implications of the model that is now consistent with the SM mass spectrum. The implications for single Higgs physics (we denote the physical Higgs by h) have been discussed in Ref. [146] (see also Ref. [147]), where it was shown that the model's single Higgs phenomenology is largely SM-like as a consequence of alternating contributions to the $H \rightarrow gg, \gamma\gamma$ decay (and production) loops. This is ultimately rooted in higher dimensional gauge invariance. Such a cancellation is broken in multi-Higgs final states and we therefore focus on this particular channel as a potentially sensitive probe of the model.

A recent projection by CMS [148] suggests that a sensitivity to $-0.18 \leq \lambda_{\text{SM}}^{95\% \text{ CL}}/\lambda_{\text{SM}} \leq 3.6$ can be achieved, which corresponds to a gluon fusion cross section extraction of $0.85 \leq \sigma(HH)/\sigma(HH)_{\text{SM}} \leq 2.39$ when assuming SM interactions. The inclusive SM di-Higgs cross section at the LHC is about 32 fb [149–158]. At a future FCC-hh, which is specifically motivated from a di-Higgs phenomenology perspective through the large inclusive cross section of 1.2 pb [156], this could be improved to $\sigma(HH)/\sigma(HH)_{\text{SM}} \simeq [0.958, 1.044]$, Ref. [159] (see also [160–166]).

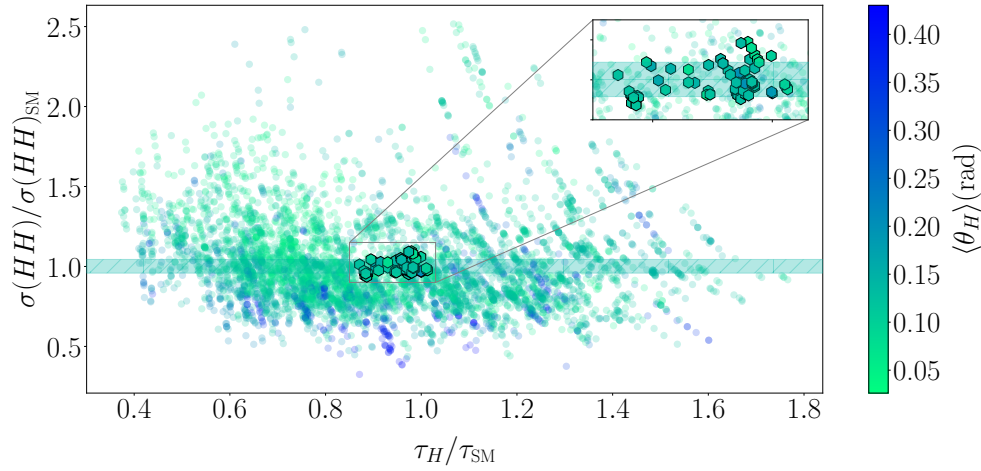
Compared to the SM where the trilinear Higgs interaction is set by the Higgs vacuum expectation value and the Higgs mass, this correlation becomes modified in the present scenario. This extends to the top quark mass correlation with the vacuum expectation value, i.e. the top quark Yukawa coupling can be modified compared to the SM [167]. Both these effects are relevant for di-Higgs production and we include them to a one-loop computation of $gg \rightarrow HH$ production [168–170]. The relevant production diagrams are shown in Fig. 7.4

We furthermore estimate the importance of the heavier states that arise in this scenario by means of the low energy effective theorem, but find that they do not significantly impact our result and their contribution is in the percent-range, below the expected theoretical uncertainty. In the following we will focus on modifications of the cross section due to modifications away from SM parameters only.

The results are summarised in Figs. 7.5a and 7.5b, from which we can see that the highlighted points have a slightly larger production cross section with respect to the SM, and are consistent with the experimental values of the Higgs and top quarks masses along with the experimental and theoretical uncertainties. We observe that



(a) Scatter plot of representative parameter space points for the $SO(11)$ model before and after differential evolution as functions of the Higgs self-coupling relative to the SM τ_H/τ_{SM} and di-Higgs cross section in relation to the SM. The color shading reflects the order parameter $\langle\theta_H\rangle$. Points highlighted as hexagons are the points that are SM-like (i.e. they obey the bound set in Eqn. (7.6)). The green band corresponds to the latest CMS di-Higgs measurement projection of Ref. [148].



(b) Scatter plot analogous to Fig. 7.3a, but for a 100 TeV FCC-hh. The green band now corresponds to the sensitivity region $0.958 \leq \sigma(HH)/\sigma(HH)_{\text{SM}} \leq 1.044$ which derives from a $\mathcal{O}(6\%)$ measurement of the Higgs self-coupling as detailed in [159].

Figure 7.3: Sensitivity bands for the di-Higgs production at CMS and the proposed FCC collider

modifications of Higgs pair production $\lesssim 20\%$ are possible in this model for our scan results. Plotting the two sensitivity bands corresponding to the CMS and FCC-hh

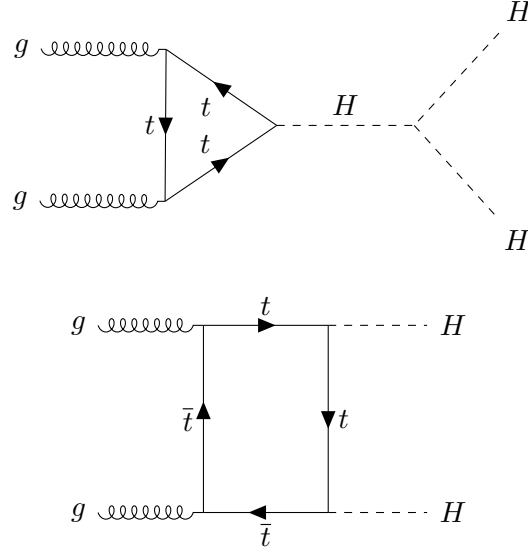
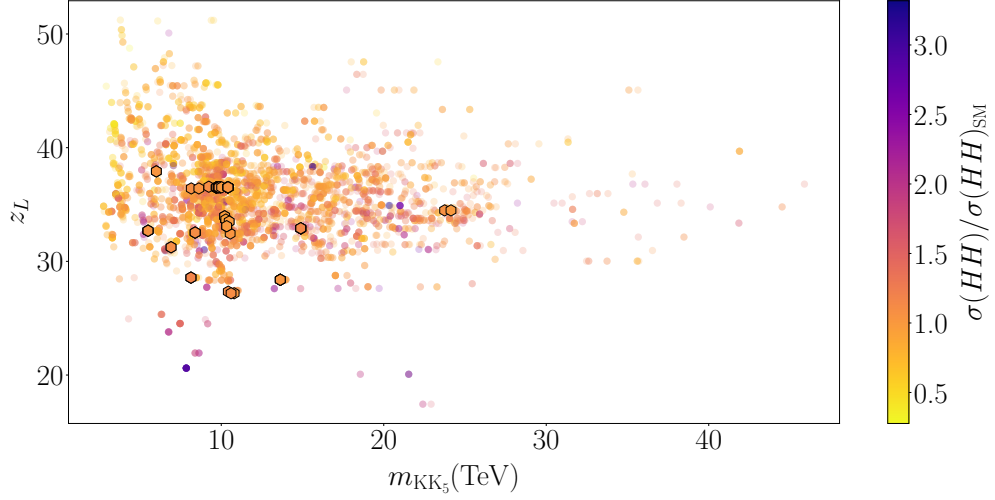


Figure 7.4: Main $gg \rightarrow HH$ 1 loop production diagrams. The trilinear Higgs coupling is given by τ_H , and the top Yukawa coupling is $\sim y_t^{\text{SM}} \cdot \cos \theta_H$, as discussed in Ref. [146]. The gluon top couplings are the same as in the SM.

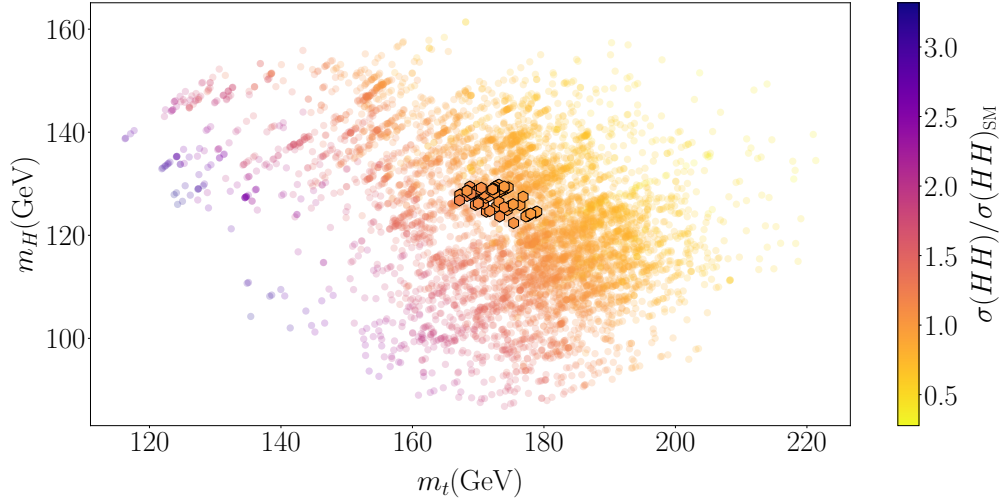
predictions in Figs. 7.3a and 7.3b, respectively, we see that some parameter points can indeed be excluded through di-Higgs analyses at future collider experiments. Given the relatively small modification of di-Higgs production (which combines with similar observations for single Higgs final states [146]), a more targeted approach to constrain this model in the near future is through its lowest lying KK resonances.

7.3.2 Exotics

We now look at the states present in the low energy description that can act as a direct probe of the model. After excluding the points that fell short of the LHC cuts specified in Sec. 7.1, we plot the lowest lying exotic mode m_ξ ($\xi = \psi^D, \tau^{(1)}, b^{(1)}$) in Fig. 7.6a; the lowest lying non-SM modes of the bottom quark, tau lepton and the “dark fermion” serve as the next accessible states. We neglect the first excited state of the top quark as it is much heavier than the other exotic states. We can see that most of the viable parameter space points predict that these states lie within the 1 TeV to 2 TeV range, which should make them accessible by the current colliders via the ongoing searches, which we have highlighted in 7.1. For the hexagonal points the next accessible state is either the first excitation of the tau lepton or the bottom quark, with the mass correlations plotted in Fig. 7.6b. Note that the



(a) Scatter plot relating the KK scale with warp factor. The colour profile reflects the di-Higgs cross section modification away from the SM expectation. This is done to highlight the cross section ratio value for the points that obey the SM like bound set in Eqn. (7.6). The highlighted hexagon points have $\sigma(HH)/\sigma(HH)_{\text{SM}}$ values within the interval $[0.961, 1.172]$, which is the envelope of cross section modifications that we observe.

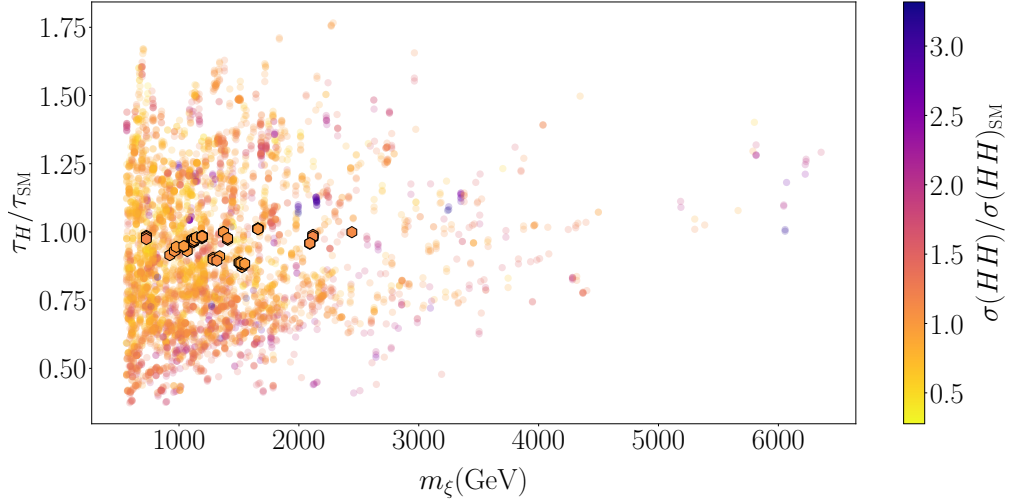


(b) Scatter plot relating top quark and Higgs mass, with di-Higgs cross section modification at 13 TeV shown as colour shading, where the highlighted hexagon points have $\sigma(HH)/\sigma(HH)_{\text{SM}}$ values within the interval $[0.961, 1.172]$.

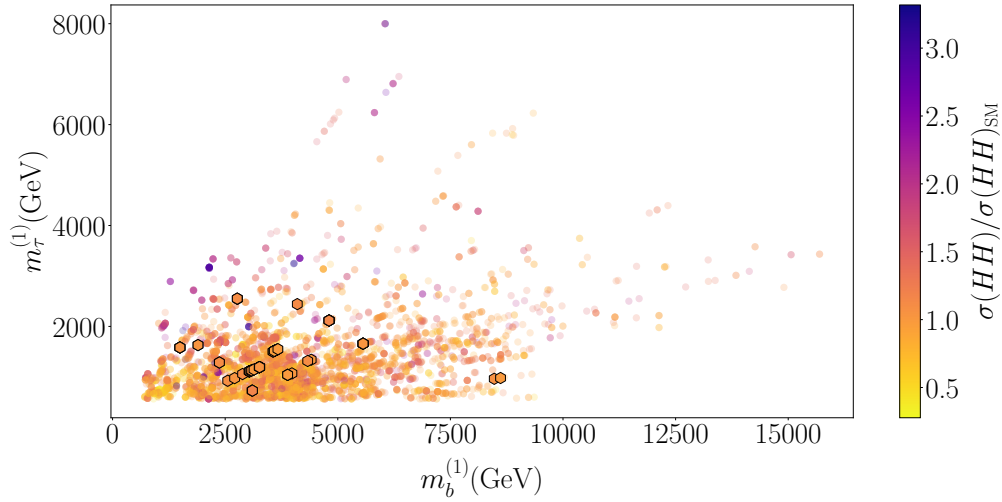
Figure 7.5: Relative cross section correlations with the UV and IR attributes.

differential evolution algorithm populates parameter regions that fall outside the LHC analyses that we consider in Sec. 7.1, i.e. the fact that these states might be accessible already with data recorded by the LHC experiments does not rule out

the model, but would be a sign of additional tuning. This shows that searches for excited leptons and quarks as they are already pursued by the LHC experiments are crucial tools in further constraining this model.



(a) Scatter plot correlating exotic mass scale m_ξ with the di-Higgs cross section modification. The lowest exotic states are summarised via $m_\xi = \min(m_{\psi D}, m_{\tau^{(1)}}, m_{b^{(1)}})$.



(b) Scatter plot relating top quark and Higgs mass, with di-Higgs cross section modification at 13 TeV shown as colour shading, where the highlighted hexagon points have $\sigma(HH)/\sigma(HH)_{SM}$ values within the interval $[0.961, 1.172]$.

Figure 7.6: Exotic scatter plots showing the lowest available mass states and relevant fields.

7.4 Gauge Coupling RGE Running in (4D & 5D) EFTs

One of the consistency arguments that is highlighted in the discussed $SO(11)$ GHGUT scenario is the tree-level prediction of the Weinberg angle

$$\sin^2 \theta_W = \frac{3}{8} \quad (7.10)$$

as a consequence of an (intermediate) $SU(5)$ unification [171]. In perturbative theories, reproducing this value in the UV is critical to support the hypothesis of unification. The relation of Eqn. (7.10) receives perturbative corrections that will modify its value in the UV as a function of the theories fundamental input parameters. However, the dominant relation between UV and TeV scales is captured in the renormalisation group running of $\sin^2 \theta_W$, i.e. starting from the observed value at the electroweak scale and including corrections from new particles becoming accessible we should approach the relation of Eqn. (7.10) or discover the necessity of additional model constraints.

Therefore the following questions naturally arise. How do we evolve the gauge couplings within the extra dimensions, taking into account the Hosotani breaking? How does $\sin \theta_W$ evolve and is the ad-hoc implementation of its electroweak value consistent with its GUT prediction?

Ideally we would like to check the full energy range of the theory (i.e. $\mu \in [M_Z, M_{\text{GUT}}]$), but due to the 6D hybrid nature of the theory we have some additional complications. Approaching this in the traditional 4D EFT way, this interpretation will only be valid up to $1/L_5$, since it is the scale at which the 5D structure becomes apparent. Therefore the maximum energy interval in which we can use a 4D EFT as an approximation to the 6D theory is only valid within the energy range $\mu \in [M_Z, 1/L_5]$.

At the TeV scale the model is effectively the 4D SM and we evolve the parameters according to the 4D theory properties. This is admissible until we approach the M_{KK_5} where the 5D structure becomes apparent. At this stage we could continue using 4D RGE equations including the additional KK states that have non-trivial quantum numbers under the SM gauge group. Alternatively, one can directly work in the 5D approximation theory to obtain identical results, see Fig. 7.7. Above the compactification scale $\sim 1/L_5$ additional KK states of the 5D theory become accessible which correct the behavior of the 5D running.

The 5D regime is determined by the Pati-Salam symmetry group together with the active KK states and thresholds. 6D compactification effects are not relevant

in this context as $M_{\text{KK}_5} \ll M_{\text{GUT}} \sim 1/R_6$. A complete evolution to the GUT scale in our one-loop analysis is not possible when there is a scale

$$\Lambda_{\text{Max}} \sim \frac{16\pi^2}{g_5^2} \ll M_{\text{GUT}}, \quad (7.11)$$

which signifies a loss of perturbative control before the unification scale. We can adopt this scale as a lower bound on the GUT scale itself and use the difference of the Weinberg angle with respect to Eqn. (7.10) as a measure of unification.

To analyse the 5D running we approximate our 6D theory down to a 5D theory dictated by the z coordinate. To do this we examine our parity assignments in the original model and look at the gauge bosons which have masses of the order of $\mathcal{O}(M_{\text{KK}_5})$. To this extent, the gauge-related states with masses $\mathcal{O}(M_{\text{KK}_5})$ relevant for our discussion are gauge fields that transform under the symmetries

$$A_M \sim \begin{cases} G_{\text{PS}}/G_{\text{SM}} \\ G_{\text{SM}} \\ SO(5)/SO(4) \end{cases}. \quad (7.12)$$

In the theory's 5D regime, these states have defined transformation properties under the Pati-Salam G_{PS} symmetry. The coset $SO(5)/SO(4)$ sector which transforms as $(1, \mathbf{2}, \mathbf{2})$ under G_{PS} which eventually triggers electroweak symmetry breaking via the Hosotani mechanism induce corrections to the gauge couplings g_{2L}, g_{2R} .

Note that the ν gauge component KK states of $SO(5)/SO(4)$ obtain large masses via brane interactions (see Ref. [116]) and are not relevant for our discussion.

Analogously, the fermionic matter content of the approximated theory is determined by the G_{PS} symmetry, and consists of states which have masses of the order of $\mathcal{O}(M_{\text{KK}_5})$ or less

$$\begin{aligned} &(\mathbf{4}, \mathbf{2}, \mathbf{1})_{L,R}, \quad (\mathbf{4}, \mathbf{1}, \mathbf{2})_{L,R}, \\ &(\mathbf{6}, \mathbf{1}, \mathbf{1})_{L,R}^{(+)}, \quad (\mathbf{6}, \mathbf{1}, \mathbf{1})_{L,R}^{(-)}, \\ &(\mathbf{1}, \mathbf{2}, \mathbf{2})_{L,R}^{(+)}, \quad (\mathbf{1}, \mathbf{2}, \mathbf{2})_{L,R}^{(-)}, \quad (\mathbf{1}, \mathbf{1}, \mathbf{1})_{L,R}^{(+)}, \quad (\mathbf{1}, \mathbf{1}, \mathbf{1})_{L,R}^{(-)}, \end{aligned} \quad (7.13)$$

which all originate from the $\Psi_{\mathbf{32}}^\alpha, \Psi_{\mathbf{11}}^\beta, \Psi_{\mathbf{11}}^{\prime\beta}$ bulk fields.

We divide the full energy range in which the 5D EFT is valid (i.e. $[M_Z, \Lambda_{\text{Max}}]$) into two regions. The first region is given by the energy range in which the 5D EFT is well-approximated by its 4D EFT counterpart. This region's cutoff energy

is dictated by the M_{KK_5} mass threshold around where the gauge bosons of the Pati-Salam symmetry become available. This corresponds to a scale given by the first non-zero mode of the photon tower.¹ Therefore we can consider the 1st region as being very well approximated by a G_{SM} theory with additional matter states (that correspond to the θ_H shifted KK towers), which is valid between $[M_Z, M_{\text{KK}_5}]$.

The remaining energy range $[M_{\text{KK}_5}, \Lambda_{\text{Max}}]$ is then described by the 5D G_{PS} , where the cutoff represents the energy at which we lose perturbative control of the 5D theory, and the more fundamental 6D theory is required.

Overall the tower of theories is schematically shown in Fig. 7.7. We will now proceed to evolve the RGEs in the broken SM phase via its 4D variant, use the evolved values as boundary conditions for the 5D theory, and finally examine the Weinberg angle at the cutoff.

We will now proceed to evolve the RGEs in the broken SM phase via its 4D variant, use the evolved values as boundary conditions for the 5D theory, and finally examine the Weinberg angle at the cutoff.

7.4.1 Methodology

To numerically analyse the RGE runnings along these lines, we proceed as follows, evolving from the IR to the UV. Starting at M_Z , we set $\alpha_S, \alpha_{\text{EM}}, \sin \theta_W$ via their experimental values [172, 173]

$$\begin{aligned} \alpha_S &= 0.11822, & (\alpha_{\text{EM}})^{-1} &= 127.916, \\ \sin^2 \theta_W &= 0.23122, \end{aligned} \tag{7.14}$$

where $\alpha_S, \alpha_{\text{EM}}$ denote the strong and electric structure constants, respectively.

We then evolve $\alpha_S, \alpha_{\text{EM}}, \sin \theta_W$ via the G_{SM} RGEs in the broken phase (using the formalism outlined in [174]) until we reach the energy scale at which a new KK state becomes available. We choose to perform the RGE runnings in the broken phase since the surviving gauge symmetry of the brane, post Hosotani breaking, is $SU(3)_C \times U(1)_{\text{EM}}$.

Upon reaching the threshold, we calculate the new β_i function contributions arising from the new KK tower state. We then proceed to run the modified RGEs and repeat this procedure until we reach the M_{KK_5} mass threshold. At this point

¹ For warp factor choices $z_L > 10$ that yield realistic low energy spectra, the solutions for the 1st photon mode and the PS gauge bosons are almost degenerate.

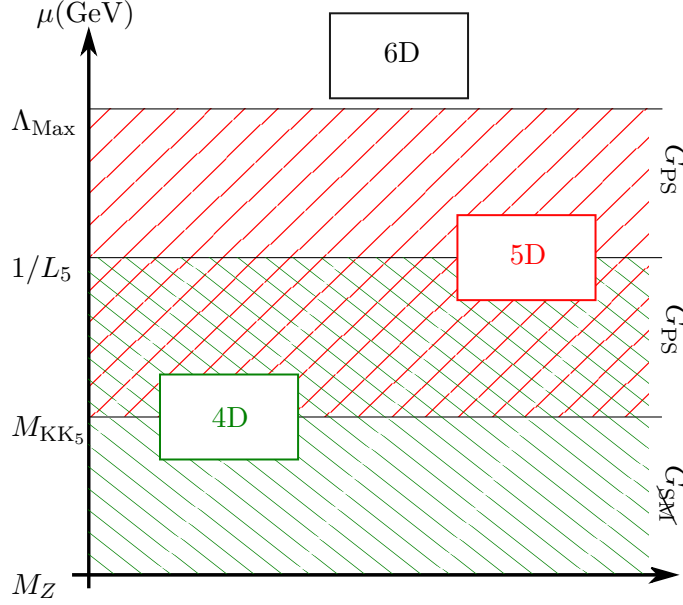


Figure 7.7: Tower of EFTs that approximate the UV 6D theory. The 4D description is valid within $[M_Z, M_{KK_5}]$ with $G_{SM} \equiv SU(3)_C \times U(1)_{EM}$ gauge symmetry and within $[M_{KK_5}, 1/L_5]$ with G_{PS} gauge symmetry. The 5D description is valid within $[M_{KK_5}, \Lambda_{Max}]$ with a G_{PS} gauge symmetry. Above Λ_{Max} the full 6D description comes into effect.

we calculate the threshold corrections λ_i corresponding to integrating out any additional states lying at M_{KK_5} along with the heavy states corresponding to the $G_{PS} \rightarrow G_{SM}$ breaking.

The electroweak couplings of the unbroken $SU(2)_L \times U(1)_Y$ phase, α_Y, α_L are related to their broken phase counterparts by

$$\begin{aligned} \frac{1}{\alpha_Y(\mu)} \Big|_{\mu=M_{KK_5}} &= \frac{3}{5}(1 - \sin^2 \theta_W) \frac{1}{\alpha_{EM}(\mu)} \Big|_{\mu=M_{KK_5}}, \\ \frac{1}{\alpha_L(\mu)} \Big|_{\mu=M_{KK_5}} &= \sin^2 \theta_W \frac{1}{\alpha_{EM}(\mu)} \Big|_{\mu=M_{KK_5}}. \end{aligned} \quad (7.15)$$

Note that this is done in the 4D framework, and where we have adopted the standard 3/5 GUT normalisation for the hypercharge coupling.

With this, we can find the values of the Pati-Salam gauge couplings $\alpha_4, \alpha_{2L}, \alpha_{2R}$

at the M_{KK_5} scale

$$\begin{aligned}\frac{1}{\alpha_{4C}} &= \frac{1}{\alpha_{3C}} + \frac{1}{12\pi}, \\ \frac{1}{\alpha_{2R}} &= \frac{5}{3} \frac{1}{\alpha_{1Y}} - \frac{2}{3} \frac{1}{\alpha_{3C}} + \frac{8}{45\pi},\end{aligned}\tag{7.16}$$

(α_{2L} is already given as the coupling of the $SU(2)_L$ group), which then serve as the boundary conditions for the 5D theory, where,

$$g_{5D} \sqrt{L_5} = g_{4D} \Big|_{\mu=M_{\text{KK}_5}}.\tag{7.17}$$

With the boundary conditions in place, we now evolve the PS couplings $\alpha_4, \alpha_{2L}, \alpha_{2R}$ within the 5D formalism introduced in Ref. [111] in the energy range $[M_{\text{KK}_5}, \Lambda_{\text{Max}}]$. Using this running we then extract the coupling values and compare the Weinberg angle

$$\sin^2 \theta_W(\mu) = \left(\frac{1}{\alpha_{2L}\alpha_{4C}} \left(\alpha_{2L}\alpha_{4C} + \frac{2}{3}\alpha_{2L}\alpha_{2R} + \alpha_{2R}\alpha_{4C} - \frac{5}{3}\alpha_{2L}\alpha_{2R}\alpha_{4C} \frac{8}{45\pi} \right) \right)^{-1} \Big|_{\mu}.\tag{7.18}$$

to its predicted GUT value.

Before we detail the RGEs in detail below, it is instructive to define a reference point that will guide our discussion. To get a qualitative understanding of how the KK thresholds modify the RG evolution of our theory, we consider the set of parameters from [116], which provide a SM-like physical mass spectrum

$$\begin{aligned}\mathcal{P}_{\text{sample}} := & \left\{ k = 89130, z_L = 35, c_1 = 0, c_2 = -0.7, \right. \\ & c'_0 = 0.5224, \mu_1 = 11.18, \mu_{11} = 0.108, \\ & \left. \tilde{\mu}_2 = 0.7091, \mu'_{11} = 0.108 \right\}.\end{aligned}\tag{7.19}$$

This choice results in the tower of states shown in Fig. 7.8, which we will use as a reference point in the following.

7.4.2 4D Approximation and RGEs

By performing the RGE analysis in the broken phase, we evolve the QCD gauge coupling g_3 , along with the electromagnetic coupling g_{EM} , which in turn determines the Weinberg angle RGE evolution $\sin \theta_W$ via the matter content. To facilitate an unambiguous transition to the Pati-Salam phase we then proceed to relate the latter to the unbroken $U(1)_Y$ hypercharge and $SU(2)_L$ weak couplings.

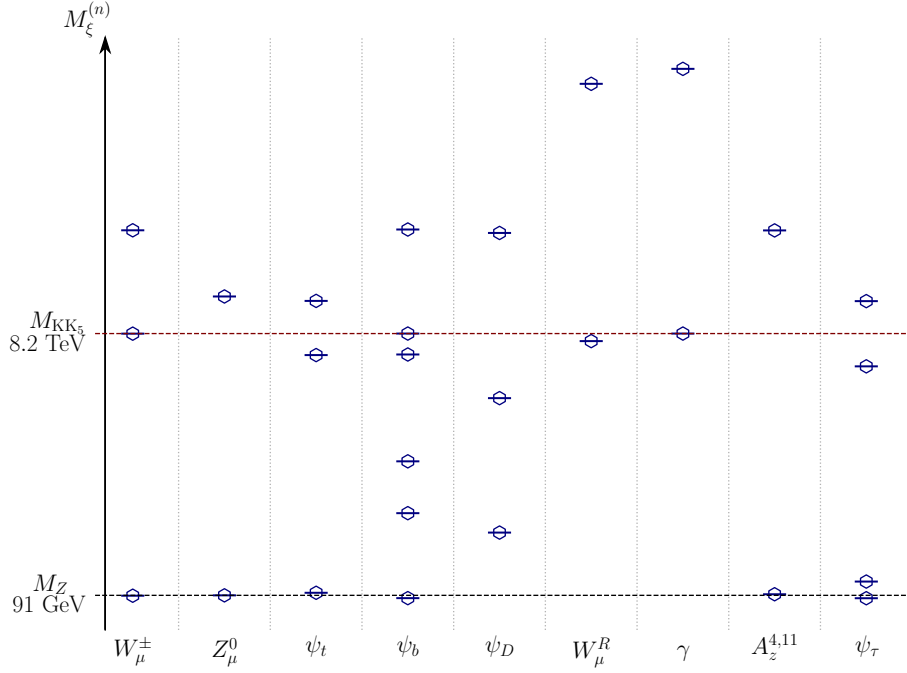


Figure 7.8: Tower of states from M_Z to the next states above M_{KK_5} . The labels on the x axis indicate the relevant fermionic and boson fields, and the markers represent the mass value of the respective KK tower state. The labels stand for: W_μ^\pm is the W boson tower, Z_μ^0 is the Z boson tower, ψ_t is the top quark tower, ψ_b is the bottom quark tower, ψ_D is the 'dark fermion' multiplet tower, W_μ^R is the Pati-Salam $SU(2)_R$ W boson tower of states, γ_μ is the photon tower of states, $A_z^{4,11}$ is the Higgs tower of states, and ψ_τ is the tau tower of states.

The renormalisation group equations are expressed in terms of the gauge couplings g_i , as,

$$\mu \frac{\partial g_i}{\partial \mu} = \beta_i(g_i, \mu), \quad \frac{1}{\alpha_i} = \frac{4\pi}{g_i^2}, \quad (7.20)$$

where β_i are the beta coefficients arising from the group representations of the $SU(N)$ gauge group. The QCD beta function β_{g_3} , has the generic form arising from a $SU(N)$ gauge theory [175] with fermions and scalars in representations F_i and S_i

$$\beta_{g_3} = (+) \frac{g_3^3}{(4\pi)^2} \left\{ -\frac{11}{3} C_2(SU(3)) + \frac{4}{3} \kappa S_2(F_i) + \frac{1}{6} \eta S_2(S_i) \right\}, \quad (7.21)$$

where $C_2(G_i)$ is the quadratic Casimir of the group G_i , $S_2(F_i)$, $S_2(S_i)$ are the Dynkin indices for the fermion/scalar representations, $\kappa = 1/2, 1$ for Weyl and

Dirac fermions, and $\eta = 1, 2$ for real and complex scalar fields.

For the RGE runnings of the QED gauge coupling g_{EM} and Weinberg angle $\sin \theta_W$, we use the formalism presented in [174]. The QED beta function is expressed as

$$\beta_{g_{\text{EM}}} = \frac{g_{\text{EM}}^3}{(4\pi)^2} \frac{1}{6} \left\{ \sum_i N_i^c \gamma_i Q_i^2 \right\}, \quad (7.22)$$

where N_i^c are the fermionic colour factors, Q_i are the EM charges and $\gamma_i = \{-22, 8, 4, 2\}$ are factors corresponding to massless gauge bosons, Dirac/chiral fermions and complex scalar fields.

We begin our RGE evolution at $M_Z \simeq 91 \text{ GeV}$. The QCD and QED couplings have beta function coefficients

$$\beta_{g_3} = -7 \frac{g_3^3}{(4\pi)^2}, \quad \beta_{g_{\text{EM}}} = 22 \frac{g_{\text{EM}}^3}{(4\pi)^2}, \quad (7.23)$$

which are determined by the SM matter content and their $SU(3)_C$ and $U(1)_{\text{EM}}$ charges. As we evolve the couplings and encounter new states, the beta functions pick up new contributions depending on the state that we encounter. The additional contributions for the QCD beta function have the form

$$\beta_{g_3} \rightarrow \beta_{g_3} + \begin{cases} -\frac{11}{3} C_2(SU(3)), \\ +\frac{4}{3} \kappa S_2(F_i) \cdot N_G, \\ +\frac{1}{6} \sum \eta S_2(S_i), \end{cases} \quad (7.24a)$$

where each conditional branch is introduced if we encounter either a gluon, a fermionic or a scalar state. Analogously, for the QED beta function we have,

$$\beta_{g_{\text{EM}}} \rightarrow \beta_{g_{\text{EM}}} + \begin{cases} -22 N_i^c \gamma_i Q_i^2, \\ +8 N_i^c \gamma_i Q_i^2 \cdot N_G, \\ +2 N_i^c \gamma_i Q_i^2. \end{cases} \quad (7.24b)$$

In Eqns. (7.24), we have introduced the N_G factor in the fermionic contributions to account for the number of matter generations present in the model. In this paper we examine the $N_G = 1, 3$ cases. For $N_G = 3$ we assume that all 3 SM generations are present and that the mass differences between the KK states corresponding to the different generations is negligible for the non-zero modes. Similarly for $N_G = 1$ we are assuming that there exists some mass separation mechanism between the 3rd family and the other two which effectively decouples the non-zero states from the theory, leaving only the 3rd as the relevant one as done in [116]. Comparing

the different assumptions will point towards future model building directions (see below) in the light of expected unification.

With this framework in place we can now form a piecewise system of differential equations valid over different energy ranges. We then solve each branch individually and use the value at the boundary of the previous region as the boundary condition for the new branch.

As an example let's look at the QCD coupling g_3 , and let's suppose that the first two relevant states that we encounter are the 1st and 2nd excited bottom quark states which sit at $m_b^{(1)}, m_b^{(2)}$. For this energy range we'll create two subranges $[M_Z, m_b^{(1)}]$ and $[m_b^{(1)}, m_b^{(2)}]$, to which we associate the piecewise system of differential equations,

$$\left\{ \begin{array}{l} \mu \frac{\partial g_3}{\partial \mu} = -7 \frac{g_3^3}{(4\pi)^2}, \quad \mu \in [M_Z, m_b^{(1)}], \quad g_3(M_Z) = \sqrt{4\pi\alpha_S^{\text{exp}}} \\ \mu \frac{\partial g_3}{\partial \mu} = \left(-7 + \frac{4}{3} \cdot \frac{1}{2} \cdot \frac{1}{2} \cdot 3 \right) \frac{g_3^3}{(4\pi)^2}, \quad \mu \in [m_b^{(1)}, m_b^{(2)}], \quad g_3(m_b^{(1)}) = g_3^{\text{Nsol}}(m_b^{(1)}), \\ \dots \end{array} \right. \quad (7.25)$$

The “Nsol” superscript refers to the value of the numerical solution from the previous branch at the upper boundary. The 1st branch is solved numerically using the initial experimental boundary condition to evolve the value of g_3 up to $m_b^{(1)}$. Once we have reached it, we use the last value to solve and evolve the next branch up to its upper limit. This is done until we reach the M_{KK_5} threshold where we switch to the 5D formalism. Note that if a state is not charged under QCD the branch is still created and run with the previous branch's β coefficient.

We treat g_{EM} in the exact same manner, creating a new branch whenever we encounter a state and performing the running with the updated β_{EM} function.

As shown in [174] the Weinberg angle's RGE running is fully determined by its experimental value at M_Z , the matter content of the theory, and the running of α_{EM}

$$\begin{aligned} \sin^2 \theta_W(\mu) = \sin^2 \theta_W(\mu_0) & \left[1 + \frac{\alpha_{\text{EM}}(\mu)}{24\pi \sin^2 \theta_W(\mu_0)} \right. \\ & \left. \times \sum_i N_i^c \gamma_i Q_i (T_i - Q_i \sin^2 \theta_W(\mu_0)) \ln \frac{\mu_0^2}{\mu^2} \right], \end{aligned} \quad (7.26)$$

where T_i is the 3rd component of the weak isospin ($T_3 = +1/2$ for u_i, ν_i , $T_3 = -1/2$ for d_i, e_i , $T_3 = \pm 1$ for W^\pm).

Name	$SU(3)_C$ Charge	$U(1)_{EM}$ Charge	T_3
Tau (τ)	1	-1	-1/2
Bottom (b)	3	-1/3	-1/2
Top (t)	3	+2/3	+1/2
Neutrino (ν)	1	0	+1/2
W^\pm	1	± 1	± 1
Dark Fermion ψ_D^ν	1	0	+1/2
Dark Fermion ψ_D^u	3	+2/3	+1/2
Dark Fermion $\psi_D^{\bar{u}}$	$\bar{3}$	-2/3	-1/2
Dark Fermion ψ_D^e	1	-1	+1/2

Table 7.2: Charge assignments for fields contributing to the RGE runnings.

Therefore, using the derived numerical solution for α_{EM} we can now create an analogous piecewise solution for $\sin \theta_W$ based on the matter content present within the respective branch. For our hypothetical example, the piecewise Weinberg angle solution is dependent on the branch solutions of $\alpha_{EM}(\mu)$ with,

$$\left\{ \begin{array}{l} s_W^2(M_Z) \left[1 + \frac{\alpha_{EM}(\mu)}{24\pi s_W^2(M_Z)} \cdot \sum_{i \in SM} N_i^c \gamma_i Q_i (T_i - Q_i s_W^2(M_Z)) \ln \frac{M_Z^2}{\mu^2} \right], \\ \quad \mu \in [M_Z, m_b^{(1)}], \quad s_W^2(M_Z) = 0.2213. \\ s_W^2(m_b^{(1)}) \left[1 + \frac{\alpha_{EM}(\mu)}{24\pi s_W^2(m_b^{(1)})} \cdot \sum_{i \in SM \oplus b^1} N_i^c \gamma_i Q_i (T_i - Q_i s_W^2(m_b^{(1)})) \ln \frac{(m_b^{(1)})^2}{\mu^2} \right], \\ \quad \mu \in [m_b^{(1)}, m_b^{(2)}], \quad s_W^2(m_b^{(1)}) = (s_W^2)^{Nsol}(m_b^{(1)}). \\ \dots \end{array} \right. \quad (7.27)$$

where s_W^2 is shorthand for $\sin^2 \theta_W$, the 'Nsol' convention applies as previously stated, and the index i runs over the matter representations that have a mass below the upper limit of the current branch.

The fields' charges under $SU(3)_C \times U(1)_{EM}$, along with their T_3 values are given in Tab. 7.2.

When we reach M_{KK_5} we can then recover the hypercharge and weak couplings

via the evolved values of α_{EM} and $\sin \theta_W$ via,

$$\begin{aligned} \frac{1}{\alpha_{2L}(\mu)} &= \frac{1}{\alpha_{\text{EM}}(\mu)} \sin^2 \theta_W(\mu), \\ \frac{1}{\alpha_{1Y}(\mu)} &= \frac{3}{5} \frac{1}{\alpha_{\text{EM}}(\mu)} (1 - \sin^2 \theta_W(\mu)), \end{aligned} \quad (7.28)$$

which relate the unbroken and broken gauge couplings.

Since M_{KK_5} is the energy threshold at which the Pati-Salam states become available, we transition to the PS phase where we obtain the gauge couplings based on the symmetry breaking $SU(4)_C \times SU(2)_L \times SU(2)_R \rightarrow SU(3)_C \times SU(2)_L \times U(1)_Y$. This in turn provides us with the aforementioned 4D/5D boundary conditions of Eqn. (7.16) evaluated at M_{KK_5} .

Following this procedure, the G_{SM} gauge coupling runnings in the energy range $[M_Z, \sim M_{\text{KK}_5}]$ for the spectrum of Fig. 7.8 is shown in Fig. 7.9. For an individual breakdown of the couplings in their “translated” unbroken phase and their broken runnings, see Appendix B.2.

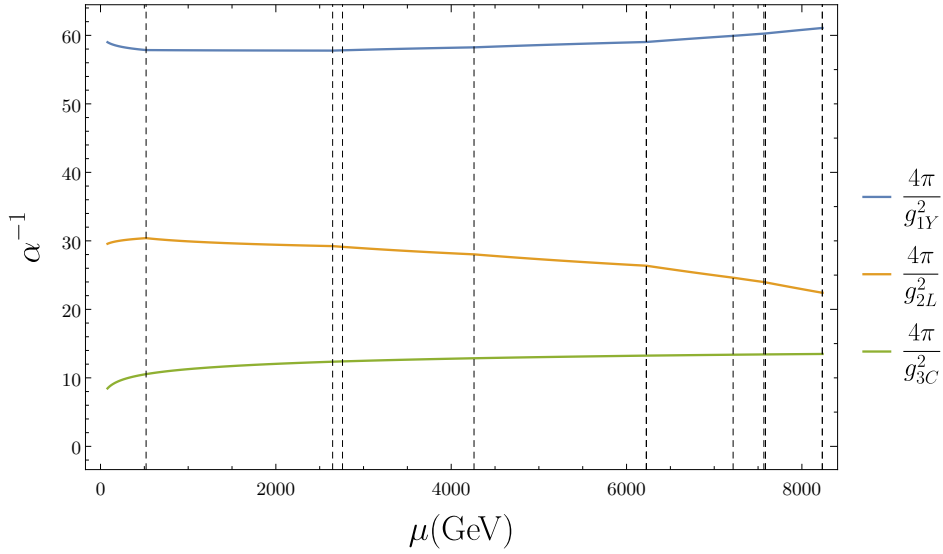


Figure 7.9: RGE evolution for the piecewise SM couplings g_{3C}, g_{2L}, g_{1Y} with the different β function changes at the multiple encountered KK states marked as dotted lines. Note that the piecewise forms for g_{2L}, g_{1Y} are obtained via Eqn. (7.26).

7.4.3 5D RGEs and Cut-offs

We now turn to the 5D running with the evolved boundary conditions at M_{KK_5} . The matter content in our approximated 5D theory was mentioned earlier in Eqn. (7.13),

in addition to the $(1, \mathbf{2}, \mathbf{2}) \sim SO(5)/SO(4)$ state.

The formalism in [111] specifies the 5D RGE running for generic 5D field parity assignments on a $S^1/\mathbb{Z}_2 \times \mathbb{Z}'_2$ orbifold. Since we started with a fully-defined 6D theory on the $\mathcal{M}_4 \times T^2/\mathbb{Z}_2$ orbifold, this has the consequence that the projected $S^1/\mathbb{Z}_2 \times \mathbb{Z}'_2$ assignments arising from our 6D \rightarrow 5D approximation, are fully determined by the corresponding translational and reflection assignments U, P that act along the warped direction in the full UV theory.

To that extent in the 6D theory we have U_5 and P_0 , which are related via the consistency condition $U_5 = P_0 P_1 = P_0^2$, or equivalently $U_5 = P_0 P'_0$, where $P'_0 = P_0 = U_5 P_0$ will now act as the *implicit* \mathbb{Z}'_2 parity assignment in the approximated 5D theory due to the way the model is set up. This is then changed by the additional complexity introduced by the η assignments acting on the spinorial fields, with $P_i \rightarrow P_i^{\text{sp}}$. For the fermions that originate from the $\alpha = \{1, 2, 3\}$ or $\beta, \beta' = \{1, 2, 3\}$ representations, we have an identical set of η assignments (either $+1, -1$ for each generation) which results in the parity assignment being unaffected by the η 's. For fermions that originate from the $\Psi_{\mathbf{32}}^4$ representation, we need to look at the effective assignments (the ones including η_j^4 , for $j = 0, 1, 2, 3$) to fully understand the parity breaking. Examining the ones that interest us (i.e. η_0^4, η_1^4), we have the new parity assignments,

$$\tilde{P}_0^{\text{sp}} = \eta_0^4 P_0^{\text{sp}} = (-1) P_0^{\text{sp}} \quad \tilde{P}_1^{\text{sp}} = \eta_1^4 P_1^{\text{sp}} = (+1) P_0^{\text{sp}}, \quad (7.29)$$

which in turn define the effective spinorial U_5 via the consistency conditions,

$$U_5^{\text{sp}} = \tilde{P}_0^{\text{sp}} \tilde{P}_1^{\text{sp}} = ((-1) P_0^{\text{sp}})((+1) P_0^{\text{sp}}) = (\tilde{P}_0^{\text{sp}})((-1) \tilde{P}_0^{\text{sp}}) \equiv \tilde{P}_0 \tilde{P}'_0. \quad (7.30)$$

Therefore, when it comes to fields originating from $\Psi_{\mathbf{32}}^4$, we can take the parity assignments of \mathbb{Z}'_2 under $S^1/\mathbb{Z}_2 \times \mathbb{Z}'_2$, as being the opposite ones of \tilde{P}_0^{sp} . For example say we're looking at $(\mathbf{4}, \mathbf{2}, 1)$ which in the original theory has the effective parity assignments $(+, -)$ under $(\tilde{P}_0^{\text{sp}}, \tilde{P}_1^{\text{sp}})$. Therefore in our approximated theory $(\mathbf{4}, \mathbf{2}, 1)$ will have $(+, (-) \times (+)) = (+, -)$ under the new \mathbb{Z}_2 assignments.

Therefore, under the $S^1/\mathbb{Z}_2 \times \mathbb{Z}'_2$ approximation the fermionic fields have the parity assignments shown in Tab. 7.3. The gauge fields and the respective scalar degrees of freedom (which show up as remnants from the 6D theory, or as the 5th dimension gauge component) have parity assignments under $S^1/\mathbb{Z}_2 \times \mathbb{Z}'_2$ as shown in Tabs. 7.4 and 7.5.

It is worth taking a pause and examining what we have done. More specifically, in terms of the gauge boson parity assignment, we have treated them separately

G_{PS} rep.	Parent Field	$(\mathbb{Z}_2, \mathbb{Z}'_2)$	G_{PS} rep.	Parent Field	$(\mathbb{Z}_2, \mathbb{Z}'_2)$
$(\mathbf{4}, \mathbf{2}, 1)_L$	$\Psi_{\mathbf{32}}^\alpha$	$(+, +)$	$(\mathbf{4}, \mathbf{2}, 1)_L$	$\Psi_{\mathbf{32}}^4$	$(+, -)$
$(\mathbf{4}, \mathbf{2}, 1)_R$	$\Psi_{\mathbf{32}}^\alpha$	$(-, -)$	$(\mathbf{4}, \mathbf{2}, 1)_R$	$\Psi_{\mathbf{32}}^4$	$(-, +)$
$(\mathbf{4}, 1, \mathbf{2})_R$	$\Psi_{\mathbf{32}}^\alpha$	$(+, +)$	$(\mathbf{4}, 1, \mathbf{2})_L$	$\Psi_{\mathbf{32}}^4$	$(-, +)$
$(\mathbf{4}, 1, \mathbf{2})_L$	$\Psi_{\mathbf{32}}^\alpha$	$(-, -)$	$(\mathbf{4}, 1, \mathbf{2})_R$	$\Psi_{\mathbf{32}}^4$	$(+, -)$

G_{PS} rep.	Parent Field	$(\mathbb{Z}_2, \mathbb{Z}'_2)$	G_{PS} rep.	Parent Field	$(\mathbb{Z}_2, \mathbb{Z}'_2)$
$(\mathbf{6}, 1, 1)_R^{(+)}$	$\Psi_{\mathbf{11}}^\beta$	$(+, +)$	$(1, \mathbf{2}, \mathbf{2})_{L,R}^{(+,-)}$	$\Psi_{\mathbf{11}}^{\beta'}$	$(+, +)$
$(\mathbf{6}, 1, 1)_L^{(-)}$	$\Psi_{\mathbf{11}}^\beta$	$(+, +)$	$(1, 1, 1)_{R,L}^{(+,-)}$	$\Psi_{\mathbf{11}}^{\beta'}$	$(+, +)$
$(\mathbf{6}, 1, 1)_L^{(+)}$	$\Psi_{\mathbf{11}}^\beta$	$(-, -)$	$(1, \mathbf{2}, \mathbf{2})_{R,L}^{(+,-)}$	$\Psi_{\mathbf{11}}^{\beta'}$	$(-, -)$
$(\mathbf{6}, 1, 1)_R^{(-)}$	$\Psi_{\mathbf{11}}^\beta$	$(-, -)$	$(1, 1, 1)_{L,R}^{(+,-)}$	$\Psi_{\mathbf{11}}^{\beta'}$	$(-, -)$

Table 7.3: Fermion parity assignments under $S^1/\mathbb{Z}_2 \times \mathbb{Z}'_2$.

G_{SM} rep.	Parent Field	$(\mathbb{Z}_2, \mathbb{Z}'_2)$
$(1, \mathbf{3}, 0)$	$A_\mu \in G_{\text{SM}}$	$(+, +)$
$(\mathbf{8}, 1, 0)$	$A_\mu \in G_{\text{SM}}$	$(+, +)$
$(1, 1, 0)$	$A_\mu \in G_{\text{SM}}$	$(+, +)$

G_{SM} rep.	Parent Field	$(\mathbb{Z}_2, \mathbb{Z}'_2)$
$(\mathbf{3}, 1, 0)$	$A_\mu \in G_{\text{PS}}/G_{\text{SM}}$	$(-, +)$
$(\bar{\mathbf{3}}, 1, 0)$	$A_\mu \in G_{\text{PS}}/G_{\text{SM}}$	$(-, +)$

G_{PS} rep.	Parent Field	$(\mathbb{Z}_2, \mathbb{Z}'_2)$
$(1, \mathbf{2}, \mathbf{2})$	$A_\mu^{a,11} \in SO(5)/SO(4)$	$(-, -)$
$(1, 1, \mathbf{3})$	$W_R^\pm, Z_R \in G_{\text{PS}}/G_{\text{SM}}$	$(-, +)$

Table 7.4: Gauge boson parity assignment under $S^1/\mathbb{Z}_2 \times \mathbb{Z}'_2$. Note that we have to treat the G_{PS} , and G_{SM} representations separately due to the mixed parity assignments in the full 6D model.

G_{PS} rep.	Parent Field	$(\mathbb{Z}_2, \mathbb{Z}'_2)$	G_{PS} rep.	Parent Field	$(\mathbb{Z}_2, \mathbb{Z}'_2)$
$(\mathbf{15}, 1, 1)$	$A_z \in G_{\text{PS}}$	$(-, -)$	$(\mathbf{15}, 1, 1)$	$A_\nu \in G_{\text{PS}}$	$(-, -)$
$(1, 1, \mathbf{3})$	$A_z \in G_{\text{PS}}$	$(-, -)$	$(1, 1, \mathbf{3})$	$A_\nu \in G_{\text{PS}}$	$(-, -)$
$(1, \mathbf{3}, 1)$	$A_z \in G_{\text{PS}}$	$(-, -)$	$(1, \mathbf{3}, 1)$	$A_\nu \in G_{\text{PS}}$	$(-, -)$

G_{PS} rep.	Parent Field	$(\mathbb{Z}_2, \mathbb{Z}'_2)$
$(1, \mathbf{2}, \mathbf{2})$	$A_z^{4,11} \in SO(5)/SO(4)$	$(+, +)$

Table 7.5: Scalar parity assignment under $S^1/\mathbb{Z}_2 \times \mathbb{Z}'_2$. In the 5D RGE formalism they are treated as scalars originating from either the gauge boson projections or as remnants from the 6D approximation.

either as part of the G_{SM} sub-algebra or the coset $G_{\text{PS}}/G_{\text{SM}}$, even though we are computing the Pati-Salam RGEs. We do this since we are effectively forced to consider how the elements in the subset and coset affect the RGEs due to the split parity assignments. I.e. we are integrating out all the Pati-Salam degrees of freedom, but we need to treat them separately due to their isometry transformation properties in the 5th dimension, dictated by the formalism in [111].

The 5D RGEs have the general form

$$\frac{1}{g_a^2(\mu)} = \frac{\pi L_5}{g_{a_{5D}}^2(\Lambda_{\text{Max}})} + \frac{1}{8\pi^2} \sum_{\xi} \bar{\Delta}_a(\xi; \mu, \ln \Lambda_{\text{Max}}), \quad (7.31)$$

where g_a is the 4D gauge coupling corresponding to the respective SU group in $SU(4)_C \times SU(2)_L \times SU(2)_R$ (where a denotes $\sim 4C, 2L, 2R$), μ is the renormalisation scale, $g_{a_{5D}}^2$ is the 5D gauge coupling with mass dimension M^1 , Λ_{Max} is the cutoff value of the 5D EFT, and $\bar{\Delta}_a$ are the various one loop corrections due to the matter fields in the theory, which are generically denoted as $\xi \in \{\phi, \psi, A_\mu\}$ with respect to scalars, fermions and gauge bosons. We will come back to specify the forms for each of the $\bar{\Delta}_a$'s.

The cutoff Λ_{Max} is defined as the scale at which we lose perturbative control of the theory,

$$\Lambda_{\text{Max}} = \frac{16\pi^2}{g_{a_{5D}}^2(\Lambda_{\text{Max}})}, \quad (7.32)$$

where the formal expansion parameter becomes too large (see Ref.[176]). To get a numerical value for Λ_{Max} we can use the RGEs evaluated at M_{KK_5} .

More specifically, we have,

$$\begin{aligned} \frac{1}{g_a^2(M_{KK_5})} &= \frac{\pi L_5}{g_{a_{5D}}^2(\Lambda_{\text{Max}})} + \frac{1}{8\pi^2} \sum_{\xi} \bar{\Delta}_a(\xi; M_{KK_5}, \ln \Lambda_{\text{Max}}) \\ &\equiv C_5^a(\Lambda_{\text{Max}}) + \frac{1}{8\pi^2} \sum_{\xi} \bar{\Delta}_a(\xi; M_{KK_5}, \ln \Lambda_{\text{Max}}). \end{aligned} \quad (7.33)$$

This implies a characterising equation for our unknown 5D gauge coupling at the cutoff scale,

$$C_5^a(\Lambda_{\text{Max}}) \equiv \frac{\pi L_5}{g_{a_{5D}}^2(\Lambda_{\text{Max}})} = \frac{1}{g_a^2(M_{KK_5})} - \frac{1}{8\pi^2} \sum_{\xi} \bar{\Delta}_a(\xi; M_{KK_5}, \ln \Lambda_{\text{Max}}). \quad (7.34)$$

To find the unknown C_5^a , and implicitly the cutoff scale Λ_{Max} , we can recast the above as a functional equation and solve it numerically for C_5^a . More specifically we can recast Λ_{Max} as

$$\Lambda_{\text{Max}} = \frac{16\pi}{L_5} C_5^a, \quad (7.35)$$

which then provides us with the functional form when substituted into Eqn. (7.34),

$$C_5^a = \frac{1}{g_a^2(M_{KK_5})} - \frac{1}{8\pi^2} \sum_{\xi} \bar{\Delta}_a\left(\xi; M_{KK_5}, \ln\left(\frac{16\pi}{L_5} C_5^a\right)\right). \quad (7.36)$$

Solving this equation numerically yields cut-off scales for each of the gauge couplings $\Lambda_{\text{Max}}^{4C}, \Lambda_{\text{Max}}^{2L}, \Lambda_{\text{Max}}^{2R}$. For the remainder of this paper we will refer to the smallest of the three when discussing the cutoff of the theory where a more fundamental 6D theory should come into effect,

$$\Lambda_{\text{Max}} = \min \{ \Lambda_{\text{Max}}^{4C}, \Lambda_{\text{Max}}^{2L}, \Lambda_{\text{Max}}^{2R} \}. \quad (7.37)$$

We now move on to specifying the full set of corrections $\bar{\Delta}_a$ coming from the fields that appear in our approximated 5D theory. The form of the $SU(N)$ corrections $\bar{\Delta}_N(\xi)$ from a generic field ξ are specified in [111].

Starting with $SU(4)_C$, the corrections due to scalars, gauge fields and fermions are,

$$\bar{\Delta}_{4C}(\phi) = 2\bar{\Delta}_{4C}^{--}(\mathbf{15}), \quad (7.38)$$

$$\begin{aligned} \bar{\Delta}_{4C}(\psi) &= 3 \left(\bar{\Delta}_{4C}^{++}(\mathbf{4}_L) + \bar{\Delta}_{4C}^{++}(\mathbf{4}_R) + \bar{\Delta}_{4C}^{--}(\mathbf{4}_L) + \bar{\Delta}_{4C}^{--}(\mathbf{4}_R) \right) \\ &\quad + 3 \left(\bar{\Delta}_{4C}^{++}(\mathbf{6}_L) + \bar{\Delta}_{4C}^{++}(\mathbf{6}_R) + \bar{\Delta}_{4C}^{--}(\mathbf{6}_L) + \bar{\Delta}_{4C}^{--}(\mathbf{6}_R) \right) \\ &\quad + \bar{\Delta}_{4C}^{+-}(\mathbf{4}_L) + \bar{\Delta}_{4C}^{+-}(\mathbf{4}_R) + \bar{\Delta}_{4C}^{-+}(\mathbf{4}_L) + \bar{\Delta}_{4C}^{-+}(\mathbf{4}_R), \end{aligned} \quad (7.39)$$

$$\bar{\Delta}_{4C}(A) = \bar{\Delta}_{3C}^{++}(\mathbf{8}) + \bar{\Delta}_{3C}^{--}(\mathbf{3}) + \bar{\Delta}_{3C}^{+-}(\mathbf{3}), \quad (7.40)$$

where the factor of 2 arises from the A_z, A_ν components, and the factors of 3 arise from generational indices $\alpha = 1, 2, 3$ and $\beta = 1, 2, 3$.

Note that the contribution of the gauge fields is obtained by splitting the $\mathbf{15} \sim SU(4)$ adjoint representation under the breaking $SU(4) \rightarrow SU(3) \times U(1)$ and adding each subcomponent's contribution separately based on their parity assignment. I.e. $\mathbf{15} \rightarrow (\mathbf{8}, 0) \oplus (\mathbf{3}, +4/3) \oplus (\bar{\mathbf{3}}, -4/3) \oplus (1, 0)$, and noting that $\Delta_3(1) = 0$ (scalar transformation under $SU(3)$). We have to treat them separately due to the original theory's $SU(5) \cap G_{PS} = G_{SM}$ projection, which results in mixed parity assignments within the 5D approximation.

Moving on to $SU(2)_L$, the corrections are

$$\bar{\Delta}_{2L}(\phi) = \bar{\Delta}_{2L}^{++}(\mathbf{2}) + 2\bar{\Delta}_{2L}^{--}(\mathbf{3}), \quad (7.41)$$

$$\begin{aligned} \bar{\Delta}_{2L}(\psi) = & 3 \left(\bar{\Delta}_{2L}^{++}(\mathbf{2}_L) + \bar{\Delta}_{2L}^{--}(\mathbf{2}_R) \right) \\ & + 3 \left(\bar{\Delta}_{2L}^{++}(\mathbf{2}_L) + \bar{\Delta}_{2L}^{++}(\mathbf{2}_R) + \bar{\Delta}_{2L}^{--}(\mathbf{2}_L) + \bar{\Delta}_{2L}^{--}(\mathbf{2}_R) \right) \\ & + \left(\bar{\Delta}_{2L}^{+-}(\mathbf{2}_L) + \bar{\Delta}_{2L}^{+-}(\mathbf{2}_R) \right), \end{aligned} \quad (7.42)$$

$$\bar{\Delta}_{2L}(A) = \bar{\Delta}_{2L}^{++}(\mathbf{3}) + \bar{\Delta}_{2L}^{--}(\mathbf{2}), \quad (7.43)$$

where the factors of 3 arise from $\alpha = 1, 2, 3$ and $\beta = 1, 2, 3$. $SU(2)_R$ has almost identical corrections apart from those originating from $\Psi_{\mathbf{32}}^4$, where $(+, -)$ and $(-, +)$ are swapped for R, L indices, and the gauge contribution,

$$\bar{\Delta}_{2R}(\phi) = \bar{\Delta}_{2R}^{++}(\mathbf{2}) + 2\bar{\Delta}_{2R}^{--}(\mathbf{3}), \quad (7.44)$$

$$\begin{aligned} \bar{\Delta}_{2R}(\psi) = & 3 \left(\bar{\Delta}_{2R}^{++}(\mathbf{2}_L) + \bar{\Delta}_{2R}^{--}(\mathbf{2}_R) \right) \\ & + 3 \left(\bar{\Delta}_{2R}^{++}(\mathbf{2}_L) + \bar{\Delta}_{2R}^{++}(\mathbf{2}_R) + \bar{\Delta}_{2R}^{--}(\mathbf{2}_L) + \bar{\Delta}_{2R}^{--}(\mathbf{2}_R) \right) \\ & + \left(\bar{\Delta}_{2R}^{+-}(\mathbf{2}_L) + \bar{\Delta}_{2R}^{+-}(\mathbf{2}_R) \right), \end{aligned} \quad (7.45)$$

$$\bar{\Delta}_{2R}(A) = \bar{\Delta}_{2R}^{++}(\mathbf{3}) + \bar{\Delta}_{2R}^{--}(\mathbf{2}). \quad (7.46)$$

Note that we have to specify the L/R handedness since the “N functions” used for the Δ corrections are depended on it (see Ref. [111]).

The corrections due to a generic field ξ are specified in [111], and consist of the following.

In the case of 5D scalars $\phi(x^\mu, y)$, we have a contribution to the gauge coupling

g_a , corresponding to $SU(N^a)$, of the form

$$\begin{aligned} \bar{\Delta}_a(\phi; \mu) = & \frac{1}{12} \left[T_a(\phi_{++}) \left[\ln \left(\frac{\Lambda}{k} \right) - 3 \int_0^1 du F(u) \ln N_{\phi_{++}} \left(\frac{iu}{2} \sqrt{\mu^2} \right) \right] - \right. \\ & - 3T_a(\phi_{+-}) \int_0^1 du F(u) \ln N_{\phi_{+-}} \left(\frac{iu}{2} \sqrt{\mu^2} \right) - \\ & - 3T_a(\phi_{-+}) \int_0^1 du F(u) \ln N_{\phi_{-+}} \left(\frac{iu}{2} \sqrt{\mu^2} \right) - \\ & \left. - T_a(\phi_{--}) \left[\ln \left(\frac{\Lambda}{k} \right) + 3 \int_0^1 du F(u) \ln N_{\phi_{--}} \left(\frac{iu}{2} \sqrt{\mu^2} \right) \right] \right], \end{aligned} \quad (7.47)$$

where $T_a(\phi)$ is the Dynkin index of the $SU(N^a)$ representation for ϕ , $F(u) = u(1-u^2)^{\frac{1}{2}}$. $N_{\phi_{\pm,\pm}}$ are the N -functions from Appendix B.3 under the assignments

$$(Z_\phi, Z'_\phi, \{\mathcal{P}_\phi\}) = (\pm, \pm, 4, 0, 0, 2), \quad (7.48)$$

where we have defined the parameter set $\{\mathcal{P}_\phi\}$ in Appendix B.3.

In the case of 5D fermionic fields $\psi(x^\mu, y)$, we have a contribution to the gauge coupling g_a , corresponding to $SU(N^a)$, of the form

$$\begin{aligned} \bar{\Delta}_a(\psi; \mu) = & \frac{1}{3} \left[T_a(\psi_{++}) \left[2 \ln \left(\frac{k}{\mu} \right) - kL_5 + 3 \int_0^1 du G(u) \ln N_{\psi_{++}} \left(\frac{iu}{2} \sqrt{\mu^2} \right) \right] + \right. \\ & T_a(\psi_{+-}) \left[-kL_5 + 3 \int_0^1 du G(u) \ln N_{\psi_{+-}} \left(\frac{iu}{2} \sqrt{\mu^2} \right) \right] + \\ & T_a(\psi_{-+}) \left[kL_5 + 3 \int_0^1 du G(u) \ln N_{\psi_{-+}} \left(\frac{iu}{2} \sqrt{\mu^2} \right) \right] + \\ & \left. T_a(\psi_{--}) \left[2 \ln \left(\frac{k}{\mu} \right) - kL_5 + 3 \int_0^1 du G(u) \ln N_{\psi_{--}} \left(\frac{iu}{2} \sqrt{\mu^2} \right) \right] \right], \end{aligned} \quad (7.49)$$

where $T_a(\psi)$ is the Dynkin index of the $SU(N^a)$ representation for ψ , $G(u) = u(1-u^2)^{\frac{1}{2}} - u(1-u^2)^{-\frac{1}{2}}$. $N_{\psi_{\pm,\pm}}$ are the N -functions under the assignments

$$(Z_\phi, Z'_\phi, \{\mathcal{P}_\phi\}) = \begin{cases} (-, -, \{1, +c, +c, |c - \frac{1}{2}|\}) & \text{for } N_{\psi_{++}} \\ (-, -, \{1, -c, -c, |c + \frac{1}{2}|\}) & \text{for } N_{\psi_{--}} \\ (+, -, \{1, -c, -c, |c + \frac{1}{2}|\}) & \text{for } N_{\psi_{+-}} \\ (-, +, \{1, -c, -c, |c + \frac{1}{2}|\}) & \text{for } N_{\psi_{-+}} \end{cases}. \quad (7.50)$$

Lastly, in the case of 5D Gauge fields $A_M(x^\mu, y)$, we have a contribution to the gauge coupling g_a , corresponding to $SU(N^a)$, of the form

$$\begin{aligned} \overline{\Delta}_a(A; \mu) = \frac{1}{12} & \left[T_a(A_{++}) \left[23 \ln \left(\frac{\mu}{\Lambda} \right) + 21 \ln \left(\frac{\mu}{k} \right) + 22kL_5 \right. \right. \\ & \left. \left. + \int_0^1 du K(u) \ln N_{A_{++}} \left(\frac{iu}{2} \sqrt{\mu^2} \right) \right] \right. \\ & + T_a(A_{+-}) \left[-kL_5 + \int_0^1 du K(u) \ln N_{A_{+-}} \left(\frac{iu}{2} \sqrt{\mu^2} \right) \right] \\ & + T_a(A_{-+}) \left[kL_5 + \int_0^1 du K(u) \ln N_{A_{-+}} \left(\frac{iu}{2} \sqrt{\mu^2} \right) \right] \\ & \left. + T_a(A_{--}) \left[23 \ln \left(\frac{\Lambda}{k} \right) + 2 \ln \left(\frac{k}{\mu} \right) - kL_5 \right. \right. \\ & \left. \left. + \int_0^1 du K(u) \ln N_{A_{--}} \left(\frac{iu}{2} \sqrt{\mu^2} \right) \right] \right], \end{aligned} \quad (7.51)$$

where $T_a(A)$ is the Dynkin index of the $SU(N^a)$ representation for A , $K(u) = -9u(1-u^2)^{\frac{1}{2}} + 24u(1-u^2)^{-\frac{1}{2}}$. $N_{\psi_{\pm, \pm}}$ are the N -functions where

$$(Z_\phi, Z'_\phi, \{\mathcal{P}_\phi\}) = \begin{cases} (-, -, \{4, 2, 2, 0\}) & \text{for } N_{A_{++}} \\ (-, -, \{2, 0, 0, 1\}) & \text{for } N_{A_{--}} \\ (+, -, \{2, 0, 0, 1\}) & \text{for } N_{A_{+-}} \\ (-, +, \{2, 0, 0, 1\}) & \text{for } N_{A_{-+}} \end{cases}. \quad (7.52)$$

Putting all of this together, the running in the 5D regime for our sample point is shown in Fig. 7.10.

7.4.4 Weinberg Angle: $SU(5)$ Prediction vs. Running

We can now turn to the comparison between the Weinberg angle prediction on the basis of our RGE analysis starting from the TeV scale.

Switching from the broken $SU(3) \times U(1)_{\text{EM}}$ phase to the G_{SM} phase, the Weinberg angle $\sin \theta_W$ and the electromagnetic fine structure constant α_{EM} , determine the weak and hypercharge couplings according to Eqn. (7.28).

Similarly the G_{SM} couplings are related to the G_{PS} ones as expressed in Eqn. (7.16), leading to the Weinberg angle expression of Eqn. (7.18).

At the unification scale, i.e. the energy at which the first non-zero GUT KK state becomes available $m_{\text{KK}_6} \sim 1/2\pi R_6$, we can write a series of identities between the

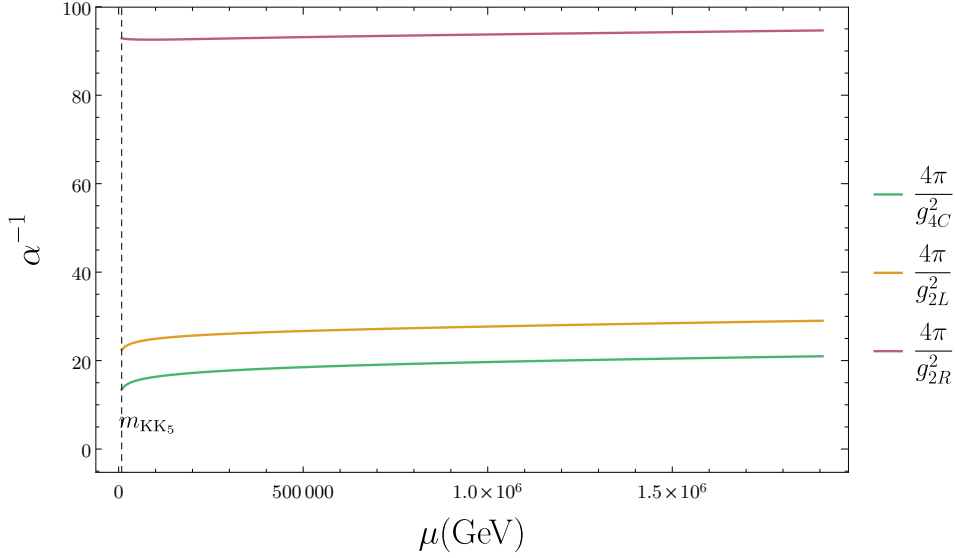


Figure 7.10: Effective 4D $SU(4)_C \times SU(2)_L \times SU(2)_R$ gauge couplings obtained via the 5D Pati-Salam approximation, using the evolved coupling values originating from the 4D formalism. The dotted line corresponds to the M_{KK_5} threshold at which we start our 5D runnings.

4D, 5D, 6D couplings based on the principle that there is only one gauge coupling in the theory. Before gauge symmetry breaking, the 5D and 4D equivalent $SO(11)$ couplings at the 5D Planck and IR branes are related to the 6D gauge coupling as,

$$\begin{aligned} \alpha_{6D}^{SO(11)} &= \frac{\alpha_{5D}^{SO(11)-IR}}{2\pi R_6} = \frac{\alpha_{5D}^{SO(11)-Pl}}{2\pi R_6} \\ &= \frac{\alpha_{4D}^{SO(11)-IR}}{2\pi R_6 L_5} = \frac{\alpha_{4D}^{SO(11)-Pl}}{2\pi R_6 L_5}. \end{aligned} \quad (7.53)$$

On the Planck brane the gauge symmetry is broken down $SO(11) \rightarrow SU(5)$ via the VEV of $\langle \Phi_{32} \rangle$. In terms of the equivalent 4D gauge couplings, the identification at 1-loop [140, 177] is equivalent to

$$\frac{1}{\alpha_{4D}^{SU(5)-Pl}} = \frac{1}{\alpha_{4D}^{SO(11)-Pl}} - \frac{1}{12\pi} [C_2(SO(11)) - C_2(SU(5))]. \quad (7.54)$$

Recasting this in terms of the 6D coupling, we have

$$\frac{1}{\alpha_{4D}^{SU(5)-Pl}} = \left\{ \frac{1}{\alpha_{6D}^{SO(11)}} - 2\pi R_6 L_5 \frac{\lambda_{11 \rightarrow 5}}{12\pi} \right\} \frac{1}{2\pi R_6 L_5}, \quad (7.55)$$

where $\lambda_{11 \rightarrow 5} = [C_2(SO(11)) - C_2(SU(5))]$.

Similarly on the IR brane we break $SO(11) \rightarrow SU(4)_C \times SU(2)_L \times SU(2)_R$ via the P_0, P_2 boundary conditions, which produce the gauge identifications at 1 loop,

$$\frac{1}{\alpha_{4D}^{SU(4)_C-IR}} = \frac{1}{\alpha_{4D}^{SO(11)-Pl}} - \frac{\lambda_{11 \rightarrow 4}}{12\pi}, \quad (7.56)$$

$$\frac{1}{\alpha_{4D}^{SU(2)_L-IR}} = \frac{1}{\alpha_{4D}^{SO(11)-Pl}} - \frac{\lambda_{11 \rightarrow 2}}{12\pi}, \quad (7.57)$$

$$\frac{1}{\alpha_{4D}^{SU(2)_R-IR}} = \frac{1}{\alpha_{4D}^{SO(11)-Pl}} - \frac{\lambda_{11 \rightarrow 2}}{12\pi}, \quad (7.58)$$

where $\lambda_{11 \rightarrow 4} = C_2(SO(11)) - C_2(SU(4))$, $\lambda_{11 \rightarrow 2} = C_2(SO(11)) - C_2(SU(2))$. In terms of the 6D couplings this means,

$$\frac{1}{\alpha_{4D}^{SU(4)_C-IR}} = \left\{ \frac{1}{\alpha_{6D}^{SO(11)-Pl}} - 2\pi R_6 L_5 \frac{\lambda_{11 \rightarrow 4}}{12\pi} \right\} \frac{1}{2\pi R_6 L_5}, \quad (7.59)$$

$$\frac{1}{\alpha_{4D}^{SU(2)_L-IR}} = \left\{ \frac{1}{\alpha_{6D}^{SO(11)-Pl}} - 2\pi R_6 L_5 \frac{\lambda_{11 \rightarrow 2}}{12\pi} \right\} \frac{1}{2\pi R_6 L_5}, \quad (7.60)$$

$$\frac{1}{\alpha_{4D}^{SU(2)_R-IR}} = \left\{ \frac{1}{\alpha_{6D}^{SO(11)-Pl}} - 2\pi R_6 L_5 \frac{\lambda_{11 \rightarrow 2}}{12\pi} \right\} \frac{1}{2\pi R_6 L_5}. \quad (7.61)$$

Ignoring the Casimirs for a moment to keep the discussion transparent, at the unification scale, instead of the Eqns. (7.55), (7.60), we have

$$\begin{aligned} \frac{1}{\alpha_{4D}^{SU(4)_C-IR}} &= \frac{1}{\alpha_{4D}^{SU(2)_L-IR}} = \frac{1}{\alpha_{4D}^{SU(2)_R-IR}} \\ &= \frac{1}{\alpha_{4D}^{SU(5)-Pl}} = \frac{1}{\alpha_{6D}^{SO(11)-Pl}} \frac{1}{2\pi R_6 L_5}. \end{aligned} \quad (7.62)$$

When combined with the expression for the Weinberg angle in the Pati-Salam phase in Eqn. (7.18) these leads to the expected

$$\sin^2 \theta_W(\mu) \Big|_{\mu=(2\pi R_6)^{-1}} = \frac{1}{\frac{2}{3} + 1 + 1} = \frac{3}{8}. \quad (7.63)$$

In essence, this is the $SU(5)$ prediction translated from the Planck brane to the IR brane. The scale of $SU(5)$ breaking is dictated by $\langle \Phi_{32} \rangle \sim R_6^{-1}$, which is localised on the UV brane $y = 0$. Again, we emphasise that this scale is not accessible within our 5D formalism, but we can infer some useful conclusions depending on the values of the RGE runnings at Λ_{Max} , as we will see in Sec. 7.5.

Including the Casimir corrections, we find the slightly modified relation

$$\sin^2 \theta_W(\mu) = \frac{36 - 18\pi\alpha_{4D}^{SO(11)}}{96 - \frac{1}{\pi}20\alpha_{4D}^{SO(11)} - 44\pi\alpha_{4D}^{SO(11)}} \Big|_{\mu=(2\pi R_6)^{-1}}. \quad (7.64)$$

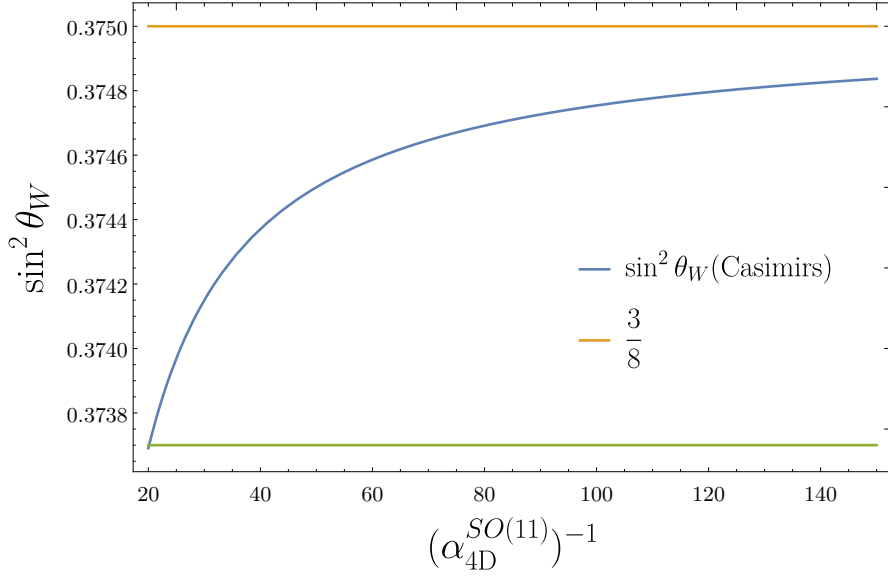


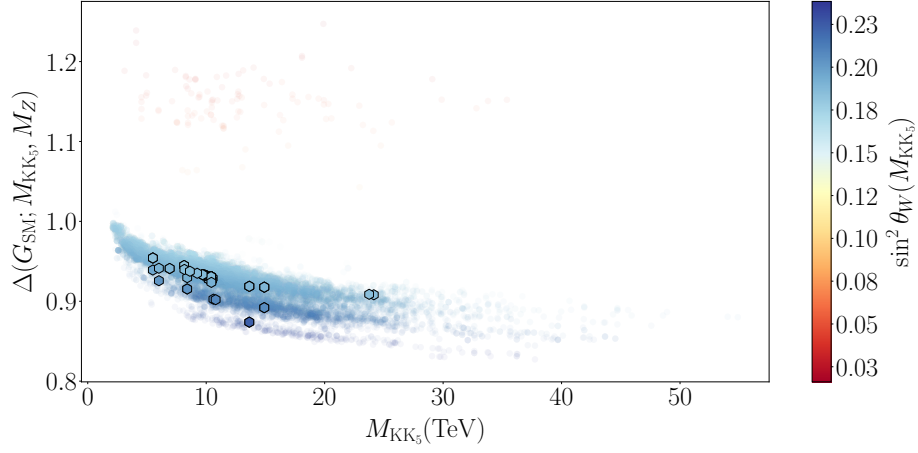
Figure 7.11: Numerical impact of the Casimir correction (blue line) as a function of the unknown inverse unified coupling $(\alpha_{4D}^{SO(11)})^{-1}$. The green line represents the low bound for the $\sim 0.4\%$ deviation occurring at $(\alpha_{4D}^{SO(11)})^{-1} \simeq 20$. The orange line represents the GUT hypothesis $3/8$. The smaller α , the less impact the Casimir corrections have on the prediction as they are weighted by $\alpha_{4D}^{SO(11)}$.

Since the Casimir-corrected Weinberg Angle requires a value for the $SO(11)$ 4D equivalent gauge coupling, we examine the possible deviation from the $3/8$ GUT prediction as a function of the possible values of $\alpha_{4D}^{SO(11)}$, as shown in Fig. 7.11. For reasonable $\alpha_{4D}^{SO(11)}$ coupling values (e.g. Ref. [140]) we see that deviations arising from the Casimir corrected values amount to $\lesssim -0.0013$, see Fig. 7.11. Since this $\sim 0.4\%$ deviation is negligible, we can safely ignore the Casimir contributions in the following without qualitatively changing our results.

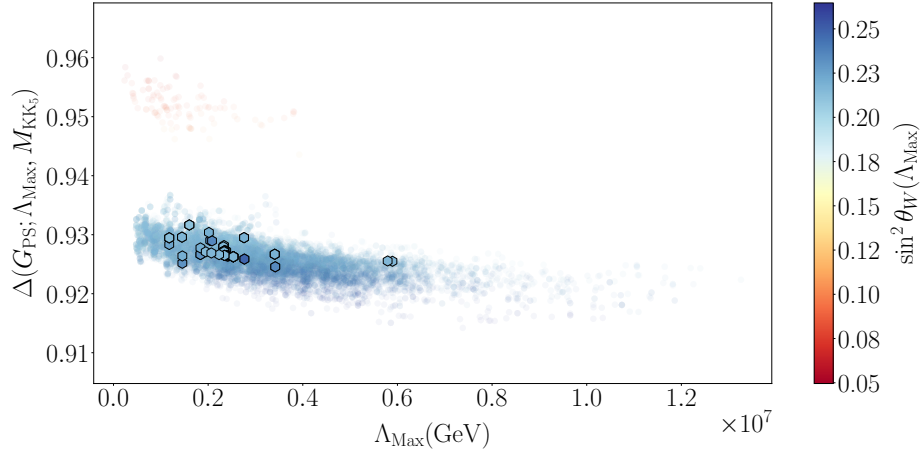
7.5 Results

The running is crucially influenced by the number of active fermion generations N_G . We will therefore comment on our results for $N_G = 1, 3$ separately.

In the first case, we include only the third fermion generation as mentioned before. This implicitly assumes that there is a large mass gap between the third family and the remaining two, decoupling the associated zero-mode KK states from the RGE flow (see Ref. [116]). In the second case, we assume that all three SM genera-



(a) Scatter plot of the parameter space points for the $N_G = 1$ case, where we use the same convention as in Fig. 7.2. We now represent each point's value for the unification measure $\Delta(G_{\text{SM}}; M_{\text{KK}_5}, M_Z)$ in the 4D SM phase between the Kaluza-Klein scale M_{KK_5} , and M_Z , the respective KK scale, and the colour shading denotes the value of the Weinberg angle $\sin^2 \theta_W(M_{\text{KK}_5})$.



(b) Correlation of the $N_G = 1$ case in the 5D phase, $\Delta(G_{\text{PS}}; \Lambda_{\text{Max}}, M_{\text{KK}_5})$, shown as a function of the cut-off scale Λ_{Max} where perturbativity is lost (see text for details). The colour shading again represents the Weinberg angle at the cut-off. Highlighted hexagon points refer to realistic low energy spectra compatible with exotics searches.

Figure 7.12: RGE evolution in the $N_G = 1$ case within the 4D and 5D approximations.

tions are present and that different generational mass states are nearly degenerate. The comparison of these avenues contrasted with implications for unification can therefore act as a guideline for future model-building in the fermion sector.

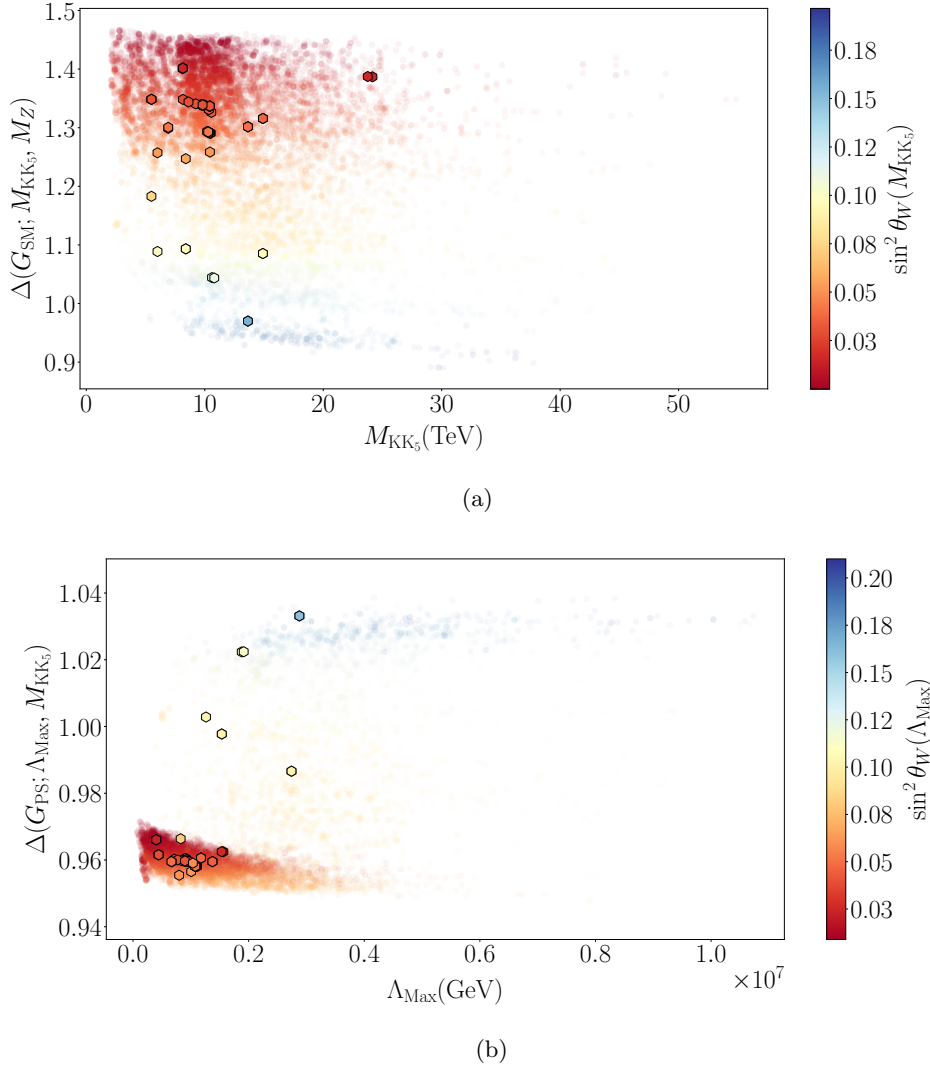


Figure 7.13: Scatter plots analogous to Figs. 7.12a and 7.12b for the degenerate $N_G = 3$ case.

To examine the extent to which the gauge couplings converge in the 4D, 5D regimes tensioned against the unification value of the Weinberg angle, we introduce a unification measure

$$\Delta(G; M_2, M_1) = \frac{\sum_{i,j \in G | i \neq j} |\alpha_i(M_2) - \alpha_j(M_2)|}{\sum_{i,j \in G | i \neq j} |\alpha_i(M_1) - \alpha_j(M_1)|}, \quad (7.65)$$

i.e. we consider the ratio of the sum of the mutual coupling deviations between two scales $M_2 > M_1$. α_i are the gauge group couplings of the subgroups that form the

gauge group G . This ratio measures how quickly the gauge couplings approach each other as a function of the energy scale. Since we are interested in gauge coupling unification at $M_2 > M_1$, values of $\Delta(G; M_2, M_1)$ refer

$$\Delta(G; M_2, M_1) \begin{cases} > 1 & \Leftrightarrow \text{departure from unification} \\ < 1 & \Leftrightarrow \text{approaching unification} \\ \sim 0 & \Leftrightarrow \text{unification} \end{cases} . \quad (7.66)$$

We plot this unification measure in the 4D SM phase between M_Z, M_{KK_5} , along with the Weinberg angle value at M_{KK_5} in Figs. 7.12a, 7.13a for the $N_G = 1$ and $N_G = 3$ cases. Figs. 7.12b and 7.13b. show the same measure for $N_G = 1$ and $N_G = 3$ in the 5D PS phase between $M_{\text{KK}_5}, \Lambda_{\text{Max}}$.

We start our discussion with the $N_G = 1$ case. Examining Fig. 7.12a we can see that within the 4D SM phase, the majority of the points that are consistent with the SM have a unification measure smaller than unity, where the evolved Weinberg angle values lie around $\sin^2 \theta_W \simeq 0.2$.

The evolution of the Weinberg angle is driven towards smaller values compared to the electroweak scale for a converging behaviour of the gauge couplings. This is due to the particular KK decomposition of the field content. The hypercharge and weak couplings receive larger corrections than the QCD coupling as there are more weakly charged states than coloured states that impact the running of QCD. The weak corrections tend to be strong enough to result in a change in the direction of the gauge coupling running away from asymptotic freedom. This leads to a smaller Weinberg angle in the UV. We can see this behaviour for the $N_G = 1, 3$ cases in Figs. 7.14a, 7.14b.

In the 5D phase shown in Fig. 7.12b, we see that the converging behaviour is maintained, with the unification measure approaching zero, while the Weinberg angle increases via the RGE flow. This reflects the need for a complete set of RGEs to be performed within higher dimensional theories (see e.g. Refs. [112, 178]). Under the assumption that in the 6D phase of the theory the coupling behaviour remains similar, we can infer that gauge coupling unification is consistent with the predicted value for the Weinberg angle. Put differently, the cutoff scale depicted in Fig. 7.12b provides us with a lower bound for the unification scale $M_{\text{GUT}} > \Lambda_{\text{Max}}$ which is dictated by gauge coupling unification and consistency with the Weinberg angle prediction.

Let us turn to the $N_G = 3$ case, where we observe an amplified behaviour of the

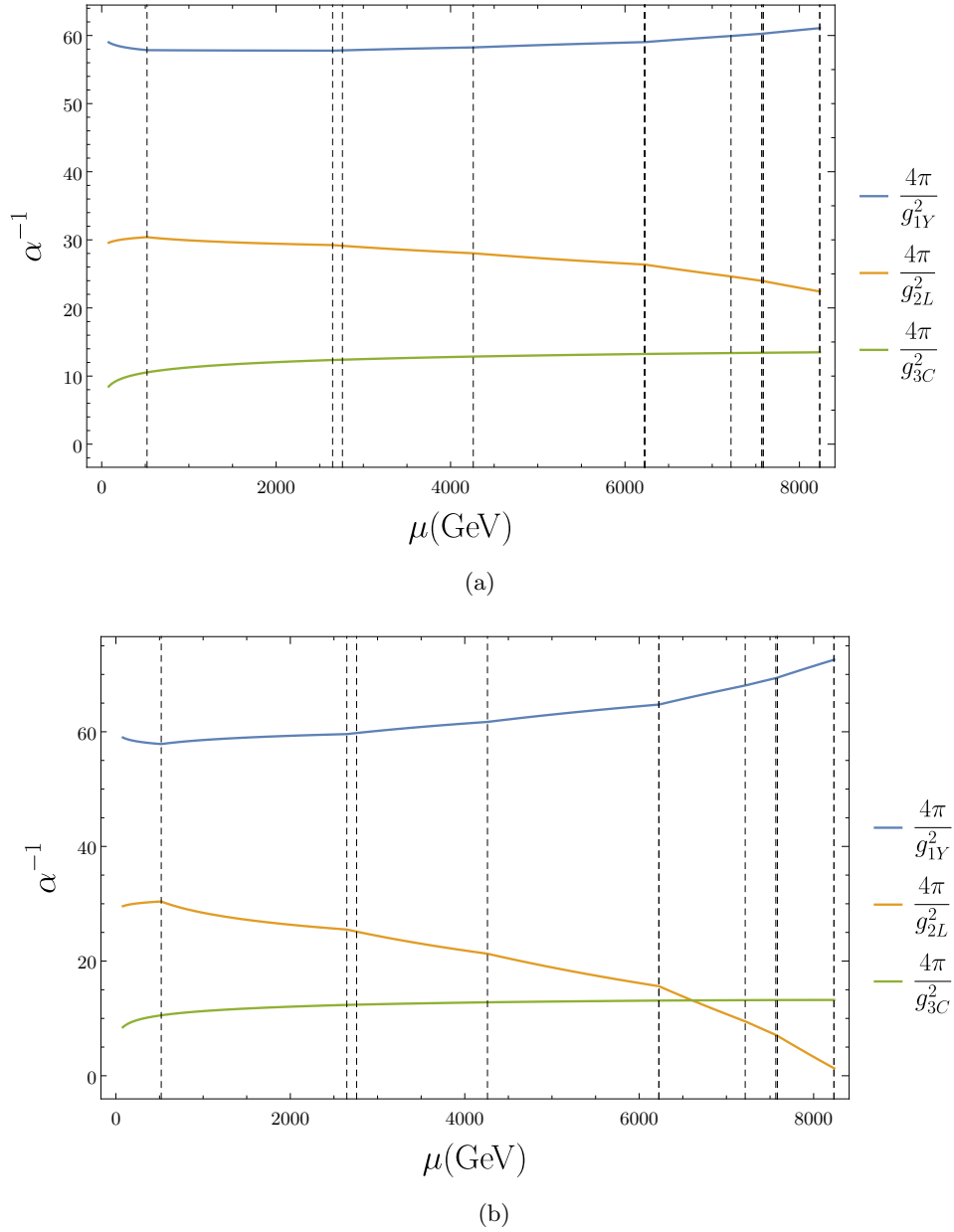


Figure 7.14: 4D SM gauge coupling running between $[M_Z, M_{KK_5}]$, for the $N_G = 1$ case (a), and the $N_G = 3$ case (b). The particular runs are of the sample point showcased in Eqn. (7.19).

aforementioned effect of the KK states (Fig. 7.13a) due to their increased number. In total, this leads to gauge couplings getting increasingly pushed away from unification, while the Weinberg angle flows to very small values. Again this behaviour is compensated to some extent in the 5D phase as indicated in Fig. 7.13b, resulting

in values $\sin^2 \theta_W \lesssim 0.07$ for the vast majority of points. Under the assumption, that this behaviour continues in the 6D theory, we could face a potential inconsistency arising from gauge coupling unification being achievable but with small Weinberg angle values. While this could be compensated by large radiative corrections that shift the Weinberg angle away from the GUT hypothesis, this sets fairly tight constraints on the dynamics of the fermion sector.

We finally comment on the impact of uncertainties, in particular uncertainties of the input parameters α_{3C} and $\sin^2 \theta_W$ at the weak scale. Errors as small as $\sigma(\alpha_{3C}) = \pm 0.00074$ are possible from a theoretical perspective (e.g. Ref. [172]), and we consider a 5% uncertainty in the value of the Weinberg Angle where $\sigma(\sin^2 \theta_W) = \pm 0.01156$ for demonstration purposes. Taking into account both of these uncertainties, we perform our analysis for the sample point highlighted in Eqn. (7.19). In the $N_G = 1$ case the percentage difference arising in the unification measure at M_{KK_5} amounts to $\sim 2\%$, whereas in the $N_G = 3$ case it reaches $\sim 5\%$. This effect is less pronounced at Λ_{Max} , where the effects stack up to $\sim 0.2\%$ for $N_G = 1$ and $\sim 0.4\%$ for $N_G = 3$.

Similarly, in the $N_G = 1$ case we look at the percentage difference in the Weinberg angle at M_{KK_5} which is roughly $\sim 7.4\%$, and comes down at Λ_{Max} to $\sim 5.8\%$. In the $N_G = 3$ case these are more pronounced, where at M_{KK_5} we obtain $\sim 170\%$, and at Λ_{Max} we have $\sim 84\%$. We note that in the latter case, the Weinberg angle has already been driven to small values $\mathcal{O}(0.01)$, i.e. while the impact is large, it does not impact a theoretically allowed parameter region from the point of view of unification.

7.6 Conclusions

Grand unified theories are attractive solutions to shortcomings of the Standard Model of Particle Physics. In non-supersymmetric realisations scale separations can be achieved by employing higher dimensional background geometry [118], where electroweak symmetry breaking can also be implemented elegantly as a radiative phenomenon [122]. Transitioning through the different phases of such scenarios is less straightforward compared to applications in “standard” 4D GUTs (see e.g. [140, 141, 179–184]).

This was the purpose of our exploratory study: a detailed analysis of the 4D and 5D phases of the model of [116, 117], contrasted with electroweak scale mea-

measurements as well as LHC constraints. We pay particular attention to the Weinberg angle, whose size is determined by $SU(5)$ relations, and can therefore be used to test gauge unification (or lack thereof). While a fully conclusive test will need a full investigation of the 6D phase of the theory, which we leave for future work, we gather evidence that the 4D and 5D effective theories can remain under perturbative control up to scales of $\sim 10^7$ GeV. If unification is to be approached in a controlled way, new dynamics should appear at scales about two orders of magnitude above the 5D compactification scale. This scale can be interpreted as a lower limit on the GUT scale ~ 5000 TeV in the light of observed physics at and around the electroweak scale.

Fermionic thresholds crucially impact the running of couplings and as a consequence, the model-building aspects related to the three fermion generations plays an important role in the high energy behaviour of the theory. Unless there is a hierarchical approach to lifting the zero modes of the fermion fields to their observed SM values, the 6D theory will play a more important role in achieving unification in the sense of Eqn. (7.63).

Furthermore, we note that the original model in Ref. [116, 117], has a series of shortcomings, such as the 6th dimension being able to develop a non-trivial Wilson line which would in turn cause a different spectrum on the IR brane. Even though proton decay is forbidden at tree level, one still needs to look at one loop contributions to gauge how much proton decay is induced by the potentially low lying Pati-Salam gauge bosons.

Summary & Conclusions

Throughout this thesis we have looked at the Standard Model of particle physics, and identified its various shortcomings and problems in trying to describe the universe as highlighted in Chapter 1. In Chapters 2, 4, 5 we then reviewed some proposed solutions, namely grand unified theories, supersymmetry, extra dimensions, and the Hosotani mechanism.

In Chapter 3 we analysed $SU(5)$ and $SU(5) \times U(1)$ supersymmetric extra dimensional orbifold models based on Scherk-Schwarz breaking. This was done by employing spectrum generators aided by numerical algorithms, which allowed us to check the models against current experimental constraints. We saw that the models struggle to obey the LHC limits and produce a consistent Higgs mass, ruling out the basic $SU(5)$ model, along with providing motivation for a next to minimal UV extension. This in turn prompted us to explore non supersymmetric alternatives.

In Chapters 6, 7 we moved on to review and analyse a $SO(11)$ GHGUT model in a hybrid 6D space time. Throughout Chapter 7, we explored the associated Higgs and exotics phenomenology, along with checking the consistency between the theory's UV and IR phases. This was achieved by employing a differential evolution algorithm based on a SM-like measure, along with RGE evolutions within 4D and 5D approximations. Within this analysis we saw the importance of current and future BSM physics searches, along with finding new measures to guide unified model building within non-supersymmetric extra dimensional scenarios.

The search for physics beyond the Standard Model is, and will be for the foreseeable future, one of the greatest challenges the particle physics community has to face. BSM models formulated under a unifying framework or that address the shortcomings of the SM, continue to provide some of the best guidance as to what direction experiments should try and probe.

With this being said, there is still a lot to be done. Further work is required in exploring non-minimal extra dimensional models incorporating Scherk-Schwarz breaking using different bulk symmetries to try and resolve the issues presented in

Chapter 3. A particular example would be a proper adaptation of the 6D E_6 model presented in Ref. [65], which has the potential of circumventing the aforementioned problems. Similarly, if we are to fully connect the UV and IR pictures in 6D extra dimensional models, we require further RGE analysis within 6D regimes, allowing us to more thoroughly probe their consistency.

Overall this has been yet another stepping stone required for a fully realistic extra dimensional Grand Unified Theory that doesn't suffer from the problems present in its 4D counterparts.

Appendices

Bessel Equation

A.1 Bessel Equation & Bessel Functions

The following review in the current section is based mainly on Chap. 12 from Ref. [185]. Bessel's equation is one of the classically named 2nd order partial differential equation. Given a function $y(x)$ of the variable x , and a real parameter $p \in \mathbb{R}$ (referred to as the *order* of the Bessel function), the standard form of the Bessel equation is

$$x^2 \frac{\partial^2 y}{\partial x^2} + x \frac{\partial y}{\partial x} + (x^2 - p^2) y = 0. \quad (\text{A.1})$$

The above can be recast in a slightly different form as

$$x \frac{\partial}{\partial x} \left(x \frac{\partial y}{\partial x} \right) + (x^2 - p^2) y = 0. \quad (\text{A.2})$$

To solve the differential equation, we can expand y in terms of a power series

$$y(x) = \sum_{n=0}^{\infty} a_n x^{n+s}, \quad (\text{A.3})$$

which when plugged into Eqn. (A.2) allows us to identify the coefficients of powers of x as

$$x^s : \quad s = \pm p, \quad (\text{A.4})$$

$$x^{s+1} : \quad a_1 = 0, \quad (\text{A.5})$$

$$x^{s+2} : \quad a_n = -\frac{a_{n-2}}{(n+s)^2 - p^2} \quad \text{for } n > 1. \quad (\text{A.6})$$

Starting of with the case $s = p$, where $p \in \mathbb{Z}$, and using the above recurrence relation for even numbers of n , we have

$$a_1 = a_3 = a_5 = \dots = 0, \quad a_{2n} = -\frac{a_{2n-2}}{2n(2n+2p)} = -\frac{a_{2n-2}}{2^2 n(n+p)}. \quad (\text{A.7})$$

The above can be simplified by using the $\Gamma(x)$ function, which is defined as the analytic continuation of the factorial product as

$$\Gamma(x) = \int_0^{\infty} t^{x-1} \exp(-t) dt, \quad (\text{A.8})$$

where $\Gamma(n) = (n-1)!$ when $n \in \mathbb{N}$. The $\Gamma(x)$ function has the property $\Gamma(p+2) = (p+1)\Gamma(p+1)$, and $\Gamma(p+3) = (p+2)(p+1)\Gamma(p+1)$, which can now be used to rewrite the recurrence relationships in Eqn. (A.7) as

$$\begin{aligned}
 a_2 &= -\frac{a_0}{2^2(1+p)} = -\frac{a_0}{2^2} \frac{\Gamma(p+1)}{\Gamma(p+2)}, \\
 a_4 &= -\frac{a_2}{2^3(2+p)} = \frac{a_0}{2^3 2^2(1+p)(2+p)} = \frac{a_0}{2!2^4} \frac{\Gamma(1+p)}{\Gamma(3+p)}, \\
 a_6 &= -\frac{a_4}{2^2 3(3+p)} = -\frac{a_0}{2^2 3!2^4(1+p)(2+p)(3+p)} = \frac{a_0}{3!2^6} \frac{\Gamma(1+p)}{\Gamma(4+p)}, \\
 &\vdots \\
 a_{2k} &= (-1)^k \frac{a_0}{k!2^{2k}} \frac{\Gamma(1+p)}{\Gamma(1+k+p)}, \\
 &\vdots
 \end{aligned} \tag{A.9}$$

Plugging in the above expression into the series solution, we get the explicit form of $y(x)$,

$$\begin{aligned}
 y &= a_0 x^p \Gamma(1+p) \left[\frac{1}{\Gamma(1+p)} - \frac{1}{\Gamma(2+p)} \left(\frac{x}{2}\right)^2 + \frac{1}{2!\Gamma(3+p)} \left(\frac{x}{2}\right)^4 + \dots \right. \\
 &\quad \left. + (-1)^k \frac{1}{k!\Gamma(1+k+p)} \left(\frac{x}{2}\right)^{2k} + \dots \right] \\
 &= a_0 2^p \left(\frac{x}{2}\right)^p \Gamma(1+p) \left[\frac{1}{\Gamma(1)\Gamma(1+p)} - \frac{1}{\Gamma(2)\Gamma(2+p)} \left(\frac{x}{2}\right)^2 + \frac{1}{\Gamma(3)\Gamma(3+p)} \left(\frac{x}{2}\right)^4 \right. \\
 &\quad \left. + \dots + (-1)^k \frac{1}{\Gamma(k)\Gamma(1+k+p)} \left(\frac{x}{2}\right)^{2k} + \dots \right].
 \end{aligned} \tag{A.10}$$

We have the freedom to set a_0 , and in order to normalise the solution we set it to $a_0 = \frac{2^p}{\Gamma(1+p)}$. With this choice, we now refer to y as a Bessel function of the 1st kind of order p

$$J_p(x) = \sum_{n=0}^{\infty} \frac{(-1)^n}{\Gamma(n+1)\Gamma(n+1+p)} \left(\frac{x}{2}\right)^{2n+p}. \tag{A.11}$$

The second case where $s = -p$, $J_{-p}(x)$ is a suitable solution which is related to $J_p(x)$ by

$$J_{-p}(x) = (-1)^p J_p(x). \tag{A.12}$$

Similarly, we can derive the solution for $p \notin \mathbb{Z}$, which has the general form

$$y(x) = AJ_p(x) + BY_p(x), \tag{A.13}$$

where A, B are arbitrary constants determined by the boundary conditions of Eqn. (A.1), and we have introduced the Bessel function of the 2nd kind Y_p ,

$$Y_p(x) = \frac{\cos(\pi p)J_p(x) - J_{-p}(x)}{\sin(\pi p)}. \quad (\text{A.14})$$

The following useful relations hold for either $J_p(x), Y_p(x)$, which we generically denote as $Z_p(x)$

$$\begin{aligned} \frac{\partial}{\partial x} (x^p Z_p(x)) &= x^p Z_{p-1}(x), & Z_{p-1}(x) + Z_{p+1}(x) &= \frac{2p}{x} Z_p(x), \\ \frac{\partial}{\partial x} (x^{-p} Z_p(x)) &= -x^{-p} Z_{p+1}(x), & Z_{p-1}(x) - Z_{p+1}(x) &= 2 \frac{\partial}{\partial x} Z_p(x), \\ \frac{\partial Z_p(x)}{\partial x} &= -\frac{p}{x} Z_p(x) + Z_{p-1}(x) = \frac{p}{x} Z_p(x) - Z_{p+1}(x). \end{aligned} \quad (\text{A.15})$$

Lastly, we note that a useful form of the Bessel equation that is often encountered consists of

$$\frac{\partial^2 y}{\partial x^2} + \frac{1-2a}{x} \frac{\partial y}{\partial x} + \left\{ \left((bcx^{c-1})^2 + \frac{a^2 - p^2 c^2}{x^2} \right) \right\} y = 0, \quad (\text{A.16})$$

where $p \in \mathbb{Z}$, and $c, a \in \mathbb{R}$ are constants. The above admits a general solution of the form

$$y(x) = x^a [AJ_p(bx^c) + BY_p(bx^c)], \quad (\text{A.17})$$

where A, B are arbitrary constants set by the boundary conditions of the problem. Eqns. (A.16), (A.17) will prove invaluable when we will solve for fermionic/bosonic equations of motion in AdS_5 space.

$SO(11)$ GHGUT

B.1 Threshold Corrections

The gauge coupling α_i of a broken subgroup G_i resulting from breaking G (recall general breaking for $SU(N+M) \rightarrow SU(N) \times SU(M) \times U(1)$) will be given in terms of the original gauge coupling α_G and a matching condition λ_i [186, 187]:

$$\frac{1}{\alpha_i(\mu)} = \frac{1}{\alpha_G(\mu)} - \frac{\lambda_i(\mu)}{12\pi}, \quad (\text{B.1})$$

where the values are valid at a matching scale μ , which lies in the vicinity of the energy breaking threshold. The matching conditions $\lambda_i(\mu)$ at one loop are given by:

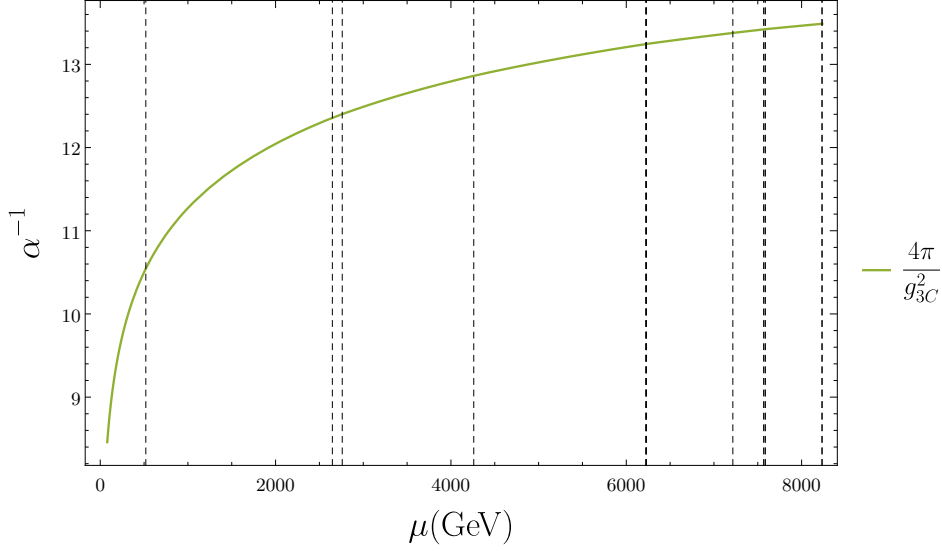
$$\begin{aligned} \lambda_i(\mu) = \{C_2(G) - C_2(G_i)\} - 21 \operatorname{Tr} \left(t_{i_V}^2 \ln \frac{M_V}{\mu} \right) \\ + \operatorname{Tr} \left(t_{i_S}^2 \ln \frac{M_S}{\mu} \right) + 8 \operatorname{Tr} \left(t_{i_F}^2 \ln \frac{M_F}{\mu} \right), \end{aligned} \quad (\text{B.2})$$

where V, F, S refer to vector, fermion and scalar particles that are integrated out at μ with their respective masses M_V, M_F, M_S .

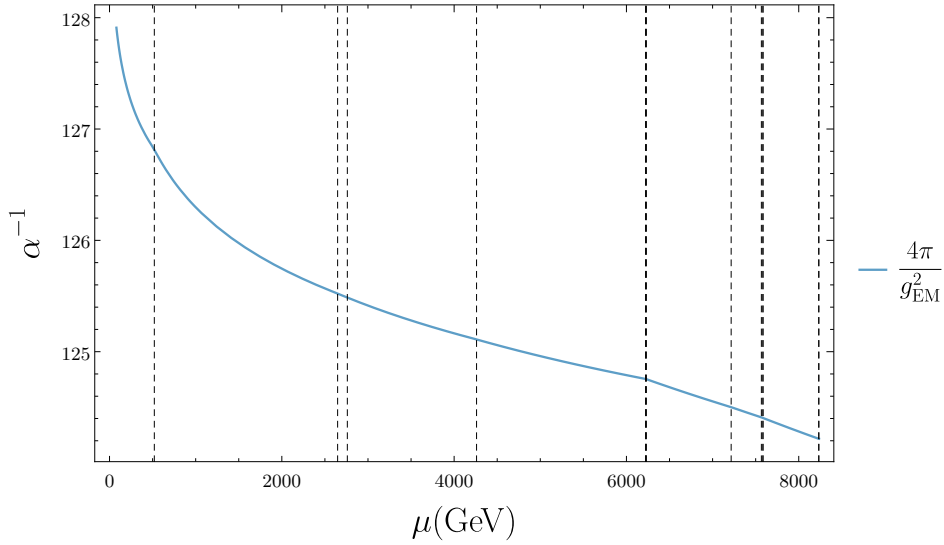
Note that the $C_2(G) - C_2(G_i)$ term is the one responsible for the ‘discrete’ jumps in gauge couplings, since all the logs go to 0 when $M_\xi = \mu$. Also note that since we are taking into account all the different KK states as we go up in energy in both the $G_{\text{SM}}, G_{\text{PS}}$ phases the threshold corrections only amount to the Casimir differences at M_{KK_5} ,

$$\lambda_i(\mu) = \delta(\mu - M_{\text{KK}_5}) \{C_2(G) - C_2(G_i)\}. \quad (\text{B.3})$$

B.2 Gauge Couplings

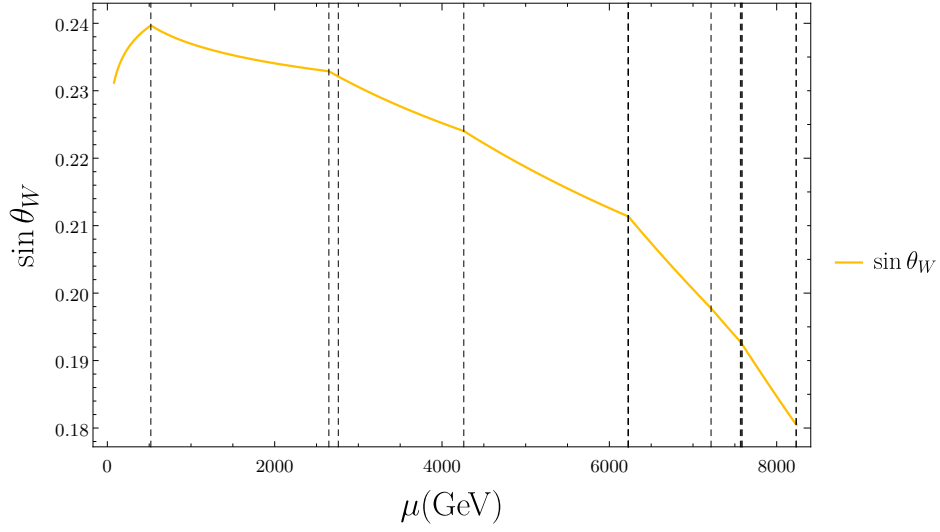


(a) RGE evolution for the piecewise QCD coupling g_{3C} with the different β function changes at the multiple encountered KK states marked as dotted lines. Note that this is evaluated in the unbroken QCD phase $SU(3)_C$.

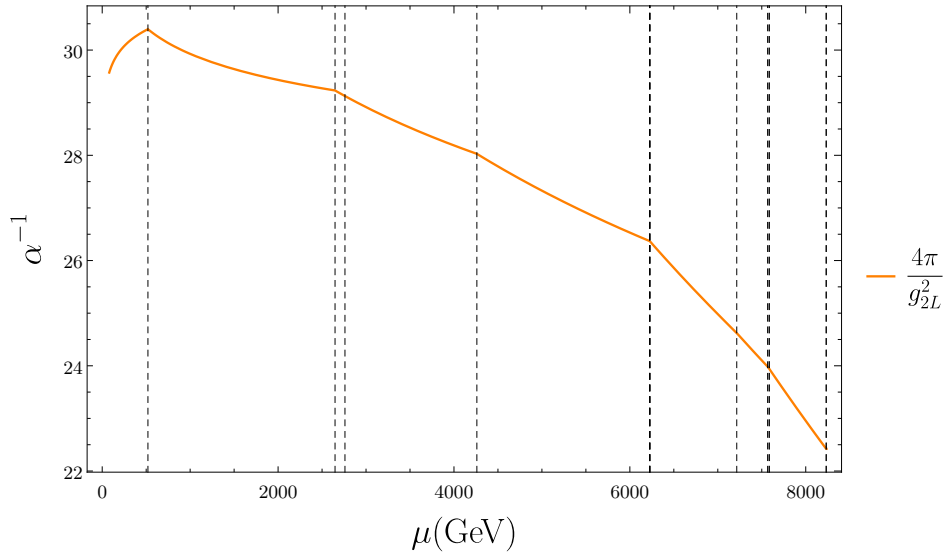


(b) RGE evolution for the piecewise electromagnetic coupling g_{EM} with the different β function changes at the multiple encountered KK states marked as dotted lines. Note that this is evaluated in the broken phase $SU(3)_C \times U(1)_{EM}$.

Figure B.1: Piecewise RGE evolutions of the electromagnetic and strong couplings for the sample point in Eqn. (7.19).



(a) RGE evolution for the piecewise Weinberg Angle $\sin \theta_W$ with the different β function changes at the multiple encountered KK states marked as dotted lines. Note that this is evaluated in the broken phase $SU(3)_C \times U(1)_{EM}$.



(b) RGE evolution for the piecewise weak coupling g_{2L} with the different β function changes at the multiple encountered KK states marked as dotted lines.

Figure B.2: Piecewise RGE evolutions of the Weinberg angle and the weak coupling for the sample point in Eqn. (7.19).

B.3 $N_{(\pm,\pm)}(\mu)$ Functions

The N -functions for a generic field ξ where $\xi \in \{A_\mu, \phi, e^{-2kL_5|y|}\psi_L, e^{-2kL_5|y|}\psi_R\}$ with $(\mathbb{Z}_2, \mathbb{Z}'_2)$ parity assignments depend on the renormalisation scale μ , the AdS

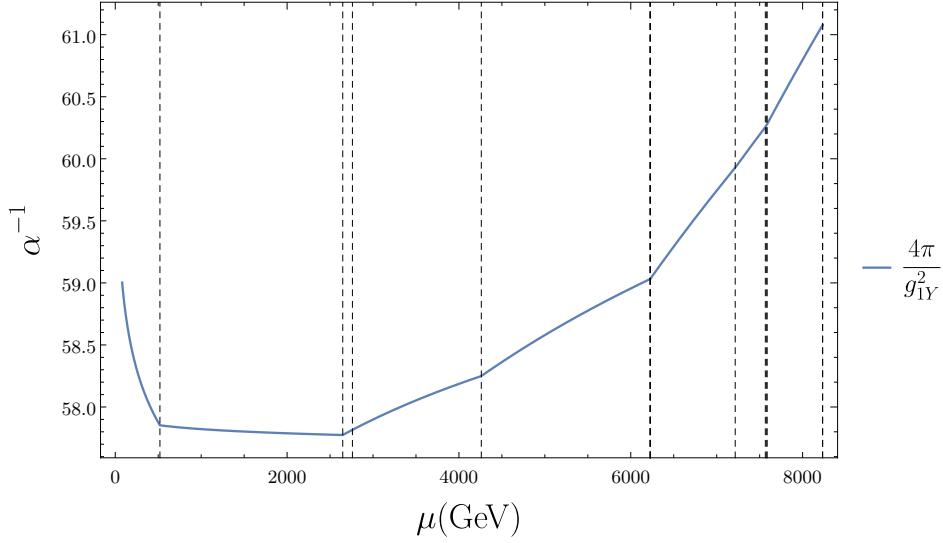


Figure B.3: RGE evolution for the piecewise hypercoupling g_{1Y} for the sample point in Eqn. (7.19), with the different β function changes at the multiple encountered KK states marked as dotted lines. Note that this is derived from the values of $\alpha_{\text{EM}}, \sin \theta_W$.

curvature k , the warp factor $z_L = \exp(kL_5)$ (note that our definition of L_5 includes the factor of π), the ξ field set of defining parameters $\{\mathcal{P}_\xi\} = \{s_\xi, (r_0)_\xi, (r_\pi)_\xi, \alpha\}$, where s is associated with the spin of the field,

$$s_\xi = \{2, 4, 1, 1, \} \quad \text{for} \quad \xi \in \left\{ A_\mu, \phi, e^{-2kL_5|y|}\psi_L, e^{-2kL_5|y|}\psi_R \right\}, \quad (\text{B.4})$$

and is related to α as

$$\alpha = \sqrt{\left(\frac{s}{2}\right)^2 + M_\xi^2} \quad \text{where} \quad M_\xi^2 \in \{0, 0, c(c+1), c(c-1)\}. \quad (\text{B.5})$$

Note that the model explored in this thesis does not have any bulk masses present for the gauge fields. The closed form for the N - functions is then given by

$$\begin{aligned} N_{\xi(+,-)}(\mu; \{\mathcal{P}_\xi\}) = & -Y_\alpha \left(\frac{\mu}{kz_L} \right) \left[\left[\frac{s_\xi}{2} - (r_0)_\xi \right] J_\alpha \left(\frac{\mu}{k} \right) + \frac{\mu}{k} J'_\alpha \left(\frac{\mu}{k} \right) \right] + \\ & + J_\alpha \left(\frac{\mu}{kz_L} \right) \left[\left[\frac{s_\xi}{2} - (r_0)_\xi \right] Y_\alpha \left(\frac{\mu}{k} \right) + \frac{\mu}{k} Y'_\alpha \left(\frac{\mu}{k} \right) \right], \end{aligned} \quad (\text{B.6})$$

$$N_{\xi(-,+)}(\mu; \{\mathcal{P}_\xi\}) = + J_\alpha\left(\frac{\mu}{k}\right) \left[\left[\frac{s_\xi}{2} - (r_\pi)_\xi \right] Y_\alpha\left(\frac{\mu}{kz_L}\right) + \frac{\mu}{kz_L} Y'_\alpha\left(\frac{\mu}{kz_L}\right) \right] + \\ - Y_\alpha\left(\frac{\mu}{k}\right) \left[\left[\frac{s_\xi}{2} - (r_\pi)_\xi \right] J_\alpha\left(\frac{\mu}{kz_L}\right) + \frac{\mu}{kz_L} J'_\alpha\left(\frac{\mu}{kz_L}\right) \right], \quad (\text{B.7})$$

$$N_{\xi(-,-)}(\mu; \{\mathcal{P}_\xi\}) = J_\alpha\left(\frac{\mu}{k}\right) Y_\alpha\left(\frac{\mu}{kz_L}\right) - J_\alpha\left(\frac{\mu}{kz_L}\right) Y_\alpha\left(\frac{\mu}{k}\right), \quad (\text{B.8})$$

$$N_{\xi(+,+)}(\mu; \{\mathcal{P}_\xi\}) = - \left[\left[\frac{s_\xi}{2} - (r_0)_\xi \right] J_\alpha\left(\frac{\mu}{k}\right) + \frac{\mu}{k} J'_\alpha\left(\frac{\mu}{k}\right) \right] \\ \times \left[\left[\frac{s_\xi}{2} - (r_\pi)_\xi \right] Y_\alpha\left(\frac{\mu}{kz_L}\right) + \frac{\mu}{kz_L} Y'_\alpha\left(\frac{\mu}{kz_L}\right) \right] \\ + \left[\left[\frac{s_\xi}{2} - (r_\pi)_\xi \right] J_\alpha\left(\frac{\mu}{kz_L}\right) + \frac{\mu}{kz_L} J'_\alpha\left(\frac{\mu}{kz_L}\right) \right] \\ \times \left[\left[\frac{s_\xi}{2} - (r_0)_\xi \right] Y_\alpha\left(\frac{\mu}{k}\right) + \frac{\mu}{k} Y'_\alpha\left(\frac{\mu}{k}\right) \right], \quad (\text{B.9})$$

where $(r_0)_\xi, (r_\pi)_\xi$ denote the 5D mass parameters at the branes. In our case, they take the simplified form for $\xi \in \{A_\mu, \phi, e^{-2kL_5|y|}\psi_L, e^{-2kL_5|y|}\psi_R\}$,

$$(r_0)_\xi = (r_\pi)_\xi = \{0, 0, -c_\xi, c_\xi\}, \quad (\text{B.10})$$

where c_ξ corresponds to the parent field's original 5D mass parameter $c_\xi \in \{c_0, c_1, c_2, c'_0\}$. Note that we don't have any artificially introduced brane masses for the scalar fields in the 5D limit.

B.4 Bessel Basis Functions

The auxiliary Bessel function constructs that are used to express the basis functions for the various fields within the 6D formalism are as follow,

$$F_{\alpha\beta}(u, v) = J_\alpha(u)Y_\beta(v) - Y_\alpha(u)J_\beta(v), \quad (\text{B.11})$$

$$\hat{F}_{\alpha,\beta}(u, v) = I_\alpha(u)K_\beta(v) - \exp(-i\pi(\alpha - \beta))K_\alpha(u)I_\beta(v), \quad (\text{B.12})$$

$$\hat{F}_c^{\pm,\pm}(q) = \hat{F}_{c\pm\frac{1}{2}, c\pm\frac{1}{2}}(qz_L^{-1}, q). \quad (\text{B.13})$$

The fermion LH/ RH basis functions, corresponding to either a sine or a cosine

6D decomposition are given by S_L, S_R , and C_L, C_R respectively, where

$$S_L(z; \lambda, c) = \frac{(-\pi)}{2} \lambda \sqrt{zz_L} F_{c+\frac{1}{2}, c+\frac{1}{2}}(\lambda z, \lambda z_L), \quad (\text{B.14})$$

$$S_R(z; \lambda, c) = \frac{(+\pi)}{2} \lambda \sqrt{zz_L} F_{c-\frac{1}{2}, c-\frac{1}{2}}(\lambda z, \lambda z_L), \quad (\text{B.15})$$

$$C_R(z; \lambda, c) = \frac{(-\pi)}{2} \lambda \sqrt{zz_L} F_{c-\frac{1}{2}, c+\frac{1}{2}}(\lambda z, \lambda z_L), \quad (\text{B.16})$$

$$S_L(z; \lambda, c) = \frac{(+\pi)}{2} \lambda \sqrt{zz_L} F_{c+\frac{1}{2}, c-\frac{1}{2}}(\lambda z, \lambda z_L). \quad (\text{B.17})$$

Similarly the vector boson basis functions, corresponding to either a sine or a cosine 6D decomposition, are given by,

$$C(z; \lambda) = \frac{(+\pi)}{2} \lambda z^{3/2} \sqrt{z_L} F_{\frac{3}{2}, \frac{1}{2}}(\lambda z, \lambda z_L), \quad (\text{B.18})$$

$$S(z; \lambda) = \frac{(-\pi)}{2} \lambda z^{3/2} \sqrt{z_L} F_{\frac{3}{2}, \frac{3}{2}}(\lambda z, \lambda z_L), \quad (\text{B.19})$$

$$C'(z; \lambda) = \frac{(+\pi)}{2} \lambda^2 z^{3/2} \sqrt{z_L} F_{\frac{1}{2}, \frac{1}{2}}(\lambda z, \lambda z_L), \quad (\text{B.20})$$

$$S'(z; \lambda) = \frac{(-\pi)}{2} \lambda^2 z^{3/2} \sqrt{z_L} F_{\frac{1}{2}, \frac{3}{2}}(\lambda z, \lambda z_L). \quad (\text{B.21})$$

B.5 Bessel Tower Equations Solutions

The relevant fields that obtain $n = 0$ modes along the GUT direction correspond to the W_R tower, photon tower, and Higgs tower, which are described by the equations

$$C(1; \lambda_{W_R}) = 0, \quad (\text{B.22})$$

$$C'(1; \lambda_\gamma) = 0, \quad (\text{B.23})$$

$$S(1; \lambda_{A^{4,11}}) = 0. \quad (\text{B.24})$$

Plotting the basis functions for a realistic value of z_L (i.e. $z_L = 35$) as shown in Fig. B.4, we can see that the photon tower and the W_R tower's first non-trivial solution are nearly degenerate at $\lambda \sim 0.8$. Note that the first non-trivial solution for the Higgs tower occurs at larger values of $\lambda \sim 0.11$. As z_L increases, the photon tower and the W_R tower become even more degenerate, further justifying our approximation.

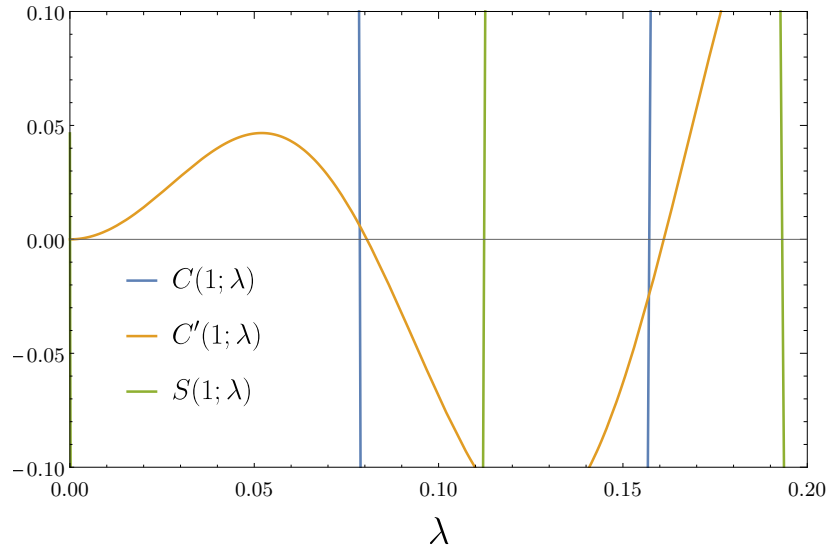


Figure B.4: Bessel basis function plot, where the blue line represents $C(1; \lambda)$, the orange line represents $C'(1; \lambda)$, and the green represents $S(1; \lambda)$. The roots of $C(1; \lambda_{W_R}) = 0$, $C'(1; \lambda_\gamma) = 0$, $S(1; \lambda_{A^{4,11}}) = 0$ correspond to the W_R tower, photon tower, and Higgs tower spectra. The above are evaluated for a warp factor of $z_L = 35$.

List of Figures

1.1	Diagrams contributing to the one loop effective $HH\Phi\Phi$ interaction. .	23
1.2	First order loop corrections in the ϕ^4 theory, where the diagrams correspond to the $n = 1, 2, 3, 4$ terms in the functional logarithm expansion in Eqn. (1.115).	27
2.1	Scalar 1 loop corrections arising from the fermionic and scalar contributions.	52
2.2	SUSY scalar B-L violating term contributing to the dimension 6 Feynman diagram for proton decay.	58
3.1	Identifying the circle S^1 as the manifold \mathbb{R}^1/\mathbb{Z} where the identification is performed by modding out the real number line \mathbb{R} via the action of the \mathbb{Z} modulo group.	77
3.2	Modding S^1 by \mathbb{Z}_2 is done by identifying the opposite ends of the circle together resulting in the interval with fixed points at $y = 0, y = \pi R$	78
3.3	The two different ways of identifying y with $-y$ within S^1/\mathbb{Z}_2 . The red lines represent translation τ by $2\pi R$, the blue lines represent a reflection ξ around 0. The dotted grey lines represent the equivalent reflection/inverse translation that produces the same identification. Note that the open ended interval symbols at 0 denote this as just a depiction of the $[0, 4\pi R]$ interval, with the end points not being identified with each other.	80
3.4	Points from the Barbieri, Hall and Nomura $SU(5)$ model with brane fermionic matter. Circles denote points that have passed the experimental constraints and have the desired Higgs mass, triangles show points that obey the Scherk-Schwarz constraint. Fainter points in the background fail these constraints but are otherwise well behaved. The x axis represents the soft SUSY scale parameter $\hat{\alpha}$, the y axis shows the corresponding value for $\tan\beta$ and the colour axis represent the value of the Higgs mass.	99
3.5	Points from the Barbieri, Hall and Nomura $SU(5)$ Model with bulk matter. We use the same conventions for the points as in Fig. 3.4. .	100

3.6	Points for the $SU(5)$ model with an additional scalar S on the brane, and brane matter. We use the same conventions for the points as in Fig. 3.4.	102
3.7	Points for the $SU(5)$ model with an additional scalar S on the brane, and bulk matter. We use the same conventions for the points as in Fig. 3.4.	103
3.8	Points for the $SU(5)$ model with an additional bulk scalar \mathcal{S} , and brane matter. We use the same conventions for the points as in Fig. 3.4.	105
3.9	Points for the $SU(5)$ model with an additional bulk scalar \mathcal{S} , and bulk matter. We use the same conventions for the points as in Fig. 3.4.	106
3.10	Points for the $SU(5)$ model with an additional bulk scalar \mathcal{S} , and bulk matter. We use the same conventions for the points as in Fig. 3.4, but this time we have plotted the deviation from the Scherk-Schwarz condition vs. the Higgs mass m_H	106
3.11	Points for the $SU(5) \times U(1)$ model with the additional scalar S and fermions both on the brane. We use the same conventions for the points as in Fig. 3.4.	108
3.12	Points for the $SU(5) \times U(1)$ model with the additional scalar S on the brane and fermions in the bulk. We use the same conventions for the points as in Fig. 3.4.	108
3.13	Points for the $SU(5) \times U(1)_N$ model with the additional scalar \mathcal{S} in the bulk and fermions on the brane. We use the same conventions for the points as in Fig. 3.4.	109
3.14	Points for the $SU(5) \times U(1)$ model with the additional scalar \mathcal{S} and fermions both in the bulk. We use the same conventions for the points as in Fig. 3.4.	109
4.1	Wilson loop $\mathbf{U}(x)$ around a square of size ϵ in $\{\hat{1}, \hat{2}\}$, where we start off at x and consecutively make ϵ increments in the $\hat{1}$ and $\hat{2}$ dimensions to form a square along the flow of the arrows.	119
4.2	One loop contributions to $V_{\text{eff}}(A_y^{\hat{a}})$ arising from fermions ψ , boson couplings $A_M^{a, \hat{a}}$, scalars ϕ , and ghosts η . The hat index $\hat{a} \in \mathcal{H}_W$ denotes the gauge components that transform under the broken coset, where the rest denote the ones transforming under the gauge symmetry imposed by $[\lambda^a, P_0] = [\lambda^a, P_1]$	128

- 4.3 Effective potential contour plots for the cases of bulk and fermionic brane matter. The color bar represents the value of the potential $V_{\text{eff}}(a, b)$, and the x, y axis represent the Wilson line phases a, b . Note that the potential is periodic, where in the case of bulk matter the global minimum lies at a non-trivial point away from the origin, whereas in the brane matter case the minimum is trivial. 132
- 6.1 Diagrammatic views of the torus as a lattice, and the orbifolding procedure resulting in T^2/\mathbb{Z}_2 148
- 6.2 $\mathcal{M}_4 \times (T^2/\mathbb{Z}_2)$ orbifold with 5D branes with a $\mathcal{M}_4 \times S^1$ topology at $y = 0, L_5$. y corresponds to the warped coordinate, and the 5D branes have the extra dimensional flat coordinate corresponding to $\nu \in [0, 2\pi R_6]$. The blue labels represent the $SO(11)$ symmetry in the 6D bulk, the same manifest UV brane symmetry, and with the effective Pati-Salam (PS) projection that results from the parity assignments intersection $G_{\text{PS}} \sim SO(6) \times SO(4) = SO(10) \cap SO(7) \times SO(4)$. The red labels represent the 5D $SO(11)$ spinor scalar field $\Phi_{\mathbf{32}}$ that breaks the UV brane symmetry down to $SU(5)$ via a Higgs mechanism, which in turn project the IR brane PS symmetry down to the SM. 150
- 6.3 $SO(11)$ breaking diagram depicting the maximal subgroups $SO(10)$ and $SO(7) \times SO(4)$, their intersection $SO(10) \cap SO(7) \times SO(4) = SU(4)_C \times SU(2)_L \times SU(2)_R \equiv G_{\text{PS}}$ highlighted in blue, and the different cosets $SO(7)/SO(6)$, $SO(5)/SO(4)$ originating from the subgroup breaking. 165
- 6.4 $SO(11)$ breaking diagram after the introduction of the $SU(5)$ UV brane breaking. Fields invariant under G_{SM} (represented as the green shaded region) have massless modes, those corresponding to the coset $G_{\text{PS}}/G_{\text{SM}}$ have masses of order $\mathcal{O}(M_{\text{KK}_5})$ (represented as the blue shaded region), and all the rest have masses of order $\mathcal{O}(M_{\text{GUT}})$ (represented as the white region). 166

7.1	Log-log sample runs of the differential evolution outlined in the text, showing the χ_G^2 value as a function of the generation number G . Note that each run (shown in different colours and denoted as “thread” specifies a parallel run) contains a population $N_P = 12$. The horizontal dotted line represents the \log_{10} value of the SM like lower bound in Eqn. (7.6), after which we terminate the thread. Note that this run was ended prematurely for Threads 5, 4, 3, 6, leading to non-SM solutions.	184
7.2	Scatter plot of representative parameter space points for the $SO(11)$ model before and after differential evolution as functions of the KK scale m_{KK_5} and warp factor z_L . The color reflects the order parameter $\langle\theta_H\rangle$. Points highlighted as hexagons are the points that are SM-like (i.e. they obey the bound set in Eqn. (7.6)). Faded points are excluded on the basis of falling short of the χ_G^2 measure bound.	185
7.3	Sensitivity bands for the di-Higgs production at CMS and the proposed FCC collider	187
7.4	Main $gg \rightarrow HH$ 1 loop production diagrams. The trilinear Higgs coupling is given by τ_H , and the top Yukawa coupling is $\sim y_t^{\text{SM}} \cdot \cos\theta_H$, as discussed in Ref. [146]. The gluon top couplings are the same as in the SM.	188
7.5	Relative cross section correlations with the UV and IR attributes.	189
7.6	Exotic scatter plots showing the lowest available mass states and relevant fields.	190
7.7	Tower of EFTs that approximate the UV 6D theory. The 4D description is valid within $[M_Z, M_{KK_5}]$ with $G_{\text{SM}} \equiv SU(3)_C \times U(1)_{\text{EM}}$ gauge symmetry and within $[M_{KK_5}, 1/L_5]$ with G_{PS} gauge symmetry. The 5D description is valid within $[M_{KK_5}, \Lambda_{\text{Max}}]$ with a G_{PS} gauge symmetry. Above Λ_{Max} the full 6D description comes into effect.	194

7.8	Tower of states from M_Z to the next states above M_{KK_5} . The labels on the x axis indicate the relevant fermionic and boson fields, and the markers represent the mass value of the respective KK tower state. The labels stand for: W_μ^\pm is the W boson tower, Z_μ^0 is the Z boson tower, ψ_t is the top quark tower, ψ_b is the bottom quark tower, ψ_D is the 'dark fermion' multiplet tower, W_μ^R is the Pati-Salam $SU(2)_R$ W boson tower of states, γ_μ is the photon tower of states, $A_z^{4,11}$ is the Higgs tower of states, and ψ_τ is the tau tower of states.	196
7.9	RGE evolution for the piecewise SM couplings g_{3C}, g_{2L}, g_{1Y} with the different β function changes at the multiple encountered KK states marked as dotted lines. Note that the piecewise forms for g_{2L}, g_{1Y} are obtained via Eqn. (7.26).	200
7.10	Effective 4D $SU(4)_C \times SU(2)_L \times SU(2)_R$ gauge couplings obtained via the 5D Pati-Salam approximation, using the evolved coupling values originating from the 4D formalism. The dotted line corresponds to the M_{KK_5} threshold at which we start our 5D runnings.	208
7.11	Numerical impact of the Casimir correction (blue line) as a function of the unknown inverse unified coupling $(\alpha_{4\text{D}}^{SO(11)})^{-1}$. The green line represents the low bound for the $\sim 0.4\%$ deviation occurring at $(\alpha_{4\text{D}}^{SO(11)})^{-1} \simeq 20$. The orange line represents the GUT hypothesis $3/8$. The smaller α , the less impact the Casimir corrections have on the prediction as they weighted by $\alpha_{4\text{D}}^{SO(11)}$	210
7.12	RGE evolution in the $N_G = 1$ case within the 4D and 5D approximations.	211
7.13	Scatter plots analogous to Figs. 7.12a and 7.12b for the degenerate $N_G = 3$ case.	212
7.14	4D SM gauge coupling running between $[M_Z, M_{\text{KK}_5}]$, for the $N_G = 1$ case (a), and the $N_G = 3$ case (b). The particular runs are of the sample point showcased in Eqn. (7.19).	214
B.1	Piecewise RGE evolutions of the electromagnetic and strong couplings for the sample point in Eqn. (7.19).	226
B.2	Piecewise RGE evolutions of the Weinberg angle and the weak coupling for the sample point in Eqn. (7.19).	227

- B.3 RGE evolution for the piecewise hypercoupling g_{1Y} for the sample point in Eqn. (7.19), with the different β function changes at the multiple encountered KK states marked as dotted lines. Note that this is derived from the values of $\alpha_{\text{EM}}, \sin \theta_W$ 228
- B.4 Bessel bassis function plot, where the blue line represents $C(1; \lambda)$, the orange line represents $C'(1; \lambda)$, and the green represents $S(1; \lambda)$. The roots of $C(1; \lambda_{W_R}) = 0$, $C'(1; \lambda_\gamma) = 0$, $S(1; \lambda_{A^{4,11}}) = 0$ correspond to the W_R tower, photon tower, and Higgs tower spectra. The above are evaluated for a warp factor of $z_L = 35$ 231

List of Tables

1.1	Table summarising the matter fields in the SM, where the columns contain the name of the field, the nomenclature, the notation for the spin 1/2 components, and the charges under the SM gauge group $G_{\text{SM}} = SU(3)_C \times SU(2)_L \times U(1)_Y$. The RH version of the fields is obtained via Hermitian conjugation.	6
1.2	Table summarising the gauge fields in the SM, where the columns contain the name of the field, the nomenclature, the notation for the spin 1 components, and the charges under the SM gauge group $G_{\text{SM}} = SU(3)_C \times SU(2)_L \times U(1)_Y$	6
2.1	Examples of common massless supermultiplets consisting of the two different helicity states along with their notation and name.	37
2.2	The available states in a supermultiplet where the left column denotes how the state is obtained via applying successive raising operators, the middle column denotes the helicity of the obtained states, and the right column contains the number of states of equivalent helicity.	40
2.3	Table summarising the gauge fields in the MSSM, where the columns contain the name of the containing superfield, the nomenclature of the components, the notations for the spin 1/2, 1 components, and their charges under the SM gauge group $G_{\text{SM}} = SU(3)_C \times SU(2)_L \times U(1)_Y$	55
2.4	Table summarising the matter fields in the MSSM, where the columns contain the name of the containing superfield, the number of copies of the superfield, the nomenclature of the components, the notations for the spin 0, 1/2 components, and their charges under the SM gauge group G_{SM}	55

7.1	Parameter values for the definition of χ_G^2 . The experimental uncertainties are the most recent bounds [22] for the Higgs boson H [9], the W^\pm bosons, the top quark t , the bottom quark b , and the tau lepton τ . We include a “theoretical” error to widen the parameter windows to discuss the phenomenological outcome in more detail below. The Z mass is obtained through the Weinberg angle, which we use as an input.	182
7.2	Charge assignments for fields contributing to the RGE runnings. . .	199
7.3	Fermion parity assignments under $S^1/\mathbb{Z}_2 \times \mathbb{Z}'_2$	202
7.4	Gauge boson parity assignment under $S^1/\mathbb{Z}_2 \times \mathbb{Z}'_2$. Note that we have to treat the G_{PS} , and G_{SM} representations separately due to the mixed parity assignments in the full 6D model.	202
7.5	Scalar parity assignment under $S^1/\mathbb{Z}_2 \times \mathbb{Z}'_2$. In the 5D RGE formalism they are treated as scalars originating from either the gauge boson projections or as remnants from the 6D approximation. . . .	203

Bibliography

- [1] Dumitru Dan Smaranda and David J. Miller, “Scherk-Schwarz orbifolds at the LHC,” [Phys. Rev. **D100**, 075016 \(2019\)](#), [arXiv:1901.10279 \[hep-ph\]](#) .
- [2] Christoph Englert, David J. Miller, and Dumitru Dan Smaranda, “Phenomenology of GUT-inspired gauge-Higgs unification,” [Physics Letters B. **802**, 135261 \(2020\)](#), [arXiv:1911.05527 \[hep-ph\]](#) .
- [3] Christoph Englert, David J. Miller, and Dumitru Dan Smaranda, “The Weinberg Angle and 5D RGE effects in a SO(11) GUT theory,” (2020), [arXiv:2003.05743 \[hep-ph\]](#) .
- [4] Sheldon L. Glashow, “Partial-symmetries of weak interactions,” [Nuclear Physics **22**, 579 – 588 \(1961\)](#).
- [5] Steven Weinberg, “A model of leptons,” [Phys. Rev. Lett. **19**, 1264–1266 \(1967\)](#).
- [6] Abdus Salam and J. C. Ward, “Weak and electromagnetic interactions,” [II Nuovo Cimento \(1955-1965\) **11**, 568–577 \(1959\)](#).
- [7] Georges Aad *et al.* (ATLAS), “Observation of a new particle in the search for the Standard Model Higgs boson with the ATLAS detector at the LHC,” [Phys. Lett. **B716**, 1–29 \(2012\)](#), [arXiv:1207.7214 \[hep-ex\]](#) .
- [8] Serguei Chatrchyan *et al.* (CMS), “Observation of a New Boson at a Mass of 125 GeV with the CMS Experiment at the LHC,” [Phys. Lett. **B716**, 30–61 \(2012\)](#), [arXiv:1207.7235 \[hep-ex\]](#) .
- [9] M. et al Tanabashi (Particle Data Group), “Review of particle physics,” [Phys. Rev. D **98**, 030001 \(2018\)](#).
- [10] G. Ross, “Beyond the Standard Model,” *43rd Annual Winter School on Physics (PNPI 2009) Repino, St. Petersburg, Russia, February 24-March 1, 2009*, [Phys. Atom. Nucl. **79**, 1445–1470 \(2016\)](#).
- [11] Steven Weinberg, “Implications of dynamical symmetry breaking,” [Phys. Rev. D **13**, 974–996 \(1976\)](#).

- [12] Leonard Susskind, “Dynamics of spontaneous symmetry breaking in the weinberg-salam theory,” [Phys. Rev. D **20**, 2619–2625 \(1979\)](#).
- [13] Eldad Gildener, “Gauge Symmetry Hierarchies,” [Phys. Rev. **D14**, 1667 \(1976\)](#).
- [14] Gerard 't Hooft, C. Itzykson, A. Jaffe, H. Lehmann, P. K. Mitter, I. M. Singer, and R. Stora, “Recent Developments in Gauge Theories. Proceedings, Nato Advanced Study Institute, Cargese, France, August 26 - September 8, 1979,” [NATO Sci. Ser. B **59**, pp.1–438 \(1980\)](#).
- [15] Steven Weinberg, “The cosmological constant problem,” [Rev. Mod. Phys. **61**, 1–23 \(1989\)](#).
- [16] Steven Weinberg, “The U(1) problem,” [Phys. Rev. D **11**, 3583–3593 \(1975\)](#).
- [17] Andrei D Sakharov, “Baryon asymmetry of the universe,” [Soviet Physics Uspekhi **34**, 417–421 \(1991\)](#).
- [18] Mark Srednicki, [*Quantum Field Theory*](#) (Cambridge Univ. Press, Cambridge, 2007).
- [19] Sidney Coleman and Jeffrey Mandula, “All possible symmetries of the s matrix,” [Phys. Rev. **159**, 1251–1256 \(1967\)](#).
- [20] S. L. Glashow, “Partial Symmetries of Weak Interactions,” [Nucl. Phys. **22**, 579–588 \(1961\)](#).
- [21] Abdus Salam, “Weak and Electromagnetic Interactions,” *8th Nobel Symposium Lerum, Sweden, May 19-25, 1968*, [Conf. Proc. **C680519**, 367–377 \(1968\)](#).
- [22] M. Tanabashi *et al.* (Particle Data Group), “Review of Particle Physics,” [Phys. Rev. **D98**, 030001 \(2018\)](#).
- [23] Ziro Maki, Masami Nakagawa, and Shoichi Sakata, “Remarks on the Unified Model of Elementary Particles,” [Progress of Theoretical Physics **28**, 870–880 \(1962\)](#).
- [24] B. Pontecorvo, “Inverse beta processes and nonconservation of lepton charge,” *Sov. Phys. JETP* **7**, 172–173 (1958), [*Zh. Eksp. Teor. Fiz.*34,247(1957)].

- [25] Nicola Cabibbo, “Unitary symmetry and leptonic decays,” [Phys. Rev. Lett. **10**, 531–533 \(1963\)](#).
- [26] Makoto Kobayashi and Toshihide Maskawa, “CP-Violation in the Renormalizable Theory of Weak Interaction,” [Progress of Theoretical Physics **49**, 652–657 \(1973\)](#).
- [27] H. Georgi, [Lie Algebras in Particle Physics](#) (Sarat Book Distributors, 2009).
- [28] C.H.Llewellyn Smith and G.G. Ross, “The real gauge hierarchy problem,” [Physics Letters B **105**, 38 – 40 \(1981\)](#).
- [29] Michael E Peskin and Daniel V Schroeder, *An Introduction to Quantum Field Theory; 1995 ed.* (Westview, Boulder, CO, 1995).
- [30] Claude Itzykson and Jean-Bernard Zuber, *Quantum field theory* (McGraw-Hill, 1980).
- [31] Sidney R. Coleman and Erick J. Weinberg, “Radiative Corrections as the Origin of Spontaneous Symmetry Breaking,” [Phys. Rev. **D7**, 1888–1910 \(1973\)](#).
- [32] N.K. Nielsen, “On the Gauge Dependence of Spontaneous Symmetry Breaking in Gauge Theories,” [Nucl. Phys. B **101**, 173–188 \(1975\)](#).
- [33] J. S. Kang, “Gauge invariance of the scalar-vector mass ratio in the coleman-weinberg model,” [Phys. Rev. D **10**, 3455–3467 \(1974\)](#).
- [34] Dimitrios Metaxas and Erick J. Weinberg, “Gauge independence of the bubble nucleation rate in theories with radiative symmetry breaking,” [Phys. Rev. D **53**, 836–843 \(1996\)](#).
- [35] Takeshi Fukuyama, “SO(10) GUT in Four and Five Dimensions: A Review,” [Int. J. Mod. Phys. **A28**, 1330008 \(2013\)](#), [arXiv:1212.3407 \[hep-ph\]](#) .
- [36] Lawrence J. Hall and Yasunori Nomura, “Gauge unification in higher dimensions,” [Phys. Rev. **D64**, 055003 \(2001\)](#), [arXiv:hep-ph/0103125 \[hep-ph\]](#) .
- [37] Guido Altarelli and Ferruccio Feruglio, “SU(5) grand unification in extra dimensions and proton decay,” [Phys. Lett. **B511**, 257–264 \(2001\)](#), [arXiv:hep-ph/0102301 \[hep-ph\]](#) .

- [38] Lawrence J. Hall, Yasunori Nomura, Takemichi Okui, and David Tucker-Smith, “SO(10) unified theories in six-dimensions,” *Phys. Rev.* **D65**, 035008 (2002), [arXiv:hep-ph/0108071 \[hep-ph\]](#) .
- [39] T. Asaka, W. Buchmuller, and L. Covi, “Gauge unification in six-dimensions,” *Phys. Lett.* **B523**, 199–204 (2001), [arXiv:hep-ph/0108021 \[hep-ph\]](#) .
- [40] Fernando Quevedo, Sven Krippendorff, and Oliver Schlotterer, “Cambridge Lectures on Supersymmetry and Extra Dimensions,” (2010), [arXiv:1011.1491 \[hep-th\]](#) .
- [41] S. P. Martin, “A supersymmetry primer,” *Adv. Ser. Direct. High Energy Phys.* **18**, 1(1998) , 1 – 98 (1997), [arXiv:hep-ph/9709356 \[hep-ph\]](#) .
- [42] B. Hall, *Lie Groups, Lie Algebras, and Representations: An Elementary Introduction*, Graduate Texts in Mathematics (Springer International Publishing, 2015).
- [43] J. Wess and B. Zumino, “Supergauge transformations in four dimensions,” *Nuclear Physics B* **70**, 39 – 50 (1974).
- [44] P. Fayet and J. Iliopoulos, “Spontaneously broken supergauge symmetries and goldstone spinors,” *Physics Letters B* **51**, 461 – 464 (1974).
- [45] Mikolaj Misiak, Stefan Pokorski, and Janusz Rosiek, “Supersymmetry and FCNC effects,” *Adv. Ser. Direct. High Energy Phys.* **15**, 795–828 (1998), [795(1997)], [arXiv:hep-ph/9703442 \[hep-ph\]](#) .
- [46] Savas Dimopoulos and David W. Sutter, “The Supersymmetric flavor problem,” *Nucl. Phys. B* **452**, 496–512 (1995), [arXiv:hep-ph/9504415](#) .
- [47] Stephen P. Martin, “Two Loop Effective Potential for a General Renormalizable Theory and Softly Broken Supersymmetry,” *Phys. Rev.* **D65**, 116003 (2002), [arXiv:hep-ph/0111209 \[hep-ph\]](#) .
- [48] Erich Poppitz and Sandip P. Trivedi, “Some remarks on gauge mediated supersymmetry breaking,” *Phys. Lett.* **B401**, 38–46 (1997), [arXiv:hep-ph/9703246 \[hep-ph\]](#) .

- [49] Morad Aaboud *et al.* (ATLAS), “Search for top-squark pair production in final states with one lepton, jets, and missing transverse momentum using 36 fb⁻¹ of $\sqrt{s} = 13$ TeV pp collision data with the ATLAS detector,” *JHEP* **06**, 108 (2018), [arXiv:1711.11520 \[hep-ex\]](#) .
- [50] Damien M. Pierce, Jonathan A. Bagger, Konstantin T. Matchev, and Renjie Zhang, “Precision corrections in the minimal supersymmetric standard model,” *Nucl. Phys.* **B491**, 3–67 (1997), [arXiv:hep-ph/9606211 \[hep-ph\]](#) .
- [51] Damien Pierce and Aris Papadopoulos, “The Complete radiative corrections to the gaugino and Higgsino masses in the minimal supersymmetric model,” *Nucl. Phys.* **B430**, 278–294 (1994), [arXiv:hep-ph/9403240 \[hep-ph\]](#) .
- [52] Damien Pierce and Aris Papadopoulos, “Radiative corrections to neutralino and chargino masses in the minimal supersymmetric model,” *Phys. Rev.* **D50**, 565–570 (1994), [arXiv:hep-ph/9312248 \[hep-ph\]](#) .
- [53] Stephen P. Martin, “Fermion self-energies and pole masses at two-loop order in a general renormalizable theory with massless gauge bosons,” *Phys. Rev.* **D72**, 096008 (2005), [arXiv:hep-ph/0509115 \[hep-ph\]](#) .
- [54] Youichi Yamada, “Two-loop SUSY QCD correction to the gluino pole mass,” *Phys. Lett.* **B623**, 104–110 (2005), [arXiv:hep-ph/0506262 \[hep-ph\]](#) .
- [55] Stephen P. Martin, “Refined gluino and squark pole masses beyond leading order,” *Phys. Rev.* **D74**, 075009 (2006), [Erratum: *Phys. Rev.* **D79**, no.11, 119901 (2009)], [arXiv:hep-ph/0608026 \[hep-ph\]](#) .
- [56] Toru Goto and Takeshi Nihei, “Effect of an RRRR dimension 5 operator on proton decay in the minimal SU(5) SUGRA GUT model,” *Phys. Rev. D* **59**, 115009 (1999).
- [57] Hitoshi Murayama and Aaron Pierce, “Not even decoupling can save the minimal supersymmetric su(5) model,” *Phys. Rev. D* **65**, 055009 (2002).
- [58] Edward Witten, “Mass hierarchies in supersymmetric theories,” *Physics Letters B* **105**, 267 – 271 (1981).
- [59] Kenzo Inoue, Akira Kakuto, and Hiroshi Takano, “Higgs as (Pseudo)Goldstone Particles,” in *Tokyo 1985, proceedings, structure and forces in elementary particle physics, 46-53.*, Vol. 75 (1986) p. 664.

- [60] Csaba Csaki, “TASI lectures on extra dimensions and branes,” in *From fields to strings: Circumnavigating theoretical physics. Ian Kogan memorial collection (3 volume set)* (2004) pp. 605–698, [967(2004)], [arXiv:hep-ph/0404096 \[hep-ph\]](#) .
- [61] J. Scherk and John H. Schwarz, “Spontaneous breaking of supersymmetry through dimensional reduction,” [Physics Letters B](#) **82**, 60 – 64 (1979).
- [62] J. Scherk and John H. Schwarz, “How to get masses from extra dimensions,” [Nuclear Physics B](#) **153**, 61 – 88 (1979).
- [63] Riccardo Barbieri, Lawrence J. Hall, and Yasunori Nomura, “Softly broken supersymmetric desert from orbifold compactification,” [Phys. Rev.](#) **D66**, 045025 (2002), [arXiv:hep-ph/0106190 \[hep-ph\]](#) .
- [64] Riccardo Barbieri, Lawrence J. Hall, and Yasunori Nomura, “Models of Scherk-Schwarz symmetry breaking in 5-D: Classification and calculability,” [Nucl. Phys.](#) **B624**, 63–80 (2002), [arXiv:hep-th/0107004 \[hep-th\]](#) .
- [65] Roman Nevzorov, “ E_6 inspired supersymmetric models with exact custodial symmetry,” [Phys. Rev.](#) **D87**, 015029 (2013), [arXiv:1205.5967 \[hep-ph\]](#) .
- [66] Savas Dimopoulos and Stuart Raby, “Supercolor,” [Nucl. Phys.](#) **B192**, 353–368 (1981).
- [67] Edward Witten, “Dynamical Breaking of Supersymmetry,” [Nucl. Phys.](#) **B188**, 513 (1981).
- [68] M. Quiros, “New ideas in symmetry breaking,” in *Summer Institute 2002 (SI 2002) Fuji-Yoshida, Japan, August 13-20, 2002* (2003) pp. 549–601, [549(2003)], [arXiv:hep-ph/0302189 \[hep-ph\]](#) .
- [69] Lisa Randall and Raman Sundrum, “A Large mass hierarchy from a small extra dimension,” [Phys. Rev. Lett.](#) **83**, 3370–3373 (1999), [arXiv:hep-ph/9905221 \[hep-ph\]](#) .
- [70] Raman Sundrum, “Tasi 2004 lectures: To the fifth dimension and back,” in *Theoretical Advanced Study Institute in Elementary Particle Physics: Many Dimensions of String Theory (TASI 2005) Boulder, Colorado, June 5-July 1, 2005* (2005) pp. 585–630, [585(2005)], [arXiv:hep-th/0508134 \[hep-th\]](#) .

- [71] Eugene A. Mirabelli and Michael E. Peskin, “Transmission of supersymmetry breaking from a four-dimensional boundary,” *Phys. Rev.* **D58**, 065002 (1998), [arXiv:hep-th/9712214 \[hep-th\]](#) .
- [72] Martin F. Sohnius, “Introducing supersymmetry,” *Physics Reports* **128**, 39 – 204 (1985).
- [73] Lawrence J. Hall, Yasunori Nomura, Takemichi Okui, and David Tucker-Smith, “SO(10) unified theories in six-dimensions,” *Phys. Rev.* **D65**, 035008 (2002), [arXiv:hep-ph/0108071 \[hep-ph\]](#) .
- [74] Yutaka Hosotani, “Dynamical Mass Generation by Compact Extra Dimensions,” *Phys. Lett.* **126B**, 309–313 (1983).
- [75] Yutaka Hosotani, “Dynamical gauge symmetry breaking as the casimir effect,” *Physics Letters B* **129**, 193 – 197 (1983).
- [76] Yutaka Hosotani, “Dynamics of non-integrable phases and gauge symmetry breaking,” *Annals of Physics* **190**, 233 – 253 (1989).
- [77] Peter Athron, Jae-hyeon Park, Dominik Stöckinger, and Alexander Voigt, “FlexibleSUSY—A spectrum generator generator for supersymmetric models,” *Comput. Phys. Commun.* **190**, 139–172 (2015), [arXiv:1406.2319 \[hep-ph\]](#) .
- [78] Peter Athron, Markus Bach, Dylan Harries, Thomas Kwasnitza, Jae-hyeon Park, Dominik Stöckinger, Alexander Voigt, and Jobst Ziebell, “FlexibleSUSY 2.0: Extensions to investigate the phenomenology of SUSY and non-SUSY models,” *Comput. Phys. Commun.* **230**, 145–217 (2018), [arXiv:1710.03760 \[hep-ph\]](#) .
- [79] B.C. Allanach, “SOFTSUSY: a program for calculating supersymmetric spectra,” *Comput.Phys.Comm.* **143**, 305–331 (2002), [arXiv:hep-ph/0104145 \[hep-ph\]](#) .
- [80] B.C. Allanach, P. Athron, Lewis C. Tunstall, A. Voigt, and A.G. Williams, “Next-to-Minimal SOFTSUSY,” *Comput.Phys.Comm.* **185**, 2322–2339 (2014), [arXiv:1311.7659 \[hep-ph\]](#) .

- [81] Florian Staub, “From Superpotential to Model Files for FeynArts and CalcHep/CompHep,” *Comput.Phys.Commun.* **181**, 1077–1086 (2010), [arXiv:0909.2863 \[hep-ph\]](#) .
- [82] Florian Staub, “Automatic Calculation of supersymmetric Renormalization Group Equations and Self Energies,” *Comput.Phys.Commun.* **182**, 808–833 (2011), [arXiv:1002.0840 \[hep-ph\]](#) .
- [83] Florian Staub, “SARAH 3.2: Dirac Gauginos, UFO output, and more,” *Comput.Phys.Commun.* **184**, pp. 1792–1809 (2013), [arXiv:1207.0906 \[hep-ph\]](#) .
- [84] Florian Staub, “SARAH 4: A tool for (not only SUSY) model builders,” *Comput.Phys.Commun.* **185**, 1773–1790 (2014), [arXiv:1309.7223 \[hep-ph\]](#) .
- [85] Georges Aad *et al.* (ATLAS), “Observation of a new particle in the search for the Standard Model Higgs boson with the ATLAS detector at the LHC,” *Phys. Lett.* **B716**, 1–29 (2012), [arXiv:1207.7214 \[hep-ex\]](#) .
- [86] Serguei Chatrchyan *et al.* (CMS), “Observation of a new boson at a mass of 125 GeV with the CMS experiment at the LHC,” *Phys. Lett.* **B716**, 30–61 (2012), [arXiv:1207.7235 \[hep-ex\]](#) .
- [87] Morad Aaboud *et al.* (ATLAS), “Search for squarks and gluinos in final states with jets and missing transverse momentum using 36 fb^{−1} of $\sqrt{s} = 13$ TeV pp collision data with the ATLAS detector,” *Phys. Rev.* **D97**, 112001 (2018), [arXiv:1712.02332 \[hep-ex\]](#) .
- [88] Albert M Sirunyan *et al.* (CMS), “Search for supersymmetry in proton-proton collisions at 13 TeV using identified top quarks,” *Phys. Rev.* **D97**, 012007 (2018), [arXiv:1710.11188 \[hep-ex\]](#) .
- [89] *SUSY July 2019 Summary Plot Update*, Tech. Rep. ATL-PHYS-PUB-2019-022 (CERN, Geneva, 2019).
- [90] Georges Aad *et al.* (ATLAS), “Search for the electroweak production of supersymmetric particles in $\sqrt{s}=8$ TeV *pp* collisions with the ATLAS detector,” *Phys. Rev.* **D93**, 052002 (2016), [arXiv:1509.07152 \[hep-ex\]](#) .
- [91] M. Aaboud *et al.* (ATLAS), “Search for electroweak production of supersymmetric particles in final states with two or three leptons at $\sqrt{s} = 13$ TeV

- with the ATLAS detector,” *Eur. Phys. J.* **C78**, 995 (2018), [arXiv:1803.02762 \[hep-ex\]](#) .
- [92] Morad Aaboud *et al.* (ATLAS), “Search for additional heavy neutral Higgs and gauge bosons in the ditau final state produced in 36 fb^{-1} of pp collisions at $\sqrt{s} = 13 \text{ TeV}$ with the ATLAS detector.” *JHEP* **01**, 055 (2018), [arXiv:1709.07242 \[hep-ex\]](#) .
- [93] G. Hinshaw *et al.* (WMAP), “Nine-Year Wilkinson Microwave Anisotropy Probe (WMAP) Observations: Cosmological Parameter Results,” *Astrophys. J. Suppl.* **208**, 19 (2013), [arXiv:1212.5226 \[astro-ph.CO\]](#) .
- [94] G. Belanger, F. Boudjema, A. Pukhov, and A. Semenov, “MicrOMEGAs: A Program for calculating the relic density in the MSSM,” *Comput. Phys. Commun.* **149**, 103–120 (2002), [arXiv:hep-ph/0112278 \[hep-ph\]](#) .
- [95] G. Belanger, F. Boudjema, A. Pukhov, and A. Semenov, “micrOMEGAs: Version 1.3,” *Comput. Phys. Commun.* **174**, 577–604 (2006), [arXiv:hep-ph/0405253 \[hep-ph\]](#) .
- [96] D. Barducci, G. Belanger, J. Bernon, F. Boudjema, J. Da Silva, S. Kraml, U. Laa, and A. Pukhov, “Collider limits on new physics within micrOMEGAs4.3,” (2016), [arXiv:1606.03834 \[hep-ph\]](#) .
- [97] Gian F. Giudice and Alessandro Strumia, “Probing High-Scale and Split Supersymmetry with Higgs Mass Measurements,” *Nucl. Phys.* **B858**, 63–83 (2012), [arXiv:1108.6077 \[hep-ph\]](#) .
- [98] Athanasios Dedes and Pietro Slavich, “Two loop corrections to radiative electroweak symmetry breaking in the MSSM,” *Nucl. Phys.* **B657**, 333–354 (2003), [arXiv:hep-ph/0212132 \[hep-ph\]](#) .
- [99] T. Asaka, W. Buchmuller, and L. Covi, “Gauge unification in six-dimensions,” *Phys. Lett.* **B523**, 199–204 (2001), [arXiv:hep-ph/0108021 \[hep-ph\]](#) .
- [100] S. F. King, S. Moretti, and R. Nevzorov, “Exceptional supersymmetric standard model,” *Phys. Lett.* **B634**, 278–284 (2006), [arXiv:hep-ph/0511256 \[hep-ph\]](#) .

- [101] S. F. King, S. Moretti, and R. Nevzorov, “Theory and phenomenology of an exceptional supersymmetric standard model,” *Phys. Rev.* **D73**, 035009 (2006), [arXiv:hep-ph/0510419 \[hep-ph\]](#) .
- [102] P. Athron, S. F. King, D. J. Miller, S. Moretti, and R. Nevzorov, “The Constrained Exceptional Supersymmetric Standard Model,” *Phys. Rev.* **D80**, 035009 (2009), [arXiv:0904.2169 \[hep-ph\]](#) .
- [103] P. Athron, S. F. King, D. J. Miller, S. Moretti, and R. Nevzorov, “Constrained Exceptional Supersymmetric Standard Model with a Higgs Near 125 GeV,” *Phys. Rev.* **D86**, 095003 (2012), [arXiv:1206.5028 \[hep-ph\]](#) .
- [104] Naoyuki Haba, Masatomi Harada, Yutaka Hosotani, and Yoshiharu Kawamura, “Dynamical rearrangement of gauge symmetry on the orbifold S^1/\mathbb{Z}_2 ,” *Nucl. Phys.* **B657**, 169–213 (2003), [Erratum: *Nucl. Phys.*B669,381(2003)], [arXiv:hep-ph/0212035 \[hep-ph\]](#) .
- [105] Lawrence J. Hall, Hitoshi Murayama, and Yasunori Nomura, “Wilson lines and symmetry breaking on orbifolds,” *Nucl. Phys.* **B645**, 85–104 (2002), [arXiv:hep-th/0107245 \[hep-th\]](#) .
- [106] Masahiro Kubo, C. S. Lim, and Hiroyuki Yamashita, “The Hosotani mechanism in bulk gauge theories with an orbifold extra space S^1/\mathbb{Z}_2 ,” *Mod. Phys. Lett.* **A17**, 2249–2264 (2002), [arXiv:hep-ph/0111327 \[hep-ph\]](#) .
- [107] Yutaka Hosotani, “Dynamical gauge symmetry breaking by Wilson lines in the electroweak theory,” in *Dynamical symmetry breaking. Proceedings, International Workshop, DSB’04, Nagoya, Japan, December 21-22, 2004* (2005) pp. 17–34, [arXiv:hep-ph/0504272 \[hep-ph\]](#) .
- [108] Michael E. Peskin and Daniel V. Schroeder, *An Introduction to quantum field theory* (Addison-Wesley, Reading, USA, 1995).
- [109] Csaba Csaki, Jay Hubisz, and Patrick Meade, “TASI lectures on electroweak symmetry breaking from extra dimensions,” in *Theoretical Advanced Study Institute in Elementary Particle Physics: Physics in $D \geq 4$* (2005) pp. 703–776, [arXiv:hep-ph/0510275](#) .
- [110] Tony Gherghetta and Alex Pomarol, “Bulk fields and supersymmetry in a slice of AdS,” *Nucl. Phys.* **B586**, 141–162 (2000), [arXiv:hep-ph/0003129 \[hep-ph\]](#) .

- [111] Ki-woon Choi and Ian-Woo Kim, “One loop gauge couplings in AdS(5),” *Phys. Rev.* **D67**, 045005 (2003), [arXiv:hep-th/0208071 \[hep-th\]](#) .
- [112] Lisa Randall and Matthew D. Schwartz, “Quantum field theory and unification in AdS5,” *JHEP* **11**, 003 (2001), [arXiv:hep-th/0108114 \[hep-th\]](#) .
- [113] Csaba Csaki, Christophe Grojean, Jay Hubisz, Yuri Shirman, and John Terning, “Fermions on an interval: Quark and lepton masses without a Higgs,” *Phys. Rev.* **D70**, 015012 (2004), [arXiv:hep-ph/0310355 \[hep-ph\]](#) .
- [114] Csaba Csáki, Salvator Lombardo, and Ofri Telem, “TASI Lectures on Non-supersymmetric BSM Models,” in *Proceedings, Theoretical Advanced Study Institute in Elementary Particle Physics : Anticipating the Next Discoveries in Particle Physics (TASI 2016): Boulder, CO, USA, June 6-July 1, 2016*, WSP (WSP, 2018) pp. 501–570, [arXiv:1811.04279 \[hep-ph\]](#) .
- [115] Atsushi Furui, Yutaka Hosotani, and Naoki Yamatsu, “Toward Realistic Gauge-Higgs Grand Unification,” *PTEP* **2016**, 093B01 (2016), [arXiv:1606.07222 \[hep-ph\]](#) .
- [116] Yutaka Hosotani and Naoki Yamatsu, “Electroweak symmetry breaking and mass spectra in six-dimensional gauge–Higgs grand unification,” *PTEP* **2018**, 023B05 (2018), [arXiv:1710.04811 \[hep-ph\]](#) .
- [117] Yutaka Hosotani and Naoki Yamatsu, “Gauge-Higgs seesaw mechanism in 6-dimensional grand unification,” *PTEP* **2017**, 091B01 (2017), [arXiv:1706.03503 \[hep-ph\]](#) .
- [118] Lisa Randall and Raman Sundrum, “A Large mass hierarchy from a small extra dimension,” *Phys. Rev. Lett.* **83**, 3370–3373 (1999), [arXiv:hep-ph/9905221 \[hep-ph\]](#) .
- [119] Y. Hosotani, K. Oda, T. Ohnuma, and Y. Sakamura, “Dynamical Electroweak Symmetry Breaking in SO(5) x U(1) Gauge-Higgs Unification with Top and Bottom Quarks,” *Phys. Rev.* **D78**, 096002 (2008), [Erratum: *Phys. Rev.* **D79**, 079902(2009)], [arXiv:0806.0480 \[hep-ph\]](#) .
- [120] Csaba Csaki, Christophe Grojean, Hitoshi Murayama, Luigi Pilo, and John Terning, “Gauge theories on an interval: Unitarity without a Higgs,” *Phys. Rev.* **D69**, 055006 (2004), [arXiv:hep-ph/0305237 \[hep-ph\]](#) .

- [121] Giacomo Cacciapaglia, Csaba Csaki, Christophe Grojean, Matthew Reece, and John Terning, “Top and bottom: A Brane of their own,” *Phys. Rev. D* **72**, 095018 (2005), [arXiv:hep-ph/0505001 \[hep-ph\]](#) .
- [122] Yutaka Hosotani, “Dynamical Mass Generation by Compact Extra Dimensions,” *Phys. Lett.* **126B**, 309–313 (1983).
- [123] Yutaka Hosotani, “Dynamics of Nonintegrable Phases and Gauge Symmetry Breaking,” *Annals Phys.* **190**, 233 (1989).
- [124] Yutaka Hosotani, “Dynamical Gauge Symmetry Breaking as the Casimir Effect,” *Phys. Lett.* **129B**, 193–197 (1983).
- [125] Yutaka Hosotani, Shusaku Noda, and Nobuhiro Uekusa, “The Electroweak gauge couplings in $SO(5) \times U(1)$ gauge-Higgs unification,” *Prog. Theor. Phys.* **123**, 757–790 (2010), [arXiv:0912.1173 \[hep-ph\]](#) .
- [126] Wolfram Research, Inc., “Mathematica, Version 11.3.0,” Champaign, IL, 2019.
- [127] Morad Aaboud *et al.* (ATLAS), “Search for new phenomena in high-mass diphoton final states using 37 fb^{-1} of proton–proton collisions collected at $\sqrt{s} = 13 \text{ TeV}$ with the ATLAS detector,” *Phys. Lett.* **B775**, 105–125 (2017), [arXiv:1707.04147 \[hep-ex\]](#) .
- [128] Kaustubh Agashe, Roberto Contino, and Alex Pomarol, “The Minimal composite Higgs model,” *Nucl. Phys.* **B719**, 165–187 (2005), [arXiv:hep-ph/0412089 \[hep-ph\]](#) .
- [129] Roberto Contino, Leandro Da Rold, and Alex Pomarol, “Light custodians in natural composite Higgs models,” *Phys. Rev.* **D75**, 055014 (2007), [arXiv:hep-ph/0612048 \[hep-ph\]](#) .
- [130] Roberto Contino, Yasunori Nomura, and Alex Pomarol, “Higgs as a holographic pseudoGoldstone boson,” *Nucl. Phys.* **B671**, 148–174 (2003), [arXiv:hep-ph/0306259 \[hep-ph\]](#) .
- [131] Kaustubh Agashe, Roberto Contino, Leandro Da Rold, and Alex Pomarol, “A Custodial symmetry for $Zb\bar{b}$,” *Phys. Lett.* **B641**, 62–66 (2006), [arXiv:hep-ph/0605341 \[hep-ph\]](#) .
- [132] Gabriele Ferretti, “Gauge theories of Partial Compositeness: Scenarios for Run-II of the LHC,” *JHEP* **06**, 107 (2016), [arXiv:1604.06467 \[hep-ph\]](#) .

- [133] Luigi Del Debbio, Christoph Englert, and Roman Zwicky, “A UV Complete Compositeness Scenario: LHC Constraints Meet The Lattice,” *JHEP* **08**, 142 (2017), [arXiv:1703.06064 \[hep-ph\]](#) .
- [134] Edward Witten, “Anti-de Sitter space and holography,” *Adv. Theor. Math. Phys.* **2**, 253–291 (1998), [arXiv:hep-th/9802150 \[hep-th\]](#) .
- [135] Nima Arkani-Hamed, Massimo Porrati, and Lisa Randall, “Holography and phenomenology,” *JHEP* **08**, 017 (2001), [arXiv:hep-th/0012148 \[hep-th\]](#) .
- [136] R. Rattazzi and A. Zaffaroni, “Comments on the holographic picture of the Randall-Sundrum model,” *JHEP* **04**, 021 (2001), [arXiv:hep-th/0012248 \[hep-th\]](#) .
- [137] Rainer Storn and Kenneth Price, “Differential evolution – a simple and efficient heuristic for global optimization over continuous spaces,” *Journal of Global Optimization* **11**, 341–359 (1997).
- [138] O. Ring, “On the usage of differential evolution for function optimization,” *Proceedings of North American Fuzzy Information Processing* , 519–523 (1996).
- [139] Peter Athron, Jae-hyeon Park, Tom Steudtner, Dominik Stöckinger, and Alexander Voigt, “Precise higgs mass calculations in (non-)minimal supersymmetry at both high and low scales,” *Journal of High Energy Physics* **2017** (2017), [10.1007/jhep01\(2017\)079](#).
- [140] K. S. Babu and S. Khan, “Minimal nonsupersymmetric $SO(10)$ model: Gauge coupling unification, proton decay, and fermion masses,” *Phys. Rev.* **D92**, 075018 (2015), [arXiv:1507.06712 \[hep-ph\]](#) .
- [141] Lawrence J. Hall, Riccardo Rattazzi, and Uri Sarid, “The Top quark mass in supersymmetric $SO(10)$ unification,” *Phys. Rev.* **D50**, 7048–7065 (1994), [arXiv:hep-ph/9306309 \[hep-ph\]](#) .
- [142] Georges Aad *et al.* (ATLAS), “Search for pair production of a new heavy quark that decays into a W boson and a light quark in pp collisions at $\sqrt{s} = 8$ TeV with the ATLAS detector,” *Phys. Rev.* **D92**, 112007 (2015), [arXiv:1509.04261 \[hep-ex\]](#) .

- [143] Morad Aaboud *et al.* (ATLAS), “Search for type-III seesaw heavy leptons in proton-proton collisions at $\sqrt{s} = 13$ TeV with the ATLAS detector,” ATLAS-CONF-2018-020 (2018).
- [144] Magnus Erik Hvass Pedersen, “Good parameters for differential evolution,” Technical Report no. HL1002 (2010).
- [145] Shuichiro Funatsu, Hisaki Hatanaka, Yutaka Hosotani, and Yuta Orikasa, “Distinct signals of the gauge-Higgs unification in e^+e^- collider experiments,” *Phys. Lett.* **B775**, 297–302 (2017), [arXiv:1705.05282 \[hep-ph\]](#) .
- [146] Shuichiro Funatsu, Hisaki Hatanaka, Yutaka Hosotani, Yuta Orikasa, and Takuya Shimotani, “Novel universality and Higgs decay $H \rightarrow \gamma\gamma, gg$ in the $SO(5) \times U(1)$ gauge-Higgs unification,” *Phys. Lett.* **B722**, 94–99 (2013), [arXiv:1301.1744 \[hep-ph\]](#) .
- [147] Yutaka Hosotani, “Gauge-Higgs unification at e^+e^- linear colliders,” *Proceedings, 18th Hellenic School and Workshops on Elementary Particle Physics and Gravity (CORFU2018): Corfu, Corfu, Greece*, *PoS CORFU2018*, 075 (2019), [arXiv:1904.10156 \[hep-ph\]](#) .
- [148] Albert M Sirunyan *et al.* (CMS), “Prospects for HH measurements at the HL-LHC,” CMS-PAS-FTR-18-019 (2018).
- [149] S. Dawson, S. Dittmaier, and M. Spira, “Neutral Higgs boson pair production at hadron colliders: QCD corrections,” *Phys. Rev.* **D58**, 115012 (1998), [arXiv:hep-ph/9805244 \[hep-ph\]](#) .
- [150] R. Frederix, S. Frixione, V. Hirschi, F. Maltoni, O. Mattelaer, P. Torrielli, E. Vryonidou, and M. Zaro, “Higgs pair production at the LHC with NLO and parton-shower effects,” *Phys. Lett.* **B732**, 142–149 (2014), [arXiv:1401.7340 \[hep-ph\]](#) .
- [151] Daniel de Florian and Javier Mazzitelli, “Higgs pair production at next-to-next-to-leading logarithmic accuracy at the LHC,” *JHEP* **09**, 053 (2015), [arXiv:1505.07122 \[hep-ph\]](#) .
- [152] Daniel de Florian, Massimiliano Grazzini, Catalin Hanga, Stefan Kallweit, Jonas M. Lindert, Philipp Maierhöfer, Javier Mazzitelli, and Dirk Rathlev, “Differential Higgs Boson Pair Production at Next-to-Next-to-Leading Order in QCD,” *JHEP* **09**, 151 (2016), [arXiv:1606.09519 \[hep-ph\]](#) .

- [153] S. Borowka, N. Greiner, G. Heinrich, S. P. Jones, M. Kerner, J. Schlenk, U. Schubert, and T. Zirke, “Higgs Boson Pair Production in Gluon Fusion at Next-to-Leading Order with Full Top-Quark Mass Dependence,” [Phys. Rev. Lett. **117**, 012001 \(2016\)](#), [Erratum: Phys. Rev. Lett.117,no.7,079901(2016)], [arXiv:1604.06447 \[hep-ph\]](#) .
- [154] S. Borowka, N. Greiner, G. Heinrich, S. P. Jones, M. Kerner, J. Schlenk, and T. Zirke, “Full top quark mass dependence in Higgs boson pair production at NLO,” [JHEP **10**, 107 \(2016\)](#), [arXiv:1608.04798 \[hep-ph\]](#) .
- [155] G. Heinrich, S. P. Jones, M. Kerner, G. Luisoni, and E. Vryonidou, “NLO predictions for Higgs boson pair production with full top quark mass dependence matched to parton showers,” [JHEP **08**, 088 \(2017\)](#), [arXiv:1703.09252 \[hep-ph\]](#) .
- [156] Massimiliano Grazzini, Gudrun Heinrich, Stephen Jones, Stefan Kallweit, Matthias Kerner, Jonas M. Lindert, and Javier Mazzitelli, “Higgs boson pair production at NNLO with top quark mass effects,” [JHEP **05**, 059 \(2018\)](#), [arXiv:1803.02463 \[hep-ph\]](#) .
- [157] Daniel De Florian and Javier Mazzitelli, “Soft gluon resummation for Higgs boson pair production including finite M_t effects,” [JHEP **08**, 156 \(2018\)](#), [arXiv:1807.03704 \[hep-ph\]](#) .
- [158] Julien Baglio, Francisco Campanario, Seraina Glaus, Margarete Mühlleitner, Michael Spira, and Jura J. Streicher, “Gluon fusion into Higgs pairs at NLO QCD and the top mass scheme,” [Eur. Phys. J. **C79**, 459 \(2019\)](#), [arXiv:1811.05692 \[hep-ph\]](#) .
- [159] R. Contino *et al.*, “Physics at a 100 TeV pp collider: Higgs and EW symmetry breaking studies,” [CERN Yellow Rep. , 255–440 \(2017\)](#), [arXiv:1606.09408 \[hep-ph\]](#) .
- [160] Weiming Yao, “Studies of measuring Higgs self-coupling with $HH \rightarrow b\bar{b}\gamma\gamma$ at the future hadron colliders,” in *Proceedings, 2013 Community Summer Study on the Future of U.S. Particle Physics: Snowmass on the Mississippi (CSS2013): Minneapolis, MN, USA, July 29-August 6, 2013* (2013) [arXiv:1308.6302 \[hep-ph\]](#) .

- [161] Alan J. Barr, Matthew J. Dolan, Christoph Englert, Danilo Enoque Ferreira de Lima, and Michael Spannowsky, “Higgs Self-Coupling Measurements at a 100 TeV Hadron Collider,” *JHEP* **02**, 016 (2015), [arXiv:1412.7154 \[hep-ph\]](#) .
- [162] Hong-Jian He, Jing Ren, and Weiming Yao, “Probing new physics of cubic Higgs boson interaction via Higgs pair production at hadron colliders,” *Phys. Rev.* **D93**, 015003 (2016), [arXiv:1506.03302 \[hep-ph\]](#) .
- [163] Andreas Papaefstathiou, “Discovering Higgs boson pair production through rare final states at a 100 TeV collider,” *Phys. Rev.* **D91**, 113016 (2015), [arXiv:1504.04621 \[hep-ph\]](#) .
- [164] Amit Adhikary, Shankha Banerjee, Rahool Kumar Barman, Biplob Bhattacharjee, and Saurabh Niyogi, “Revisiting the non-resonant Higgs pair production at the HL-LHC,” *JHEP* **07**, 116 (2018), [arXiv:1712.05346 \[hep-ph\]](#) .
- [165] Shankha Banerjee, Christoph Englert, Michelangelo L. Mangano, Michele Selvaggi, and Michael Spannowsky, “ hh +jet production at 100 TeV,” *Eur. Phys. J.* **C78**, 322 (2018), [arXiv:1802.01607 \[hep-ph\]](#) .
- [166] Shankha Banerjee, Frank Krauss, and Michael Spannowsky, “Revisiting the $t\bar{t}hh$ channel at the FCC-hh,” *Phys. Rev.* **D100**, 073012 (2019), [arXiv:1904.07886 \[hep-ph\]](#) .
- [167] Yutaka Hosotani and Yoshikazu Kobayashi, “Yukawa Couplings and Effective Interactions in Gauge-Higgs Unification,” *Phys. Lett.* **B674**, 192–196 (2009), [arXiv:0812.4782 \[hep-ph\]](#) .
- [168] E. W. Nigel Glover and J. J. van der Bij, “Higgs boson pair production via gluon fusion,” *Nucl. Phys.* **B309**, 282–294 (1988).
- [169] Ulrich Baur, Tilman Plehn, and David L. Rainwater, “Measuring the Higgs boson self coupling at the LHC and finite top mass matrix elements,” *Phys. Rev. Lett.* **89**, 151801 (2002), [arXiv:hep-ph/0206024 \[hep-ph\]](#) .
- [170] Matthew J. Dolan, Christoph Englert, and Michael Spannowsky, “Higgs self-coupling measurements at the LHC,” *JHEP* **10**, 112 (2012), [arXiv:1206.5001 \[hep-ph\]](#) .

- [171] William J. Marciano, “Weak mixing angle and grand unified gauge theories,” *Phys. Rev. D* **20**, 274–288 (1979).
- [172] Bipasha Chakraborty, C. T. H. Davies, B. Galloway, P. Knecht, J. Koponen, G. C. Donald, R. J. Dowdall, G. P. Lepage, and C. McNeile, “High-precision quark masses and QCD coupling from $n_f = 4$ lattice QCD,” *Phys. Rev.* **D91**, 054508 (2015), [arXiv:1408.4169 \[hep-lat\]](#) .
- [173] Peter J. Mohr, David B. Newell, and Barry N. Taylor, “CODATA Recommended Values of the Fundamental Physical Constants: 2014,” *Rev. Mod. Phys.* **88**, 035009 (2016), [arXiv:1507.07956 \[physics.atom-ph\]](#) .
- [174] Jens Erler and Michael J. Ramsey-Musolf, “The Weak mixing angle at low energies,” *Phys. Rev.* **D72**, 073003 (2005), [arXiv:hep-ph/0409169 \[hep-ph\]](#) .
- [175] Marie E. Machacek and Michael T. Vaughn, “Two-loop renormalization group equations in a general quantum field theory: (iii). scalar quartic couplings,” *Nuclear Physics B* **249**, 70 – 92 (1985).
- [176] Raman Sundrum, “Tasi 2004 lectures: To the fifth dimension and back,” in *Theoretical Advanced Study Institute in Elementary Particle Physics: Many Dimensions of String Theory (TASI 2005) Boulder, Colorado, June 5-July 1, 2005* (2005) pp. 585–630, [585(2005)], [arXiv:hep-th/0508134 \[hep-th\]](#) .
- [177] Lawrence Hall, “Grand unification of effective gauge theories,” *Nuclear Physics B* **178**, 75 – 124 (1981).
- [178] Lisa Randall and Matthew D. Schwartz, “Unification and the hierarchy from AdS5,” *Phys. Rev. Lett.* **88**, 081801 (2002), [arXiv:hep-th/0108115 \[hep-th\]](#) .
- [179] G. Lazarides, Q. Shafi, and C. Wetterich, “Proton lifetime and fermion masses in an $so(10)$ model,” *Nuclear Physics B* **181**, 287 – 300 (1981).
- [180] Stephen M. Barr, “A New Symmetry Breaking Pattern for $SO(10)$ and Proton Decay,” *Phys. Lett.* **112B**, 219–222 (1982).
- [181] Savas Dimopoulos and Howard Georgi, “Softly Broken Supersymmetry and $SU(5)$,” *Nucl. Phys. B* **193**, 150–162 (1981).
- [182] J.P. Derendinger, Jihn E. Kim, and Dimitri V. Nanopoulos, “Anti- $SU(5)$,” *Phys. Lett. B* **139**, 170–176 (1984).

-
- [183] Ignatios Antoniadis, John R. Ellis, J.S. Hagelin, and Dimitri V. Nanopoulos, “Supersymmetric Flipped SU(5) Revitalized,” *Phys. Lett. B* **194**, 231–235 (1987).
- [184] Nobuhiro Maekawa and Toshifumi Yamashita, “E(6) unification, doublet triplet splitting and anomalous U(1)(A) symmetry,” *Prog. Theor. Phys.* **107**, 1201–1233 (2002), [arXiv:hep-ph/0202050](#) .
- [185] Mary L Boas, *Mathematical methods in the physical sciences; 3rd ed.* (Wiley, Hoboken, NJ, 2006).
- [186] Steven Weinberg, “Effective gauge theories,” *Physics Letters B* **91**, 51 – 55 (1980).
- [187] Lawrence J. Hall, “Grand Unification of Effective Gauge Theories,” *Nucl. Phys.* **B178**, 75–124 (1981).